Compiled properties of nucleonic matter and nuclear and neutron star models from nonrelativistic and relativistic interactions

Boyang Sun, Saketh Bhattiprolu, and James M. Lattimer
Department of Physics & Astronomy, Stony Brook University, Stony Brook, New York 11794, USA

(Received 26 October 2023; accepted 8 April 2024; published 3 May 2024)

This paper compiles the model parameters and zero-temperature properties of an extensive collection of published theoretical nuclear interactions, including 255 nonrelativistic (Skyrme-like) forces, 270 relativistic mean field (RMF) and point-coupling (RMF-PC) forces, and 13 Gogny-like forces. This forms the most exhaustive tabulation of model parameters to date. The properties of uniform symmetric matter and pure neutron matter at the saturation density are determined. Symmetry properties found from the second-order term of a Taylor expansion in neutron excess are compared with the energy difference of pure neutron and symmetric nuclear matter at the saturation density. Selected liquid-droplet model parameters, including the surface tension and surface symmetry energy, are determined for semi-infinite surfaces. Theoretical liquid droplet model neutron skin thicknesses of the neutron-rich closed-shell nuclei ^{48}Ca and ^{208}Pb are compared with published theoretical Hartree-Fock and experimental results. A similar comparison is made between theoretical liquid-droplet and experimental values of dipole polarizabilities. In addition, radii, binding energies, moments of inertia and tidal deformabilities of 1.2M$_\odot$, 1.4M$_\odot$ and 1.6M$_\odot$ neutron stars are computed. An extensive correlation analysis of bulk matter, nuclear structure, and low-mass neutron star properties is performed and compared with nuclear experiments and astrophysical observations.

DOI: 10.1103/PhysRevC.109.055801

I. INTRODUCTION

The properties of uniform matter consisting of neutrons and protons at zero temperature are functions of the total baryon density n and the proton fraction x. The equation of state of uniform matter between about half the nuclear saturation density $n_0 \approx 0.16\ \mathrm{fm}^{-3}$ and $2n_0$ is an essential ingredient in models of neutron stars and in calculations of gravitational collapse supernovae and in neutron star mergers. For example, the radii of typical neutron stars between $1.3M_\odot$ and $1.6M_\odot$ depends strongly on the symmetry energy near n_0, and the amount of mass ejected in a binary neutron star merger, in which both components are likely in this mass range, is very sensitive to the neutron star radius.

Many microscopic models of dense matter begin with a two-body nucleon-nucleon interaction with parameters fitted to nucleon-nucleon phase shifts and to properties of the deuteron. But many-body formalisms based on these inputs have historically had difficulty in matching the saturation properties established, for example, from experimental binding energies using the empirical liquid droplet or Hartree-Fock nuclear models. As a result, the vast majority of published interactions have instead followed more empirical approaches.

The simplest ones employ nonrelativistic effective density-dependent zero-range two-and three-nucleon interactions, whose parameters are fit to the properties of nuclei and/or symmetric matter at the saturation density. These zero-range nonrelativistic interactions are collectively known as Skyrme-type interactions, and lead to an energy density that is, effectively, a power-law series expressed in terms of the wave number or baryon density. A more complicated non-relativistic approach (Gogny-type) utilizes short finite-range interactions.

A distinctly different theoretical relativistic mean field (RMF) approach is based on quantum hadrodynamics and involves forces mediated by two to four meson fields, which leads to an energy density that depends not only on the baryon density and the proton fraction, but also on the meson field strengths. The meson fields are determined at each baryon density and proton fraction by energy minimization, which leads to a more complex density-dependence of the energy density than for Skyrme-type interactions. Several variations of the RMF approach, depending on whether the couplings are linear or nonlinear in the fields, have been proposed.

The uniform matter properties for hundreds of published models using these two main approaches were compiled by Dutra *et al.* in Ref. [1] for 240 Skyrme-like interactions and in Ref. [2] for 263 RMF interactions (see also Ref. [3]). The main purposes of this paper are to

(1) create a database of interaction parameters for Skyrme-, RMF- and Gogny-type forces, which were not tabulated in Refs. [1,2].
(2) remove duplicated forces and include additional forces, as well as correcting typos in previous works.
(3) compare symmetry properties of these forces found by both differencing the energies of pure neutron and symmetric matter and computing the quadratic term of an expansion of the energy in powers of the neutron excess.

(4) compute properties of a semi-infinite surface, including the surface tension and surface symmetry energy.
(5) tabulate the liquid droplet model (DM) neutron skin thicknesses and dipole polarizabilities of ^{48}Ca and ^{208}Pb and compare the former to Hartree-Fock computations and experiments.
(6) compute low-mass neutron star properties, such as radii, binding energies, moments of inertia and tidal deformabilities.
(7) produce extensive correlation analyses among bulk matter, nuclear structure, and low-mass neutron star properties.

The creation of this parameter database will greatly ease future studies, alleviating the need to peruse hundreds of individual publications for this information.

The bulk of the force models we consider were included in Refs. [1,2]. We include additional force models and correct a few published parameter sets. At the same time, in the case of RMF models, we selectively omit a few models because of ambiguities in their published parameters or the models' complexity. We did not include some recent RMF forces because they do not fit into the parametrization schemes of Ref. [2], such as the 18 forces [V,S,M][P,Z,N][E,R] in Ref. [4]. These will be included in future work.

II. SKYRME-TYPE INTERACTIONS

A. Energy density

The energy density of bulk matter in Skyrme-type models contains multiple parameters t_i, x_i and σ_i:

$$\begin{aligned}\mathcal{E} = {} & \frac{3\hbar^2}{10M}\left(\frac{3\pi^2}{2}\right)^{2/3} n^{5/3}H_{5/3} + \frac{t_0}{4}n^2\left[x_0+2-\left(x_0+\frac{1}{2}\right)H_2\right] + \frac{1}{24}\sum_{i=1}^{3} t_{3i}n^{\sigma_i+2}\left[x_{3i}+2-\left(x_{3i}+\frac{1}{2}\right)H_2\right]\\ & + \frac{3}{40}\left(\frac{3\pi^2}{2}\right)^{2/3} n^{8/3}(aH_{5/3}+bH_{8/3}) + \frac{3}{40}\left(\frac{3\pi^2}{2}\right)^{2/3} n^{8/3+\delta}\left[t_4(x_4+2)H_{5/3} - t_4\left(x_4+\frac{1}{2}\right)H_{8/3}\right]\\ & + \frac{3}{40}\left(\frac{3\pi^2}{2}\right)^{2/3} n^{8/3+\gamma}\left[t_5(x_5+2)H_{5/3} + t_5\left(x_5+\frac{1}{2}\right)H_{8/3}\right]\\ & + \frac{1}{2}[Q_{nn}(\vec{\nabla}n_n)^2 + 2Q_{np}\vec{\nabla}n_n\cdot\vec{\nabla}n_p + Q_{pp}(\vec{\nabla}n_p)^2],\end{aligned} \tag{1}$$

with a and b being the parameter combinations

$$a = t_1(x_1+2) + t_2(x_2+2), \quad b = t_2\left(x_2+\tfrac{1}{2}\right) - t_1\left(x_1+\tfrac{1}{2}\right), \tag{2}$$

and $H_n(x) = 2^{n-1}[x^n + (1-x)^n]$, such that $H_n(x=0) = 2^{n-1}$ for pure neutron matter (PNM) and $H_n(x=1/2) = 1$ for symmetric nuclear matter (SNM). The coefficients Q_{ij} in the spatially varying part of the Skyrme Hamiltonian density are

$$\begin{aligned} Q_{nn} = Q_{pp} &= \frac{3}{16}\left[t_1(1-x_1) - t_2(1+x_2) + t_4n^\delta\left\{1-x_4+\frac{4\delta}{3}\left[1+\frac{x_4}{2}-x_t\left(\frac{1}{2}+x_4\right)\right]\right\} - t_5n^\gamma(1+x_5)\right],\\ Q_{np} = Q_{pn} &= \frac{1}{8}\left[3t_1\left(1+\frac{x_1}{2}\right) - t_2\left(1+\frac{x_2}{2}\right) + \frac{3t_4n^\delta}{2}(2+x_4+\delta) - t_5n^\gamma\left(1+\frac{x_5}{2}\right)\right].\end{aligned} \tag{3}$$

The first term in Eq. (1) is the kinetic energy density for noninteracting neutrons and protons. Together with the terms involving a, b and t_4, it forms the total kinetic energy density. Equivalently, the bare nucleon mass M is replaced by the effective neutron ($t=n$) and proton ($t=p$) masses M_t^*:

$$\frac{\hbar^2}{2M_t^*} = \frac{\hbar^2}{2M} + \frac{n}{4}\left(\frac{a}{2} + bx_t + t_4n^\delta\left[1+\frac{x_4}{2}-\left(\frac{1}{2}+x_4\right)x_t\right] + t_5n^\gamma\left[1+\frac{x_5}{2}+\left(\frac{1}{2}+x_5\right)x_t\right]\right). \tag{4}$$

where $x_n = 1-x$ and $x_p = x$. We ignored contributions from Coulomb and spin-orbit interactions which do not contribute to the energy density of uniform bulk matter.

Modifications to the conventional, original form of $\mathcal{E}$, as described by Vautherin and Brink in Ref. [5], include the summation over index i in the t_{3i} term introduced by Agrawal *et al.* in Ref. [6] and additional terms involving t_4, x_4, t_5 and x_5 used by Chamel *et al.* in Refs. [7,8].

B. Uniform nuclear matter

In uniform matter, the density gradients $\vec{\nabla} n_n = \vec{\nabla} n_p = 0$. The energy per particle $E = \mathcal{E}_B/n$ is then obtained as

$$E(n,x) = \frac{3\hbar^2}{10M}\left(\frac{3\pi^2}{2}\right)^{2/3} n^{2/3} H_{5/3} + \frac{t_0}{4} n\left[x_0 + 2 - \left(x_0 + \frac{1}{2}\right)H_2\right] + \frac{1}{24}\sum_{i=1}^{3} t_{3i} n^{\sigma_i+1}\left[x_{3i} + 2 - \left(x_{3i} + \frac{1}{2}\right)H_2\right]$$
$$+ \frac{3}{40}\left(\frac{3\pi^2}{2}\right)^{2/3} n^{5/3}\left(aH_{5/3} + bH_{8/3}\right) + \frac{3t_4}{40}\left(\frac{3\pi^2}{2}\right)^{2/3} n^{5/3+\delta}\left[(x_4+2)H_{5/3} - \left(x_4 + \frac{1}{2}\right)H_{8/3}\right]$$
$$+ \frac{3t_5}{40}\left(\frac{3\pi^2}{2}\right)^{2/3} n^{5/3+\gamma}\left[(x_5+2)H_{5/3} + \left(x_5 + \frac{1}{2}\right)H_{8/3}\right]. \tag{5}$$

The pressure is given as

$$P(n,x) = n^2\frac{\partial E}{\partial n} = \frac{\hbar^2}{5M}\left(\frac{3\pi^2}{2}\right)^{2/3} n^{5/3} H_{5/3} + \frac{1}{48}\sum_{i=1}^{3} t_{3i}(\sigma_i+1) n^{\sigma_i+2}[2(x_{3i}+2) - (2x_{3i}+1)H_2]$$
$$+ \frac{1}{8}\left(\frac{3\pi^2}{2}\right)^{2/3} n^{8/3}(aH_{5/3} + bH_{8/3}) + \frac{t_4}{40}\left(\frac{3\pi^2}{2}\right)^{2/3}(5+3\delta) n^{\frac{8}{3}+\delta}\left[(x_4+2)H_{5/3} - \left(x_4+\frac{1}{2}\right)H_{8/3}\right]$$
$$+ \frac{t_0}{8} n^2[2(x_0+2) - (2x_0+1)H_2] + \frac{t_5}{40}\left(\frac{3\pi^2}{2}\right)^{2/3}(5+3\gamma) n^{\frac{8}{3}+\gamma}\left[(x_5+2)H_{5/3} + \left(x_5+\frac{1}{2}\right)H_{8/3}\right]. \tag{6}$$

The saturation density n_0 is defined by $P(n_0, 1/2) = 0$. The volume incompressibility is defined as

$$\mathcal{K}(n,x) = 9n^2\frac{\partial^2 E}{\partial n^2} = -\frac{3\hbar^2}{5M}\left(\frac{3\pi^2}{2}\right)^{2/3} n^{2/3} H_{5/3} + \frac{3}{16}\sum_{i=1}^{3} t_{3i}\sigma_i(\sigma_i+1) n^{\sigma_i+1}[2(x_{3i}+2) - (2x_{3i}+1)H_2]$$
$$+ 3\left(\frac{3\pi^2}{2}\right)^{2/3} n^{5/3}(aH_{5/3} + bH_{8/3}) + \frac{3t_4}{40}\left(\frac{3\pi^2}{2}\right)^{2/3}(2+3\delta)(5+3\delta) n^{\frac{5}{3}+\delta}\left[(x_4+2)H_{5/3} - \left(x_4+\frac{1}{2}\right)H_{8/3}\right]$$
$$+ \frac{3t_5}{40}\left(\frac{3\pi^2}{2}\right)^{2/3}(2+3\gamma)(5+3\gamma) n^{\frac{5}{3}+\gamma}\left[(x_5+2)H_{5/3} + \left(x_5+\frac{1}{2}\right)H_{8/3}\right]. \tag{7}$$

Finally, the skewness is defined as

$$\mathcal{Q}(n,x) = 27n^3\frac{\partial^3 E}{\partial n^3} = \frac{12\hbar^2}{5M}\left(\frac{3\pi^2}{2}\right)^{2/3} n^{2/3} H_{5/3} - \frac{3}{4}\left(\frac{3\pi^2}{2}\right)^{2/3} n^{5/3}(aH_{5/3} + bH_{8/3})$$
$$+ \frac{9}{16}\sum_{i=1}^{3} t_{3i}\sigma_i\left(\sigma_i^2 - 1\right) n^{\sigma_i+1}[2(x_{3i}+2) - (2x_{3i}+1)H_2]$$
$$+ \frac{3t_4}{40}\left(\frac{3\pi^2}{2}\right)^{2/3}(2+3\delta)(5+3\delta)(3\delta-1) n^{\frac{5}{3}+\delta}\left[(x_4+2)H_{5/3} - \left(x_4+\frac{1}{2}\right)H_{8/3}\right]$$
$$+ \frac{3t_5}{40}\left(\frac{3\pi^2}{2}\right)^{2/3}(2+3\gamma)(5+3\gamma)(3\gamma-1) n^{\frac{5}{3}+\gamma}\left[(x_5+2)H_{5/3} + \left(x_5+\frac{1}{2}\right)H_{8/3}\right]. \tag{8}$$

Relevant properties of SNM include $E_0 = E(n_0, 1/2)$, $P_0 = P(n_0, 1/2) = 0$, $K_0 = \mathcal{K}(n_0, 1/2)$, and $Q_0 = \mathcal{Q}(n_0, 1/2)$ and those of PNM include $E_{N0} = E(n_0, 0)$, $P_{N0} = P(n_0, 0)$, $K_{N0} = \mathcal{K}(n_0, 0)$, and $Q_{N0} = \mathcal{Q}(n_0, 0)$.

C. Symmetry energy

The symmetry energy can be defined in two ways. First it can be expressed as the difference of the PNM energy and the SNM energy

$$\mathcal{S}_1(n) = E(n,0) - E(n,1/2), \tag{9}$$

and second, as the second derivative of E with respect to the neutron excess $1-2x$ at $x=1/2$,

$$\mathcal{S}_2(n)=\frac{1}{8}\left(\frac{\partial^2 E}{\partial x^2}\right)_{x=1/2}. \tag{10}$$

If higher than quadratic terms in an expansion of S in $1-2x$ are negligible, then S_1 and S_2 would be identical. The symmetry energy defined in either way can be expanded in a Taylor series in $y=(n-n_0)/(3n_0)$ around the saturation density n_0:

$$\mathcal{S}_{1,2}(n)=J_{1,2}+L_{1,2}y+\frac{1}{2!}K_{\mathrm{sym}1,2}y^2+\frac{1}{3!}Q_{\mathrm{sym}1,2}y^3+O(y^4), \tag{11}$$

where $J_{1,2}$, $L_{1,2}$, $K_{\mathrm{sym}1,2}$, and $Q_{\mathrm{sym}1,2}$ are the so-called symmetry energy parameters.

In the first case, one finds

$$\begin{aligned}
J_1 &= E_{N0}-E_0=\frac{3\hbar^2}{10M}\left(\frac{3\pi^2 n_0}{2}\right)^{2/3}(2^{2/3}-1)-\frac{t_0}{8}n_0(2x_0+1)-\frac{1}{48}\sum_{i=1}^{3}t_{3i}n_0^{\sigma_i+1}(2x_{3i}+1)\\
&\quad+\frac{3}{40}\left(\frac{3\pi^2}{2}\right)^{2/3}n_0^{5/3}[(2^{2/3}-1)a+(2^{5/3}-1)b]+\frac{3t_4}{40}\left(\frac{3\pi^2}{2}\right)^{2/3}n_0^{5/3+\delta}\left[2^{2/3}(1-x_4)-\frac{3}{2}\right]\\
&\quad+\frac{3t_5}{40}\left(\frac{3\pi^2}{2}\right)^{2/3}n_0^{5/3+\gamma}\left[3\times 2^{2/3}(1+x_5)-\frac{5}{2}\left(1+\frac{4}{5}x_5\right)\right],\\
L_1 &= \frac{3}{n_0}(P_{N0}-P_0)=\frac{3\hbar^2}{5M}\left(\frac{3\pi^2 n_0}{2}\right)^{2/3}(2^{2/3}-1)-\frac{3t_0}{8}n_0(2x_0+1)-\frac{1}{16}\sum_{i=1}^{3}t_{3i}n_0^{\sigma_i+1}(\sigma_i+1)(2x_{3i}+1)\\
&\quad+\frac{3}{8}\left(\frac{3\pi^2}{2}\right)^{2/3}n_0^{5/3}[(2^{2/3}-1)a+(2^{5/3}-1)b]+\frac{3t_4}{40}\left(\frac{3\pi^2}{2}\right)^{2/3}n_0^{5/3+\delta}(5+3\delta)\left[2^{2/3}(1-x_4)-\frac{3}{2}\right]\\
&\quad+\frac{3t_5}{40}\left(\frac{3\pi^2}{2}\right)^{2/3}n_0^{5/3+\gamma}(5+3\gamma)\left[3\times 2^{2/3}(1+x_5)-\frac{5}{2}\left(1+\frac{4x_5}{5}\right)\right],\\
K_{\mathrm{sym}1} &= K_{N0}-K_0=-\frac{3\hbar^2}{5M}\left(\frac{3\pi^2}{2}n_0\right)^{2/3}(2^{2/3}-1)+3\left(\frac{3\pi^2}{2}\right)^{2/3}n_0^{5/3}[(2^{2/3}-1)a+(2^{5/3}-1)b]\\
&\quad-\frac{3}{16}\sum_{i=1}^{3}t_{3i}\sigma_i(\sigma_i+1)n_0^{\sigma_i+1}(2x_{3i}+1)+\frac{3t_4}{40}\left(\frac{3\pi^2}{2}\right)^{2/3}(2+3\delta)(5+3\delta)n_0^{\frac{5}{3}+\delta}\left[2^{2/3}(1-x_4)-\frac{3}{2}\right]\\
&\quad+\frac{3t_5}{40}\left(\frac{3\pi^2}{2}\right)^{2/3}(2+3\gamma)(5+3\gamma)n_0^{\frac{5}{3}+\gamma}\left[3\times 2^{2/3}(1+x_5)-\frac{5}{2}\left(1+\frac{4}{5}x_5\right)\right],\\
Q_{\mathrm{sym}1} &= Q_{N0}-Q_0=\frac{12\hbar^2}{5M}\left(\frac{3\pi^2}{2}\right)^{2/3}n_0^{2/3}(2^{2/3}-1)\\
&\quad-\frac{3}{4}\left(\frac{3\pi^2}{2}\right)^{2/3}n_0^{5/3}[(2^{2/3}-1)a+(2^{5/3}-1)b]-\frac{9}{16}\sum_{i=1}^{3}t_{3i}\sigma_i(\sigma_i+1)(\sigma_i-1)n_0^{\sigma_i+1}(2x_{3i}+1)\\
&\quad+\frac{3t_4}{40}\left(\frac{3\pi^2}{2}\right)^{2/3}(2+3\delta)(5+3\delta)(3\delta-1)n_0^{\frac{5}{3}+\delta}\left[2^{2/3}(1-x_4)-\frac{3}{2}\right]\\
&\quad+\frac{3t_5}{40}\left(\frac{3\pi^2}{2}\right)^{2/3}(2+3\gamma)(5+3\gamma)(3\gamma-1)n_0^{\frac{5}{3}+\gamma}\left[3\times 2^{2/3}(1+x_5)-\frac{5}{2}\left(1+\frac{4}{5}x_5\right)\right].
\end{aligned} \tag{12}$$

In the second case,

$$\begin{aligned}
\mathcal{S}_2(n) &= \frac{\hbar^2}{6M}\left(\frac{3\pi^2}{2}\right)^{2/3}n^{2/3}-\frac{t_0}{8}(2x_0+1)n-\frac{1}{48}\sum_{i=1}^{3}t_{3i}(2x_{3i}+1)n^{\sigma_i+1}\\
&\quad+\frac{1}{24}\left(\frac{3\pi^2}{2}\right)^{2/3}(a+4b)n^{5/3}-\frac{t_4}{8}\left(\frac{3\pi^2}{2}\right)^{2/3}x_4 n^{\frac{5}{3}+\delta}+\frac{t_5}{24}\left(\frac{3\pi^2}{2}\right)^{2/3}(5x_5+4)n^{\frac{5}{3}+\gamma}.
\end{aligned} \tag{13}$$

At the saturation density, we have $J_2 = \mathcal{S}_2(n_0)$. Other saturation properties are consequently given as

$$\begin{aligned}
L_2 &= 3n_0\left(\frac{\partial \mathcal{S}_2}{\partial n}\right)_{n=n_0} = \frac{\hbar^2}{3M}\left(\frac{3\pi^2}{2}\right)^{2/3} n_0^{2/3} - \frac{3t_0}{8}(2x_0+1)n_0 - \frac{1}{16}\sum_{i=1}^{3} t_{3i}(2x_{3i}+1)(\sigma_i+1)n_0^{\sigma_i+1} \\
&\quad + \frac{5}{24}\left(\frac{3\pi^2}{2}\right)^{2/3}(a+4b)n_0^{5/3} - \frac{t_4}{8}\left(\frac{3\pi^2}{2}\right)^{2/3}(5+3\delta)x_4 n_0^{\frac{5}{3}+\delta} + \frac{t_5}{24}\left(\frac{3\pi^2}{2}\right)^{2/3}(5+3\gamma)(5x_5+4)n_0^{\frac{5}{3}+\gamma}, \\
K_{\rm sym2} &= 9n_0^2\left(\frac{\partial^2 \mathcal{S}_2}{\partial n^2}\right)_{n=n_0} = -\frac{\hbar^2}{3M}\left(\frac{3\pi^2}{2}\right)^{2/3} n_0^{2/3} - \frac{3}{16}\sum_{i=1}^{3} t_{3i}(2x_{3i}+1)(\sigma_i+1)\sigma_i n_0^{\sigma_i+1} \\
&\quad + \frac{5}{12}\left(\frac{3\pi^2}{2}\right)^{2/3}(a+4b)n_0^{5/3} - \frac{t_4}{8}\left(\frac{3\pi^2}{2}\right)^{2/3}(5+3\delta)(2+3\delta)x_4 n_0^{\frac{5}{3}+\delta} \\
&\quad + \frac{t_5}{24}\left(\frac{3\pi^2}{2}\right)^{2/3}(5+3\gamma)(2+3\gamma)(5x_5+4)n_0^{\frac{5}{3}+\gamma}, \\
Q_{\rm sym2} &= 27n_0^3\left(\frac{\partial^3 \mathcal{S}_2}{\partial n^3}\right)_{n=n_0} = \frac{4\hbar^2}{3M}\left(\frac{3\pi^2}{2}\right)^{2/3} n_0^{2/3} - \frac{9}{16}\sum_{i=1}^{3} t_{3i}(2x_{3i}+1)(\sigma_i+1)\sigma_i(\sigma_i-1)n_0^{\sigma_i+1} \\
&\quad - \frac{5}{12}\left(\frac{3\pi^2}{2}\right)^{2/3}(a+4b)n_0^{5/3} - \frac{t_4}{8}\left(\frac{3\pi^2}{2}\right)^{2/3}(5+3\delta)(2+3\delta)(3\delta-1)x_4 n_0^{\frac{5}{3}+\delta} \\
&\quad + \frac{t_5}{24}\left(\frac{3\pi^2}{2}\right)^{2/3}(5+3\gamma)(2+3\gamma)(3\gamma-1)(5x_5+4)n_0^{\frac{5}{3}+\gamma}. \qquad (14)
\end{aligned}$$

The list of saturation properties of Skyrme forces is given in Table II of Appendix A.

III. RELATIVISTIC MEAN-FIELD MODELS

In contrast with Skyrme-like models, RMF models describe the strong interaction by an exchange of mesons which are usually assumed to couple minimally to nucleons. These include the isospin scalar-scalar σ, the isospin scalar-vector ω, and, in some cases, the isospin vector-vector ρ and, in additional cases, the isospin vector-scalar δ mesons. The meson fields are approximated by their mean fields. An interesting property of RMF models is the occurrence of two different particle number densities: vector densities n_n and n_p, which are equivalent to the baryon densities occurring in Skyrme-type interactions, and scalar densities n_{sn} and n_{sp}. Their interplay is essential to describe the saturation of nuclear matter. Most models considered assume the meson-nucleon couplings to be constant, but we also consider models in which either the couplings depend on baryon-density or the nucleons interact with each other only through effective point-like couplings not involving mesons.

A. Models with constant couplings

1. Energy density

The total energy density of infinite bulk nuclear matter is assumed to be dependent both on the baryon densities n_i ($i = n, p$) and the meson fields σ, ω, and ρ and δ when the model contains them:

$$\mathcal{E}_B = \sum_{i=n,p} \mathcal{E}_{{\rm kin},i} + g_\omega \omega n + \frac{1}{2} g_\rho \rho (n_n - n_p) + V(\sigma) - F(\omega,\sigma) - G(\rho,\omega,\sigma) + I(\delta), \qquad (15)$$

with potential-energy densities

$$\begin{aligned}
V(\sigma) &= \frac{\sigma^2}{(\hbar c)^3}\left[\frac{1}{2}m_\sigma^2 + \sigma\left(\frac{A}{3} + \frac{B}{4}\sigma\right)\right], \quad F(\omega,\sigma) = \frac{\omega^2}{(\hbar c)^3}\left\{\frac{1}{2}m_\omega^2 + g_\omega^2\left(g_\sigma\sigma\left[\alpha_1 + \frac{\alpha_1'}{2}g_\sigma\sigma\right] + \frac{C}{4}g_\omega^2\omega^2\right)\right\}, \\
G(\rho,\omega,\sigma) &= \frac{\rho^2}{(\hbar c)^3}\left\{\frac{1}{2}m_\rho^2 + g_\rho^2\left(g_\sigma\sigma\left[\alpha_2 + \frac{\alpha_2'}{2}g_\sigma\sigma\right] + \frac{1}{2}\alpha_3' g_\omega^2\omega^2 + \frac{1}{4}D g_\rho^2\rho^2\right)\right\}, \quad I(\delta) = \frac{\delta^2}{(\hbar c)^3}\frac{m_\delta^2}{2}. \qquad (16)
\end{aligned}$$

The kinetic contributions to the energy density are

$$\mathcal{E}_{{\rm kin},i} = \frac{1}{\pi^2}\int_0^{k_{Fi}} k^2\sqrt{(\hbar c k)^2 + M_i^{*2}}\,dk = \frac{3}{4}E_{Fi}n_i + \frac{1}{4}M_i^* n_{si}, \qquad (17)$$

with Fermi energies for nucleons $E_{Fi} = [M_i^{*2} + (\hbar c k_{Fi})^2]^{1/2}$, wave numbers $k_{Fi} = (3\pi^2 n_i)^{1/3}$, and effective masses

$$M_n^* = M - g_\sigma \sigma - g_\delta \delta, \quad M_p^* = M - g_\sigma \sigma + g_\delta \delta. \tag{18}$$

As opposed to the case with Skyrme interactions, the neutron and proton effective masses differ only when δ mesons are included. The total vector and scalar densities are defined as $n = n_p + n_n$ and $n_s = n_{sp} + n_{sn}$, where

$$n_{si} = \frac{M_i^*}{\pi^2} \int_0^{k_{Fi}} \frac{k^2 dk}{\sqrt{(\hbar c k)^2 + M_i^{*2}}} = \frac{1}{2\pi^2}\left(\frac{M_i^*}{\hbar c}\right)^3 \left[\frac{\hbar c k_{Fi} E_{Fi}}{M_i^{*2}} - \ln\left(\frac{\hbar c k_{F,i} + E_{F,i}}{M_i^*}\right)\right]. \tag{19}$$

Our notation follows that of Ref. [2] with the exception that the opposite sign is used for the ρ and δ meson fields, such that here they are both positive for neutron-rich matter.

The values for the fields are determined from energy minimization at fixed baryon densities. As discussed below in Sec. VI, in spatially varying matter the total energy density for RMF forces also receives contributions from gradient terms:

$$\mathcal{E} = \mathcal{E}_B + \frac{1}{2\hbar c}\left[\left(\frac{d\sigma}{dr}\right)^2 - \left(\frac{d\omega}{dr}\right)^2 - \left(\frac{d\rho}{dr}\right)^2 + \left(\frac{d\delta}{dr}\right)^2\right]. \tag{20}$$

The Euler-Lagrange equations expressing minimization of the total energy density [Eq. (20)] with respect to the meson fields, in spatially nonuniform semi-infinite systems where curvature corrections can be ignored, and for fixed k_{Fn} and k_{Fp}, are [9]

$$\begin{aligned}
\frac{d^2\sigma}{dr^2} &= \hbar c\left[-g_\sigma n_s + \frac{\partial V(\sigma)}{\partial \sigma} - \frac{\partial F(\omega,\sigma)}{\partial \sigma} - \frac{\partial G(\rho,\omega,\sigma)}{\partial \sigma}\right],\\
\frac{d^2\omega}{dr^2} &= \hbar c\left[-g_\omega n + \frac{\partial F(\omega,\sigma)}{\partial \omega} + \frac{\partial G(\rho,\omega,\sigma)}{\partial \omega}\right],\\
\frac{d^2\rho}{dr^2} &= \hbar c\left[-\frac{g_\rho}{2}(n_n - n_p) + \frac{\partial G(\rho,\omega,\sigma)}{\partial \rho}\right],\\
\frac{d^2\delta}{dr^2} &= \hbar c\left[-g_\delta(n_{sn} - n_{sp}) + \frac{\partial I(\delta)}{\partial \delta}\right].
\end{aligned} \tag{21}$$

We used the facts that

$$(\partial \mathcal{E}_{\mathrm{kin},i}/\partial M_i^*)_{k_{Fi}} = n_{si}, \quad (\partial \mathcal{E}_{\mathrm{kin},i}/\partial \sigma)_{k_{Fi},\delta} = -g_\sigma n_{si}, \quad (\partial \mathcal{E}_{\mathrm{kin},i}/\partial \delta)_{k_{Fi},\sigma} = -\tau_i g_\delta n_{si}, \tag{22}$$

where $\tau_i = \pm 1$ for neutrons and protons, respectively. We can write Eq. (21) as a vector equation:

$$\frac{d^2\mathbf{X}}{dr^2} = \hbar c(\mathbf{W} - \mathbf{H}), \quad \mathbf{X} = \begin{pmatrix}\sigma\\ \omega\\ \rho\\ \delta\end{pmatrix}, \quad \mathbf{H} = \frac{\partial(F + G - V - I)}{\partial \mathbf{X}}, \quad \mathbf{W} = \begin{pmatrix} -g_\sigma n_s\\ g_\omega n\\ \frac{g_\rho}{2}(1-2x)n\\ -g_\delta(n_{sn} - n_{sp})\end{pmatrix}, \tag{23}$$

where the proton fraction is defined as $x = n_p/n$.

2. Uniform nuclear matter

In uniform matter, the gradients are zero, and the meson fields can be solved implicitly in terms of the densities:

$$\begin{aligned}
g_\sigma n_s &= \frac{\sigma}{(\hbar c)^3}\left[m_\sigma^2 + \sigma(A + B\sigma) - g_\omega^2 g_\sigma \omega^2(\alpha_1 + \alpha_1' g_\sigma \sigma) - g_\rho^2 g_\sigma \rho^2(\alpha_2 + \alpha_2' g_\sigma \sigma)\right],\\
g_\omega n &= \frac{\omega}{(\hbar c)^3}\left[m_\omega^2 + g_\omega^2\left(g_\sigma \sigma\left[\alpha_1 + \frac{\alpha_1'}{2} g_\sigma \sigma\right] + C g_\omega^2 \omega^2 + g_\rho^2 \rho^2 \alpha_3'\right)\right],\\
\frac{g_\rho}{2}(n_n - n_p) &= \frac{\rho}{(\hbar c)^3}\left[m_\rho^2 + g_\rho^2\left(g_\sigma \sigma\left[\alpha_2 + \frac{\alpha_2'}{2} g_\sigma \sigma\right] + \frac{\alpha_3'}{2} g_\omega^2 \omega^2 + D g_\rho^2 \rho^2\right)\right],\\
g_\delta(n_{s,n} - n_{s,p}) &= \frac{\delta}{(\hbar c)^3} m_\delta^2.
\end{aligned} \tag{24}$$

The energy density of bulk uniform matter can then be expressed as

$$\mathcal{E}_B = \sum_{i=n,p} \mathcal{E}_{\mathrm{kin},i} + V - F - G + I + g_\omega \omega n + \frac{g_\rho}{2}\rho(n_n - n_p). \tag{25}$$

We note the fact that, operating on Eq. (20),

$$\frac{d\mathcal{E}_B}{dn} \equiv \mathcal{E}_B' = \left(\frac{\partial \mathcal{E}_B}{\partial n}\right)_{\sigma,\omega,\rho,\delta} + \left(\frac{\partial \mathcal{E}_B}{\partial \sigma}\right)_{n,\omega,\rho,\delta}\left(\frac{\partial \sigma}{\partial n}\right)_{\omega,\rho,\delta} + \left(\frac{\partial \mathcal{E}_B}{\partial \omega}\right)_{n,\sigma,\rho,\delta}\left(\frac{\partial \omega}{\partial n}\right)_{\sigma,\rho,\delta}$$
$$+\left(\frac{\partial \mathcal{E}_B}{\partial \rho}\right)_{n,\sigma,\omega,\delta}\left(\frac{\partial \rho}{\partial n}\right)_{\sigma,\omega,\delta} + \left(\frac{\partial \mathcal{E}_B}{\partial \delta}\right)_{n,\sigma,\omega,\rho}\left(\frac{\partial \delta}{\partial n}\right)_{\sigma,\omega,\rho} = \left(\frac{\partial \mathcal{E}_B}{\partial n}\right)_{\sigma,\omega,\rho,\delta}, \tag{26}$$

where we denote total derivatives with respect to the density with primes hereafter. The final four terms vanish due to the fact that the fields are determined from the Euler-Lagrange equations expressing energy minimization. Since M^* and n_s are functions of σ and δ, they are treated as constants in determining the first derivative of $\mathcal{E}_B$ (but not for higher-order derivatives). Thus one obtains, operating on Eq. (15), and using μ_i for the nucleon chemical potentials,

$$\frac{\partial \mathcal{E}_B}{\partial n_i} = \mu_i = E_{Fi} + g_\omega \omega + \frac{g_\rho \rho}{2}\tau_i. \tag{27}$$

We then also have $\mathcal{E}_B + P_B = \sum_{i=n,p} \mu_i n_i$ and $\mathcal{E}_{\text{kin},i} + P_{\text{kin},i} = \sum_{i=n,p} E_{Fi} n_i$. The kinetic contribution to the pressure is

$$P_{\text{kin},i} = \frac{\hbar c}{3\pi^2}\int_0^{k_{Fi}} \frac{k^4 dk}{\sqrt{(\hbar c k)^2 + M_i^{*2}}} = (E_{Fi} n_i - M_i^* n_{si})/4. \tag{28}$$

The pressure and total chemical potential are

$$P_B = n^2 \frac{d(\mathcal{E}_B/n)}{dn} = \sum_{i=n,p} P_{\text{kin},i} - V + F + G - I,$$
$$\mu = \frac{d\mathcal{E}_B}{dn} = (1-x)\mu_n + x\mu_p = (1-x)E_{Fn} + xE_{Fp} + g_\omega \omega + \frac{g_\rho \rho}{2}(1-2x). \tag{29}$$

For general fixed proton fraction x, we need the solution of the simultaneous equations for σ and ω, and in the case of asymmetric matter, additionally ρ and, if $g_\delta \neq 0$, δ, i.e., Eq. (24), which we express as $\mathbf{H} = \mathbf{W}$. For nearly all the RMF forces described by Eq. (15), however, this set of equations can be dimensionally reduced by eliminating ρ and δ. First, almost all the force models have $D = 0$, for which

$$\rho = g_\rho (\hbar c)^3 n\left\{m_\rho^2 + g_\rho^2\left(\frac{\alpha_3'}{2} g_\omega^2 \omega^2 + g_\sigma \sigma\left[\alpha_2 + \frac{\alpha_2'}{2} g_\sigma \sigma\right]\right)\right\}^{-1},$$
$$\rho' = \frac{\rho}{n}\left[1 - \frac{g_\rho \rho}{(\hbar c)^3}(\alpha_3' g_\omega^2 \omega \omega' + g_\sigma \sigma'[\alpha_2 + \alpha_2' g_\sigma \sigma])\right],$$
$$\rho'' = 2\left(\frac{\rho'^2}{\rho} - \frac{\rho'}{n}\right) - \frac{g_\rho \rho^2}{n(\hbar c)^3}\left\{\alpha_3' g_\omega^2(\omega'^2 + \omega\omega'') + g_\sigma[\alpha_2 \sigma'' + \alpha_2' g_\sigma(\sigma''\sigma + \sigma'^2)]\right\},$$
$$\rho''' = 2\left(3\frac{\rho'\rho''}{\rho} - 3\frac{\rho'^3}{\rho^2} - \frac{\rho''}{n} + \frac{\rho'}{n^2} + \frac{\rho'^2}{\rho n}\right) - \frac{g_\rho \rho^2}{n(\hbar c)^3}\left\{\alpha_3' g_\omega^2(3\omega'\omega'' + \omega\omega''') + g_\sigma[\alpha_2 \sigma''' + g_\sigma \alpha_2'(3\sigma''\sigma' + \sigma'''\sigma)]\right\}. \tag{30}$$

Second, in these models with δ mesons, δ can be expressed solely in terms of the scalar densities,

$$\delta = \frac{d}{g_\delta}\sum_i \tau_i n_{si},$$
$$\delta' = \frac{d}{g_\delta}\sum_i \tau_i\left(\frac{\partial n_{si}}{\partial n} - g_\sigma \mathcal{A}_i \sigma'\right)\left(1 + d\sum_i \mathcal{A}_i\right)^{-1},$$
$$\delta'' = \frac{d}{g_\delta}\sum_i \tau_i\left(\frac{\partial^2 n_{si}}{\partial n^2} + 2M_i^{*\prime}\frac{\partial^2 n_{si}}{\partial n \partial M_i^*} + M_i^{*\prime 2}\frac{\partial n_{si}^2}{\partial M_i^{*2}} - g_\sigma \mathcal{A}_i \sigma''\right)\left(1 + d\sum_i \mathcal{A}_i\right)^{-1},$$
$$\delta''' = \frac{d}{g_\delta}\sum_i \tau_i\left(\frac{\partial^3 n_{si}}{\partial n^3} + 3\frac{\partial^3 n_{si}}{\partial n^2 \partial M_i^*}M_i^{*\prime} + 3\frac{\partial^3 n_{si}}{\partial n \partial M_i^{*2}}M_i^{*\prime 2} + \frac{\partial^3 n_{si}}{\partial M_i^{*3}}M_i^{*\prime 3} + \frac{\partial^2 n_{s,i}}{\partial n \partial M_i^*}M_i^{*\prime} + \frac{\partial^2 n_{si}}{\partial M_i^{*2}}M_i^{*\prime}M_i^{*\prime\prime} - g_\sigma \mathcal{A}_i \sigma'''\right)$$
$$\times\left(1 + d\sum_i \mathcal{A}_i\right)^{-1}, \tag{31}$$

where $d = (\hbar c)^3 g_\delta^2/m_\delta^2$.

The needed derivatives of the scalar densities are

$$\frac{\partial n_{si}}{\partial n_i} = \frac{M_i^*}{E_{F,i}}, \quad \frac{\partial n_{si}}{\partial M_i^*} = -\frac{1}{g_\sigma}\frac{\partial n_{si}}{\partial \sigma} = -\frac{\tau_i}{g_\delta}\frac{\partial n_{si}}{\partial \delta} = 3\left(\frac{n_{si}}{M_i^*} - \frac{n_i}{E_{Fi}}\right) \equiv \mathcal{A}_i, \tag{32}$$

$$\frac{\partial^2 n_{si}}{\partial n_i^2} = -\frac{M_i^*(\hbar c k_{Fi})^2}{3n_i E_{Fi}^3}, \quad \frac{\partial^2 n_{si}}{\partial n_i \partial M_i^*} = \frac{(\hbar c k_{Fi})^2}{E_{Fi}^3},$$

$$\frac{\partial^2 n_{si}}{\partial M_i^{*2}} = \frac{3}{M_i^*}\left[\frac{2n_{si}}{M_i^*} - \frac{n_i}{E_{Fi}^3}\left(3E_{Fi}^2 - M_i^{*2}\right)\right], \tag{33}$$

and

$$\frac{\partial^3 n_{si}}{\partial n_i^3} = \frac{M_i^*(\hbar c k_{Fi})^2}{9n_i^2 E_{Fi}^5}\left(4E_{Fi}^2 - 3M_i^{*2}\right), \quad \frac{\partial^3 n_{si}}{\partial n_i^2 \partial M_i^*} = \frac{(\hbar c k_{Fi})^2}{3n_i E_{Fi}^5}\left(3M_i^{*2} - E_{Fi}^2\right),$$

$$\frac{\partial^3 n_s}{\partial n_i \partial M_i^{*2}} = -\frac{3M_i^*(\hbar c k_{Fi})^2}{E_{Fi}^5}, \quad \frac{\partial^3 n_s}{\partial M_i^{*3}} = \frac{9}{M_i^{*2}}\left[\frac{2n_{si}}{3M_i^*} - \frac{n_i}{E_{Fi}}\left(1 - \frac{4M_i^{*2}}{3E_{Fi}^2} + \frac{M_i^{*4}}{E_{Fi}^4}\right)\right]. \tag{34}$$

It follows that

$$\frac{\partial n_s}{\partial n} = \sum_i x_i \frac{\partial n_{si}}{\partial n_i} = \sum_i x_i \frac{M_i^*}{E_{F,i}}, \quad \frac{\partial^2 n_s}{\partial n^2} = \sum_i x_i \frac{\partial^2 n_{si}}{\partial n_i^2}, \tag{35}$$

where $x_n = 1 - x$ and $x_p = x$. We note the derivatives of the effective masses are

$$M_i^{*\prime} = -g_\sigma \sigma' - g_\delta \tau_i \delta', \quad M_i^{*\prime\prime} = -g_\sigma \sigma'' - g_\delta \tau_i \delta'', \quad M_i^{*\prime\prime\prime} = -g_\sigma \sigma''' - g_\delta \tau_i \delta'''. \tag{36}$$

To compute the standard properties of matter at the saturation density, we are also required to determine $\mathbf{X}'$, $\mathbf{X}''$, and $\mathbf{X}'''$. The first-order field derivatives are found from $\mathbf{H}' = \mathbf{W}'$, which we write as $\mathbf{X}' = \mathbf{A}^{-1}\mathbf{B}$ where

$$\mathbf{A} = \frac{\partial(\mathbf{H} - \mathbf{W})}{\partial \mathbf{X}} = \begin{pmatrix} \frac{\partial^2(F+G-V)}{\partial\sigma^2} + g_\sigma \frac{\partial n_s}{\partial \sigma} & \frac{\partial^2 F}{\partial\sigma\partial\omega} & \frac{\partial^2 G}{\partial\sigma\partial\rho} & g_\sigma \frac{\partial n_s}{\partial\delta} \\ \frac{\partial^2 F}{\partial\sigma\partial\omega} & \frac{\partial^2(F+G)}{\partial\omega^2} & \frac{\partial^2 G}{\partial\omega\partial\rho} & 0 \\ \frac{\partial^2 G}{\partial\sigma\partial\rho} & \frac{\partial^2 G}{\partial\omega\partial\rho} & \frac{\partial^2 G}{\partial\rho^2} & 0 \\ g_\delta \sum_i \frac{\partial n_{si}}{\partial\sigma}\tau_i & 0 & 0 & -\frac{\partial^2 I}{\partial\delta^2} + g_\delta \sum_i \frac{\partial n_{si}}{\partial\delta}\tau_i \end{pmatrix},$$

$$\mathbf{B} = \frac{\partial \mathbf{W}}{\partial n} = \begin{pmatrix} -g_\sigma \frac{\partial n_s}{\partial n} \\ g_\omega \\ g_\rho \frac{1-2x}{2} \\ -g_\delta \sum_i \frac{\partial n_{si}}{\partial n}\tau_i \end{pmatrix}. \tag{37}$$

The second-order field derivatives then follow from $\mathbf{H}'' = \mathbf{W}''$, or

$$\mathbf{X}'' = \mathbf{A}^{-1}(\mathbf{B}' - \mathbf{A}'\mathbf{X}') \equiv \mathbf{A}^{-1}\mathbf{C}, \tag{38}$$

where the vector $\mathbf{C}$ has components

$$C_i = \frac{\partial B_i}{\partial n} + 2\frac{\partial B_i}{\partial X_j}X_j' - \frac{\partial A_{ij}}{\partial X_k}X_k'X_j', \tag{39}$$

and summation over repeated indices is assumed. The fact that $\partial A_{ij}/\partial n = -\partial B_i/\partial X_j$ was used; note that only its [1,1] component, $-g_\sigma^2 \sum_i \partial^2 n_{si}/(\partial n \partial M_i^*)$, and when g_δ is nonzero, its [1,4] and [4,1] components, both $-g_\sigma g_\delta \sum_i \tau_i \partial n_{si}^2/(\partial n \partial M_i^*)$, and its [4,4] component, $-g_\delta^2 \sum_i \partial^2 n_{si}/(\partial n \partial M_i^*)$, are nonzero.

The third-order derivatives, similarly, follow from $\mathbf{H}''' = \mathbf{W}'''$, or

$$\mathbf{X}''' = \mathbf{A}^{-1}(\mathbf{B}'' - \mathbf{A}''\mathbf{X}' - 2\mathbf{A}'\mathbf{X}'') \equiv \mathbf{A}^{-1}\mathbf{D}, \tag{40}$$

where the vector $\mathbf{D}$ has components

$$D_i = \frac{\partial^2 B_i}{\partial n^2} + 3\left(\frac{\partial^2 B_i}{\partial n \partial X_j}X_j' + \frac{\partial^2 B_i}{\partial X_k \partial X_j}X_k'X_j' + \frac{\partial B_i}{\partial X_j}X_j'' - \frac{\partial A_{ij}}{\partial X_k}X_k'X_j''\right) - \frac{\partial^2 A_{ij}}{\partial X_\ell \partial X_k}X_\ell'X_k'X_j'. \tag{41}$$

The general expressions for the incompressibility and skewness of uniform matter are given by

$$K = 9n^2\frac{d^2(\mathcal{E}_B/n)}{dn^2} = 9\left(n\mathcal{E}_B'' - 2\mathcal{E}_B' + \frac{2\mathcal{E}_B}{n}\right) = 9n\mathcal{E}_B'' - 18\frac{P_B}{n},$$
$$Q = 27n^3\frac{d^3(\mathcal{E}_B/n)}{dn^3} = 27\left(n^2\mathcal{E}_B''' - 3n\mathcal{E}_B'' + 6\mathcal{E}_B' - \frac{6\mathcal{E}_B}{n}\right) = 27n^2\mathcal{E}_B''' - 9K, \tag{42}$$

where the second and third derivatives of energy density are

$$\mathcal{E}_B'' = xE_{Fp}' + (1-x)E_{Fn}' + g_\omega\omega' + \frac{g_\rho}{2}(1-2x)\rho',$$
$$\mathcal{E}_B''' = xE_{Fp}'' + (1-x)E_{Fn}'' + g_\omega\omega'' + \frac{g_\rho}{2}(1-2x)\rho'', \tag{43}$$

with

$$E_{Fi}' = E_{Fi}^{-1}\left[\frac{(\hbar ck_{Fi})^2}{3n} + M_i^*M_i^{*\prime}\right],$$
$$E_{Fi}'' = E_{Fi}^{-1}\left[-\frac{(\hbar ck_{Fi})^2}{9n^2} - E_{Fi}'^2 + M_i^{*\prime 2} + M_i^*M_i^{*\prime\prime}\right]. \tag{44}$$

3. Uniform symmetric matter

In this case, $\rho = \delta = G = I = 0$. We define $k_F = k_{Fn} = k_{Fp} = (3\pi^2 n/2)^{1/3}$, $M^* = M_n^* = M_p^*$, and $E_F = E_{Fn} = E_{Fp} = [M^{*2} + (\hbar ck_F)^2]^{1/2}$, and therefore find

$$n_s = \frac{1}{\pi^2}\left(\frac{M^*}{\hbar c}\right)^3\left[\frac{\hbar ck_F E_F}{M^{*2}} - \ln\left(\frac{\hbar ck_F + E_F}{M^*}\right)\right]. \tag{45}$$

Note that

$$\frac{\partial n_s}{\partial n} = \frac{M^*}{E_F}, \quad \frac{\partial n_s}{\partial M^*} = 3\left(\frac{n_s}{M^*} - \frac{n}{E_F}\right) \equiv \mathcal{A}, \tag{46}$$

which defines $\mathcal{A}$.

The internal energy per particle and the pressure are

$$E_{1/2} = \frac{3E_F + M^*n_s/n}{4} + g_\omega\omega + \frac{V-F}{n} - M, \quad P_{1/2} = \frac{E_F n - M^*n_s}{4} - V + F. \tag{47}$$

The needed derivatives of the energy density of symmetric matter are

$$\mathcal{E}_{B,1/2}' = E_F + g_\omega\omega, \quad \mathcal{E}_{B,1/2}'' = E_F' + g_\omega\omega', \quad \mathcal{E}_{B,1/2}''' = E_F'' + g_\omega\omega''. \tag{48}$$

Derivatives of E_F and M^* are given by the same expressions as in Eqs. (44) and (36), respectively, but ignoring the subscript i. The σ and ω fields and derivatives are determined by the two-dimensional vector $\mathbf{H} = \mathbf{W}$ and the 2×2 matrix $\mathbf{AX}' = \mathbf{B}$ equations. The incompressibility and skewness are found from Eq. (42).

4. Uniform neutron matter

Now $k_{Fn} = (3\pi^2 n)^{1/3}$ and $E_{Fn} = [M_n^{*2} + (\hbar ck_{Fn})^2]^{1/2}$. The internal energy per particle and pressure of neutron matter are

$$E_N = \frac{3E_{Fn} + M^*n_{sn}/n}{4} + g_\omega\omega + \frac{g_\rho}{2}\rho + \frac{V-F-G+I}{n} - M,$$
$$P_N = \frac{E_{Fn}n - M_n^*n_{sn}}{4} - V + F + G - I. \tag{49}$$

where

$$n_{sn} = \frac{1}{2\pi^2}\left(\frac{M_n^*}{\hbar c}\right)^3\left[\frac{\hbar ck_{Fn}E_{Fn}}{M_n^{*2}} - \ln\left(\frac{\hbar ck_{Fn} + E_{Fn}}{M_n^*}\right)\right]. \tag{50}$$

The values of the fields can be determined using three (or four, in the case $g_\delta \neq 0$) simultaneous equations $\mathbf{H} = \mathbf{W}$, although these can be reduced for the forces considered here as noted in Eqs. (30) and (31). Their nth derivatives are obtained from

$\mathbf{H}^{n'} = \mathbf{W}^{n'}$. The components of the matrices **A** and **B** are given by Eq. (37), noting that

$$\frac{\partial n_{sn}}{\partial n} = \frac{M_n^*}{E_{Fn}}, \quad \frac{\partial n_{sn}}{\partial M_n^*} = 3\left(\frac{n_{sn}}{M_n^*} - \frac{n}{E_{Fn}}\right) = \mathcal{A}_n. \tag{51}$$

The derivatives of the uniform neutron matter energy density become

$$\mathcal{E}_N' = E_{Fn} + g_\omega \omega + \frac{g_\rho \rho}{2}, \quad \mathcal{E}_N'' = E_{Fn}' + g_\omega \omega' + \frac{g_\rho \rho'}{2}, \quad \mathcal{E}_N''' = E_{Fn}'' + g_\omega \omega'' + \frac{g_\rho \rho''}{2}. \tag{52}$$

The derivatives of E_{Fn} and M_n^* are given in Eqs. (44) and (36), respectively. The incompressibility and skewness are given by Eq. (42).

5. Symmetry energy

Two approaches for the calculation of symmetry energy have been shown in Eqs. (9) and (10). For the constant coupling models, the second approach gives the formula for symmetry energy as

$$\begin{aligned}\mathcal{S}_2 = \frac{1}{8}\frac{d^2(\mathcal{E}/n)}{dx^2}\bigg|_{x=1/2} &= \frac{(\hbar c k_F)^2}{6E_F} + \frac{g_\rho^2}{8}\left(\frac{\partial^2 G}{\partial \rho^2}\right)^{-1} n + \frac{g_\delta}{8}\left(4\frac{\partial n_s}{\partial n} + \frac{g_\delta}{n}\frac{\partial n_s}{\partial M^*}\frac{\partial \delta}{\partial x}\right)\frac{\partial \delta}{\partial x} + \frac{1}{8n}\frac{\partial^2 I}{\partial \delta^2}\left(\frac{\partial \delta}{\partial x}\right)^2 \\ &= \mathcal{S}_{\text{kin},0} + \frac{g_\rho^2}{8m_\rho^*}(\hbar c)^3 n + \mathcal{S}_\delta, \end{aligned} \tag{53}$$

with

$$\mathcal{S}_{\text{kin},0} = \frac{(\hbar c k_F)^2}{6E_F} \tag{54}$$

being the kinetic contribution in the absence of δ mesons,

$$m_\rho^* = (\hbar c)^3 \frac{\partial^2 G}{\partial \rho^2} = m_\rho^2 + g_\sigma g_\rho^2 \sigma (2\alpha_2 + \alpha_2' g_\sigma \sigma) + \alpha_3' g_\omega^2 g_\rho^2 \omega^2, \tag{55}$$

and

$$\frac{\partial \delta}{\partial x} = -4 g_\delta \frac{\partial n_s}{\partial n}\left(\frac{\partial^2 I}{\partial \delta^2} + 2g_\delta^2 \frac{\partial n_s}{\partial M^*}\right)^{-1}. \tag{56}$$

$\mathcal{S}_\delta$ is the contribution of δ mesons to both the kinetic and potential symmetry energies,

$$\mathcal{S}_\delta = -\frac{dM^{*2} n}{2E_F^2(1 + d\mathcal{A})} \equiv \frac{d\mathcal{B}}{1 + d\mathcal{A}}, \tag{57}$$

which defines $\mathcal{B}$. Note that the quantity $d = (\hbar c)^3 g_\delta^2 / m_\delta^2$ has been defined immediately following Eq. (31). The slope, curvature and skewness of the symmetry energy are, respectively,

$$\begin{aligned} \mathcal{L}_2 &= 3n\mathcal{S}_2' = \mathcal{L}_{\text{kin},0} - \frac{3g_\rho^2(\hbar c)^3}{8m_\rho^*}\left(\frac{n}{m_\rho^*}m_\rho^{*\prime} - 1\right)n + \mathcal{L}_\delta, \\ \mathcal{K}_{\text{sym},2} &= 9n^2\mathcal{S}_2'' = \mathcal{K}_{\text{kin},0} - \frac{9g_\rho^2(\hbar c)^3}{4m_\rho^{*2}}\left(m_\rho^{*\prime} - \frac{n}{m_\rho^*}m_\rho^{*\prime 2} + \frac{n}{2}m_\rho^{*\prime\prime}\right)n^2 + \mathcal{K}_\delta, \\ \mathcal{Q}_{\text{sym},2} &= 27n^3\mathcal{S}_2''' = \mathcal{Q}_{\text{kin},0} - \frac{27g_\rho^2(\hbar c)^3}{4m_\rho^{*3}}\left(\frac{3n}{m_\rho^*}m_\rho^{*\prime 3} - 3m_\rho^{*\prime 2} + \frac{3}{2}m_\rho^* m_\rho^{*\prime\prime} - 3nm_\rho^{*\prime}m_\rho^{*\prime\prime} + \frac{1}{2}nm_\rho^* m_\rho^{*\prime\prime\prime}\right)n^3 + \mathcal{Q}_\delta, \end{aligned} \tag{58}$$

where the kinetic-energy contributions in the absence of δ mesons are

$$\begin{aligned} \mathcal{L}_{\text{kin},0} &= 3n\mathcal{S}_{\text{kin},0}' = \mathcal{S}_{\text{kin},0}\left(2 - 3n\frac{E_F'}{E_F}\right), \\ \mathcal{K}_{\text{kin},0} &= 9n^2\mathcal{S}_{\text{kin},0}'' = -2\mathcal{S}_{\text{kin},0} - \frac{3}{E_F}(3n^2\mathcal{S}_{\text{kin},0}E_F'' + 2n\mathcal{L}_{\text{kin},0}E_F'), \\ \mathcal{Q}_{\text{kin},0} &= 27n^3\mathcal{S}_{\text{kin},0}''' = 8\mathcal{S}_{\text{kin}}, 0 - \frac{9}{E_F}(3n^3 S_{\text{kin},0}E_F''' + 3n^2\mathcal{L}_{\text{kin},0}E_F'' + n\mathcal{K}_{\text{kin},0}E_F'), \end{aligned} \tag{59}$$

with

$$E_F''' = E_F^{-1}\left(-3E_F''E_F' + \frac{4(\hbar c k_F)^2}{27n^3} + 3M^{*\prime}M^{*\prime\prime} + M^*M^{*\prime\prime\prime}\right), \tag{60}$$

and

$$\begin{aligned}
m_\rho^{*\prime} &= 2g_\rho^2\big[g_\sigma\sigma'(\alpha_2 + \alpha_2' g_\sigma\sigma) + \alpha_3' g_\omega^2\omega'\omega + 3Dg_\rho^2\rho\rho'\big],\\
m_\rho^{*\prime\prime} &= 2g_\rho^2\big[g_\sigma\alpha_2\sigma'' + \alpha_2' g_\sigma^2(\sigma\sigma'' + \sigma'^2) + \alpha_3' g_\omega^2(\omega'^2 + \omega\omega'') + 3Dg_\rho^2(\rho'^2 + \rho\rho'')\big],\\
m_\rho^{*\prime\prime\prime} &= 2g_\rho^2\big[g_\sigma\alpha_2\sigma''' + \alpha_2' g_\sigma^2(3\sigma'\sigma'' + \sigma\sigma''') + \alpha_3' g_\omega^2(3\omega'\omega'' + \omega\omega''') + 3Dg_\rho^2(3\rho'\rho'' + \rho\rho''')\big].
\end{aligned} \tag{61}$$

The contributions from the δ mesons are

$$\begin{aligned}
\mathcal{L}_\delta &= 3n\mathcal{S}_\delta' = 3dn(\mathcal{B}' - \mathcal{S}_\delta\mathcal{A}')(1 + d\mathcal{A})^{-1},\\
\mathcal{K}_\delta &= 9n^2\mathcal{S}_\delta'' = 9dn^2(\mathcal{B}'' - 2\mathcal{S}_\delta'\mathcal{A}' - \mathcal{S}_\delta\mathcal{A}'')(1 + d\mathcal{A})^{-1},\\
\mathcal{Q}_\delta &= 27n^3\mathcal{S}_\delta''' = 27dn^3(\mathcal{B}''' - 3[\mathcal{S}_\delta''\mathcal{A}' + \mathcal{S}_\delta'\mathcal{A}''] - \mathcal{S}_\delta\mathcal{A}''')(1 + d\mathcal{A})^{-1},
\end{aligned} \tag{62}$$

where, for example,

$$\mathcal{A}' = \frac{3M^{*\prime}}{M^*}\left(\mathcal{A} + \frac{nM^{*2}}{E_F^3}\right) + \frac{(\hbar c k_F)^2}{E_F^3}, \quad \mathcal{B}' = \mathcal{B}\left(\frac{1}{n} + \frac{2M^{*\prime}}{M^*} - \frac{2E_F'}{E_F}\right). \tag{63}$$

The higher-order derivatives of $\mathcal{A}$ and $\mathcal{B}$ are more complicated and are not explicitly indicated.

To calculate $\mathcal{Q}_{\rm sym,2}$, the following derivatives are also needed

$$\begin{aligned}
&\frac{\partial^4 n_s}{\partial n\partial M^{*3}} = -\frac{3(\hbar c k_F)^2}{E_F^7}\big(E_F^2 - 5M^{*2}\big), \quad \frac{\partial^4 n_s}{\partial n^2\partial M^{*2}} = -\frac{M^*}{3n}\frac{(\hbar c k_F)^2}{E_F^7}\big(E_F^2 + 5M^{*2}\big),\\
&\frac{\partial^4 n_s}{\partial n^3\partial M^*} = \frac{1}{9n^2}\frac{(\hbar c k_F)^2}{E_F^5}\left(4E_F^2 + \frac{15M^{*4}}{E_F^2} - 21M^{*2}\right),
\end{aligned} \tag{64}$$

where all the symbols are for symmetric nuclear matter.

At the saturation density n_0, we have

$$\begin{aligned}
&J_1 = E_N(n_0) - E_0, \quad L_1 = \frac{3P_N(n_0)}{n_0},\\
&K_{\rm sym,1} = \mathcal{K}_N(n_0) - \mathcal{K}_{1/2}(n_0) \equiv K_N - K_{1/2}, \quad Q_{\rm sym,1} = \mathcal{Q}_N(n_0) - \mathcal{Q}_{1/2}(n_0) \equiv Q_N - Q_{1/2},\\
&J_2 = \mathcal{S}_2(n_0), \quad L_2 = \mathcal{L}_2(n_0), \quad K_{\rm sym,2} = \mathcal{K}_{\rm sym,2}(n_0), \quad Q_{\rm sym,2} = \mathcal{Q}_{\rm sym,2}(n_0).
\end{aligned} \tag{65}$$

These meson-exchange models with constant couplings can be divided into five types following the classification of Dutra *et al.* [2]:

Type 1 (linear finite-range models) models in which $g_\delta = A = B = C = D = \alpha_1 = \alpha_2 = \alpha_1' = \alpha_2' = \alpha_3' = 0$. This is the case of the linear Walecka model, and there are up to three effective parameters, including g_σ/m_σ, g_ω/m_ω, and g_ρ/m_ρ, which could correspond to unique values of n_0, E_0 and, in the case that $g_\rho \neq 0$, J_1 (or J_2).

Type 2 ($\sigma^3 + \sigma^4$ models) models in which $g_\delta = C = D = \alpha_1 = \alpha_2 = \alpha_1' = \alpha_2' = \alpha_3' = 0$. This type corresponds to parametrizations related to the Boguta-Bodmer model, and has up to five effective parameters, including g_σ/m_σ, g_ω/m_ω, g_ρ/m_ρ, A/m_σ^3, and B/m_σ^4, which could correspond to unique values of n_0, E_0, J_1, $K_{1/2}$, and L_1.

Type 3 ($\sigma^3 + \sigma^4 + \omega^4$ models) models in which $g_\delta = D = \alpha_1 = \alpha_2 = \alpha_1' = \alpha_2' = \alpha_3' = 0$. These parametrizations include a quartic self-interaction in the ω field, and have up to six effective parameters, including g_σ/m_σ, g_ω/m_ω, g_ρ/m_ρ, A/m_σ^3, B/m_σ^4, and C, which could correspond to unique values of n_0, E_0, J_1, $K_{1/2}$, L_1, and K_N.

Type 4 ($\sigma^3 + \sigma^4 + \omega^4 +$ cross terms models) models in which $g_\delta = D = 0$ and at least one of the coupling constants α_1, α_2, α_1', α_2', or α_3' is different from zero. These models could have up to 11 effective parameters.

Type 7 models which have δ mesons. Since the models included here all have $D = \alpha_1 = \alpha_2 = \alpha_1' = \alpha_2' = 0$, there are up to seven effective parameters, including g_σ/m_σ, g_ω/m_ω, g_ρ/m_ρ, g_δ/m_δ, A/m_σ^3, B/m_σ^4, C, and α_3', which could correspond to unique values of n_0, E_0, J_1, $K_{1/2}$, L_1, K_N, and $Q_{1/2}$.

B. Relativistic models with density-dependent couplings

In the density-dependent (DD) coupling model, denoted type 5 by Ref. [2], the nucleon-meson couplings between nucleons and mesons are taken to be functions of baryon density, and the parameters of the models we consider have $g_\delta = A = B = C = D = \alpha_1 = \alpha_2 = \alpha_1' = \alpha_2' = \alpha_3' = 0$. These models represent extensions of type 1 models with the substitutions

$$g_\sigma \rightarrow \Gamma_\sigma(n), \quad g_\omega \rightarrow \Gamma_\omega(n), \quad g_\rho \rightarrow \Gamma_\rho(n), \tag{66}$$

where the density dependencies are parametrized with

$$\Gamma_\alpha(u) = \Gamma_\alpha(n_0) f_\alpha(u) = a_\alpha \frac{1 + b_\alpha(u + d_\alpha)^2}{1 + c_\alpha(u + d_\alpha)^2}, \quad \alpha \in [\sigma, \omega],$$
$$\Gamma_\alpha(u) = \Gamma_\alpha(n_0) e^{-a_\alpha(u-1)}, \quad \alpha \in [\rho], \tag{67}$$

with $u = n/n_0$. The magnitudes of the meson fields follow from minimization of the energy density with respect to the meson fields, giving the equivalent of Eq. (24):

$$\sigma = (\hbar c)^3 \frac{\Gamma_\sigma}{m_\sigma^2} n_s, \quad \omega = (\hbar c)^3 \frac{\Gamma_\omega}{m_\omega^2} n, \quad \rho = (\hbar c)^3 \frac{\Gamma_\rho}{2m_\rho^2}(1 - 2x)n. \tag{68}$$

The definition for scalar and vector densities, proton and neutron effective masses and Fermi energies are also the same as previously with the substitution Eq. (66). The energy density and pressure, respectively, are therefore

$$\mathcal{E}_{\rm DD} = \sum_{i=n,p} \mathcal{E}_{{\rm kin},i} + \frac{1}{2(\hbar c)^3}\left[m_\sigma^2\sigma^2 - m_\omega^2\omega^2 - m_\rho^2\rho^2\right] + \Gamma_\omega \omega n + \frac{1-2x}{2}\Gamma_\rho \rho n, \tag{69}$$

and

$$P_{\rm DD} = \sum_{i=n,p} P_{{\rm kin},i} - \frac{1}{2(\hbar c)^3}\left[m_\sigma^2\sigma^2 - m_\omega^2\omega^2 - m_\rho^2\rho^2\right] + n\Sigma_R(n), \tag{70}$$

where $\Sigma_R(n)$ is an additional term involving the density derivatives of the density-dependent couplings

$$\Sigma_R(n) = -\Gamma_\sigma'\sigma n_s + \Gamma_\omega'\omega n + \frac{1-2x}{2}\Gamma_\rho'\rho n = -(\hbar c)^3 \frac{\Gamma_\sigma \Gamma_\sigma'}{m_\sigma^2} n_s^2 + \sum_{\alpha=\omega,\rho} C_\alpha \Gamma_\alpha \Gamma_\alpha' n^2, \tag{71}$$

where $C_\omega = (\hbar c)^3/m_\omega^2$ and $C_\rho = (1-2x)^2(\hbar c)^3/(4m_\rho^2)$, for the models considered here. The chemical potentials are then analogs of Eq. (27), and the expressions for vectors **X**, **W**, and **H** are the same as previously, with the substitution of Eq. (66). For uniform matter, **H** = **W** is given by Eq. (68).

From Eq. (68), the matrix **A** becomes diagonal and the vector **B** now has additional terms containing vector field coupling derivatives,

$$\mathbf{A} = \mathrm{diag}\left(-\frac{m_\sigma}{(\hbar c)^3} + \Gamma_\sigma \frac{\partial n_s}{\partial \sigma}, \quad \frac{m_\omega^2}{(\hbar c)^3}, \quad \frac{m_\rho^2}{(\hbar c)^3}\right), \tag{72}$$

$$\mathbf{B} = \begin{pmatrix} -\Gamma_\sigma \frac{\partial n_s}{\partial n} - n_s\Gamma_\sigma', \\ \Gamma_\omega + n\Gamma_\omega' \\ (\Gamma_\rho + n\Gamma_\rho')\frac{1-2x}{2} \end{pmatrix}. \tag{73}$$

The required derivatives of **X** and n_s are identical to Eqs. (32)–(34), and the computation of **B** and the derivatives of **A** and **B** now require the coupling derivatives

$$\Gamma_\alpha' = \frac{2a_\alpha \Gamma_\alpha(n_0)}{n_0}\frac{(b_\alpha - c_\alpha)(x + d_\alpha)}{[1 + c_\alpha(x + d_\alpha)^2]^2}, \quad \Gamma_\alpha'' = \frac{2a_\alpha \Gamma_\alpha(n_0)}{n_0^2}\frac{(b_\alpha - c_\alpha)[1 - 3c_\alpha(x + d_\alpha)^2]}{[1 + c_\alpha(x + d_\alpha)^2]^3},$$
$$\Gamma_\alpha''' = \frac{-24a_\alpha \Gamma_\alpha(n_0)}{n_0^3}\frac{(b_\alpha - c_\alpha)c_\alpha(x + d_\alpha)[1 - c_\alpha(x + d_\alpha)^2]}{[1 + c_\alpha(x + d_\alpha)^2]^4}, \tag{74}$$

for $\alpha = \sigma, \omega$, and

$$\Gamma_\rho' = -a_\rho\Gamma_\rho/n_0, \quad \Gamma_\rho'' = a_\rho^2\Gamma_\rho/n_0^2, \quad \Gamma_\rho''' = -a_\rho^3\Gamma_\rho/n_0^3. \tag{75}$$

The effective masses for neutrons and protons are equal and their derivatives become

$$M^{*\prime} = -(\Gamma_\sigma \sigma' + \sigma \Gamma'_\sigma), \quad M^{*\prime\prime} = -(\Gamma_\sigma \sigma'' + 2\sigma' \Gamma'_\sigma + \sigma \Gamma''_\sigma), \quad M^{*\prime\prime\prime} = -(\Gamma_\sigma \sigma''' + 3\sigma'' \Gamma'_\sigma + 3\sigma' \Gamma''_\sigma + \sigma \Gamma'''_\sigma). \tag{76}$$

The general formulas for the incompressibility and skewness of uniform ANM, Eq. (42), require different expressions for the derivatives of $\mathcal{E}_{\rm DD}$,

$$\mathcal{E}''_{\rm DD} = x E'_{Fp} + (1-x) E'_{Fn} + \sum_{\alpha=\omega,\rho} C_\alpha \left(\Gamma_\alpha^2 + 2\Gamma_\alpha \Gamma'_\alpha n\right) + \Sigma'_R, \tag{77}$$

$$\mathcal{E}'''_{\rm DD} = x E''_{Fp} + (1-x) E''_{Fn} + \sum_{\alpha=\omega,\rho} C_\alpha \left[2n\left(\Gamma_\alpha \Gamma''_\alpha + \Gamma'^2_\alpha\right) + 4\Gamma_\alpha \Gamma'_\alpha\right] + \Sigma''_R, \tag{78}$$

with

$$\Sigma'_R = -\frac{(\hbar c)^3}{m_\sigma^2}\left[\left(\Gamma'^2_\sigma + \Gamma_\sigma \Gamma''_\sigma\right) n_s^2 + 2\Gamma_\sigma \Gamma'_\sigma n_s n'_s\right] + \sum_{\alpha=\omega,\rho} C_\alpha \left[\left(\Gamma'^2_\alpha + \Gamma_\alpha \Gamma''_\alpha\right) n^2 + 2n \Gamma_\alpha \Gamma'_\alpha\right], \tag{79}$$

$$\Sigma''_R = -\frac{(\hbar c)^3}{m_\sigma^2}\left[(\Gamma_\sigma \Gamma'''_\sigma + 3\Gamma'_\sigma \Gamma''_\sigma) n_s^2 + 2\Gamma_\sigma \Gamma'_\sigma n_s n''_s + 2\Gamma_\sigma \Gamma'_\sigma n'^2_s + 4\left(\Gamma'^2_\sigma + \Gamma_\sigma \Gamma''_\sigma\right) n_s n'_s\right] \\ + \sum_{\alpha=\omega,\rho} C_\alpha \left[(\Gamma_\alpha \Gamma'''_\alpha + 3\Gamma'_\alpha \Gamma''_\alpha) n^2 + 4n\left(\Gamma'^2_\alpha + \Gamma_\alpha \Gamma''_\alpha\right) + 2\Gamma_\alpha \Gamma'_\alpha)\right]. \tag{80}$$

Derivatives of the scalar density are needed, and can be found from

$$n'_{si} = \frac{\partial n_{si}}{\partial n} + \frac{\partial n_{si}}{\partial M^*} M^{*\prime}, \quad n''_{si} = \frac{\partial^2 n_{si}}{\partial n^2} + 2\frac{\partial^2 n_{si}}{\partial n \partial M^*} M^{*\prime}_i + \frac{\partial n_{si}}{\partial M^*} M^{*\prime\prime}, \tag{81}$$

where the partial derivatives are given in Eqs. (32) and (33).

Similarly, the symmetry energy functions are given as follows:

$$\begin{aligned} \mathcal{S}_2^{\rm DD} &= \mathcal{S}_{\rm kin,0} + \frac{(\hbar c)^3}{8m_\rho^2}\Gamma_\rho^2 n, \\ \mathcal{L}_2^{\rm DD} &= \mathcal{L}_{\rm kin,0} - \frac{3n(\hbar c)^3}{8m_\rho^2}\left(2\Gamma_\rho \Gamma'_\rho n + \Gamma_\rho^2\right), \\ \mathcal{K}_{\rm sym,2}^{\rm DD} &= \mathcal{K}_{\rm kin,0} - \frac{9n^2(\hbar c)^3}{4m_\rho^2}\left[\left(\Gamma_\rho \Gamma''_\rho + \Gamma'^2_\rho\right) n + 2\Gamma_\rho \Gamma'_\rho\right], \\ \mathcal{Q}_{\rm sym,2}^{\rm DD} &= \mathcal{Q}_{\rm kin,0} - \frac{27n^3(\hbar c)^3}{4m_\rho^2}\left[\left(\Gamma_\rho \Gamma'''_\rho + 3\Gamma'_\rho \Gamma''_\rho\right) n + 3\left(\Gamma_\rho \Gamma''_\rho + \Gamma'^2_\rho\right)\right], \end{aligned} \tag{82}$$

where the kinetic parts are given in Eq. (59).

C. Relativistic nonlinear point-coupling models

In the nonlinear point-coupling (PC) model [10], nucleons interact with each other only through effective point-like interactions, without exchanging mesons. Although this model is classified as a type 6 RMF model by Ref. [2], technically it is closer to a Skyrme-like model, albeit with a more complicated density dependence.

1. Energy density

The energy density and the pressure for uniform nuclear matter are

$$\mathcal{E}_{\rm PC} = \sum_{i=n,p} \mathcal{E}_{{\rm kin},i} + \frac{\alpha'_{\rm V}}{2} n^2 + \frac{\alpha'_{\rm TV}}{2}(n_n - n_p)^2 + \frac{\gamma'_{\rm V}}{4} n^4 + \frac{\gamma'_{\rm TV}}{4}(n_n - n_p)^4 - \eta'_2 n_s^2 n^2 - \frac{\alpha'_s}{2} n_s^2 - \frac{2\beta'_s}{3} n_s^3 - \frac{3\gamma'_s}{4} n_s^4 - \frac{\alpha'_{\rm TS}}{2}(n_{sn} - n_{sp})^2, \tag{83}$$

$$P_{\rm PC} = \sum_{i=n,p} P_{{\rm kin},i} + \frac{\alpha'_{\rm V}}{2} n^2 + \frac{\alpha'_{\rm TV}}{2}(n_n - n_p)^2 + \frac{3\gamma'_{\rm TV}}{4}(n_n - n_p)^4 + 2\eta'_1 n_s n^2 + 3\eta'_2 n_s^2 n^2 \\ + 2\eta'_3 n_s (n_n - n_p)^2 + \frac{\alpha'_s}{2} n_s^2 + \frac{2\beta'_s}{3} n_s^3 + \frac{3\gamma'_s}{4} n_s^4 + \frac{\alpha'_{\rm TS}}{2}(n_{sn} - n_{sp})^2, \tag{84}$$

where $\mathcal{E}_{\rm kin}$ is the RMF kinetic-energy density. We simplified the expressions by using

$$\alpha'_{s,{\rm V,TV,TS}} = (\hbar c)^3\alpha_{s,{\rm V,TV,TS}}, \quad \beta'_s = (\hbar c)^6\beta_s, \quad \gamma'_{s,{\rm V,TV}} = (\hbar c)^9\gamma_{s,{\rm V,TV}}, \quad \eta'_{1,3} = (\hbar c)^6\eta_{1,3}, \quad \eta'_2 = (\hbar c)^9\eta_2. \tag{85}$$

The effective masses for protons and neutrons are defined as

$$M_t^* = M + \alpha'_s n_s + \beta'_s n_s^2 + \gamma'_s n_s^3 + \eta'_1 n^2 + 2\eta'_2 n_s n^2 + \eta'_3(n_n - n_p)^2 - \tau_i\alpha'_{TS}(n_{sn} - n_{sp}). \tag{86}$$

Note that the α parameters are related to constant coupling RMF parameters by

$$\alpha_s = -\frac{g_\sigma^2}{m_\sigma^2}, \quad \alpha_{\rm V} = \frac{g_\omega^2}{m_\omega^2}, \quad \alpha_{\rm TV} = \frac{g_\rho^2}{m_\rho^2}, \quad \alpha_{\rm TS} = \frac{g_\delta^2}{m_\delta^2}. \tag{87}$$

The incompressibility and skewness are given by analogous expressions to Eq. (42), which require derivatives of the energy density:

$$\begin{aligned}
\mathcal{E}'_{\rm PC} &= xE_{Fp} + (1-x)E_{Fn} + n[\alpha'_{\rm V} + \alpha'_{\rm TV}(1-2x)^2] + n^3[\gamma'_{\rm V} + \gamma'_{\rm TV}(1-2x)^4] + 2nn_s[\eta'_1 + \eta'_3(1-2x)^2 + \eta'_2 n_s],\\
\mathcal{E}''_{\rm PC} &= xE'_{Fp} + (1-x)E'_{Fn} + \alpha'_{\rm V} + \alpha'_{\rm TV}(1-2x)^2 + 3n^2[\gamma'_{\rm V} + \gamma'_{\rm TV}(1-2x)^4]\\
&\quad + 2(n'_s n + n_s)[\eta'_1 + \eta'_3(1-2x)^2] + 2\eta'_2 n_s(2n'_s n + n_s),\\
\mathcal{E}'''_{\rm PC} &= xE''_{Fp} + (1-x)E''_{Fn} + 6n[\gamma'_{\rm V} + \gamma'_{\rm TV}(1-2x)^4] + 2(n''_s n + 2n'_s)[\eta'_1 + \eta'_3(1-2x)^2] + 4\eta'_2\left(n''_s n_s n + n_s'^2 n + 2n_s n'_s\right).
\end{aligned} \tag{88}$$

2. Uniform symmetric matter

In the symmetric-matter case, we can take $\alpha_{\rm TV} = \alpha_{\rm TS} = \gamma_{\rm TV} = 0$, so we have $M_n^* = M_p^* = M^*$ as well as $k_F = k_{Fn} = k_{Fp} = (3\pi^2 n/2)^{1/3}$ and $E_F = E_{Fn} = E_{Fp} = [M^{*2} + (\hbar c k_F)^2]^{1/2}$. Formulae for the relevant properties at the saturation density are easily obtained in analogy with the RMF constant coupling case. The derivative of the scalar density is

$$n'_s = \frac{\partial n_s}{\partial n} + \frac{\partial n_s}{\partial M^*}M^{*\prime} \equiv \mathcal{C} + \mathcal{A}M^{*\prime}, \tag{89}$$

and the derivatives of the effective mass are

$$\begin{aligned}
M^{*\prime} &= n'_s\left(\alpha'_s + 2\beta'_s n_s + 3\gamma'_s n_s^2 + 2\eta'_2 n^2\right) + 2n(\eta'_1 + \eta'_2 n_s) \equiv n'_s M_1 + M_2,\\
M^{*\prime\prime} &= n''_s M_1 + n'_s M'_1 + M'_2,\\
M^{*\prime\prime\prime} &= n'''_s M_1 + 2n''_s M'_1 + n'_s M''_1 + M''_2.
\end{aligned} \tag{90}$$

We therefore find

$$\begin{aligned}
n'_s &= [\mathcal{C} + \mathcal{A}M_2](1 - \mathcal{A}M_1)^{-1},\\
n''_s &= [\mathcal{C}' + \mathcal{A}'(M_2 + n'_s M_1) + \mathcal{A}(M'_2 + n'_s M'_1)](1 - \mathcal{A}M_1)^{-1},\\
n'''_s &= [\mathcal{C}'' + \mathcal{A}''(M_2 + n'_s M_1) + 2\mathcal{A}'(M'_2 + n''_s M'_1 + n'_s M'_1) + \mathcal{A}(M''_2 + 2n''_s M'_1 + n'_s M''_1)](1 - \mathcal{A}M_1)^{-1},
\end{aligned} \tag{91}$$

3. Uniform neutron matter

In the case of uniform neutron matter, the definitions for k_{Fn} and E_{Fn} are the same as previously. The derivative of the scalar density is

$$n'_{sn} = \frac{\partial n_{sn}}{\partial n} + \frac{\partial n_{sn}}{\partial M_n^*}M_n^{*\prime} \equiv \mathcal{C}_n + \mathcal{A}_n M_n^{*\prime}, \tag{92}$$

and the derivative of the effective mass is

$$M_n^{*\prime} = n'_s\left(\alpha'_s - \alpha'_{TS} + 2\beta'_s n_{sn} + 3\gamma'_s n_{sn}^2 + 2\eta'_2 n^2\right) + 2n(\eta'_1 + \eta'_3 + \eta'_2 n_{sn}) \equiv n'_{sn}M_{1n} + M_{2n}, \tag{93}$$

thus $M_{1n} = M_1 - \alpha'_{TS}$ and $M_{2n} = M_2 + 2n\eta'_3$. Higher-order derivatives of n_{sn} and M_n^* follow in analogy to the symmetric-matter case, Eqs. (90) and (91).

4. Symmetry energy

The symmetry energy functions for the second approach are

$$\begin{aligned}
\mathcal{S}_2^{\rm PC} &= \mathcal{S}_{\rm kin,0} + \frac{\alpha'_{\rm TV}}{2}n + \eta'_3 n n_s + \mathcal{S}_{\rm TS},\\
\mathcal{L}_2^{\rm PC} &= \mathcal{L}_{\rm kin,0} + \frac{3\alpha'_{\rm TV}}{2}n + 3\eta'_3 n(nn'_s + n_s) + \mathcal{L}_{\rm TS},
\end{aligned}$$

$$\mathcal{K}_{\rm sym,2}^{\rm PC} = \mathcal{K}_{\rm kin,0} + 9\eta_3' n^2(2n_s' + nn_s'') + \mathcal{K}_{\rm TS},$$
$$\mathcal{Q}_{\rm sym,2}^{\rm PC} = \mathcal{Q}_{\rm kin,0} + 27\eta_3' n^3(3n_s'' + nn_s''') + \mathcal{Q}_{\rm TS}, \tag{94}$$

where

$$\mathcal{S}_{\rm TS} = -\frac{\alpha_{\rm TS}'}{2}\frac{\mathcal{B}}{1-\alpha_{TS}'\mathcal{A}},$$
$$\mathcal{L}_{\rm TS} = 3n\mathcal{S}_{\rm TS}' = -\frac{3\alpha_{TS}'}{2}n\frac{\mathcal{B}'-2\mathcal{S}_{\rm TS}\mathcal{A}'}{1-\alpha_{TS}'\mathcal{A}},$$
$$\mathcal{K}_{\rm TS} = 9n^2\mathcal{S}_{\rm TS}'' = -\frac{9\alpha_{\rm TS}'}{2}n^2\frac{\mathcal{B}''-4\mathcal{S}_{\rm TS}'\mathcal{A}'-2\mathcal{S}_{\rm TS}\mathcal{A}''}{1-\alpha_{TS}'\mathcal{A}},$$
$$\mathcal{Q}_{\rm TS} = 27n^3\mathcal{S}_{\rm TS}''' = -\frac{27\alpha_{\rm TS}'}{2}n^3\frac{\mathcal{B}'''-6\mathcal{S}_{\rm TS}''\mathcal{A}'-6\mathcal{S}_{\rm TS}'\mathcal{A}''-2\mathcal{S}_{\rm TS}\mathcal{A}'''}{1-\alpha_{TS}'\mathcal{A}}. \tag{95}$$

All the needed quantities are given in Eqs. (32)–(34) and (64). Table VIII of Appendix B lists the saturation properties for all types of RMF forces.

IV. GOGNY INTERACTIONS

The Gogny two-body effective nuclear model is characterized by potential-energy contributions from a finite-range interaction and a spin-orbit interaction. It bears a closer resemblance to a Skyrme-like than an RMF-like model.

1. Energy density

The total energy per particle can be expressed as an explicit function of number density and proton fraction, using the notation of Ref. [11],

$$E(n,x) = \frac{3\hbar^2k_F^2}{10M}H_{5/3} + \sum_{i=1}^{2}\frac{t_{3i}}{4}n^{\alpha_i+1}\left[x_{3i}+2-\left(x_{3i}+\frac{1}{2}\right)H_2\right] + \frac{\pi^{3/2}}{2}n\sum_{i=1}^{2}\mu_i^3[\mathcal{A}_i+\mathcal{B}_i(1-2x)^2]$$
$$-\sum_{i=1}^{2}\frac{\mathcal{C}_i[\mathbf{e}(k_{Fn}\mu_i)+\mathbf{e}(k_{Fp}\mu_i)]-\mathcal{D}_i\bar{\mathbf{e}}(k_{Fn}\mu_i,k_{Fp}\mu_i)}{2(k_F\mu_i)^3}, \tag{96}$$

where the Fermi momentum of SNM is defined as $k_F = (3\pi^2 n/2)^{1/3}$ and k_{Fn} and k_{Fp} stand for the Fermi momenta of neutrons and protons, respectively. The function $H_n(x)$ is defined in Eq. (2). Note that the kinetic contribution, which is nonrelativistic, and the zero-range many-body contribution correspond to the first and third terms of the Skyrme force in Eq. (5). The parameters μ_i are interaction lengths, and the coefficients $\mathcal{A}_i$, $\mathcal{B}_i$, $\mathcal{C}_i$, and $\mathcal{D}_i$ are combinations of the spin-isospin exchange parameters B_i, $\mathbf{H}_i$, M_i, and W_i:

$$\mathcal{A}_i = \frac{1}{4}(4W_i+2B_i-2\mathbf{H}_i-M_i), \quad \mathcal{B}_i = -\frac{1}{4}(2\mathbf{H}_i+M_i),$$
$$\mathcal{C}_i = \frac{1}{\sqrt{\pi}}(W_i+2B_i-\mathbf{H}_i-2M_i), \quad \mathcal{D}_i = \frac{1}{\sqrt{\pi}}(\mathbf{H}_i+2M_i). \tag{97}$$

$\mathbf{e}(\eta)$ and $\bar{\mathbf{e}}(\eta_1,\eta_2)$ are finite-range functions defined as

$$\mathbf{e}(\eta) = \frac{\sqrt{\pi}}{2}\eta^3\mathrm{erf}(\eta) + \left(\frac{\eta^2}{2}-1\right)\exp\left(-\eta^2\right) - \frac{3\eta^2}{2}+1,$$
$$\bar{\mathbf{e}}(\eta_1,\eta_2) = \sum_{s=\pm1}s\left[\frac{\sqrt{\pi}}{2}(\eta_1^3+s\eta_2^3)\mathrm{erf}\left(\frac{\eta_1+s\eta_2}{2}\right) + \left(\eta_1^2+\eta_2^2-s\eta_1\eta_2-2\right)\exp\left(-\frac{1}{4}[\eta_1+s\eta_2]^2\right)\right], \tag{98}$$

where $\mathrm{erf}(x) = (2/\sqrt{\pi})\int_0^x \exp(-t^2)\,dt$ is the error function. Note that $\mathbf{e}(0) = \bar{\mathbf{e}}(\eta,0) = 0$ and $\bar{\mathbf{e}}(\eta,\eta) = 2\mathbf{e}(\eta)$.

The pressure in isospin asymmetric matter is

$$P(n,x) = n^2E'(n,x) = n\left[\frac{\hbar^2k_F^2}{5M}H_{5/3} + \sum_{i=1}^{2}(\alpha_i+1)\frac{t_{3i}}{4}n^{\alpha_i+1}\left[x_{3i}+2-\left(x_{3i}+\frac{1}{2}\right)H_2\right] + \frac{\pi^{3/2}}{2}n\sum_{i=1}^{2}\mu_i^3[\mathcal{A}_i+\mathcal{B}_i(1-2x)^2]\right.$$
$$\left.-\sum_{i=1}^{2}\left\{\mathcal{C}_i[(1-x)\mathbf{p}(k_{Fn}\mu_i)+x\mathbf{p}(k_{Fp}\mu_i)] - \frac{\mathcal{D}_i}{2}\bar{\mathbf{p}}(k_{Fn}\mu_i,k_{Fp}\mu_i)\right\}\right], \tag{99}$$

with

$$\mathbf{p}(\eta) = n\left[\frac{\mathbf{e}(\eta)}{\eta^3}\right]' = \frac{1}{2\eta} - \frac{1}{\eta^3} + \left(\frac{1}{\eta^3} + \frac{1}{2\eta}\right)\exp(-\eta^2),$$
$$\bar{\mathbf{p}}(\eta_1, \eta_2) = n\left[\frac{\bar{\mathbf{e}}(\eta_1, \eta_2)}{\eta_1^3 + \eta_2^3}\right]' = \frac{2}{\eta_1^3 + \eta_2^3}\sum_{s=\pm 1}(\eta_1\eta_2 + 2s)\exp\left(-\frac{1}{4}[\eta_1 + s\eta_2]^2\right), \quad (100)$$

which, like $\bar{\mathbf{e}}$, also satisfies $\bar{\mathbf{p}}(\eta, \eta) = 2\mathbf{p}(\eta)$ and $\bar{\mathbf{p}}(\eta, 0) = 0$. Note that $\eta' = \eta/(3n)$.

2. Uniform symmetric matter

For uniform symmetric matter, one finds

$$E_{1/2}(n) = \frac{3\hbar^2 k_F^2}{10M} + \frac{3}{8}\sum_{i=1}^{2} t_{3i} n^{\alpha_i + 1} + \frac{\pi^{3/2}}{2} n \sum_{i=1}^{2} \mu_i^3 \mathcal{A}_i - \sum_{i=1}^{2}\frac{\mathcal{C}_i - \mathcal{D}_i}{(k_F\mu_i)^3}\mathbf{e}(k_F\mu_i),$$
$$P_{1/2}(n) = n\left[\frac{\hbar^2 k_F^2}{5M} + \frac{3}{8}\sum_{i=1}^{2} t_{3i}(\alpha_i + 1) n^{\alpha_i + 1} + \frac{\pi^{3/2}}{2} n \sum_{i=1}^{2}\mu_i^3\mathcal{A}_i - \sum_{i=1}^{2}(\mathcal{C}_i - \mathcal{D}_i)\mathbf{p}(k_F\mu_i)\right]. \quad (101)$$

The incompressibility and skewness can be derived from the pressure

$$\mathcal{K}_{1/2}(n) = 9P'_{1/2}(n) - \frac{18P_{1/2}(n)}{n} = -\frac{3\hbar^2 k_F^2}{5M} + \frac{27}{8}\sum_{i=1}^{2}\alpha_i(\alpha_i + 1)t_{3i}n^{\alpha_i + 1} + 9\sum_{i=1}^{2}(\mathcal{C}_i - \mathcal{D}_i)[\mathbf{p}(k_F\mu_i) - n\mathbf{p}'(k_F\mu_i)],$$
$$\mathcal{Q}_{1/2}(n) = 27nP''_{1/2}(n) - \frac{54P_{1/2}(n)}{n} - 12\mathcal{K}_{1/2}(n) = \frac{12\hbar^2 k_F^2}{5M} + \frac{81}{8}\sum_{i=1}^{2}\alpha_i\left(\alpha_i^2 - 1\right)t_{3i}n^{\alpha_i + 1} - 27\sum_{i=1}^{2}(\mathcal{C}_i - \mathcal{D}_i)$$
$$\times [2\mathbf{p}(k_F\mu_i) - 2n\mathbf{p}'(k_F\mu_i) + n^2\mathbf{p}''(k_F\mu_i)], \quad (102)$$

where the logarithmic derivatives of $\mathbf{p}$ are

$$n\mathbf{p}'(\eta) = n\frac{d\mathbf{p}}{dn} = \frac{\eta}{3}\frac{d\mathbf{p}}{d\eta} = \frac{1}{\eta^3} - \frac{1}{6\eta} - \left(\frac{1}{\eta^3} + \frac{5}{6\eta} + \frac{\eta}{3}\right)\exp(-\eta^2),$$
$$n^2\mathbf{p}''(\eta) = \frac{\eta^2}{9}\frac{d^2\mathbf{p}}{d\eta^2} - \frac{2\eta}{9}\frac{d\mathbf{p}}{d\eta} = \frac{2}{9\eta} - \frac{2}{\eta^3} + \left(\frac{2}{\eta^3} + \frac{16}{9\eta} + \frac{7}{9}\eta + \frac{2}{9}\eta^3\right)\exp(-\eta^2). \quad (103)$$

3. Uniform neutron matter

In the case of uniform neutron matter, $k_{Fn} = (3\pi^2 n)^{1/3}$, and

$$E_N(n) = \frac{3\hbar^2 k_{Fn}^2}{10M} + \sum_{i=1}^{2}\frac{t_{3i}}{4}n^{\alpha_i + 1}(1 - x_{3i}) + \frac{\pi^{3/2}}{2}n\sum_{i=1}^{2}\mu_i^3(\mathcal{A}_i + \mathcal{B}_i) - \sum_{i=1}^{2}\frac{\mathcal{C}_i\mathbf{e}(k_{Fn}\mu_i)}{2(k_{Fn}\mu_i)^3},$$
$$P_N(n) = n\left[\frac{\hbar^2 k_{Fn}^2}{5M} + \sum_{i=1}^{2}\frac{t_{3i}}{4}(\alpha_i + 1)n^{\alpha_i + 1}(1 - x_{3i}) + \frac{\pi^{3/2}}{2}n\sum_{i=1}^{2}\mu_i^3(\mathcal{A}_i + \mathcal{B}_i) - \sum_{i=1}^{2}\mathcal{C}_i\mathbf{p}(k_{Fn}\mu_i)\right],$$
$$\mathcal{K}_N(n) = -\frac{3\hbar^2 k_{Fn}^2}{5M} + \frac{9}{4}\sum_{i=1}^{2}\alpha_i(\alpha_i + 1)t_{3i}n^{\alpha_i + 1}(1 - x_{3i}) + 9\sum_{i=1}^{2}\mathcal{C}_i[\mathbf{p}(k_{Fn}\mu_i) - n\mathbf{p}'(k_{Fn}\mu_i],$$
$$\mathcal{Q}_N(n) = \frac{12\hbar^2 k_{Fn}^2}{5M} + \frac{27}{4}\sum_{i=1}^{2}\alpha_i\left(\alpha_i^2 - 1\right)t_{3i}n^{\alpha_i + 1}(1 - x_{3i}) - 27\sum_{i=1}^{2}\mathcal{C}_i[2\mathbf{p}(k_{Fn}\mu_i) - 2n\mathbf{p}'(k_{Fn}\mu_i) + n^2\mathbf{p}''(k_{Fn}\mu_i)]. \quad (104)$$

4. Symmetry properties

The symmetry energy and its derivatives at saturation density can be expressed in the first approach as

$$\mathcal{S}_1 = E_N(n) - E_{1/2}(n) = \frac{3\hbar^2\left(k_{Fn}^2 - k_F^2\right)}{10M} - \sum_{i=1}^{2}\frac{t_{3i}}{8}n^{\alpha_i + 1}(1 + 2x_{3i}) + \frac{\pi^{3/2}}{2}n\sum_{i=1}^{2}\mu_i^3\mathcal{B}_i - \sum_{i=1}^{2}\frac{\mathcal{C}_i\mathbf{e}(k_{Fn}\mu_i) - 2(\mathcal{C}_i - \mathcal{D}_i)\mathbf{e}(k_F\mu_i)}{2(k_F\mu_i)^3}, \quad (105)$$

The slope of symmetric energy can be calculated from $3[P_N(n) - P_{1/2}(n)]/n$:

$$\mathcal{L}_1 = \frac{3\hbar^2(k_{Fn}^2 - k_F^2)}{5M} - \frac{3}{8}\sum_{i=1}^{2}(\alpha_i+1)t_{3i}n^{\alpha_i+1}(1+2x_{3i}) + \frac{3\pi^{3/2}}{2}n\sum_{i=1}^{2}\mu_i^3\mathcal{B}_i - 3\sum_{i=1}^{2}[\mathcal{C}_i\mathbf{p}(k_{Fn}\mu_i) - (\mathcal{C}_i - \mathcal{D}_i)\mathbf{p}(k_F\mu_i)]. \tag{106}$$

The symmetry incompressibility and skewness are further obtained as

$$\begin{aligned}\mathcal{K}_{\mathrm{sym}1} = & -\frac{3\hbar^2(k_{Fn}^2 - k_F^2)}{5M} - \frac{9}{8}\sum_{i=1}^{2}\alpha_i(\alpha_i+1)t_{3i}n^{\alpha_i+1}(1+2x_{3i}) + 9\sum_{i=1}^{2}\{\mathcal{C}_i[\mathbf{p}(k_{Fn}\mu_i) - n\mathbf{p}'(k_{Fn}\mu_i)] \\ & - (\mathcal{C}_i - \mathcal{D}_i)[\mathbf{p}(k_F\mu_i) - n\mathbf{p}'(k_F\mu_i)]\} \\ \mathcal{Q}_{\mathrm{sym}1} = & \frac{12\hbar^2(k_{Fn}^2 - k_F^2)}{5M} - \frac{27}{8}\sum_{i=1}^{2}\alpha_i(\alpha_i^2-1)t_{3i}n^{\alpha_i+1}(1+2x_{3i}) - 27\sum_{i=1}^{2}\{\mathcal{C}_i[2\mathbf{p}(k_{Fn}\mu_i) - 2n\mathbf{p}'(k_{Fn}\mu_i) + n^2\mathbf{p}''(k_{Fn}\mu_i)] \\ & - (\mathcal{C}_i - \mathcal{D}_i)[2\mathbf{p}(k_F\mu_i) - 2n\mathbf{p}'(k_F\mu_i) + n^2\mathbf{p}''(k_F\mu_i)]\}.\end{aligned} \tag{107}$$

The second approach gives the symmetry energy as

$$\mathcal{S}_2 = \frac{1}{8}\frac{\partial^2 E(n,x)}{\partial x^2}\bigg|_{x=1/2} = \frac{\hbar^2}{6M}\left(\frac{3\pi^2}{2}\right)^{2/3}n^{2/3} - \frac{1}{8}\sum_{i=1}^{2}t_{3i}n^{\alpha_i+1}(2x_{3i}+1) + \frac{\pi^{3/2}}{2}n\sum_{i=1}^{2}\mu_i^3\mathcal{B}_i - \frac{1}{6}\sum_{i=1}^{2}[\mathcal{C}_i\mathbf{s}_1(k_F\mu_i) - \mathcal{D}_i\mathbf{s}_2(k_F\mu_i)], \tag{108}$$

with

$$\mathbf{s}_1(\eta) = \frac{1}{\eta} - \left(\eta + \frac{1}{\eta}\right)\exp(-\eta^2), \quad \mathbf{s}_2(\eta) = \frac{1}{\eta} - \eta - \frac{1}{\eta}\exp(-\eta^2). \tag{109}$$

Then its derivatives can be obtained as

$$\begin{aligned}\mathcal{L}_2 &= 3nS_2' = \frac{\hbar^2}{3M}(3\pi^2n/2)^{2/3} - \frac{3}{8}\sum_{i=1}^{2}(\alpha_i+1)t_{3i}n^{\alpha_i+1}(2x_{3i}+1) + \frac{3\pi^{3/2}}{2}n\sum_{i=1}^{2}\mu_i^3\mathcal{B}_i - \frac{n}{2}\sum_{i=1}^{2}[\mathcal{C}_i\mathbf{s}_1'(k_F\mu_i) - \mathcal{D}_i\mathbf{s}_2'(k_F\mu_i)], \\ \mathcal{K}_{\mathrm{sym}2} &= 9n^2S_2'' = -\frac{\hbar^2}{3M}(3\pi^2n/2)^{2/3} - \frac{9}{8}\sum_{i=1}^{2}\alpha(\alpha_i+1)t_{3i}n^{\alpha_i+1}(2x_{3i}+1) - \frac{3n^2}{2}\sum_{i=1}^{2}[\mathcal{C}_i\mathbf{s}_1''(k_F\mu_i) - \mathcal{D}_i\mathbf{s}_2''(k_F\mu_i)], \\ \mathcal{Q}_{\mathrm{sym}2} &= 27n^3S_3''' = -\frac{4\hbar^2}{3M}(3\pi^2n/2)^{2/3} - \frac{27}{8}\sum_{i=1}^{2}\alpha(\alpha_i^2-1)t_{3i}n^{\alpha_i+1}(2x_{3i}+1) - \frac{9n^3}{2}\sum_{i=1}^{2}[\mathcal{C}_i\mathbf{s}_1'''(k_F\mu_i) - \mathcal{D}_i\mathbf{s}_2'''(k_F\mu_i)],\end{aligned} \tag{110}$$

where the logarithmic derivatives of $\mathbf{s}_{1,2}$ are

$$\begin{aligned} n\mathbf{s}_1' &= \frac{\eta}{3}\frac{d\mathbf{s}_1}{d\eta} = -\frac{1}{3\eta} + \left(\frac{1}{3\eta} + \frac{\eta}{3} + \frac{2\eta^3}{3}\right)e^{-\eta^2}, \quad n\mathbf{s}_2' = \frac{\eta}{3}\frac{d\mathbf{s}_2}{d\eta} = -\frac{1}{3\eta} - \frac{\eta}{3} + \left(\frac{1}{3\eta} + \frac{2\eta}{3}\right)e^{-\eta^2}, \\ n^2\mathbf{s}_1'' &= \frac{4}{9\eta} - \left(\frac{4}{9\eta} + \frac{4\eta}{9} + \frac{2\eta^3}{9} + \frac{4\eta^5}{9}\right)e^{-\eta^2}, \quad n^2\mathbf{s}_2'' = \frac{4}{9\eta} + \frac{2\eta}{9} - \left(\frac{4}{9\eta} + \frac{2\eta}{3} + \frac{4\eta^3}{9}\right)e^{-\eta^2}, \\ n^3\mathbf{s}_1''' &= -\frac{7}{9\eta} + \left(\frac{7}{9\eta} + \frac{7\eta}{9} + \frac{26\eta^3}{27} - \frac{26\eta^5}{27} + \frac{8\eta^7}{27}\right)e^{-\eta^2}, \quad n^3\mathbf{s}_2''' = -\frac{7}{9\eta} - \frac{5\eta}{27} + \left(\frac{7}{9\eta} + \frac{26\eta}{27} + \frac{20\eta^3}{27} + \frac{8\eta^5}{27}\right)e^{-\eta^2}.\end{aligned} \tag{111}$$

All the saturation properties of Gogny interactions are included in Table XII of Appendix C.

V. COMPARISONS OF PROPERTIES AT THE SATURATION DENSITY

Figure 1 displays the symmetric-matter densities n_0, energies $-E_0$ and incompressibilities K_0 at saturation for symmetric matter for the Skyrme, RMF and Gogny forces considered in this paper. Similarly, the left panel of Fig. 2 compares n_0, K_0 and skewnesses Q_0 at saturation. It is notable that n_0, E_0, and K_0 cluster in regions, often called the saturation window, which therefore represents predictions resulting from fitting these forces mainly to binding energies. There are distinct differences in the saturation windows for Skyrme and RMF forces; RMF forces typically suggest a smaller saturation density, for example, as well as larger mean values of $-E_0$, K_0, and Q_0. The saturation window for Skyrme forces is defined by $n_0 = 0.160 \pm 0.006\ \mathrm{fm}^{-3}$, $E_0 = -15.96 \pm 0.55$ MeV, and $K_0 = 246.4 \pm 43.0$ MeV, and

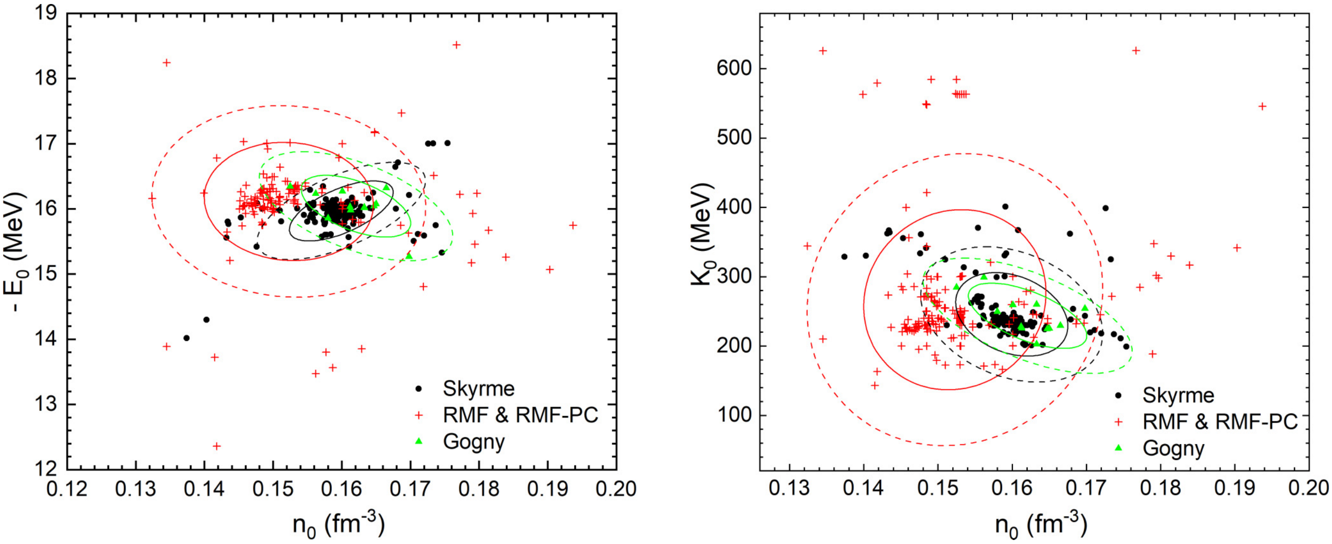

FIG. 1. The correlations between the saturation density n_0 and the bulk energy per particle E_0 (left panel) and the incompressibility K_0 (right panel) of symmetric matter at n_0 for Skyrme (black filled circles), Gogny (green triangles) and RMF (red pluses) models. Solid and dashed lines indicate 1σ and 2σ confidence ellipses for each force type.

for RMF forces $n_0 = 0.152 \pm 0.008$ fm^{-3}, $E_0 = -16.11 \pm 0.59$ MeV, and $K_0 = 266.9 \pm 485.2$ MeV. For reference, for Skyrme forces $Q_0 = -326 \pm 161$ MeV and, for RMF forces, $Q_0 = -179 \pm 678$ MeV. The parameters n_0, E_0, and K_0 are largely uncorrelated. Q_0 is not as well localized as the other parameters, but their values are highly correlated with K_0 (and with n_0 for Skyrme forces), as seen in Fig. 2.

It is also useful to compare symmetry properties at the saturation density. Figure 3 displays the saturation densities and the symmetry parameters J_2 and L_2. It is seen that RMF forces have larger average values of J_2 and L_2 than do Skyrme and Gogny forces, and correlations between n_0 and both J_2 and L_2 are very weak. On the other hand, as shown in Fig. 4, J_2 and L_2 are strongly correlated for all kinds of forces. This correlation is one of the most powerful predictions of nuclear mass-fitting, and, interestingly, has a similar slope and centroid to that determined from chiral effective field theory expansions of nuclear matter [12]. RMF forces show a smaller correlation slope than for Skyrme forces.

Figure 5 compares the incompressibilities of both symmetric and pure neutron matter with the symmetry energy slope L_2, at the saturation density. Similarly, Fig. 6 shows the skewnesses versus L_2. All types of forces show stronger correlations between K_{N0} and L_2 than between K_0 and L_2. Globally, both skewness parameters are largely uncorrelated with L_2, except that Q_{N0} for Skyrme forces does correlate with L_2. The average values of these parameters for neutron

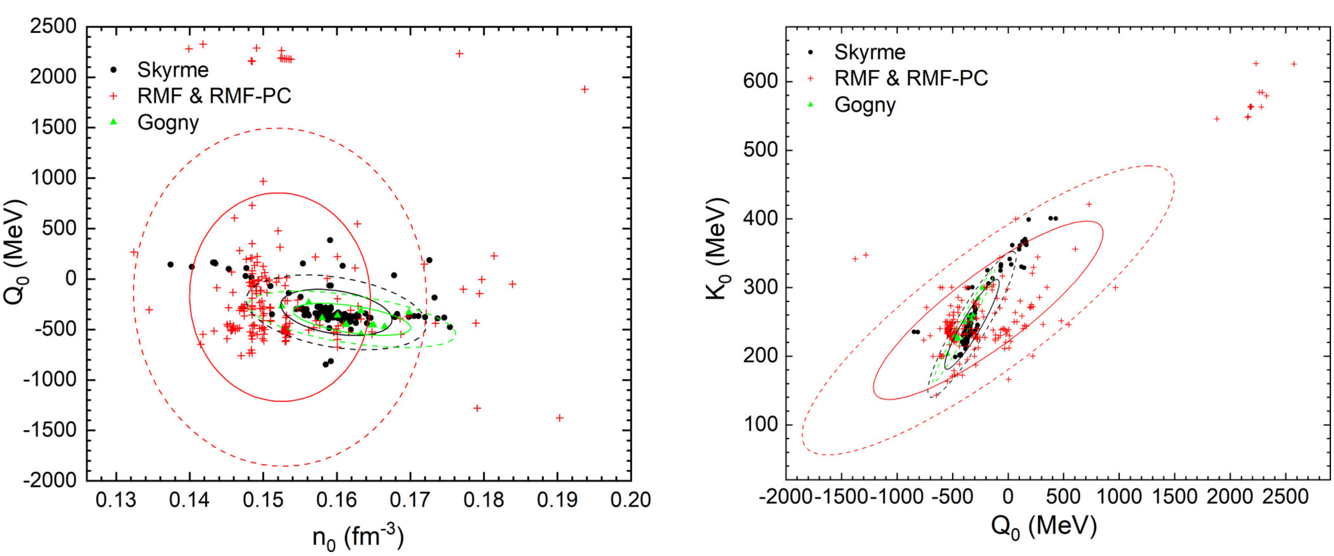

FIG. 2. Similar to Fig. 1, but for the correlations between the symmetric-matter skewness Q_0 with n_0 (left panel) and Q_0 with K_0 (right panel).

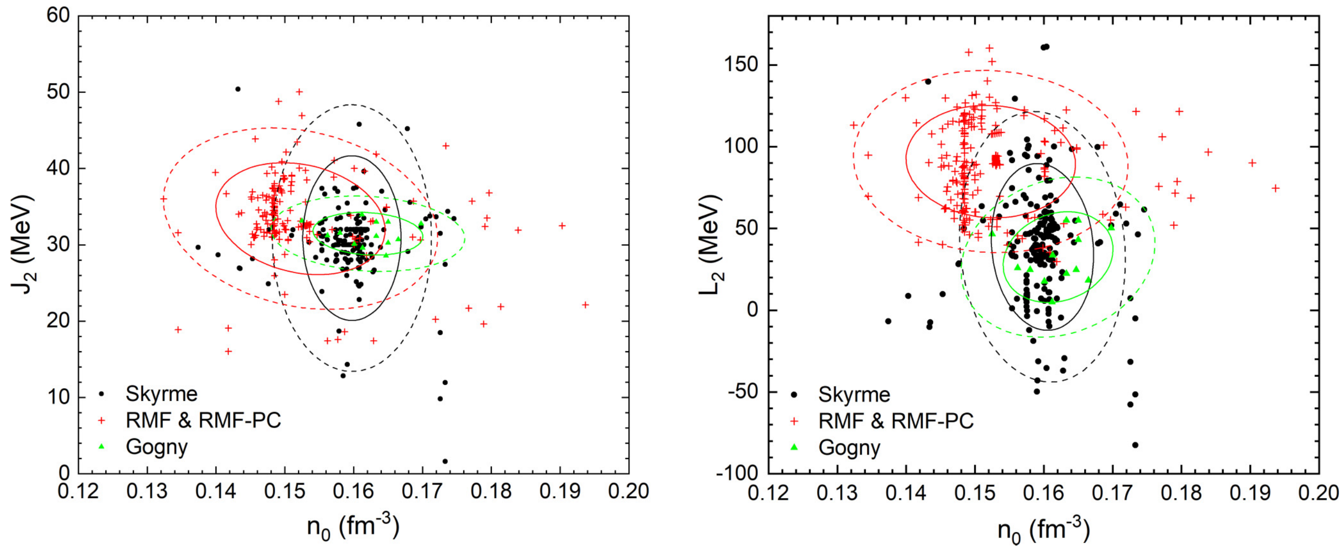

FIG. 3. Similar to Fig. 1, but for correlations between the parameters J_2 and n_0 (left panel) and L_2 and n_0 (right panel).

matter are all larger than for those of symmetric matter. These differences are especially significant for both L and K.

The moderate degrees of correlation of K_{N0} and Q_{N0} with L_2 suggest a similar degree of correlation between the corresponding symmetry energy parameters with L_2. This is confirmed in Fig. 7. The slopes of these correlations differ depending on the type of force considered, especially for $Q_{\rm sym2}$.

There are two methods of computing the symmetry energy parameters at the saturation density. Figures 3–7 employed the second method, using the second-order term of a Taylor expansion of the symmetry energy in the neutron excess. Figure 8 shows the extent to which the two methods differ. The mean difference $\langle J_1 - J_2\rangle = 1.00 \pm 0.30$ MeV, while $\langle L_1 - L_2\rangle = 2.58 \pm 8.31$ MeV, $\langle K_{\rm sym,1} - K_{\rm sym,2}\rangle = 1.40 \pm 4.44$ MeV, and $\langle Q_{\rm sym,1} - Q_{\rm sym,2}\rangle = 2.79 \pm 38.6$ MeV. The mean differences are quite small and nearly identical for

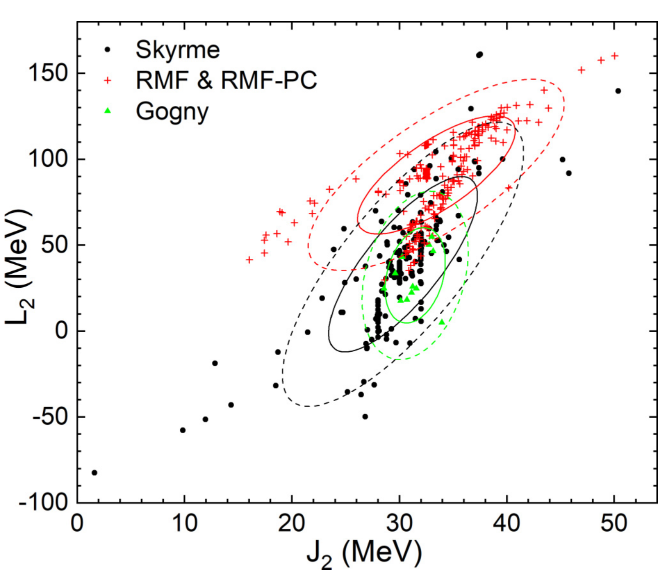

FIG. 4. Similar to Fig. 1 but showing the correlation between L_2 and J_2.

Skyrme and RMF forces, but the standard deviations for Skyrme forces are about double those of RMF forces, except for the Skyrme skewness standard deviation which is 4.5 times smaller than that for RMF. The primary contribution to the differences in the symmetry parameters arises from their kinetic-energy contributions. For Skyrme forces, this leads to

$$\begin{aligned} J_{1,\rm kin} - J_{2,\rm kin} &= \frac{\hbar^2}{M}\left(\frac{3\pi^2 n_0}{2}\right)^{2/3}\left[\frac{3}{10}(2^{2/3}-1) - \frac{1}{6}\right] \\ &\approx 0.69 \text{ MeV}, \\ L_{1,\rm kin} - L_{2,\rm kin} &= 2(J_{1,\rm kin} - J_{2,\rm kin}) \approx 1.39 \text{ MeV}, \\ K_{\rm sym,1,kin} - K_{2,\rm sym,kin} &= -2(J_{1,\rm kin} - J_{2,\rm kin}) \approx -1.39 \text{ MeV}, \\ Q_{\rm sym,1,kin} - Q_{\rm sym,2,kin} &= 8(J_{1,\rm kin} - J_{2,\rm kin}) \approx 5.56 \text{ MeV}. \end{aligned} \quad (112)$$

RMF forces give a similar result. The kinetic terms are important, but not the sole, contributions to these average differences, which are, nevertheless, relatively small, being of order 1% or less for all symmetry parameters. To the extent that the differences between the two methods are insignificant, which is not always the case as seen in Fig. 8, truncation of the Taylor expansion at quadratic order is justified. The few forces with the largest deviations from the quadratic approximation are identified in each panel of Fig. 8. It should be emphasized that Fig. 8 displays the deviations at saturation density; these deviations become larger at higher densities.

VI. NUCLEAR STRUCTURE PROPERTIES

The previous sections developed expressions for the energy density and pressure of uniform matter. It is useful to also study the properties of nonuniform matter as exists within nuclei, so that deductions about nuclear structure can be made. Within nuclei, in general, the neutron/proton ratio also varies with position. In consequence, contributions to the total energy of a nucleus from the existence of a surface, as well as global properties such as the neutron skin thickness and dipole polarizability, can be evaluated. In this paper, we evaluate

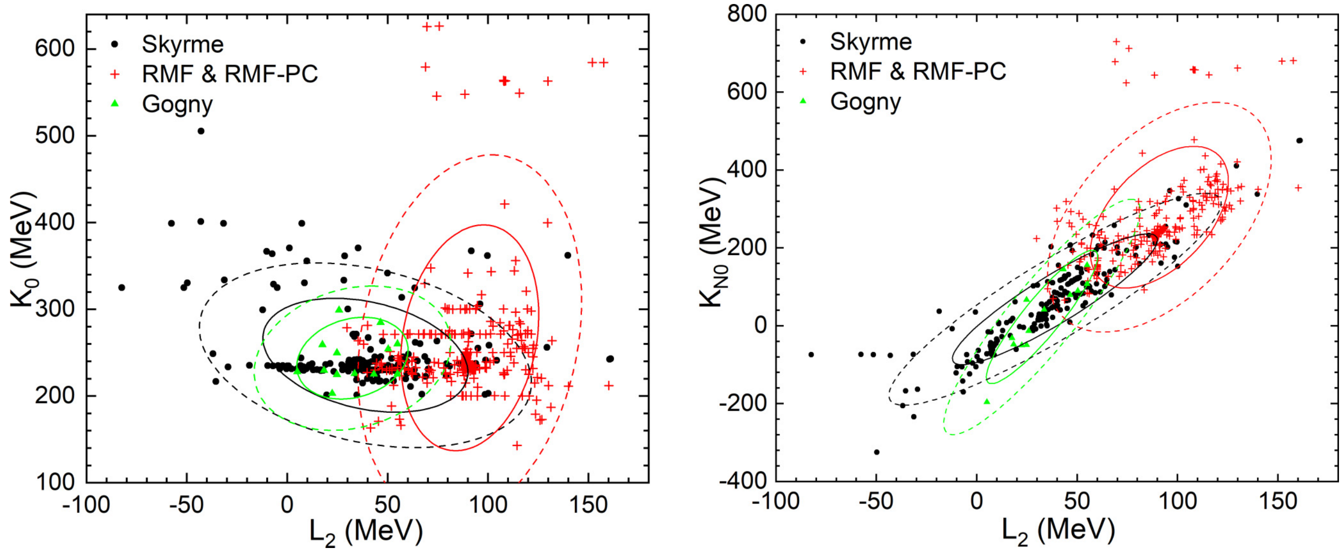

FIG. 5. Similar to Fig. 1, but for correlations between K_0 and L_2 (left panel) and K_{N0} and L_2 (right panel).

such quantities in a Thomas-Fermi approach and using the DM for nuclear structure [13]. The hydrodynamical model [9] gives the same results. Where available, we compare with the neutron skin thicknesses computed through the more accurate Hartree-Fock approximation.

The general expression for the total energy density of nucleonic matter within a nucleus, ignoring Coulomb, spin-orbit, shell and pairing effects, in Skyrme-like interactions can be expressed as

$$\mathcal{E} = \mathcal{E}_B + \tfrac{1}{2}[Q_{nn}(\vec{\nabla} n_n)^2 + 2Q_{np}\vec{\nabla} n_n \cdot \vec{\nabla} n_p + Q_{pp}(\vec{\nabla} n_p)^2], \tag{113}$$

where $\mathcal{E}_B(n, x)$ describes spatially homogeneous infinite bulk matter and the last factor expresses the contributions due to density gradients (as exist, for example, within nuclei). The coefficients Q_{ij} are given in Eq. (3). These coefficients are spatially constant unless t_4 or t_5 are nonzero.

For RMF models, the expression for the total energy density is not conveniently expressed in terms of neutron and proton density gradients, but rather in terms of the gradient contributions from the meson fields as given in Eq. (20), which is valid in the case of both constant and density-dependent coupling models. The surface properties of point-coupling and Gogny interactions, which have different gradient contributions, will not be considered further in this paper.

We be particularly interested in the case of symmetric matter, which is sufficient in the DM to determine the surface symmetry energy, the neutron skin thickness, and the dipole polarizability. For Skyrme interactions, in this case,

$$\mathcal{E} = \mathcal{E}_B + \frac{Q_{nn} + Q_{np}}{4}\left(\frac{dn}{dr}\right)^2 \equiv \mathcal{E}_B + \frac{\mathcal{Q}}{2}\left(\frac{dn}{dr}\right)^2, \tag{114}$$

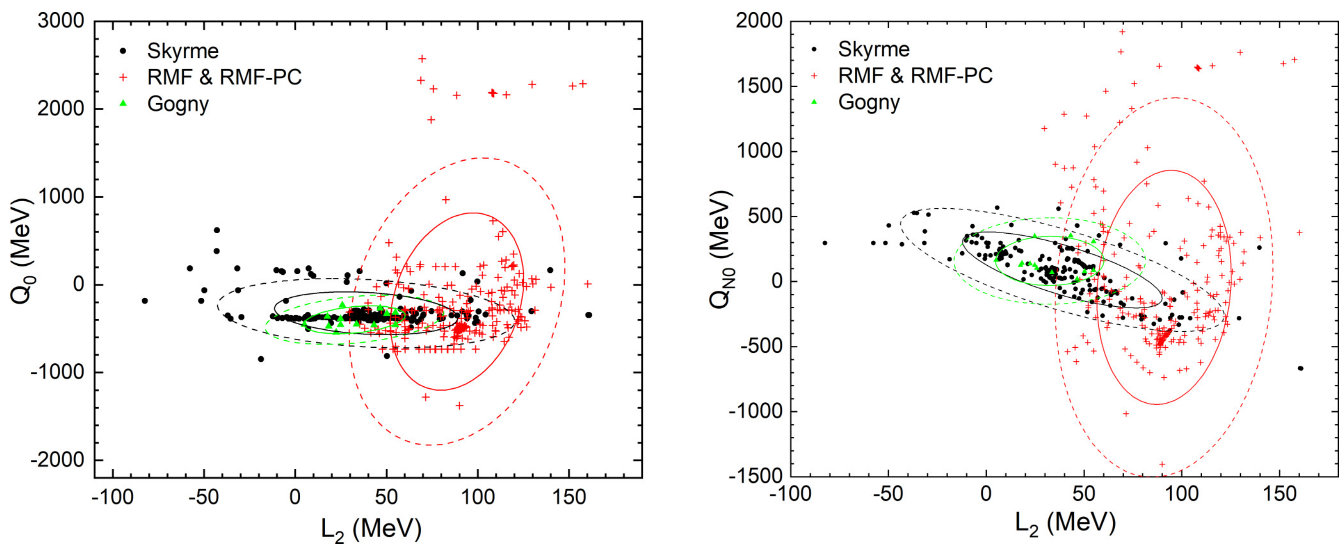

FIG. 6. Similar to Fig. 1, but for correlations between Q_0 and L_2 (left panel) and Q_{N0} and L_2 (right panel).

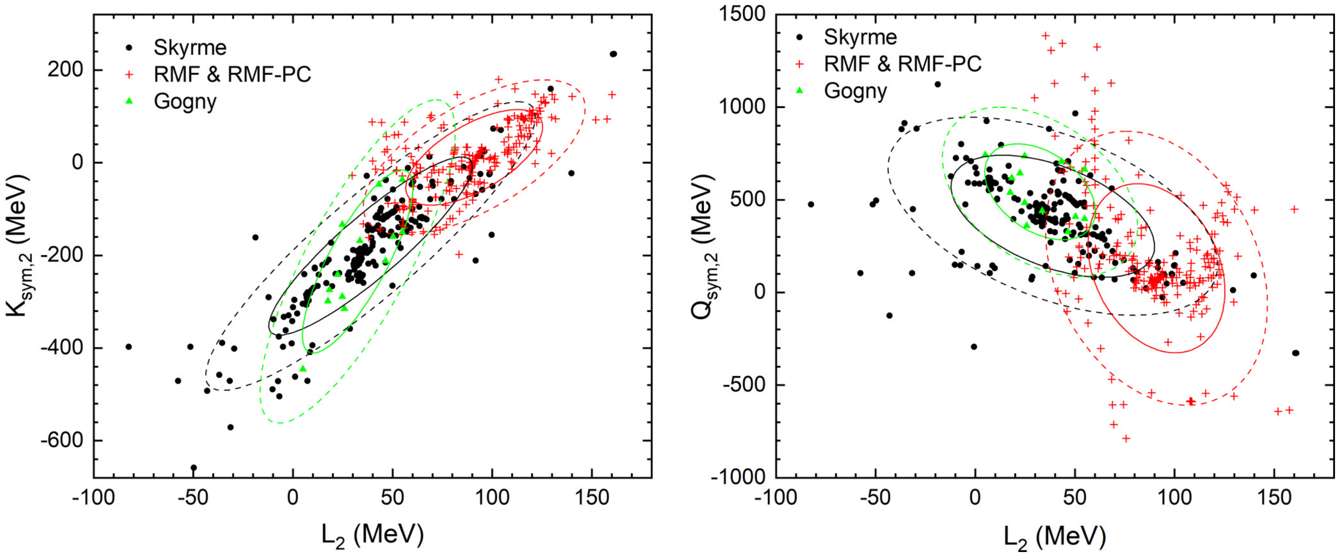

FIG. 7. Similar to Fig. 1, but for correlations between $K_{\rm sym}$ and L_2 (left panel) $Q_{\rm sym}$ and L_2 (right panel).

which defines $\mathcal{Q}$. For RMF interactions, we assume the Thomas-Fermi approximation, which holds that the field gradients are small enough that the fields at any point within the nucleus are given by their uniform matter expressions, i.e., those given by Euler-Lagrange minimization Eq. (24). In the case of symmetric matter, comparison of Eqs. (114) and (20) allow the identification of the corresponding expression for $\mathcal{Q}$,

$$\mathcal{Q} = \frac{\sigma'^2 - \omega'^2 - \rho'^2 + \delta'^2}{\hbar c} = \frac{\sigma'^2 - \omega'^2}{\hbar c}. \tag{115}$$

Note that in RMF interactions, $\mathcal{Q}$ always varies with density. It would also be possible, by algebraic manipulation, to evaluate corresponding expressions for Q_{nn} and Q_{np} individually, but this will not be necessary in this paper.

A. Semi-infinite interface and the surface energy

In general, phase equilibrium exists in zero temperature but arbitrary proton fraction matter, as long as the average density is below the nuclear saturation density for that proton fraction (where the pressure of a single phase of uniform matter would be negative). To minimize the total energy, matter separates into two phases with different densities and proton fractions. Neglecting the Coulomb interaction, in the limit that the surface region is negligible compared with the overall volume, the system may be considered as consisting of two semi-infinite regions (the dense region corresponding to the matter within a nucleus, and the vacuous region corresponding to the region outside the nucleus) separated by a plane-parallel surface. The Euler-Lagrange minimization of the total energy per unit area of this system, for fixed numbers of neutrons and protons per unit area, leads to an expression, which, after integrating by parts, is

$$\mathcal{E} - \mu_{n0}n_n - \mu_{p0}n_p = \frac{1}{2}\sum_{ij} Q_{ij}\frac{dn_i}{dr}\frac{dn_j}{dr}, \tag{116}$$

where the Lagrange parameters for fixed neutrons and protons per unit area are the chemical potentials μ_{n0} and μ_{p0}, which are constants. This equation turns out to be the same whether the coefficients Q_{ij} are constant or spatially varying, or on whether the interaction is a nonrelativistic Skyrme-type or an RMF-type force. It states that the bulk and gradient contributions to the total energy density are equal. This expression provides explicit representations of the density gradients as functions of the densities. In the case of symmetric matter, this expression can be straightforwardly integrated to yield the density profile $n(r)$ throughout the interface.

The left-hand side of Eq. (116) is simply the thermodynamic potential density. For a semi-infinite geometry, the net surface thermodynamic potential per unit area, often referred to as the surface tension σ, is

$$\sigma(\delta_L) = \int_{-\infty}^{+\infty} [\mathcal{E} - \mu_{n0}n_n - \mu_{p0}n_p]dz, \tag{117}$$

where δ_L is the neutron excess in the dense phase far from the interface and z is the coordinate perpendicular to the surface. This is recognizable as the difference of the total energy per unit area between the configuration in which the density profile is optimized through the interface and the configuration in which the densities are taken to be spatially uniform with a sharp discontinuity at the interface where the density changes abruptly from its value (n_0 in the case of $\delta_L = 0$) to zero, at least in the case when $\delta_L \lesssim 0.2$, i.e., less than the neutron-drip value where the density in the external phase becomes finite. It is precisely the surface tension, σ, that is maximized when performing the Euler-Lagrange minimization of the total energy density per unit area of the semi-infinite system.

In the case of small, nonzero, asymmetry δ_L, Eq. , (117) can be expanded as a Taylor series in δ_L^2,

$$\sigma(\delta_L) = \sigma_o - \sigma_\delta \delta_L^2 + \cdots, \tag{118}$$

where σ_o is the surface tension for symmetric matter $\delta_L = 0$ and σ_δ is the surface tension symmetry parameter. In the case of symmetric matter, $\mu_{n0} = \mu_{p0} = M + E_0$ (in the case of nonrelativistic interactions, M is not included in the chemical potentials). Also, since $\mathcal{E}_B = \mathcal{E}_{1/2}$ is the energy density for

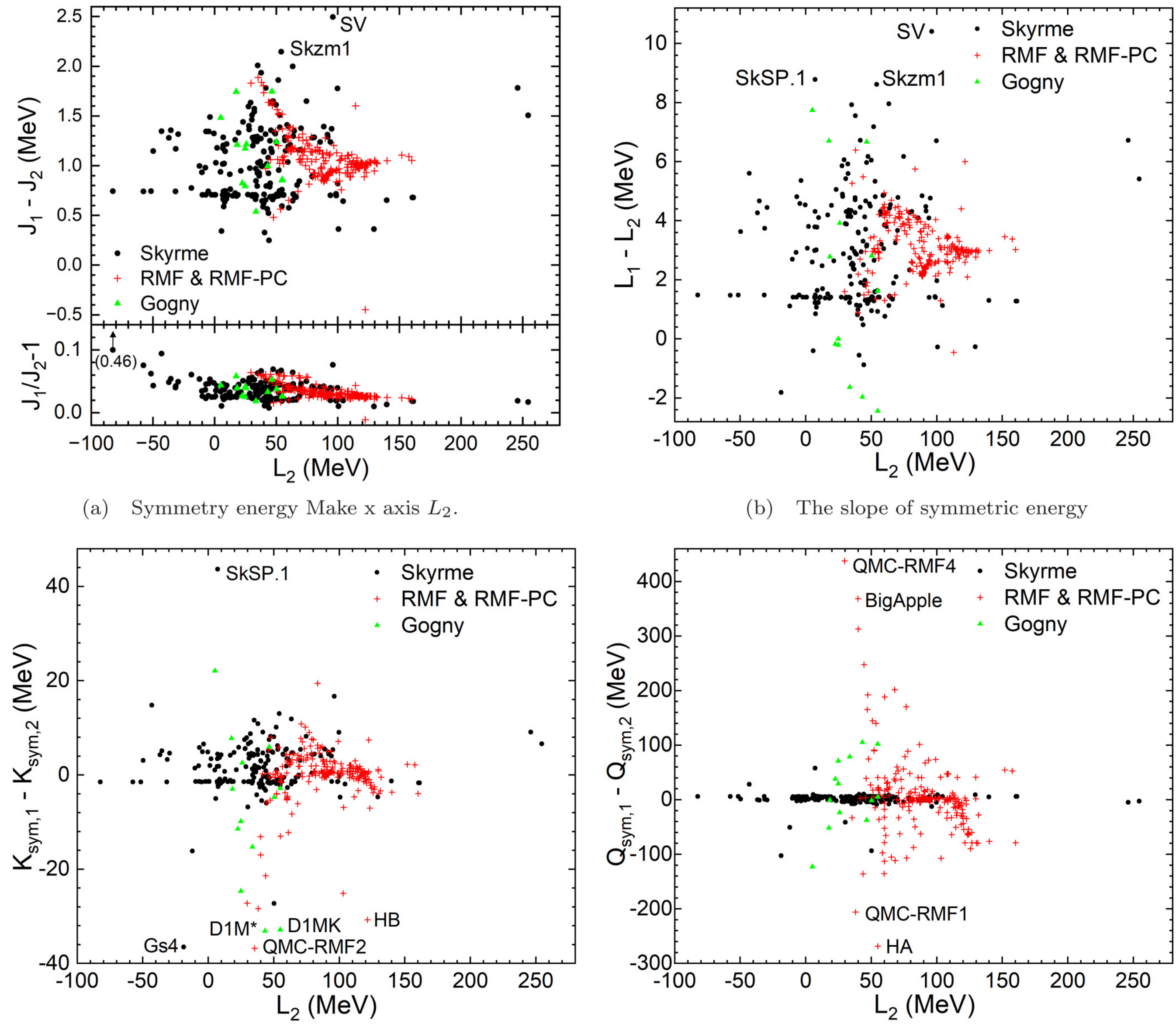

(a) Symmetry energy Make x axis L_2.

(b) The slope of symmetric energy

(c) Volume incompressibility

(d) Skewness

FIG. 8. Differences between the two methods for determining symmetry energy parameters.

uniform symmetric matter, one finds

$$\sigma_o \equiv \sigma(\delta_L = 0) = 2\int_{-\infty}^{+\infty}[E_{1/2}(n) - E_0]n dz$$
$$= \int_{-\infty}^{+\infty} \mathcal{Q}\left(\frac{dn}{dz}\right)^2 dz. \tag{119}$$

The gradient dn/dz can be eliminated by substituting Eq. (116), noting that for a semi-infinite interface $r \to z$, which removes the spatial dependence to form the quadrature

$$\sigma_o = \int_0^{n_0} \sqrt{2\mathcal{Q}n(E_{1/2}(n) - E_0)}dn. \tag{120}$$

The integrand of this equation vanishes at both boundaries.

Figure 9 shows that the parameter σ_0 is only weakly correlated with either n_0 or E_0 for both types of forces. However, it is more strongly correlated with K_0, especially for RMF forces, as shown in the left panel of Fig. 10. This can be understood from Eq. (120) if one approximates $E_{1/2}(n) = E_0 + (K_0/18)(n - n_0)^2 + \cdots$. Then one finds that $\sigma_o \propto \sqrt{K_0}$.

The surface tension symmetry parameter σ_δ in Eq. (118) can be found by expanding Eq. (117), after substituting Eq. (25), in powers of δ_L^2. This leads to

$$\sigma(\delta_L) = \int_0^{n_0} \sqrt{\frac{\mathcal{Q}n}{2}}\left[E_{1/2}(n) - E_0 - \delta_L^2\left(\frac{J_2}{\mathcal{S}_2(n)} - 1\right)\right]^{1/2} dn, \tag{121}$$

and further expanding the integrand of Eq. (121), one finds

$$\sigma_\delta = \frac{J_2}{\sqrt{2}}\int_0^{n_0}\sqrt{\frac{\mathcal{Q}n}{E_{1/2}(n) - E_0}}\left[\frac{J_2}{\mathcal{S}_2(n)} - 1\right]dn, \tag{122}$$

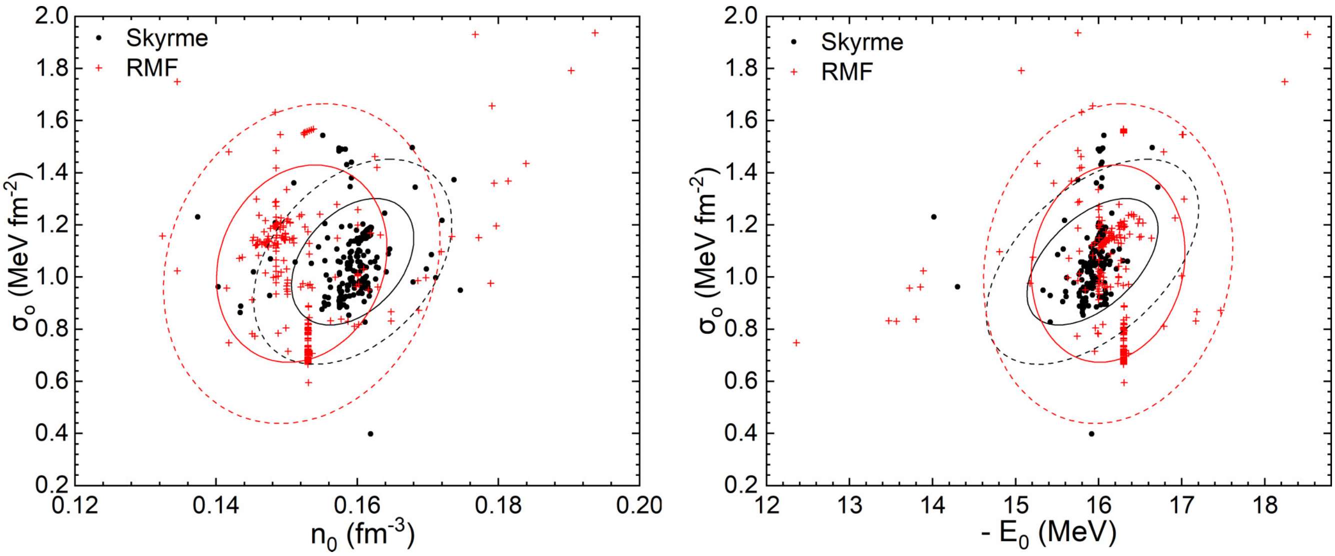

FIG. 9. Correlations between the surface tension σ_0 and the saturation density n_0 (left panel) and the binding energy $-E_0$ at saturation (right panel) in Skyrme (black) and RMF (red) models. 1σ and 2σ confidence ellipses are indicated by solid and dashed lines for each force type.

which is also, therefore, another quadrature. The integral Eq. (122) is well-behaved: in the limit where $n \to 0$, $\mathcal{Q}(n=0)/[E_{1/2}(n=0)-E_0]$ is a constant and $\mathcal{S}_2(n) \to n^{2/3}$, so the integrand diverges as $n^{-1/6}$. But its contribution to the integral at small density is proportional to $n^{5/6}$ and therefore vanishes. In the opposite limit where $n \to n_0$, one has $E_{1/2}(n) - E_0 \to K_{1/2}(1-u)^2/18$ and $J_2/\mathcal{S}_2(n) - 1 \to L_2(u-1)/(3J_2)$, where $u = n/n_0$, so the integrand approaches the constant $L_2\sqrt{\mathcal{Q}(n=n_0)n_0/K_{1/2}}$.

We note that in the DM, the surface energy E_S and the surface symmetry energy S_S parameters are respectively given as

$$E_S = 4\pi r_o^2 \sigma_o, \quad S_S = 4\pi r_o^2 \sigma_\delta, \tag{123}$$

where the nucleon radius r_o satisfies $4\pi r_o^3 n_0/3 = 1$. Values of σ_o, σ_δ, and S_S of Skyrme (RMF) parametrizations are included in Table III (IX). Integration of Eq. (122) results in a strong correlation between S_S/J_2 and L_2, which is, furthermore, linear to an excellent approximation as shown in the right panel of Fig. 10. For Skyrme and RMF forces, they are, respectively,

$$\frac{S_S}{J_2} = (0.905 \pm 0.378) + 0.02091\frac{L_2}{\text{MeV}},$$
$$\frac{S_S}{J_2} = (0.777 \pm 0.439) + 0.02535\frac{L_2}{\text{MeV}}. \tag{124}$$

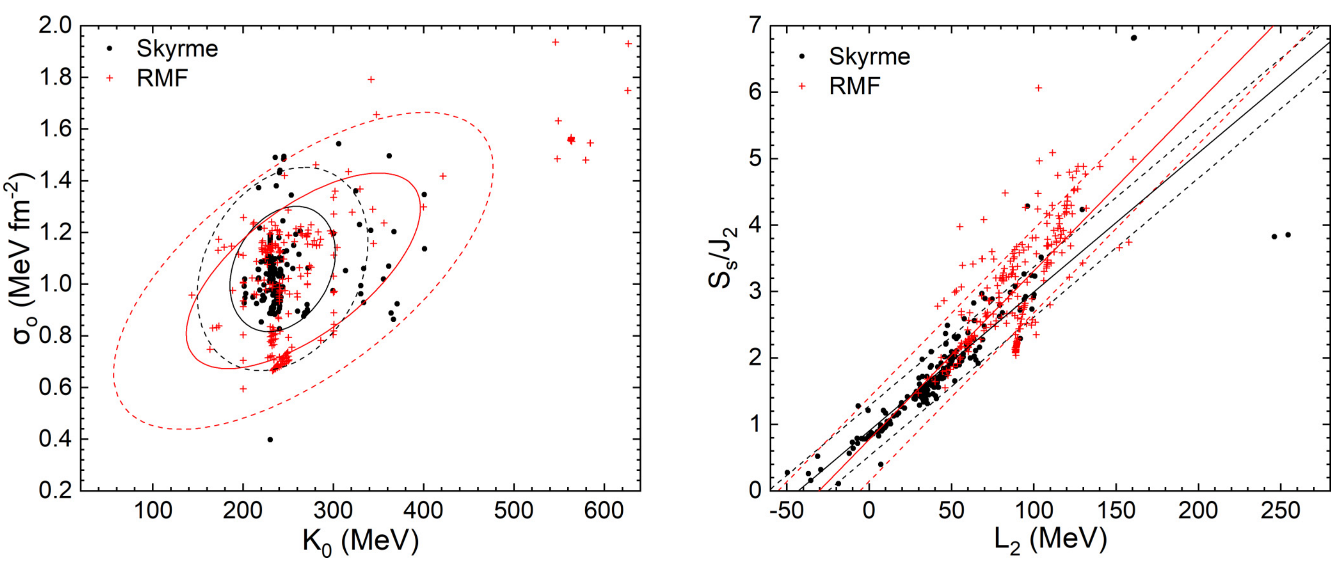

FIG. 10. The left panel is the same as Fig. 9 except for the surface tension σ_o and the incompressibility at saturation K_0. The right panel shows the nearly linear correlations, with standard deviations, between S_s/J_2 and the symmetry energy slope L_2.

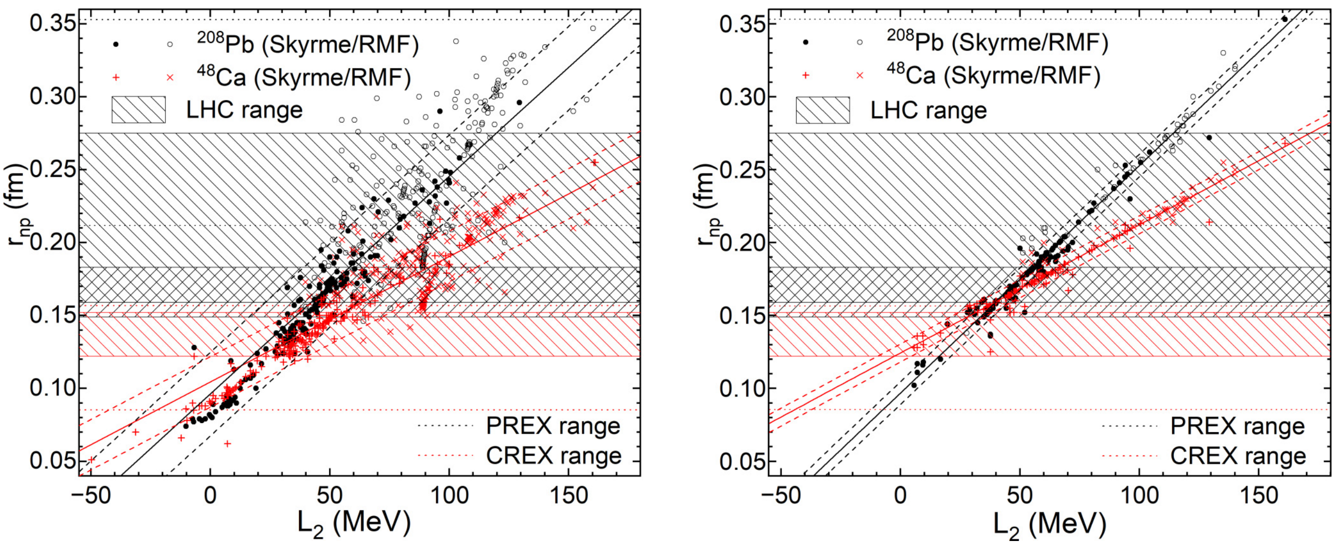

FIG. 11. Skyrme and RMF predictions of the neutron skin thicknesses of ^{48}Ca (red) and ^{208}Pb (black) for the DM, including surface diffuseness corrections, (left panel) and Hartree-Fock calculations (right panel). Linear correlations and one standard deviation are shown as solid and dashed diagonal lines, respectively. The narrow hatched horizontal bands indicate the one standard deviation ranges of the previous averaged experimental results for these nuclei [12]. The dotted black (red) lines indicate the one standard deviation ranges of r_{np}^{208} (r_{np}^{48}) from PREX I + II [17] (CREX [18]). The wide black hatched band shows the one standard deviation range of the Large Hadron Collider ^{208}Pb neutron skin measurement [19].

B. Neutron skin thickness

Other quantities of interest are the neutron skin thickness and the dipole polarizability. Both the DM and hydrodynamical (h) models predict that the difference between the mean neutron and proton radii for a nucleus with mass A and charge Z is [9,14,15]

$$R_n - R_p = \frac{2r_o}{3}\left(1+\frac{S_S}{J_2A^{1/3}}\right)^{-1} \times\left[I\frac{S_S}{J_2} - \frac{3Ze^2}{140 r_o J_2}\left(1+\frac{10S_S}{3J_2A^{1/3}}\right)\right], \quad (125)$$

where the nuclear isospin parameter is $I=(N-Z)/A$ [not to be confused with the RMF potential energy density $I(\delta)$]. The neutron skin thickness is defined as the difference of the mean square neutron and proton radii, or $r_{np}\approx\sqrt{3/5}(R_n-R_p)$. The nominal nuclear radius is $R=r_oA^{1/3}$. The last term in the square brackets of these formulas represents the effects of Coulomb polarization. In addition, one can include a correction

$$\Delta r_{np}^{\rm surf} = \sqrt{\frac{3}{5}}\frac{5\left(b_n^2-b_p^2\right)}{2R} \quad (126)$$

due to the difference of the surface widths b_n and b_p of the neutron and proton density distributions [13,16], respectively. For ^{208}Pb, this correction is about 0.05 fm and for ^{48}Ca it is about 0.04 fm [16], amounts which are not negligible. We included this correction to the DM values of r_{np}^{48} and r_{np}^{208} for Skyrme (RMF) parametrizations in Table III (IX). Equation (125) indicates that r_{np} should be highly correlated with S_S/J_2, and therefore, with L_2. In spite of the various nonlinear factors in Eq. (125), they largely cancel, resulting in a nearly linear correlation between r_{np} and L_2, as indicated in Fig. 11. This is true for both nuclei, and also for both Skyrme and RMF force models. The slopes of these linear correlations, to the lowest order, are proportional to I and therefore steeper for Pb relative to Ca.

For predicting neutron skin thicknesses, the DM leaves a lot to be desired. Coulomb corrections and density variations within the nucleus are only treated approximately, and the DM truncates the leptodermous expansion so that curvature and higher-order corrections are ignored. Figure 11 compares the correlations between r_{np} and L_2 for the DM with those of more accurate Hartree-Fock (HF) computations from Ref. [20]. It is therefore somewhat surprising that the mean trends, including the slopes, averaged over all forces are nearly the same for both models. The greater accuracy of HF computations results in linear correlations between r_{np} and L_2 that have significantly smaller standard deviations for both nuclei by a factor $\approx$2–2.5 for ^{208}Pb and $\approx$3–4 for ^{48}Ca.

The overall differences in the correlations between force types are small; for example, for the HF computations, the slope of the Skyrme (RMF) correlation for ^{208}Pb, is 0.00149 (0.00153) fm MeV^{-1} and for ^{48}Ca, the slope of the Skyrme (RMF) correlation is 0.000840 (0.000836) fm MeV^{-1}. Similarly, small differences are found for DM computations as well.

To explore the differences between DM and HF predictions for neutron skin thicknesses in more detail, in Fig. 12 we display the ratio of the DM and HF values of r_{np}^{48} (left panel) and r_{np}^{208} (right panel). In both cases, the average DM skin thickness is smaller than the HF values, especially for forces with small L_2 values. The DM predictions are, however, closer to the HF predictions for Pb than for Ca. The contribution of the Coulomb term in Eq. (125) compared with the leading-order asymmetry (IS_S/J_2) term scales like $Z/(IS_S)$. It is reasonable

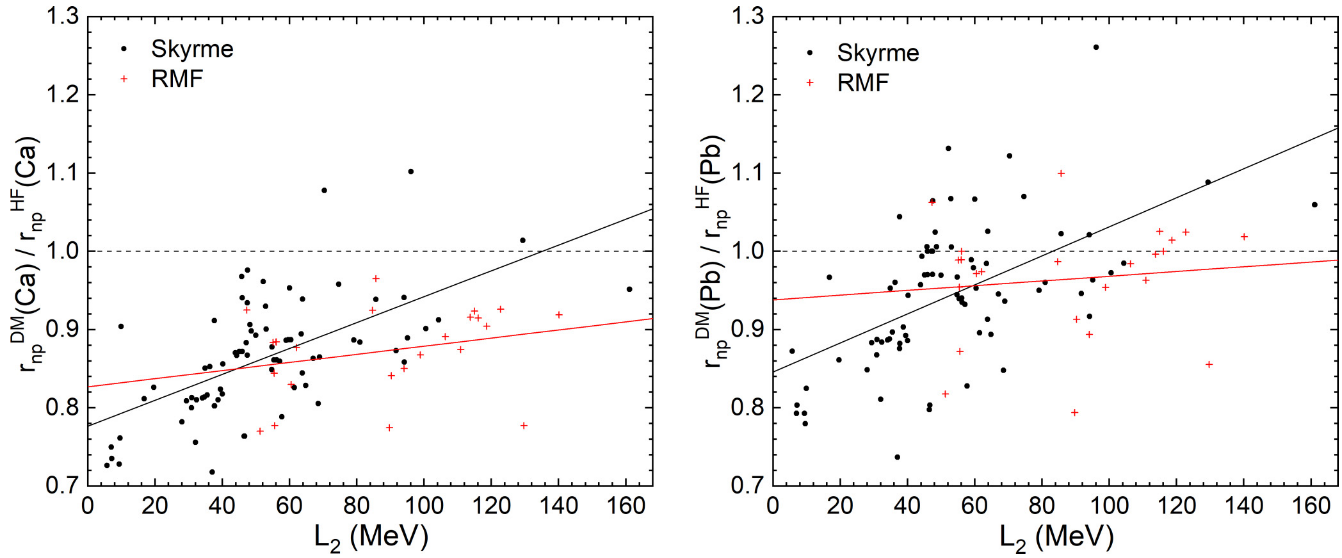

FIG. 12. Comparison of the neutron skin thicknesses of ^{48}Ca and ^{208}Pb calculated from the DM including surface diffuseness corrections with those from the HF method, for selected Skyrme (left panel) and RMF (right panel) models.

that DM predictions would increase in accuracy for larger A where the Coulomb corrections and the leptodermous truncation are more accurately represented. The trend that DM predictions become more accurate as L_2 is increased for a given nuclei is due to the decreasing importance of Coulomb corrections with increasing S_S, and therefore, L_2.

C. Dipole polarizability

The liquid droplet [14] and the hydrodynamical [9] models predict slightly different dipole polarizabilities

$$\alpha_D^{\rm h} = \frac{1}{20}\frac{AR^2}{J_2}\left(1+\frac{5S_S}{3J_2A^{1/3}}\right),$$
$$\alpha_D^{\rm DM} = \frac{\pi e^2}{90}\frac{AR^2}{J_2}\left(1+\frac{5S_S}{3J_2A^{1/3}}\right). \tag{127}$$

The factor $\pi e^2/90 \approx 1/19.894$ in the DM model is almost identical to the factor $1/20$ from the hydrodynamical model, so the two predictions differ by only 0.5%. Hydrodynamical model predictions of α_D for ^{48}Ca and ^{208}Pb for Skyrme (RMF) parametrizations are included in Table III (IX), and are shown in Fig. 13. This figure shows that, in comparison to the experimentally measured values (from Refs. [21,22], respectively) the hydrodynamical (or DM) model largely overpredicts their values. The theoretical results indicate a positive correlation with L_2, and reconciling them with experimental data would suggest rather small values of $L_2 \approx 0$ MeV. No Hartree-Fock estimates are readily available in tabular form for the forces considered here.

VII. SELECTED NEUTRON STAR PROPERTIES

We are also interested in the dependence of neutron star properties on the equation of state (EOS). However, it is unreasonable to naively extrapolate EOSs determined from fitting nuclear structure properties, for which the maximum density is n_0, to $(5-10)n_0$, the central density of the most massive neutron stars. Therefore, we largely confine our attention to low-mass neutron stars, those with $M \lesssim 1.6M_\odot$, for which the central densities are just a few n_0. An exception is made to include the calculation of $M_{\rm max}$, the maximum neutron star mass predicted by an EOS. Many of the EOSs included here cannot satisfy the minimal constraint that $M_{\rm max} \gtrsim 2M_\odot$, the mass of the most massive measured pulsar, but in practice one could replace a given EOS at densities in excess of n_0 with another model that could satisfy this condition. Since this replacement is arbitrary, given the lack of experimental information for densities in excess of n_0, we do not pursue such replacements in this paper.

In principle, each EOS predicts a specific core-crust boundary, and a crust EOS at lower densities that contains finite nuclei in addition to nucleons. Ideally, one would compute this crustal EOS for each force using a scheme such as that of Ref. [23]. Instead, for simplicity and computational expediency, we assume the crust EOS is a piecewise-polytropic EOS fitted to the Skyrme EOS SLy4 [24]. The crust EOS is assumed for $n \lesssim 0.04$ fm^{-3}. For Skyrme and Gogny forces, we use the given EOS as PNM at densities in excess of 0.12 fm^{-3} and smoothly interpolate in between with a smooth scheme that matches energies, pressures and incompressibilities at both boundaries. For RMF forces, we use the same crust EOS below 0.04 fm^{-3}, and the EOS in the in-between range is obtained through an interpolation based on Neville's algorithm. We checked that small variations in the EOS resulting from these interpolations do not significantly affect the quantities we seek. The quantity most sensitive to the way this region is treated is the tidal deformability, for which a lack of smoothness in the transition region has large effects. But varying the interpolation scheme, as long as it is smooth, has only very small effect. Although neutron-star matter has a small proton fraction, determined by beta equilibrium, and a

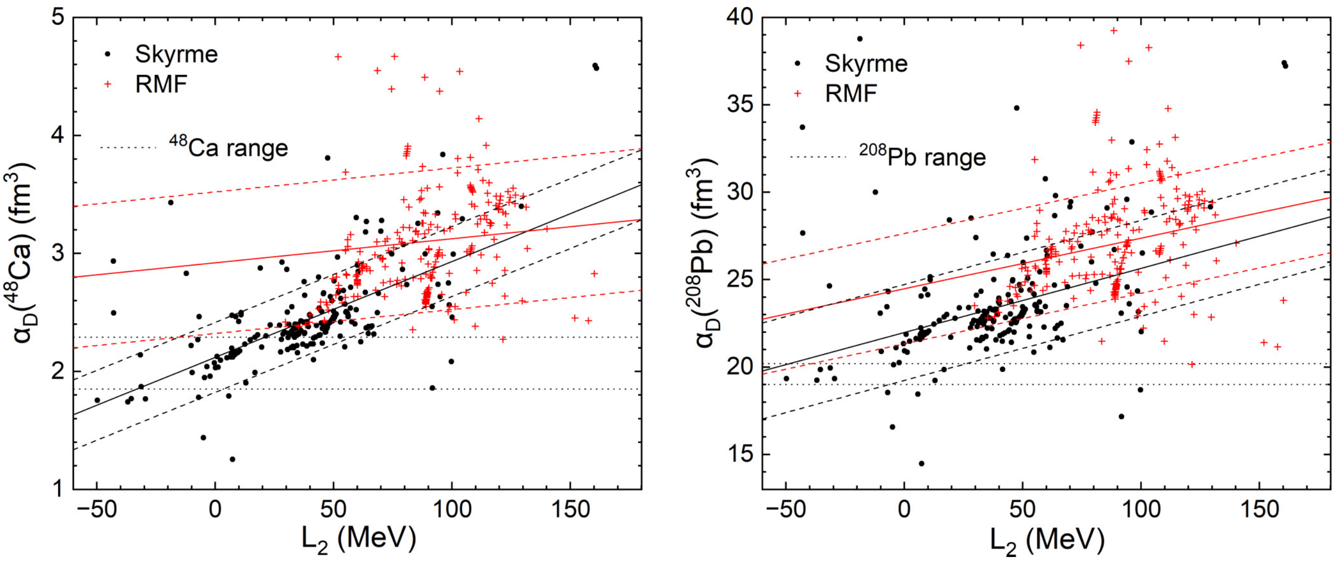

FIG. 13. Skyrme and RMF predictions of the dipole polarizability of ^{48}Ca (left) and ^{208}Pb (right) calculated with hydrodynamical model. The dotted black lines in both figures indicate the ranges of the experimental results for these nuclei, Refs. [21,22], respectively.

slightly smaller pressure than PNM, we ignore this complication. Primarily this omission will affect predictions of $M_{\rm max}$, but given the unreliability of these interactions at the relevant densities, these differences have little consequence.

A. Radius

The basic relations determining the mass-radius relation are the traditional Tolman–Oppenheimer–Volkoff (TOV) differential equations

$$\frac{dP}{dr} = -\frac{G(\mathcal{E}+P)(mc^2+4\pi r^3 P)}{rc^2(rc^2-2Gm)}, \quad \frac{dm}{dr} = 4\pi r^2 \frac{\mathcal{E}}{c^2}, \tag{128}$$

where $m(r)$ is the gravitational mass interior to the radius r. Boundary conditions for these equations are $m(r=0)=0$ and $(dP/dr)_{r=0}=0$. The integrations are terminated when $P=0$, which defines the surface $r=R$. A specified value of central pressure $P_c = P(r=0)$ determines the total mass $M = m(r=R)$. Note that the only EOS relation needed is the pressure-energy density relation $P(\mathcal{E})$, which in the neutron star core is assumed to be PNM. Tables IV, X, and XIII give the radii $R_{1.2}$, $R_{1.4}$, and $R_{1.6}$ corresponding to the masses $1.2M_\odot$, $1.4M_\odot$, and $1.6M_\odot$, for Skyrme, RMF and Gogny forces, respectively. Radii for larger masses are not considered, due to the large central densities of such structures. For informational purposes, the maximum masses $M_{\rm max}$ are also tabulated. Besides the radii of low-mass neutron stars, we also consider other potentially observable quantities, including moments of inertia, tidal deformabilities and binding energies.

It has long been known that there is a high degree of correlation between the typical (i.e., $1.4M_\odot$) neutron star radius $R_{1.4}$ and the pressure of neutron-star matter in the range n_0 to $2n_0$ [25]. We update the relations found by Ref. [25] at n_s and $1.5n_s$, assuming $M_{\rm max} \geqslant 2M_\odot$:

$$R_{1.4} = (9.46 \pm 0.38)\left(\frac{P(n_s)}{\text{MeV fm}^{-3}}\right)^{1/4} \text{km}$$
$$= (6.99 \pm 0.26)\left(\frac{P(1.5n_s)}{\text{MeV fm}^{-3}}\right)^{1/4} \text{km}. \tag{129}$$

This implies a similar correlation exists between $R_{1.4}$ and L_2, which is shown in Fig. 14. The fitted curve satisfies

$$R_{1.4} = (3.84 \pm 0.74)(L_2/\text{MeV})^{0.282} \text{ km}; \tag{130}$$

note the exponent is close to 1/4, but the correlation is less significant than with $P(n_s)$, partly due to variations of n_s, that $L_2 \neq L_1 = 3P_N(n_s)/n_s$, and that the former correlation assumes $M_{\rm max} \geqslant 2M_\odot$.

B. Moment of inertia

The moment of inertia of a neutron star, the ratio of its rotational angular momentum to its angular velocity, is given for a slowly uniformly rotating star by [26]

$$I = \frac{c^2}{G}\frac{R^3 u_R}{6+2u_R}, \tag{131}$$

where $u_R = u(R)$ is the surface value of a function $u(r)$ that obeys the first-order differential equation

$$\frac{du}{dr} = \frac{4\pi G r^2}{c^2}\frac{(\mathcal{E}+P)(4+u)}{c^2 r - 2Gm} - \frac{u}{r}(3+u), \tag{132}$$

with the boundary condition $u(0)=0$ that is solved together with the TOV equations. Note that u is not to be confused with the earlier usage as $u = n/n_0$. It is useful to define the dimensionless moment of inertia as

$$\bar{I} = \frac{c^4 I}{G^2 M^3} = \frac{u_R}{\beta^3(6+2u_R)}, \tag{133}$$

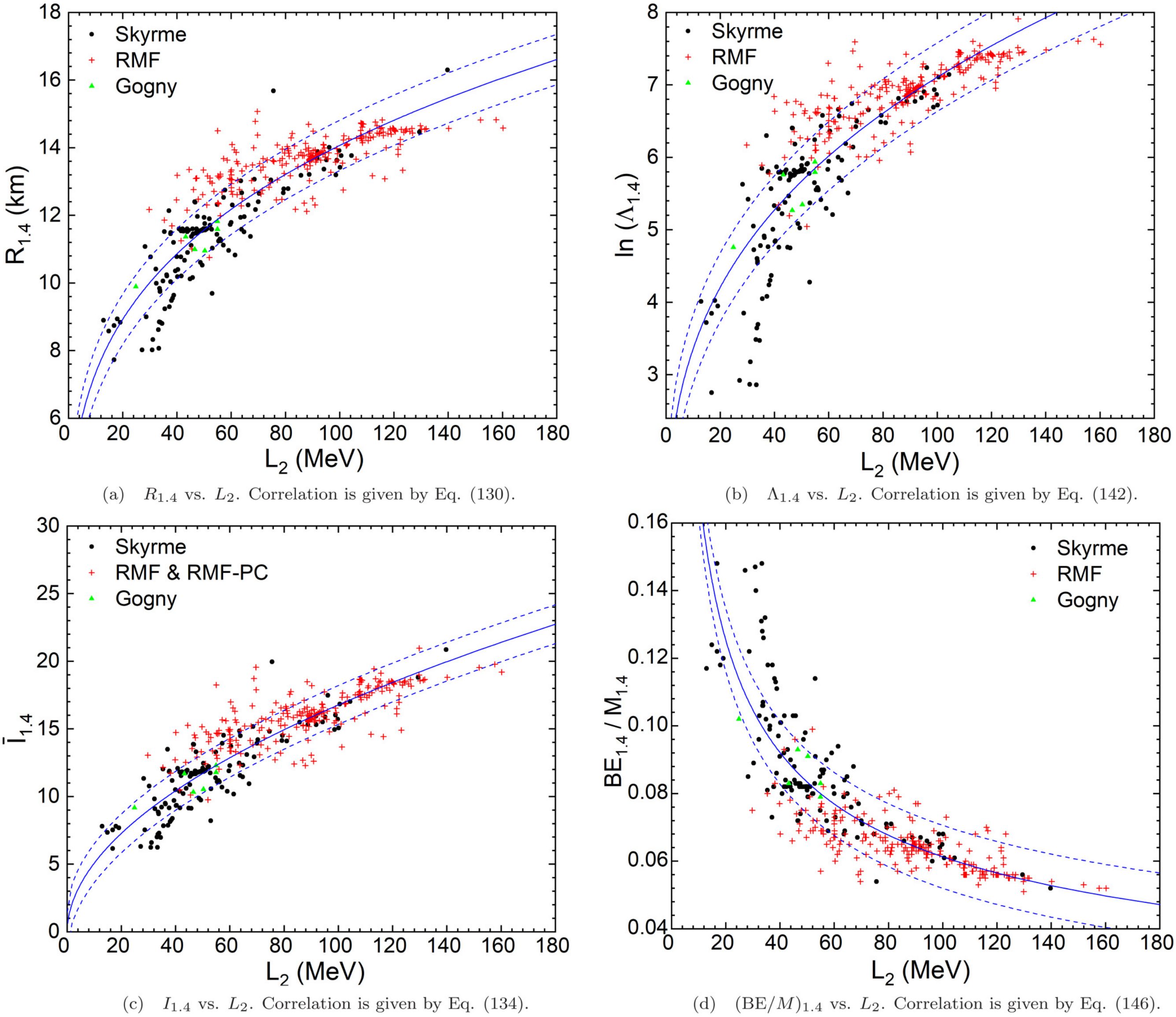

(a) $R_{1.4}$ vs. L_2. Correlation is given by Eq. (130).

(b) $\Lambda_{1.4}$ vs. L_2. Correlation is given by Eq. (142).

(c) $I_{1.4}$ vs. L_2. Correlation is given by Eq. (134).

(d) $(\mathrm{BE}/M)_{1.4}$ vs. L_2. Correlation is given by Eq. (146).

FIG. 14. Relationship between neutron star parameters and slope of symmetric energy.

where $\beta = GM/(Rc^2)$ is the dimensionless compactness parameter. Like the M-R relation, the only EOS relation required is $P(\mathcal{E})$. Tables IV, X, and XIII give the quantities $\bar{I}_{1.2}$, $\bar{I}_{1.4}$, and $\bar{I}_{1.6}$ for Skyrme, RMF and Gogny forces, respectively.

Since one expects that $I \propto MR^2$ in the Newtonian case, a correlation between $\bar{I}_{1.4}$ and L is anticipated. This is shown in Fig. 14, where the fitted relation satisfies

$$\bar{I}_{1.4} = 0.542(L_2/\mathrm{MeV})^{0.183} \pm 1.435. \tag{134}$$

The correlation between $\bar{I}_{1.4}$ and $R_{1.4}$ itself is shown in Fig. 15, where the fitted curve is given by

$$\bar{I}_{1.4} = 0.1478(R_{1.4}/\mathrm{km})^{1.789} \pm 0.4649. \tag{135}$$

Note that this relation is less steep than $\bar{I} \propto R^2$, due to general relativistic corrections that become more important for small radii. Indeed, the average correlation for RMF forces is noticeably steeper than for Skyrme forces, due to the fact that RMF forces typically have larger values of $R_{1.4}$. Also note that the moment of inertia correlation with radius is much more accurate than with L_2.

C. Tidal deformability

The tidal deformability λ quantifies how easily a star is deformed when subjected to an external tidal field. A larger tidal deformability signals a larger, less compact star that is easily deformable. Specifically, the tidal deformability is defined as the ratio of the induced quadrupole moment to the external perturbing tidal field. In the Newtonian limit, the perturbing tidal field is defined as the second spatial derivative of the external field. Formally, the tidal deformability is defined as $\lambda = (2/5)k_2R^5$, where k_2 is the gravitational Love number [27]

$$k_2 = \frac{8\beta^5}{5\mathcal{R}}(1-2\beta)^2[2 - y_R + 2\beta(y_R - 1)], \tag{136}$$

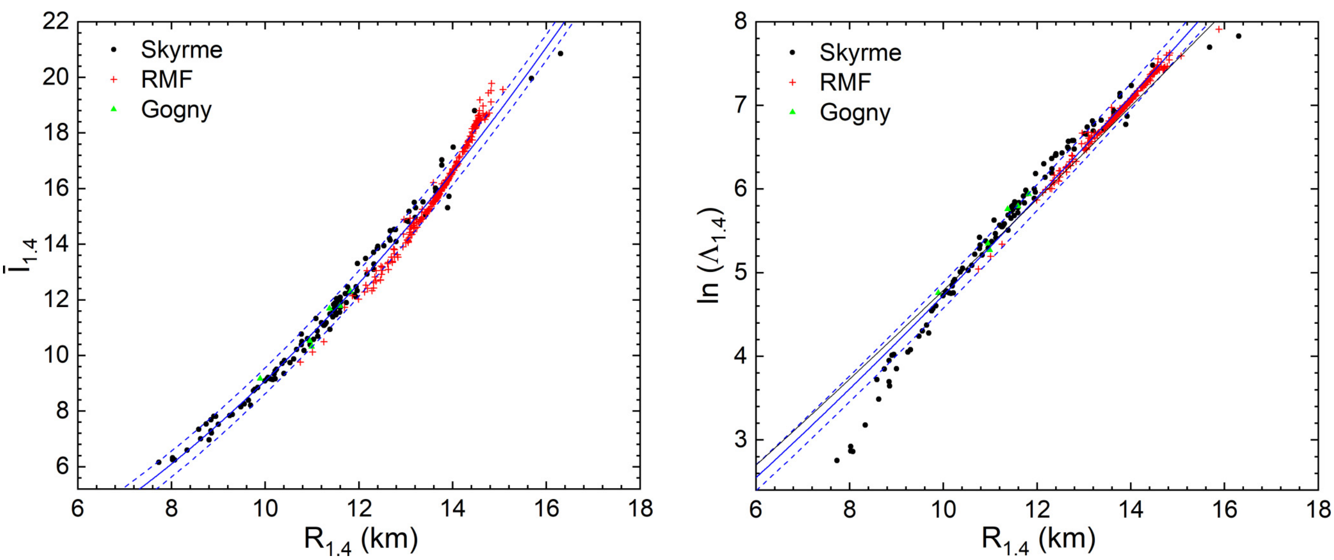

FIG. 15. (left) $I_{1.4}$ vs $R_{1.4}$. The correlation is given in Eq. (135). (right) ln $\Lambda_{1.4}$ vs $R_{1.4}$. The correlation is given in Eq. (142).

the parameter $\mathcal{R}$ being

$$\mathcal{R} = 6\beta[2 - y_R + \beta(5y_R - 8)] + 3(1 - \beta^2) \times [2 - y_R + 2\beta(y_R - 1)] \ln(1 - 2\beta) + 4\beta^3[13 - 11y_R + \beta(3y_R - 2) + 2\beta^2(1 + y_R)]. \quad (137)$$

$y_R = y(R)$ is the surface value of the dimensionless function $y(r)$, which is the solution of the differential equation

$$\frac{dy(r)}{dr} = -\frac{y(r)^2}{r} - \frac{y(r)F(r)}{r} - rQ(r), \quad (138)$$

which is solved together with the TOV equations. The central boundary condition is $y(0) = 2$. The functions $F(r)$ and $Q(r)$ are expressed as

$$F(r) = \left(1 - \frac{4\pi G}{c^4} r^2[\mathcal{E}(r) - P(r)]\right)\left[1 - \frac{2Gm(r)}{rc^2}\right]^{-1},$$
$$Q(r) = \frac{4\pi G}{c^4}\left[5\mathcal{E}(r) + 9P(r) + \frac{\mathcal{E}(r) + P(r)}{dP(r)/d\mathcal{E}(r)} - \frac{6}{4\pi r^2}\right] \times \left[1 - \frac{2Gm(r)}{rc^2}\right]^{-1} - \left(\frac{2Gm(r)}{r^2c^2}\right)^2 \times \left[1 + \frac{4\pi r^3 P(r)}{m(r)c^2}\right]^2\left[1 - \frac{2Gm(r)}{rc^2}\right]^{-2}. \quad (139)$$

Note that $dP/d\mathcal{E}$ is the square of the sound speed in units of the speed of light, and, once again, only $P(\mathcal{E})$ is the only EOS relation required. The appearance of the sound speed in a denominator in a term of $Q(r)$ means that the evaluation of y_R is sensitive to how the core-crust interface is treated. Physically unrealistic discontinuities in thermodynamic quantities near the interface will introduce anomalous contributions to y_R, so smoothing the $P(\mathcal{E})$ relation is important.

As for the moment of inertia, it is convenient to introduce the dimensionless tidal deformability

$$\Lambda = \frac{2k_2}{3\beta^5}. \quad (140)$$

Tables IV, X, and XIII give the quantities $\Lambda_{1.2}$, $\Lambda_{1.4}$, and $\Lambda_{1.6}$ for Skyrme, RMF and Gogny forces, respectively.

Λ is known to scale approximately as $(R/M)^6$ [28], rather than as $(R/M)^5$ as suggested by Eq. (140), a result we validate

$$\Lambda_{1.4} = 0.000\,136\,3R_{1.4}^{6.021} \pm 102.7. \quad (141)$$

Thus correlations among $\Lambda_{1.4}$, $R_{1.4}$, and L_2 are expected. These are shown in Figs. 14 and 15, where the relations

$$\ln \Lambda_{1.4} = 1.591(L_2/\text{MeV})^{0.3251} \pm 0.4728 = 0.3605(R_{1.4}/\text{km})^{1.123} \pm 0.2127 \quad (142)$$

are drawn. These relations can be made even more accurate if the restriction $M_{\max} > 2M_\odot$, which also implies $R_{1.4} > 11$ km for the Skyrme and RMF forces used here, is applied, as the right-hand panel of Fig. 15 suggests.

Reference [29] discovered a powerful correlation connecting the dimensionless tidal deformability and moment of inertia. This correlation does not depend on the mass. For the case of $1.4M_\odot$ stars only, in order to limit the number of data points to a legible value, we confirm their result in Fig. 16.

D. Binding energy

In addition to the gravitational mass M of a neutron star, one can consider the total baryon mass $N_B m_B$, where N_B is the number of baryons in the star and m_B is the mass of a single baryon. N_B is defined as [30]

$$N_B = \int_0^R 4\pi r^2\left[1 - \frac{2Gm(r)}{rc^2}\right]^{-1/2} n(r)dr, \quad (143)$$

where $n(r)$ is the baryon number density at r. The binding energy of a neutron star is the energy released during its formation through gravitational collapse, which is

$$\text{BE} = (M_B - M)c^2. \quad (144)$$

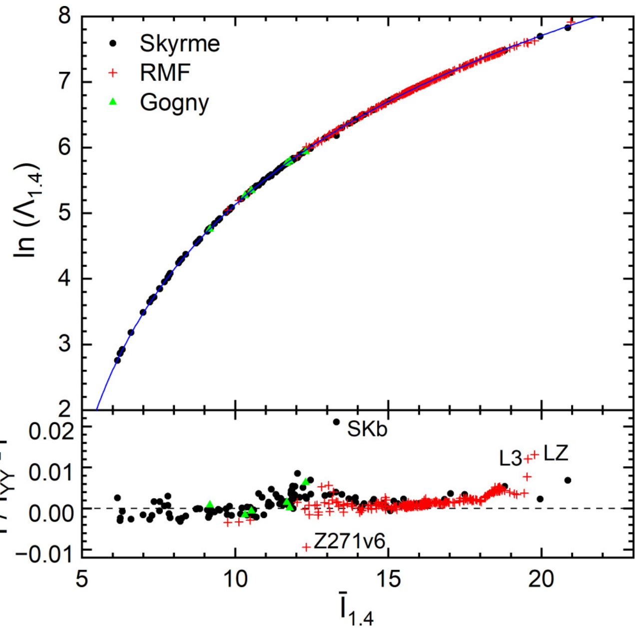

FIG. 16. The relation between tidal deformability and moment of inertia for neutron stars with 1.4 solar mass is shown in the upper panel. The line in the upper panel is the Yagi-Yunes (YY) universal relation [29], and the lower panel shows the deviation from it. Equations of state with the largest deviations, which in no case exceed 2%, are indicated.

Calculation of the binding energy thus requires specification of the baryon density $n(r)$, which is found from the differential equation

$$\frac{d\mathcal{E}}{dn} = \frac{\mathcal{E}+P}{n}, \tag{145}$$

with the boundary condition $\mu_0 = [(\mathcal{E}+P)/n]_{n\to 0} \approx -9$ MeV, the binding energy, per nucleon, of iron. Tables IV, X, and XIII give the quantities $(\mathrm{BE}/Mc^2)_{1.2}$, $(\mathrm{BE}/Mc^2)_{1.4}$, and $(\mathrm{BE}/Mc^2)_{1.6}$ for Skyrme, RMF and Gogny forces, respectively.

The binding energy per unit mass is correlated with L as shown in Fig. 14, where the relation

$$(\mathrm{BE}/Mc^2)_{1.4} = 0.474(L_2/\mathrm{MeV})^{-0.4444} \pm 0.00931 \tag{146}$$

is shown. Since in Newtonian gravity, the binding energy of a uniform sphere is $(3/5)GM^2/R$, and Eq. (130) indicates $R_{1.4} \propto L_2^{0.28}$, one expects an inverse relationship between BE/M and L_2. Correlations between $(\mathrm{BE}/Mc^2)_{1.4}$ and $R_{1.4}$ or $\beta_{1.4}$ have even more significance.

VIII. DISCUSSION AND CONCLUSIONS

In this paper we have compiled a large number of interaction parameters for Skyrme, RMF and Gogny forces, largely culled from the publications of Dutra *et al.* [1,2]. Importantly, we created a complete database of interaction parameters for these forces including Table I (Skyrme), Table V, VI, VII (different types of RMF) and Table XI (Gogny), which are not contained in Refs. [1,2]. This should greatly ease future studies using these force collections. We have given explicit formulas for the calculation of properties for both cold symmetric and pure neutron uniform matter. We have also given prescriptions for calculating symmetry energy parameters, where the symmetry energy is alternately defined as the difference between the symmetric and pure neutron uniform matter energies or as the quadratic term in a Taylor expansion of the uniform matter energy in the neutron excess away from symmetric matter.

In addition, selected properties related to nuclear structure, such as the surface energy, neutron skin thickness, and dipole polarizability were computed for most forces. We compared the approximate liquid droplet model determinations of the neutron skin thicknesses for both ^{48}Ca and ^{208}Pb with those from more accurate Hartree-Fock computations. We found that the high degree of correlation between the neutron skin thickness and L seen in HF computations is remarkably well reproduced by the DM. We also computed the properties of relatively low-mass neutron stars (including radii, moments of inertia, tidal deformabilities and binding energies), which involve computations at densities for which the EOSs included here remain plausibly relevant. The predicted neutron star maximum mass was found for all forces, although we argued that the specific values should be treated with caution since they necessarily involve the properties of matter at densities far in excess of those found in nuclei, which renders their $P(\mathcal{E})$ relations unreliable.

Many of the calculated properties are highly correlated, which can lead to semi-universal relations among them. Those relations involving nuclear structure are very useful in interpreting experiments, while those involving neutron star properties are important in interpreting astronomical observations of neutron stars. Those correlations that cross over between nuclear physics and astrophysics are especially interesting. Figures 17 and 18 show correlation matrices involving many of these parameters for Skyrme and RMF forces, respectively.

A. Correlation matrices

The highest degrees of correlation exist among J_2, L_2, r_{np}(Pb), σ_δ, $R_{1.4}$, $\Lambda_{1.4}$, $\bar{I}_{1.4}$, and $\mathrm{BE}_{1.4}$. In most cases, the correlations are stronger for Skyrme forces than for RMF forces. In particular, this is true for computations of $\mathrm{BE}_{1.4}$, which exhibits only mild correlations with $R_{1.4}$ and none with the other parameters for RMF models. The parameters K_0 and Q_0 are highly correlated, and $K_{\mathrm{sym},2}$ and L_2 are mildly correlated, for both types of forces. For RMF forces, the parameter σ_o is mildly correlated with K_0 and Q_0 but this is not the case for Skyrme forces. For Skyrme forces, the parameters n_0 and E_0 are moderately correlated, but this is not the case for RMF forces.

In many cases where relatively strong correlations exist, we have determined in Secs. VI and VII simple fits with standard deviations which can be regarded as semi-universal relations. We caution that since we do not explicitly consider interactions leading to strong phase transitions in dense matter, those semi-universal relations involving neutron stars in such cases could be violated.

In a future work, there are a number of improvements that could be made, including

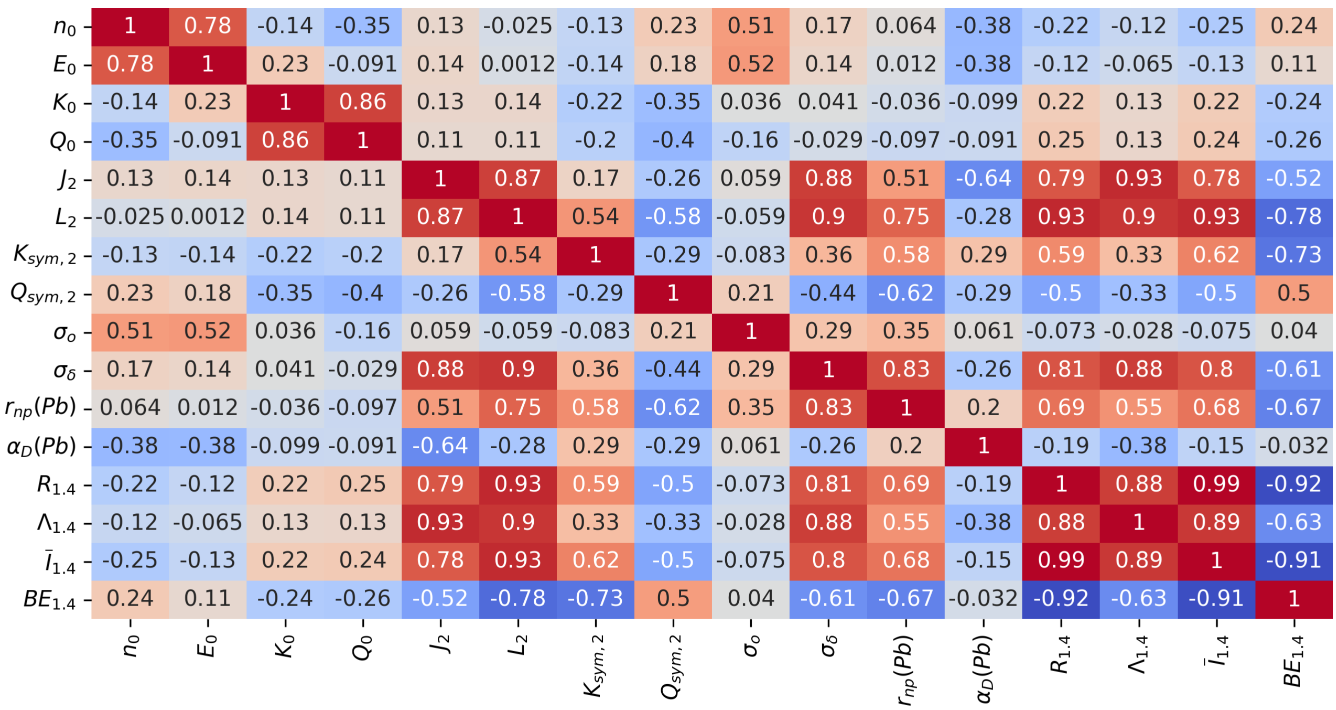

FIG. 17. Correlation matrix for Skyrme forces.

(1) computation of Hartree-Fock values for surface energies, dipole polarizabilities, neutron skin thicknesses and giant resonance frequencies.
(2) inclusion of additional forces, including those in more recent publications and those from the extensive compilation of Ref. [20], who computed HF neutron skin thicknesses for many additional forces but did not tabulate their model parameters.
(3) more detailed explorations of correlations among low-mass neutron star properties and bulk matter properties, not just at the saturation density, but at other densities such as $0.5n_0$, $1.5n_0$, and $2n_0$.

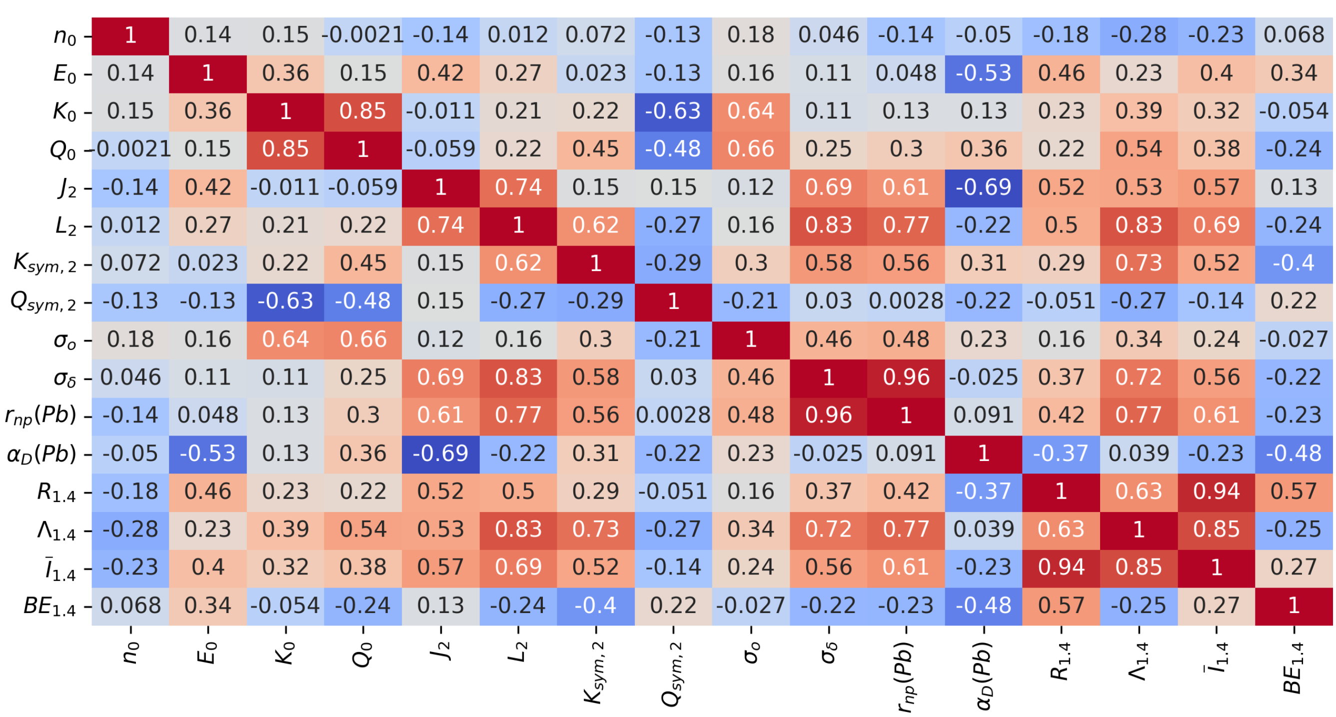

FIG. 18. Correlation matrix for RMF forces.

ACKNOWLEDGMENTS

We acknowledge useful discussions with Yeunhwan Lim and Tianqi Zhao, and thank M. Dutra for providing valuable information, including some interaction parameters from models in Refs. [1,2]. We also thank the anonymous referee for valuable corrections and suggestions, and the CompOSE team as well as Hristijan Kochankovski for proposing the inclusion of additional interactions. Funding for this research was provided by the US Department of Energy under Grant DE-FG02-87ER40317.

APPENDIX A: PARAMETERS AND PROPERTIES OF SKYRME MODELS

This Appendix contains Tables I–IV.

TABLE I. Parameters of Skyrme models. The unit for t_0 is MeV fm^3. t_1 and t_2 are both in MeV fm^5, t_{3i} is in MeV fm$^{3+3\alpha_i}$, and t_4 and t_5 are in MeV fm$^{5+3\delta}$ and MeV fm$^{5+3\gamma}$, respectively. Other parameters are dimensionless.

	t_0	t_1	t_2	t_{31}	t_{32}	t_{33}	t_4	t_5					
Model	x_0	x_1	x_2	x_{31}	x_{32}	x_{33}	x_4	x_5	σ_1	σ_2	σ_3	δ	γ
BSk1 [31]	−1830.45	262.97	−296.446	13444.7					1/3				
	0.599988	−0.5	−0.5	0.823074									
BSk2 [32]	−1790.62	260.996	−147.167	13215.1					0.343295				
	0.498986	−0.08975	0.224411	0.515675									
BSk2′ [32]	−1792.71	259.053	−146.768	13267.9					0.343295				
	0.498612	−0.08976	0.242854	0.509818									
BSk3 [33]	−1755.1297	233.262	−135.284	13543.2					0.361194				
	0.476585	−0.03257	0.470393	0.422501									
BSk4 [34]	−1776.9376	306.884	−105.67	12302.1					1/3				
	0.542594	−0.53517	0.494738	0.759028									
BSk5 [34]	−1778.8934	312.727	−102.883	12318.37					1/3				
	0.44451	−0.48872	0.58459	0.569304									
BSk6 [34]	−2043.3174	382.127	−173.879	12511.7					0.25				
	0.735859	−0.799153	−0.358983	1.234779									
BSk7 [34]	−2044.2484	385.973	−131.525	12518.8					0.25				
	0.729193	−0.932335	−0.050127	1.23628									
BSk8 [35]	−2035.525	398.8208	−196.0032	12433.36					0.25				
	0.773828	−0.822006	−0.38964	1.309331									
BSk9 [36]	−2043.918	411.5987	−194.1886	12497.169					0.25				
	0.51492	−0.953799	−0.332249	0.899435									
BSk10 [37]	−1771.37	322.432	−80.6445	12219					1/3				
	0.266859	−0.461021	1.18713	0.23156									
BSk11 [37]	−1773.9	310.45	−78.3014	12254.7					1/3				
	0.259339	−0.46419	1.14268	0.225045									
BSk12 [37]	−1773.71	309.046	−75.2529	12253.1					1/3				
	0.263418	−0.46164	1.22561	0.229978									
BSk13 [37]	−1773.86	307.766	−73.428	12254.3					1/3				
	0.253076	−0.47147	1.27406	0.215541									
BSk14 [38]	−1822.67	377.47	−2.41056	11406.3					0.3				
	0.302096	−0.82358	61.9411	0.47346									
BSk15 [39]	−1832.91	372.552	17.982	11483					0.3				
	0.436279	−0.78526	−9.53228	0.675865									
BSK16 [7]	−1837.23	383.521	−3.41736	11523					0.3				
	0.4326	−0.82411	44.652	0.689797									
BSK17 [40]	−1837.33	389.102	−3.17417	11523.8					0.3				
	0.411377	−0.8321	49.4875	0.654962									
BSK18 [8]	−1837.96	428.88	−3.23704	11528.9			−400	−400	0.3			1	1
	0.42129	−0.90718	57.7185	0.683926			−2	−2					
BSK19 [41]	−4115.21	403.072	1	23670.4			−60	−90	1/12			1/3	1/12
	0.398848	−0.13796	−1055.55	0.375201			−6	−13					
BSK20 [41]	−4056.04	438.219	1	23256.6			−100	−120	1/12			1/6	1/12
	0.569613	−0.39205	−1147.64	0.614276			−3	−11					

TABLE I. (*Continued.*)

Model	t_0 / x_0	t_1 / x_1	t_2 / x_2	t_{31} / x_{31}	t_{32} / x_{32}	t_{33} / x_{33}	t_4 / x_4	t_5 / x_5	σ_1	σ_2	σ_3	δ	γ
BSK21 [41]	−3961.39	396.131	1	22588.2			−100	−150	1/12			0.5	1/12
	0.885231	0.0648452	−1390.38	1.03928			2	−11					
BSK22 [42]	−3978.97	404.461	1	22704.7			−100	−150	1/12			0.5	1/12
	0.472558	0.062754	−1396.13	0.514386			2	−11					
BSK23 [42]	−3974.58	400.199	1	22676.3			−100	−150	1/12			0.5	1/12
	0.673839	0.062754	−1392.94	0.770751			2	−11					
BSK24 [42]	−3970.29	395.766	1	22648.6			−100	−150	1/12			0.5	1/12
	0.894371	0.056354	−1389.61	1.05119			2	−11					
BSK25 [42]	−4068.39	431.093	1	23342.8			−200	−150	1/12			0.5	1/12
	1.20467	0.111366	−1387.47	1.44777			2	−11					
BSK26 [42]	−4072.53	439.536	1	23369.1			−100	−120	1/12			1/6	1/12
	0.577367	−0.404961	−1147.7	0.624831			−3	−11					
E [43]	−1140.25	309.61	−122.22	11608.1					0.8				
	0.7979			1.632									
Es [43]	−1664.05	358.83	−137.22	10931.5					0.35				
	1.077			1.6918									
f_- [44]	−1848.246	476.7814	−530.4592	14017.936	−4315.172				1/3	2/3			
	0.826263	−0.553989	−0.990625	1.813282	2.27293								
f_+ [44]	−1849.486	478.0776	−324.437	14050.844	−4351.536				1/3	2/3			
	0.826648	0.085961	−0.821841	1.77001	3.932								
f_0 [44]	−1849.082	477.2767	−412.8245	14035.192	−4331.235				1/3	2/3			
	0.824349	−0.137469	−0.91558	1.780474	3.29576								
FPLyon [45]	−2498.9	382.19	−336.96	15230.5					0.18832				
	0.5469	−0.7624	−0.6813	0.8094									
Gs [43]	−1800.16	336.23	−85.74	11113.5					0.3				
	−0.4862			−1.0295									
Gs1 [46]	−1268	887	−77.3	14485			−1853		1			1	
	0.15			1			1						
Gs2 [46]	−1177	670	−49.7	11054			−775		1			1	
	0.124			1			1						
Gs3 [46]	−1037	336	−7.63	5774			883		1			1	
	0.074			1			1						
Gs4 [46]	−1242	760	−146.2	19362			−2157		1			1	
	0.026			1			1						
Gs5 [46]	−1152	543	−118.6	15989			−1079		1			1	
	0.182			1			1						
Gs6 [46]	−1012	209	−76.3	10619			579		1			1	
	0.139			1			1						
GSkI [6]	−1855.45	397.23	264.63	13858.02	−2694.06	−319.86			1/3	2/3	1		
	0.118	−1.7586	−1.8068	0.1261	−1.1881	−0.4594							
GSkII [6]	−1855.99	393.08	266.08	13842.9	−2689.68				1/3	2/3			
	0.0909	−0.7203	−1.8369	−0.1005	−0.3529								
KDE [47]	−2532.8842	403.7285	−394.5578	14575.0234					0.169				
	0.7707	−0.5229	−0.8956	1.1716									
KDE0v [47]	−2526.511	430.9418	−398.3775	14235.5193					0.1676				
	0.7583	−0.3087	−0.9495	1.1445									
KDE0v1 [47]	−2553.0843	411.6963	−419.8712	14603.6069					0.1673				
	0.6483	−0.3472	−0.9268	0.9475									
LNS [48]	−2484.97	266.735	−337.135	14588.2					1/6				
	0.06277	0.65845	−0.95382	−0.03413									
MSk1 [49]	−1813.03	274.828	−274.828	13050.1					1/3				
	0.365395	−0.5	−0.5	0.449882									
MSk2 [49]	−1830.67	260.301	−293.742	13442.1					1/3				
	0.356875	−0.5	−0.5	0.409759									
MSk3 [49]	−1810.32	269.092	−269.092	13027.5					1/3				
	0.631485	−0.5	−0.5	0.90368									

TABLE I. (*Continued.*)

	t_0	t_1	t_2	t_{31}	t_{32}	t_{33}	t_4	t_5					
Model	x_0	x_1	x_2	x_{31}	x_{32}	x_{33}	x_4	x_5	σ_1	σ_2	σ_3	δ	γ
MSk4 [49]	−1827.96	254.129	−287.569	13419.5					1/3				
	0.61036	−0.5	−0.5	0.835063									
MSk5 [49]	−1827.96	254.326	−287.766	13419.5					1/3				
	0.605152	−0.5	−0.5	0.827182									
MSk5*[50]	−1728.73	362.859	−126.139	11084.8					1/3				
	0.647	−0.1	−0.145864	0.994321									
MSk6 [49]	−1827.96	258.483	−291.924	13419.5					1/3				
	0.576591	−0.5	−0.5	0.783956									
MSk7 [51]	−1828.23	259.4	−292.84	13421.7					1/3				
	0.576761	−0.5	−0.5	0.78529									
MSk8 [51]	−1844.2	242.743	−306.583	13777.5					1/3				
	0.574829	−0.5	−0.5	0.752727									
MSk9 [51]	−1810.73	273.844	−273.844	13030.9					1/3				
	0.5846	−0.5	−0.5	0.831332									
MSkA [52]	−1218.828	370.265	−106.883	10834.819					0.7179				
	0.119	0.0157	0.0335	−0.199									
MSL0 [53]	−2118.06	395.196	−63.9531	12857.7					0.235879				
	−0.0709496	−0.332282	1.3583	−0.228181									
NRAPR [9]	−2719.7	417.64	−66.687	15042					0.14416				
	0.16154	−0.047986	0.02717	0.13611									
PRC45 [54]	−1089			17480.4					1				
	0.5			−0.5									
RATP [55]	−2160	513	121	11600					0.2				
	0.418	−0.36	−2.29	0.586									
Rs [43]	−1798	335.97	−84.81	11083.9					0.3				
	−0.4036			−0.8705									
SAMi [56]	−1877.75	475.6	−85.2	10219.6					0.25614				
	0.32	−0.532	−0.014	0.688									
SAMi-T [56]	−2199.38	533.036	−88.1692	11293.5					0.17955				
	0.51471	−0.531674	−0.02634	0.944603									
Sefm068 [45]	−2010.772	450.169	149.831	10974.273					0.227111				
	0.325938	−0.344503	−1.901577	−0.790546									
Sefm074 [45]	−1846.054	389.115	110.885	10809.466					0.276096				
	−0.323949	−0.332954	−2.258584	−0.799724									
Sefm081 [45]	−1798.334	330.052	69.948	11262.011					0.3				
	−0.333179	−0.31821	−3.073331	−0.777484									
Sefm09 [45]	−1663.007	267.154	28.846	11388.487					0.353679				
	−0.337644	−0.29787	−6.116109	−0.772582									
Sefm1 [45]	−1600.735	205.894	−13.894	11875.792					0.386048				
	−0.350069	−0.26687	9.864514	−0.746603									
SGI [57]	−1603	515.9	84.5	8000					1/3				
	−0.02	−0.5	−1.731	0.1381									
SGII [57]	−2645	340	−41.9	15595					1/6				
	0.09	−0.0588	1.425	0.06044									
SGOI [58]	−1089	558.8	−83.7	8272					1				
	0.412												
SGOII [58]	−2248	558.8	−83.7	11224					1/6				
	0.715												
SI [5]	−1057.3	235.9	−100	14463.5					1				
	0.56			1									
SI′ [59]	−1057.3	235.9	−100	14463.5					1				
	0.2885			0.2257									
SII [5]	−1169.9	585.6	−27.1	9331.1					1				
	0.34			1									
SIII [60]	−1128.75	395	−95	14000					1				
	0.45			1									

TABLE I. (*Continued.*)

Model	t_0	t_1	t_2	t_{31}	t_{32}	t_{33}	t_4	t_5	σ_1	σ_2	σ_3	δ	γ
	x_0	x_1	x_2	x_{31}	x_{32}	x_{33}	x_4	x_5					
SIII*[61]	−1121	400	−533.33	14000					1				
	0.43225	0.35	−0.9875	1									
SIV [60]	−1205.6	765	35	5000					1				
	0.05			1									
SK255 [62]	−1689.35	389.3	−126.07	10989.6					0.3563				
	−0.1461	0.116	0.0012	−0.7449									
SK272 [62]	−1496.84	397.66	−112.82	10191.64					0.4492				
	0.0008	0.0102	0.002	−0.5519									
SKa [63]	−1602.78	570.88	−67.7	8000					1/3				
	−0.02			−0.286									
Ska25s20 [45]	−2180.5	281.5	−160.4	14577.8					0.25				
	0.14	−0.8		0.06									
Ska35s15 [45]	−1768.97	249.37	−155.56	12978.71					0.35				
	0.42553	−0.8		0.5274									
Ska35s20 [45]	−1768.8	263.9	−158.3	12904.8					0.35				
	0.13	−0.8		0.01									
Ska35s25 [45]	−1772.73	276.85	−162.36	12899.78					0.35				
	−0.14393	−0.8		−0.49481									
Ska45s20 [45]	−1537.89	245.47	−157.2	12461.12					0.45				
	0.12318	−0.8		−0.05608									
SKb [63]	−1602.78	570.88	−67.7	8000					1/3				
	−0.165			−0.286									
SkI1 [64]	−1913.619	439.809	2697.594	10592.267					0.25				
	−0.954536	−5.782388	−1.287379	−1.561421									
SkI2 [64]	−1915.43	438.449	305.446	10548.9					0.25				
	−0.2108	−1.7376	−1.5336	−0.178									
SkI3 [64]	−1762.88	561.608	−227.09	8106.2					0.25				
	0.3083	−1.1722	−1.0907	1.2926									
SkI4 [64]	−1855.827	473.829	1006.855	9703.607					0.25				
	0.405082	−2.889148	−1.32515	1.145203									
SkI5 [64]	−1772.91	550.84	−126.685	8206.25					0.25				
	−0.1171	−1.3088	−1.0487	0.341									
SkI6 [65]	−1849.347	483.913	528.43	9553.404					0.25				
	0.491825	−2.137409	−1.381416	1.337188									
SkM [66]	−2645	385	−120	15595					1/6				
	0.09												
SkM1 [67]	−2645	410	−135	15595					1/6				
	1.3			1.734									
SkM*[68]	−2645	410	−135	15595					1/6				
	0.09												
SkMP [69]	−2372.24	503.623	57.2783	12585.3					1/6				
	−0.157563	−0.402886	−2.95571	−0.267933									
SkO [70]	−2103.653	303.352	791.674	13553.252					0.25				
	−0.210701	−2.810752	−1.461595	−0.429881									
SkO′ [70]	−2099.419	301.531	154.781	13526.464					0.25				
	−0.029503	−1.325732	−2.323439	−0.147404									
SkP [71]	−2931.7	320.62	−337.41	18708.97					1/6				
	0.29215	0.65318	−0.53732	0.18103									
SKRA [72]	−2895.4	405.5	−89.1	16660					0.1422				
	0.08		0.2										
SkS1 [73]	−2013.4	359.8	−171.9	12754					0.2601				
	0.15	0.456	−0.179	−0.049									
SkS2 [73]	−2015.9	364.6	−49	12755					0.2602				
	−0.106	0.874	2.52	−0.615									
SkS3 [73]	−2014.7	361	−29.5	12756					0.2604				
	−0.319	0.732	4.95	−0.904									

TABLE I. (*Continued.*)

Model	t_0	t_1	t_2	t_{31}	t_{32}	t_{33}	t_4	t_5					
	x_0	x_1	x_2	x_{31}	x_{32}	x_{33}	x_4	x_5	σ_1	σ_2	σ_3	δ	γ
SkS4 [73]	−2011.7	348.7	−317	12781					0.2597				
	0.256	0.675	−0.67	0.144									
SkSC1 [74]	−1788.59	282.623	−282.623	12775.3					1/3				
	0.72	−0.5	−0.5	1.04564									
SkSC2 [74]	−1791.64	290.601	−290.601	12800.6					1/3				
	0.38	−0.5	−0.5	0.59276									
SkSC3 [74]	−1788.11	289.901	−96.6337	12771.4					1/3				
	0.65	−1	1	0.960976									
SkSC4 [75]	−1789.42	283.467	−283.467	12782.42					1/3				
	0.79	−0.5	−0.5	1.13871									
SkSC4o [76]	−1788.76	283.037	−283.037	12775					1/3				
	0.79434	−0.5	−0.5	1.18439									
SkSC5 [77]	−1788.17	281.931	−281.931	12771.9					1/3				
	0.98	−0.5	−0.5	1.38526									
SkSC6 [77]	−1792.47	291.964	−291.964	12805.7					1/3				
	0.370038	−0.5	−0.5	0.581085									
SkSC10 [77]	−1795.12	298.95	−298.95	12827.7					1/3				
	0.159124	−0.5	−0.5	0.292918									
SkSC11 [78]	−1789.42	283.467	−283.467	12782.3					1/3				
	0.79	−0.5	−0.5	1.13871									
SkSC14 [76]	−1792.47	291.334	−291.334	12805.7					1/3				
	0.364025	−0.5	−0.5	0.455431									
SkSC15 [76]	−1789.81	285.6	−285.6	12783.7					1/3				
	0.621299	−0.5	−0.5	0.895573									
SkSP.1 [50]	−1507.6	−632.324	−483.786	23288	−28415.5		2332.61		0.55	1.1		0.4	
	0.533774	1.68964	−0.75	0.933215	1		1						
SkT [79]	−1144.7	402.1	56.1	9656.3					1				
	0.07			1									
SkT1a [45]	−1794	298	−298	12812					1/3				
	0.154	−0.5	−0.5	0.089									
SkT2a [45]	−1791.6	300	−300	12792					1/3				
	0.154	−0.5	−0.5	0.089									
SkT3a [45]	−1791.8	298	−99.5	12794					1/3				
	0.138	−1	1	0.075									
SkT4a [45]	−1808.8	303.4	−303.4	12980					1/3				
	−0.177	−0.5	−0.5	−0.5									
SkT5a [45]	−2917.1	328.2	−328.2	18584					1/6				
	−0.295	−0.5	−0.5	−0.5									
SkT6a [45]	−1794.2	294	−294	12817					1/3				
	0.392	−0.5	−0.5	0.5									
SkT7a [45]	−1892.5	366.6	−21	11983					0.285				
	0.334	−0.359	6.9	0.366									
SkT8a [45]	−1892.5	367	−228.76	11983					0.285				
	0.448	−0.5	−0.5	0.695									
SkT9a [45]	−1891.4	377.4	−239.16	11982					0.285				
	0.441	−0.5	−0.5	0.686									
SkTK [80]	−2248	558.8	−83.7	11224					1/6				
	0.715			1									
SKX [81]	−1445.32	246.867	−131.786	12103.86					0.5				
	0.34	0.58	0.127	0.03									
Skχ414 [82]	−1734.0261	255.655	−264.0678	12219.5884	556.132				1/3	1			
	0.4679	−0.5756	−0.3955	0.7687	−15.8761								
Skχ450 [82]	−1803.2928	301.8208	−273.2827	12783.8619	564.1049				1/3	1			
	0.443	−0.3622	−0.4105	0.6545	−11.316								
Skχ500 [82]	−1747.4826	241.3197	−331.0412	12491.5053	405.0317				1/3	1			
	0.5953	−1.1589	−0.5843	1.2005	−25.4938								

TABLE I. (*Continued.*)

Model	t_0 x_0	t_1 x_1	t_2 x_2	t_{31} x_{31}	t_{32} x_{32}	t_{33} x_{33}	t_4 x_4	t_5 x_5	σ_1	σ_2	σ_3	δ	γ
SKXce [81]	−1438	244.3	−133.7	12116.3					0.5				
	0.288	0.611	0.145	−0.056									
Skxcsb [83]	−1437.353	238.39	−111.766	12157.747					0.5				
	0.348	−0.845	0.407	0.373									
SKXm [81]	−1803.1	273.8	−95.9	12755.1					1/3				
	0.306	0.225	0.698	0.116									
Skxs15 [84]	−2883.29	291.6	−314.89	18239.55					1/6				
	0.4762	−0.25433	−0.61109	0.52936									
Skxs20 [84]	−2885.24	302.73	−323.42	18237.49					1/6				
	0.13746	−0.25548	−0.60744	0.05428									
Skxs25 [84]	−2887.81	315.5	−329.3	18229.81					1/6				
	−0.18594	−0.24766	−0.60119	−0.40902									
Skxta [83]	−1443.18	257.229	−137.843	12139.42					1/2				
	0.341	0.58	0.167	0									
Skxtb [83]	−1446.8	250.9	−133	12127.6					1/2				
	0.329	0.518	0.139	0.018									
Skz−1 [85]	−2471.1	439.85	−299.14	13732.8					0.1694				
	−0.2665	1.2968	−0.8899	−0.7282									
Skz0 [85]	−2471.1	439.85	−258.18	13732.8					0.1694				
	0.1986	1.0413	−0.8328										
Skz1 [85]	−2471.1	439.85	−262.98	13732.8					0.1694				
	0.6052	0.4933	−0.8404	0.7282									
Skz2 [85]	−2471.1	439.85	−267.78	13732.8					0.1694				
	1.029	0.0546	−0.8478	1.4564									
Skz3 [85]	−2471.1	439.85	−272.66	13732.8					0.1694				
	1.4174	−0.6082	−0.8549	2.1846									
Skz4 [85]	−2471.1	439.85	−277.5	13732.8					0.1694				
	1.8226	−1.164	−0.8618	2.9127									
SLy0 [86]	−2486.43	485.25	−440.46	13783					1/6				
	0.7947	−0.4983	−0.9323	1.2893									
SLy1 [86]	−2487.64	488.29	−568.86	13791					1/6				
	0.7955	−0.3056	−1	1.2902									
SLy2 [86]	−2484.23	482.19	−289.95	13763					1/6				
	0.7893	−0.7279	−0.7754	1.2824									
SLy230a [87]	−2490.23	489.53	−566.58	13803					1/6				
	1.1318	−0.8426	−1	1.9219									
SLy230b [87]	−2488.91	486.82	−546.39	13777					1/6				
	0.834	−0.3438	−1	1.3539									
SLy3 [86]	−2481.1	481	−540.8	13731					1/6				
	0.838	−0.3381	−1	1.3578									
SLy4 [88]	−2488.91	486.82	−546.39	13777					1/6				
	0.834	−0.3438	−1	1.354									
SLy5 [88]	−2484.88	483.13	−549.4	13763					1/6				
	0.778	−0.328	−1	1.267									
SLy6 [88]	−2479.5	462.18	−448.61	13673					1/6				
	0.825	−0.465	−1	1.355									
SLy7 [88]	−2482.41	457.97	−419.85	13677					1/6				
	0.846	−0.511	−1	1.391									
SLy8 [86]	−2481.4	480.8	−538.3	13731					1/6				
	0.8	−0.34	−1	1.31									
SLy9 [86]	−2511.1	510.6	−429.8	13716					1/6				
	0.8	−0.62	−1	1.3701									
SLy10 [88]	−2506.77	430.98	−304.95	13826.41					1/6				
	1.0398	−0.6745	−1	1.6833									
SQMC1 [89]	−1071	651	−352	16620					1				
	0.89			1									

TABLE I. (*Continued.*)

Model	t_0 x_0	t_1 x_1	t_2 x_2	t_{31} x_{31}	t_{32} x_{32}	t_{33} x_{33}	t_4 x_4	t_5 x_5	σ_1	σ_2	σ_3	δ	γ
SQMC2 [89]	−1082	400	−146	14926					1				
	0.59			1									
SQMC3 [89]	−1047	373	−136	12531					1				
	0.61			1									
SQMC600 [90]	−2510.0376	520.9512	−221.0096	14651.7525					1/6				
	0.17												
SQMC650 [90]	−2462.6784	436.0993	−151.9441	14154.4809					1/6				
	0.13												
SQMC700 [90]	−2429.1323	370.9804	−96.6917	13773.634					1/6				
	0.1												
SQMC750 [90]	−2403.4794	319.6746	−55.2524	13473.6924					1/6				
	0.08												
SSK [6]	−2523.52	435	−382.04	14234.94					0.1682				
	0.6835	−0.4519	−0.9214	1.0508									
SV [60]	−1248.29	970.56	107.22						1				
	−0.17			1									
SV-bas [91]	−1879.64	313.749	112.677	12527.4					0.3				
	0.258546	−0.381689	−2.82364	0.123229									
SV-min [91]	−2112.25	295.781	142.268	13988.6					0.255368				
	0.243886	−1.43493	−2.6259	0.25807									
SVI [60]	−1101.81	271.67	−138.33	17000					1				
	0.583			1									
SVII [61]	−1096.8	246.2	−148	17626					1				
	0.62			1									
SV-K218 [91]	−2295.82	320.278	330.798	14557.2					0.22				
	0.191803	−0.925134	−1.80081	0.068066									
SV-K226 [91]	−2055.77	317.043	247.652	13344.4					0.26				
	0.217498	−0.717223	−1.97595	0.0819									
SV-K241 [91]	−1745.18	310.497	5.7047	11975.6					0.34				
	0.291787	−0.10699	−31.9044	0.157335									
SV-Kap00 [91]	−1877.891	312.6	7.104	12509.993					0.3				
	0.393391	−1.45482	−26.089659	0.640506									
SV-Kap02 [91]	−1878.883	313.245	44.042	12519.929					0.3				
	0.331398	−0.879672	−5.267351	0.390236									
SV-Kap06 [91]	−1880.594	314.373	194.94	12537.049					0.3				
	0.183805	0.082542	−2.16197	−0.146674									
SV-mas07 [91]	−2203.66	438.349	566.846	12222.7					0.2				
	0.354369	−1.78294	−1.43693	0.632534									
SV-mas08 [91]	−1982.65	368.228	274.611	12141.1					0.26				
	0.285653	−1.0374	−1.78083	0.339364									
SV-mas10 [91]	−1813.91	270.452	57.2151	12965.5					0.33				
	0.232898	0.127181	−4.7952	−0.062346									
SV-sym28 [91]	−1877.431	307.255	140.868	12511.94					0.3				
	0.517821	−0.431291	−2.474137	0.568794									
SV-sym32 [91]	−1883.28	319.184	197.329	12559.5					0.3				
	0.007688	−0.594307	−2.16921	−0.309537									
SV-sym34 [91]	−1887.37	323.804	351.782	12597.3					0.3				
	−0.23011	−0.959586	−1.77548	−0.721854									
SV-tls [91]	−1879.892	317.952	30.265	12531.858					0.3				
	0.246413	−0.197627	−7.212765	0.103793									
T [43]	−1788.9	301.5	502.5	12764					1/3				
	0.353	−2.5	−1.7	0.475									
T1 [92]	−1794	298	−298	12812					1/3				
	0.154	−0.5	−0.5	0.089									
T11 [93]	−2484.69	480.674	−522.233	13785.81					1/6				
	0.734532	−0.357956	−0.981127	1.195657									

TABLE I. (*Continued.*)

Model	t_0 x_0	t_1 x_1	t_2 x_2	t_{31} x_{31}	t_{32} x_{32}	t_{33} x_{33}	t_4 x_4	t_5 x_5	σ_1	σ_2	σ_3	δ	γ
T12 [93]	−2482.571	480.605	−523.692	13762.34					1/6				
	0.741577	−0.3579	−0.98452	1.208913									
T13 [93]	−2481.315	480.343	−531.133	13749.16					1/6				
	0.741208	−0.346965	−0.989822	1.209875									
T14 [93]	−2479.458	479.87	−530.397	13732.47					1/6				
	0.744308	−0.348138	−0.9909	1.215762									
T15 [93]	−2482.479	478.923	−317.302	13764.91					1/6				
	0.733926	−0.677015	−0.813783	1.196671									
T16 [93]	−2485.64	481.672	−316.779	13791.07					1/6				
	0.736004	−0.680207	−0.805749	1.198185									
T1*[92]	−1800.5	296	−296	12884					1/3				
	0.157	−0.5	−0.5	0.092									
T2 [92]	−1791.6	300	−300	12792					1/3				
	0.154	−0.5	−0.5	0.089									
T21 [93]	−2486.26	484.633	−445.88	13807.35					1/6				
	0.721464	−0.480492	−0.924422	1.173067									
T22 [93]	−2484.397	484.495	−471.454	13786.97					1/6				
	0.73012	−0.442635	−0.944655	1.188194									
T23 [93]	−2483.501	484.291	−440.089	13776.29					1/6				
	0.732464	−0.492071	−0.924856	1.1931									
T24 [93]	−2482.931	484.346	−433.185	13768.56					1/6				
	0.729639	−0.503889	−0.921044	1.190192									
T25 [93]	−2480.434	485.519	−478.822	13735.27					1/6				
	0.754456	−0.439566	−0.956135	1.231884									
T26 [93]	−2476.673	484.49	−482.591	13699.04					1/6				
	0.767612	−0.434554	−0.962725	1.254753									
T3 [93]	−1791.8	298.5	−99.5	12794					1/3				
	0.138	−1	1	0.075									
T31 [93]	−2486.963	490.158	−418.307	13808.78					1/6				
	0.724547	−0.532406	−0.89494	1.178613									
T32 [93]	−2486.155	489.073	−438.565	13804.97					1/6				
	0.712439	−0.499144	−0.912063	1.16036									
T33 [93]	−2486.688	489.683	−405.609	13804.2					1/6				
	0.728149	−0.551901	−0.885872	1.184753									
T34 [93]	−2485.496	488.412	−351.129	13799.05					1/6				
	0.716858	−0.632712	−0.829737	1.167295									
T35 [93]	−2483.136	490.586	−377.114	13762.06					1/6				
	0.74039	−0.6014	−0.863924	1.208476									
T36 [93]	−2478.946	488.365	−427.188	13729.53					1/6				
	0.752195	−0.522097	−0.912891	1.22718									
T3*[92]	−1800.5	296	−98.67	12884					1/3				
	0.142	−1	1	0.076									
T4 [92]	−1808.8	303.4	−303.4	12980					1/3				
	−0.177	−0.5	−0.5	−0.5									
T41 [93]	−2492.261	494.721	−262.766	13874.45					1/6				
	0.689383	−0.767147	−0.653878	1.117874									
T42 [93]	−2492.153	494.635	−251.272	13869.06					1/6				
	0.690625	−0.785802	−0.630399	1.121129									
T43 [93]	−2490.275	494.608	−255.534	13847.12					1/6				
	0.698702	−0.781655	−0.646302	1.135795									
T44 [93]	−2485.67	494.477	−337.961	13794.75					1/6				
	0.721557	−0.661848	−0.803184	1.175908									
T45 [93]	−2485.014	492.671	−304.046	13793.28					1/6				
	0.727016	−0.710368	−0.755428	1.182969									
T46 [93]	−2484.405	495.225	−356.435	13769.07					1/6				
	0.735176	−0.639443	−0.833399	1.201318									

TABLE I. (*Continued.*)

Model	t_0	t_1	t_2	t_{31}	t_{32}	t_{33}	t_4	t_5					
	x_0	x_1	x_2	x_{31}	x_{32}	x_{33}	x_4	x_5	σ_1	σ_2	σ_3	δ	γ
T5 [92]	−2917.1	328.2	−328.2	18584					1/6				
	−0.295	−0.5	−0.5	−0.5									
T51 [93]	−2492.67	500.414	−272.332	13871.38					1/6				
	0.691985	−0.760015	−0.663662	1.123486									
T52 [93]	−2494.783	499.204	−141.125	13886.86					1/6				
	0.692186	−0.955937	−0.126512	1.123414									
T53 [93]	−2486.978	499.333	−363.964	13807.83					1/6				
	0.719761	−0.627515	−0.823595	1.171935									
T54 [93]	−2489.087	497.774	−248.404	13829.43					1/6				
	0.710724	−0.797929	−0.625993	1.156397									
T55 [93]	−2487.084	497.823	−227.658	13815.23					1/6				
	0.711011	−0.829103	−0.567634	1.157022									
T56 [93]	−2484.179	497.603	−258.182	13775.24					1/6				
	0.725926	−0.788228	−0.661928	1.185298									
T6 [93]	−1794.2	294	−294	12817					1/3				
	0.392	−0.5	−0.5	0.5									
T61 [93]	−2494.625	501.033	−125.512	13895.88					1/6				
	0.683145	−0.977518	0.040183	1.1071									
T62 [93]	−2495.048	499.981	−197.374	13901.24					1/6				
	0.690739	−0.86851	−0.431559	1.117413									
T63 [93]	−2492.495	500.627	−121.265	13875.17					1/6				
	0.680914	−0.985108	0.07644	1.105776									
T64 [93]	−2487.323	501.096	−284.539	13818.03					1/6				
	0.70532	−0.74642	−0.694782	1.148322									
T65 [93]	−2489.413	497.52	−194.992	13841.04					1/6				
	0.699857	−0.875605	−0.446926	1.137559									
T66 [93]	−2485.363	500.799	−228.479	13794.56					1/6				
	0.715164	−0.832653	−0.56642	1.165944									
T7 [92]	−1892.5	366.6	−21	11983					0.285				
	0.334	−0.359	6.9	0.366									
T8 [92]	−1892.5	367	−228.76	11983					0.285				
	0.448	−0.5	−0.5	0.695									
T9 [92]	−1891.4	377.4	−239.16	11982					0.285				
	0.441	−0.5	−0.5	0.686									
UNEDF0 [94]	−1883.688	277.5002	608.4309	13901.948					0.321956				
	0.009744	−1.777844	−1.67699	−0.38079									
UNEDF1 [94]	−2078.328	239.4008	1575.1195	14263.646					0.270018				
	0.053757	−5.077232	−1.366506	−0.162491									
v070 [95]	−1828.64	248.527	−176.49	13425.1					1/3				
	0.517539	1.2	−0.051769	0.329698									
v075 [95]	−1828.64	252.349	−171.327	13425.1					1/3				
	0.521301	0.75	0.001069	0.408383									
v080 [95]	−1827.96	251.271	−168.233	13419.5					1/3				
	0.528552	0.4	0.019271	0.483059									
v090 [95]	−1827.96	253.565	−199.305	13419.5					1/3				
	0.559906	−0.1	−0.169977	0.637001									
v100 [95]	−1827.96	253.702	−220.261	13419.5					1/3				
	0.564938	−0.5	−0.272269	0.729808									
v105 [95]	−1827.96	253.114	−286.554	13419.5					1/3				
	0.611956	−0.5	−0.5	0.837479									
v110 [95]	−1827.96	252.949	−347.19	13419.5					1/3				
	0.627871	−0.5	−0.631341	0.894757									
Z [43]	−1137.57	284.67	−92.73	11269.5					0.8				
	0.926			2.1561									
ZR1a [54]	−1003.9			13287.2					1				
				1									

TABLE I. (*Continued.*)

Model	t_0	t_1	t_2	t_{31}	t_{32}	t_{33}	t_4	t_5					
	x_0	x_1	x_2	x_{31}	x_{32}	x_{33}	x_4	x_5	σ_1	σ_2	σ_3	δ	γ
ZR1b [54]	−1003.9			13287.2					1				
	0.2			1									
ZR1c [54]	−1003.9			13287.2					1				
	0.5			1									
ZR2a [54]	−1192.2			11041					2/3				
				1									
ZR2b [54]	−1192.2			11041					2/3				
	0.2			1									
ZR2c [54]	−1192.2			11041					2/3				
	0.5			1									
ZR3a [54]	−4392.2			26967.3					0.1				
				1									
ZR3b [54]	−4392.2			26967.3					0.1				
	0.2			1									
ZR3c [54]	−4392.2			26967.3					0.1				
	0.5			1									
Zs [43]	−1983.76	362.25	−104.27	11861.4					0.25				
	1.1717			1.762									
Zs*[43]	−1987.64	380.92	−109.88	11837.7					0.25				
	0.8897			1.278									

TABLE II. Properties of Skyrme models at their saturation densities. Entries are in MeV except for the saturation density n_0, which has units of fm^{-3}.

Model	n_0	E_0	K_0	Q_0	J_1	J_2	L_1	L_2	$K_{\mathrm{sym},1}$	$K_{\mathrm{sym},2}$	$Q_{\mathrm{sym},1}$	$Q_{\mathrm{sym},2}$
BSk1	0.1574	−15.82	231.45	−385.93	28.46	27.80	8.37	7.14	−283.67	−281.95	612.56	606.67
BSk2	0.1575	−15.81	233.80	−380.40	29.01	27.99	10.94	7.93	−295.26	−297.10	560.42	558.09
BSk2′	0.1575	−15.81	233.47	−381.19	29.01	27.99	10.74	7.74	−296.33	−298.15	561.17	558.81
BSk3	0.1575	−15.82	234.95	−381.17	28.94	27.93	9.72	6.73	−305.24	−307.04	552.91	550.53
BSk4	0.1575	−15.79	236.99	−367.49	28.91	27.99	14.97	12.50	−265.27	−266.04	561.99	558.58
BSk5	0.1575	−15.82	237.34	−368.19	29.64	28.69	24.02	21.38	−239.28	−240.39	503.14	500.08
BSk6	0.1575	−15.76	229.29	−370.96	28.72	27.99	18.33	16.81	−216.39	−215.26	609.03	603.72
BSk7	0.1575	−15.77	229.41	−371.24	28.69	27.99	19.33	17.95	−210.84	−209.42	603.94	598.33
BSk8	0.1590	−15.84	230.46	−372.71	28.69	27.99	16.20	14.82	−222.38	−220.95	630.71	625.08
BSk9	0.1590	−15.94	231.58	−375.25	30.61	30.00	40.86	39.87	−147.60	−145.37	482.30	475.87
BSk10	0.1593	−15.92	238.99	−370.67	31.01	30.00	40.17	37.22	−193.27	−194.97	399.61	397.10
BSk11	0.1586	−15.87	238.24	−369.51	30.99	30.00	41.20	38.33	−188.34	−189.88	392.91	390.25
BSk12	0.1586	−15.87	238.21	−369.44	30.99	30.00	40.87	37.98	−189.85	−191.42	395.26	392.64
BSk13	0.1586	−15.87	238.24	−369.50	30.99	30.00	41.66	38.80	−186.45	−187.97	389.34	386.67
BSk14	0.1586	−15.87	239.48	−358.99	30.92	30.00	46.40	43.89	−151.24	−152.06	391.73	388.36
BSk15	0.1590	−16.05	241.72	−363.46	30.97	30.00	36.32	33.57	−193.12	−194.41	469.55	466.64
BSk16	0.1586	−16.07	241.83	−363.90	30.92	30.00	37.38	34.85	−186.58	−187.43	465.36	462.01
BSk17	0.1586	−16.07	241.84	−363.94	30.92	30.00	38.78	36.26	−181.05	−181.89	453.95	450.59
BSk18	0.1586	−16.08	241.94	−364.14	30.89	30.00	38.58	36.19	−180.37	−180.96	458.26	454.64
BSk19	0.1592	−16.04	236.75	−297.20	31.58	30.01	38.14	32.22	−181.53	−190.25	469.99	470.87
BSk20	0.1592	−16.04	240.78	−281.65	31.38	30.00	42.41	37.63	−130.32	−135.71	546.46	547.39
BSk21	0.1578	−16.02	245.22	−273.51	31.14	29.99	49.85	46.67	−37.73	−37.18	703.05	706.92
BSk22	0.1574	−16.05	245.33	−274.96	33.13	31.97	71.75	68.50	12.48	12.87	556.91	560.93
BSk23	0.1574	−16.03	245.15	−274.43	32.11	30.96	60.92	57.71	−12.10	−11.62	627.75	631.68
BSk24	0.1574	−16.01	244.95	−273.90	31.13	29.99	49.65	46.52	−38.20	−37.58	704.33	708.11
BSk25	0.1583	−15.99	235.51	−315.64	30.04	29.00	39.39	37.04	−32.95	−28.72	875.11	882.36

TABLE II. (*Continued.*)

Model	n_0	E_0	K_0	Q_0	J_1	J_2	L_1	L_2	$K_{\mathrm{sym},1}$	$K_{\mathrm{sym},2}$	$Q_{\mathrm{sym},1}$	$Q_{\mathrm{sym},2}$
BSk26	0.1585	−16.03	240.20	−282.30	31.36	30.00	42.44	37.73	−129.63	−134.89	546.51	547.33
E	0.1592	−16.14	333.65	−63.91	28.82	27.65	−27.59	−31.34	−567.67	−570.96	449.64	448.72
Es	0.1628	−16.03	248.76	−352.73	27.71	26.43	−32.68	−36.94	−453.70	−457.96	880.35	880.34
f−	0.1616	−16.04	230.16	−405.28	32.52	32.00	44.25	43.77	−108.35	−105.06	662.63	655.08
f+	0.1619	−16.06	230.16	−406.52	33.31	32.00	45.98	41.52	−113.31	−117.97	660.86	661.26
f0	0.1617	−16.05	230.16	−405.80	33.01	32.00	45.35	42.40	−111.75	−113.40	660.15	657.55
FPLyon	0.1619	−15.94	217.18	−399.79	31.49	30.93	43.43	42.75	−138.51	−135.62	493.06	485.92
Gs	0.1576	−15.60	237.39	−349.03	32.61	31.38	98.12	94.03	18.01	14.00	−26.66	−26.83
Gs1	0.1592	−16.04	235.19	−813.11	30.09	28.86	51.17	50.22	−85.17	−57.91	872.82	966.14
Gs2	0.1590	−16.03	300.30	−322.05	27.42	25.96	34.15	30.24	−195.63	−188.82	426.93	467.95
Gs3	0.1821	−20.10	505.31	620.22	19.11	16.94	−32.20	−42.89	−536.79	−570.58	−359.37	−415.26
Gs4	0.1585	−15.97	235.25	−847.51	13.60	12.83	−20.55	−18.75	−197.88	−161.39	1019.21	1121.95
Gs5	0.1579	−15.92	299.36	−358.97	19.69	18.69	−11.08	−12.19	−306.91	−290.75	575.05	625.73
Gs6	0.1591	−16.06	401.08	383.67	15.67	14.32	−37.43	−43.04	−477.63	−492.41	−97.49	−125.83
GSkI	0.1590	−16.03	230.35	−487.83	32.67	32.03	64.57	63.44	−97.26	−95.31	301.86	293.49
GSkII	0.1587	−16.13	233.55	−399.08	31.83	30.49	53.19	48.62	−152.95	−157.89	309.59	310.34
KDE	0.1644	−16.01	224.05	−382.15	32.62	31.97	42.53	41.40	−143.90	−141.85	549.81	543.47
KDE0v	0.1609	−16.11	228.86	−373.71	33.80	32.98	47.18	45.19	−145.08	−144.81	527.91	523.40
KDE0v1	0.1646	−16.25	227.70	−385.19	35.34	34.58	56.32	54.68	−128.17	−127.14	489.90	484.57
LNS	0.1746	−15.33	210.93	−382.91	34.63	33.43	65.25	61.45	−124.27	−127.41	303.87	302.53
MSk1	0.1575	−15.85	233.88	−380.30	30.69	30.00	35.28	33.89	−201.49	−200.10	454.35	448.78
MSk2	0.1575	−15.85	231.80	−386.55	30.66	30.00	34.55	33.32	−205.24	−203.52	455.74	449.84
MSk3	0.1575	−15.81	233.40	−379.34	28.69	27.99	8.39	6.99	−285.03	−283.64	621.43	615.86
MSk4	0.1575	−15.81	231.32	−385.59	28.66	27.99	8.38	7.15	−285.89	−284.17	617.04	611.14
MSk5	0.1575	−15.81	231.32	−385.59	28.66	27.99	8.75	7.52	−284.39	−282.67	614.04	608.14
MSk5*	0.1561	−15.80	243.90	−346.46	29.17	27.99	10.76	6.97	−287.35	−290.77	596.03	595.31
MSk6	0.1575	−15.81	231.32	−385.59	28.66	27.99	10.81	9.58	−276.17	−274.44	597.59	591.69
MSk7	0.1576	−15.81	231.37	−385.69	28.61	27.94	10.59	9.36	−276.47	−274.74	598.19	592.28
MSk8	0.1576	−15.81	229.46	−391.35	28.56	27.92	9.29	8.21	−282.16	−280.13	604.00	597.79
MSk9	0.1576	−15.81	233.48	−379.49	28.69	27.99	11.71	10.32	−271.73	−270.33	594.83	589.26
MSkA	0.1535	−16.00	313.51	−138.36	31.60	30.34	61.37	57.15	−131.05	−135.38	197.53	197.75
MSL0	0.1601	−16.01	230.15	−380.65	31.19	30.00	63.85	59.99	−95.87	−99.36	225.05	224.31
NRAPR	0.1606	−15.87	225.80	−362.85	34.18	32.78	64.50	59.63	−117.84	−123.36	310.38	311.67
PRC45	0.1432	−15.56	362.11	164.12	51.03	50.38	141.04	139.74	−24.10	−22.79	96.41	91.18
RATP	0.1599	−16.06	239.68	−350.14	30.79	29.25	37.97	32.37	−184.32	−191.29	438.05	440.81
Rs	0.1578	−15.60	237.51	−348.71	31.82	30.59	89.81	85.71	−5.11	−9.13	22.35	22.18
SAMi	0.1588	−15.94	245.16	−339.01	29.24	28.16	46.97	43.67	−117.56	−119.97	373.79	372.00
SAMi-T	0.1639	−16.16	243.95	−342.10	30.84	29.67	49.44	45.73	−112.49	−115.62	415.82	414.66
Sefm068	0.1602	−15.94	240.26	−347.42	90.09	88.59	259.91	254.50	−25.49	−32.10	56.98	59.35
Sefm074	0.1604	−15.82	240.25	−350.46	34.80	33.40	93.59	88.74	−27.68	−33.14	57.13	58.36
Sefm081	0.1609	−15.70	237.20	−356.98	32.05	30.77	83.68	79.39	−35.21	−39.54	66.61	66.70
Sefm09	0.1610	−15.57	240.21	−350.07	28.94	27.78	73.63	69.96	−37.70	−40.80	71.73	70.59
Sefm1	0.1611	−15.42	240.23	−346.67	25.85	24.81	62.60	59.55	−45.03	−46.90	83.87	81.49
SGI	0.1545	−15.91	261.92	−298.21	29.62	28.33	68.28	63.86	−47.27	−51.99	193.86	194.45
SGII	0.1584	−15.61	214.79	−381.24	28.10	26.83	41.88	37.61	−141.61	−145.96	330.34	330.49
SGOI	0.1678	−16.65	361.80	37.22	46.97	45.20	106.46	99.76	−146.63	−155.69	139.63	144.33
SGOII	0.1682	−16.71	253.44	−346.49	95.78	94.00	252.80	246.08	−110.52	−119.60	267.70	272.43
SI	0.1554	−16.01	370.58	152.23	30.26	29.23	4.24	1.17	−460.03	−462.02	143.56	141.41
SI′	0.1554	−16.01	370.58	152.23	30.38	29.35	38.38	35.31	−257.25	−259.25	143.56	141.41
SII	0.1484	−16.00	341.59	15.62	35.77	34.15	56.05	50.00	−257.74	−265.82	100.64	104.71
SIII	0.1453	−15.87	355.56	101.28	29.37	28.15	13.98	9.87	−389.62	−393.88	130.11	130.42
SIII*	0.1477	−16.08	361.35	107.84	32.94	31.96	31.54	28.66	−356.75	−358.50	87.04	84.79
SIV	0.1510	−15.97	324.73	−69.01	33.21	31.22	71.45	63.49	−124.90	−136.76	71.61	79.40
SK255	0.1573	−16.35	255.09	−350.40	38.77	37.40	99.83	95.06	−52.98	−58.34	93.01	94.19
SK272	0.1554	−16.29	271.67	−305.60	38.71	37.40	96.16	91.67	−62.96	−67.79	133.65	134.33
SKa	0.1554	−16.01	263.32	−300.41	34.56	32.91	80.79	74.62	−70.27	−78.47	170.47	174.53

TABLE II. (*Continued.*)

Model	n_0	E_0	K_0	Q_0	J_1	J_2	L_1	L_2	$K_{\mathrm{sym},1}$	$K_{\mathrm{sym},2}$	$Q_{\mathrm{sym},1}$	$Q_{\mathrm{sym},2}$
Ska25s20	0.1607	−16.09	220.89	−413.80	34.50	33.78	65.25	63.80	−119.60	−118.26	319.77	314.20
Ska35s15	0.1581	−16.02	239.04	−379.21	31.25	30.55	31.94	30.57	−224.43	−222.99	487.76	482.13
Ska35s20	0.1581	−16.09	240.42	−378.98	34.26	33.57	66.21	64.82	−121.75	−120.35	290.17	284.59
Ska35s25	0.1577	−16.15	241.45	−379.27	37.68	36.98	100.31	98.90	−24.92	−23.56	102.97	97.42
Ska45s20	0.1559	−16.09	260.37	−330.86	34.07	33.39	67.54	66.20	−121.49	−120.02	257.41	251.80
SKb	0.1554	−16.01	263.32	−300.41	25.53	23.88	53.71	47.54	−70.27	−78.47	170.47	174.53
SkI1	0.1604	−15.97	242.88	−346.39	38.21	37.53	162.38	161.10	233.12	234.79	−322.33	−328.22
SkI2	0.1576	−15.79	241.09	−340.01	34.02	33.38	105.49	104.36	68.83	70.76	57.65	51.55
SkI3	0.1578	−15.99	258.35	−304.15	35.20	34.84	100.27	100.55	68.39	73.13	220.43	211.51
SkI4	0.1602	−15.96	248.08	−331.46	30.08	29.50	61.16	60.40	−43.20	−40.50	358.05	351.12
SkI5	0.1558	−15.86	255.95	−302.23	37.01	36.65	129.11	129.37	155.02	159.69	20.44	11.62
SkI6	0.1600	−15.92	242.31	−345.26	38.07	37.39	161.83	160.55	232.64	234.31	−321.36	−327.25
SkM	0.1604	−15.79	216.75	−386.42	32.07	30.74	53.82	49.33	−144.10	−148.86	322.88	323.42
SkM1	0.1604	−15.79	216.75	−386.42	26.51	25.16	−30.78	−35.45	−383.96	−389.06	912.33	913.21
SkM*	0.1604	−15.79	216.75	−386.42	31.39	30.03	50.42	45.76	−150.89	−156.00	329.68	330.55
SkMP	0.1571	−15.58	231.03	−338.35	31.26	29.89	75.10	70.31	−44.41	−49.82	158.19	159.43
SkO	0.1605	−15.85	223.49	−393.20	32.86	31.97	81.48	79.15	−42.73	−43.17	134.90	131.11
SkO′	0.1602	−15.77	222.47	−391.10	32.79	31.95	71.03	68.93	−78.86	−78.83	227.62	223.37
SkP	0.1626	−15.96	201.11	−435.79	31.33	30.00	24.16	19.63	−261.96	−266.74	508.03	508.54
SKRA	0.1595	−15.79	217.13	−379.09	32.71	31.32	57.84	53.02	−133.92	−139.34	309.70	310.90
SkS1	0.1613	−15.87	228.58	−383.10	30.25	28.74	35.91	30.49	−212.19	−218.79	376.99	379.35
SkS2	0.1609	−15.90	229.16	−383.07	31.16	29.22	45.37	37.81	−207.31	−218.18	263.46	270.10
SkS3	0.1609	−15.89	228.98	−382.95	30.70	28.84	58.90	51.72	−147.34	−157.47	148.19	154.08
SkS4	0.1627	−15.89	228.23	−385.79	29.78	28.34	28.31	23.25	−232.68	−238.52	436.62	438.20
SkSC1	0.1607	−15.87	234.73	−380.84	28.80	28.09	1.49	0.08	−313.57	−312.16	679.20	673.55
SkSC2	0.1607	−15.91	235.28	−381.94	25.44	24.73	12.37	10.96	−229.72	−228.31	511.49	505.85
SkSC3	0.1607	−15.86	234.64	−380.66	27.70	27.00	2.17	0.76	−297.73	−296.32	647.52	641.87
SkSC4	0.1607	−15.88	234.87	−381.11	29.50	28.79	−0.76	−2.18	−331.02	−329.61	714.10	708.46
SkSC4o	0.1608	−15.88	234.89	−381.13	27.70	26.99	−8.32	−9.73	−339.58	−338.17	731.24	725.59
SkSC5	0.1607	−15.86	234.65	−380.68	31.68	30.98	−5.62	−7.03	−376.65	−375.23	805.35	799.71
SkSC6	0.1608	−15.94	235.56	−382.47	25.27	24.57	12.37	10.96	−227.76	−226.35	507.60	501.95
SkSC10	0.1608	−15.98	236.04	−383.42	23.53	22.82	20.51	19.10	−174.24	−172.83	400.56	394.91
SkSC11	0.1607	−15.88	234.87	−381.12	29.50	28.79	−0.76	−2.18	−331.03	−329.62	714.13	708.48
SkSC14	0.1608	−15.94	235.56	−382.47	30.70	30.00	34.52	33.10	−204.32	−202.90	460.71	455.06
SkSC15	0.1608	−15.90	235.08	−381.50	28.70	27.99	8.09	6.67	−285.99	−284.58	624.07	618.42
SkSP.1	0.1619	−15.92	230.16	−503.11	29.20	27.99	15.91	7.12	−246.01	−289.67	720.66	662.94
SkT	0.1476	−15.42	333.55	28.88	26.25	24.89	33.03	28.21	−231.17	−236.81	68.18	69.81
SkT1a	0.1611	−15.99	236.31	−383.86	32.72	32.02	57.58	56.17	−136.29	−134.87	324.71	319.06
SkT2a	0.1611	−15.96	235.88	−383.01	32.70	32.00	57.57	56.15	−136.12	−134.71	324.38	318.73
SkT3a	0.1612	−15.98	236.09	−383.52	32.20	31.50	56.64	55.22	−133.85	−132.44	319.70	314.04
SkT4a	0.1591	−15.97	235.65	−383.28	36.16	35.46	95.55	94.15	−25.85	−24.45	103.41	97.80
SkT5a	0.1641	−16.01	201.83	−437.18	37.73	37.01	99.98	98.55	−26.39	−24.96	105.57	99.85
SkT6a	0.1609	−15.98	236.10	−383.49	30.67	29.96	32.24	30.82	−213.02	−211.61	478.15	472.50
SkT7a	0.1607	−15.95	235.79	−372.55	30.71	29.51	34.98	31.09	−206.40	−209.93	440.17	439.47
SkT8a	0.1607	−15.96	235.85	−372.69	30.77	29.92	35.82	33.70	−187.58	−187.59	480.61	476.38
SkT9a	0.1604	−15.90	235.06	−371.30	30.60	29.75	35.83	33.71	−185.67	−185.68	476.33	472.11
SkTK	0.1682	−16.71	253.44	−346.49	37.35	35.56	48.28	41.56	−212.78	−221.86	523.35	528.07
SKX	0.1555	−16.07	271.24	−297.74	32.35	31.10	37.38	33.16	−247.93	−252.23	379.64	379.80
Skχ414	0.1408	−14.47	252.34	−111.63	56.86	57.82	280.04	291.51	1141.73	1206.44	3210.58	3331.46
Skχ450	0.1332	−14.50	248.33	−135.84	45.90	46.16	187.60	193.61	645.65	684.36	2149.92	2222.25
Skχ500	0.1453	−14.69	246.89	−168.79	79.13	80.85	400.54	417.32	1552.61	1639.70	3921.76	4078.58
SKXce	0.1554	−15.88	268.35	−294.88	31.40	30.14	37.69	33.45	−234.15	−238.48	356.82	357.02
Skxcsb	0.1550	−15.81	267.20	−293.94	32.19	31.47	41.83	40.34	−215.28	−214.12	382.62	377.33
SKXm	0.1589	−16.06	238.24	−380.72	32.44	31.20	36.19	32.05	−238.78	−242.87	428.97	428.86
Skxs15	0.1617	−15.77	201.23	−424.93	32.67	31.87	36.61	34.76	−197.72	−197.17	521.26	516.46
Skxs20	0.1618	−15.83	202.09	−425.92	36.30	35.50	68.95	67.06	−122.82	−122.35	333.33	328.60
Skxs25	0.1615	−15.88	203.05	−426.04	40.42	39.61	102.09	100.12	−50.59	−50.28	150.53	145.98

TABLE II. (*Continued.*)

Model	n_0	E_0	K_0	Q_0	J_1	J_2	L_1	L_2	$K_{\mathrm{sym},1}$	$K_{\mathrm{sym},2}$	$Q_{\mathrm{sym},1}$	$Q_{\mathrm{sym},2}$
Skxta	0.1559	−16.05	270.91	−298.28	32.45	31.16	37.14	32.78	−251.09	−255.66	380.17	380.60
Skxtb	0.1553	−16.07	271.26	−297.90	32.39	31.15	38.64	34.50	−242.44	−246.58	372.86	372.86
Skz0	0.1601	−16.02	230.23	−365.56	34.00	32.00	42.99	35.07	−230.68	−242.31	397.88	405.28
Skz1	0.1601	−16.02	230.23	−365.56	33.60	32.00	33.49	27.64	−235.00	−242.49	532.27	535.54
Skz2	0.1601	−16.02	230.22	−365.55	33.26	32.00	20.96	16.77	−255.58	−259.75	682.90	682.84
Skz3	0.1601	−16.02	230.24	−365.58	32.77	32.01	14.61	12.92	−242.81	−241.98	800.24	795.18
Skz4	0.1601	−16.02	230.24	−365.57	32.35	32.00	5.31	5.71	−245.93	−240.91	933.42	924.17
Skzm1	0.1601	−16.02	230.23	−365.57	34.15	32.00	62.74	54.13	−171.17	−184.18	208.29	217.08
SLy0	0.1604	−15.99	229.81	−364.33	32.67	31.98	48.43	47.10	−117.80	−116.23	514.60	508.80
SLy1	0.1604	−16.00	229.97	−364.67	32.68	31.99	48.38	47.05	−118.07	−116.50	515.27	509.47
SLy2	0.1606	−16.00	230.07	−364.53	32.69	32.00	48.77	47.44	−116.71	−115.13	512.44	506.63
SLy230a	0.1600	−16.00	230.04	−364.50	32.23	31.98	43.43	44.31	−104.17	−98.20	613.20	603.01
SLy230b	0.1596	−15.99	230.06	−363.41	32.68	32.00	47.24	45.95	−121.36	−119.73	527.46	521.62
SLy3	0.1605	−15.98	230.03	−363.69	32.67	31.99	46.61	45.29	−123.77	−122.17	531.81	525.98
SLy4	0.1596	−15.99	230.06	−363.41	32.68	32.00	47.22	45.93	−121.37	−119.74	527.49	521.65
SLy5	0.1604	−16.00	230.09	−364.29	32.71	32.02	49.57	48.26	−113.94	−112.34	506.43	500.61
SLy6	0.1590	−15.93	230.01	−360.56	32.62	31.96	48.67	47.44	−114.44	−112.71	516.68	510.74
SLy7	0.1581	−15.91	229.85	−359.25	32.65	31.99	48.41	47.20	−115.10	−113.32	521.29	515.32
SLy8	0.1604	−15.98	230.02	−363.55	32.64	31.95	48.27	46.95	−117.59	−116.00	516.19	510.37
SLy9	0.1512	−15.81	229.97	−350.68	32.57	31.98	55.73	54.79	−83.82	−81.62	468.89	462.62
SLy10	0.1556	−15.92	229.83	−358.63	32.62	31.98	39.87	38.73	−144.05	−142.20	597.37	591.37
SQMC1	0.1374	−14.02	328.94	143.70	31.02	29.67	−1.94	−6.76	−498.64	−504.46	216.09	218.08
SQMC2	0.1403	−14.30	330.29	121.66	29.83	28.69	12.41	8.63	−404.87	−408.57	145.69	145.53
SQMC3	0.1608	−16.00	367.18	130.12	47.07	45.78	96.12	91.79	−206.60	−211.02	163.26	163.45
SQMC600	0.1737	−15.75	217.16	−388.97	36.02	34.38	52.33	46.36	−207.78	−215.26	393.95	396.97
SQMC650	0.1720	−15.59	218.26	−377.09	35.16	33.65	58.24	52.90	−167.00	−173.23	348.03	349.84
SQMC700	0.1705	−15.51	219.77	−368.36	34.81	33.40	63.85	59.00	−134.99	−140.29	311.85	312.75
SQMC750	0.1711	−15.61	223.02	−366.17	35.10	33.75	69.20	64.67	−112.89	−117.55	288.22	288.47
SSK	0.1615	−16.17	229.46	−375.70	34.25	33.50	54.37	52.77	−120.21	−119.16	487.65	482.35
SV	0.1551	−16.06	305.87	−176.01	35.32	32.83	106.51	96.10	40.88	24.21	35.39	47.93
SV-bas	0.1597	−15.92	233.60	−379.61	31.28	30.00	36.65	32.33	−217.43	−221.85	410.85	411.05
SV-min	0.1612	−15.93	221.91	−403.42	31.44	30.65	46.61	44.79	−157.24	−156.62	394.51	389.66
SVI	0.1435	−15.77	363.84	153.41	27.85	26.88	−4.46	−7.39	−469.55	−471.48	148.01	146.02
SVII	0.1434	−15.80	366.63	164.43	27.88	26.95	−7.52	−10.21	−487.62	−489.08	152.18	149.71
SV-K218	0.1615	−15.91	218.37	−403.49	31.29	30.00	38.94	34.59	−202.53	−206.96	401.51	401.70
SV-K226	0.1606	−15.92	225.97	−392.47	31.29	30.00	38.40	34.07	−207.58	−212.01	401.75	401.95
SV-K241	0.1588	−15.92	241.21	−364.84	31.28	30.00	35.22	30.92	−226.44	−230.84	415.90	416.10
SV-Kap00	0.1598	−15.92	233.59	−379.49	30.58	30.00	40.23	39.42	−164.41	−161.82	453.87	447.06
SV-Kap02	0.1597	−15.92	233.59	−379.54	30.93	30.00	38.08	35.51	−192.35	−193.26	435.33	432.03
SV-Kap06	0.1596	−15.92	233.60	−379.66	31.63	30.00	35.36	29.30	−241.96	−249.87	385.26	388.96
SV-mas07	0.1599	−15.90	233.70	−357.25	30.95	30.00	54.80	52.14	−97.69	−98.78	368.88	365.75
SV-mas08	0.1598	−15.91	233.28	−371.61	31.14	30.00	43.72	40.13	−169.49	−172.45	398.80	397.54
SV-mas10	0.1595	−15.92	234.48	−383.55	31.40	30.00	32.90	28.00	−247.04	−252.62	406.82	408.19
SV-sym28	0.1596	−15.88	233.07	−378.56	29.28	28.00	11.47	7.16	−292.22	−296.63	567.88	568.09
SV-sym32	0.1595	−15.95	233.96	−380.44	33.28	32.00	61.37	57.06	−144.44	−148.85	257.55	257.75
SV-sym34	0.1593	−15.98	234.22	−381.15	35.28	34.00	85.26	80.95	−74.70	−79.11	111.06	111.26
SV-tls	0.1596	−15.91	233.45	−379.36	31.28	30.00	37.51	33.19	−214.10	−218.52	403.81	404.01
T	0.1613	−15.95	235.82	−382.77	29.05	28.35	28.57	27.15	−208.26	−206.84	468.71	463.05
T1	0.1611	−15.99	236.31	−383.86	32.72	32.02	57.58	56.17	−136.29	−134.87	324.71	319.06
T11	0.1613	−16.03	230.17	−366.07	32.69	32.00	50.81	49.45	−110.28	−108.76	492.85	487.09
T12	0.1612	−16.02	230.17	−365.43	32.69	32.00	50.72	49.37	−110.29	−108.75	494.39	488.61
T13	0.1611	−16.01	230.17	−365.10	32.69	32.00	50.86	49.52	−109.62	−108.06	493.47	487.67
T14	0.1611	−16.01	230.17	−364.80	32.69	32.00	50.80	49.47	−109.68	−108.12	494.26	488.46
T15	0.1613	−16.02	230.17	−365.64	32.69	32.00	50.99	49.64	−109.45	−107.92	491.71	485.93
T16	0.1612	−16.03	230.17	−366.00	32.69	32.00	50.80	49.44	−110.28	−108.75	493.11	487.34
T1*	0.1603	−15.99	236.14	−383.82	32.72	32.02	57.50	56.10	−136.64	−135.23	325.24	319.60
T2	0.1611	−15.96	235.88	−383.01	32.70	32.00	57.57	56.15	−136.12	−134.71	324.38	318.73
T21	0.1615	−16.04	230.16	−366.80	32.70	32.00	51.14	49.76	−109.52	−108.03	489.09	483.35

TABLE II. (*Continued.*)

Model	n_0	E_0	K_0	Q_0	J_1	J_2	L_1	L_2	$K_{\mathrm{sym},1}$	$K_{\mathrm{sym},2}$	$Q_{\mathrm{sym},1}$	$Q_{\mathrm{sym},2}$
T22	0.1614	−16.03	230.17	−366.27	32.70	32.00	50.92	49.56	−110.02	−108.51	491.60	485.85
T23	0.1614	−16.03	230.17	−365.95	32.69	32.00	50.94	49.58	−109.79	−108.27	491.83	486.06
T24	0.1613	−16.02	230.17	−365.68	32.69	32.00	51.20	49.84	−108.75	−107.22	489.88	484.11
T25	0.1609	−16.00	230.17	−364.56	32.69	32.00	50.44	49.11	−110.79	−109.22	497.77	491.95
T26	0.1609	−15.99	230.17	−363.80	32.69	32.00	50.06	48.75	−111.75	−110.15	501.87	496.03
T3	0.1611	−15.96	235.90	−383.03	32.20	31.50	56.72	55.30	−133.51	−132.09	319.15	313.50
T31	0.1614	−16.04	230.17	−366.60	32.70	32.00	51.11	49.74	−109.50	−108.00	489.67	483.93
T32	0.1615	−16.04	230.17	−366.70	32.70	32.00	51.65	50.27	−107.70	−106.20	484.82	479.08
T33	0.1613	−16.04	230.17	−366.41	32.70	32.00	51.01	49.65	−109.74	−108.23	490.74	484.99
T34	0.1615	−16.04	230.17	−366.60	32.70	32.00	51.46	50.08	−108.31	−106.81	486.56	480.82
T35	0.1610	−16.01	230.17	−365.16	32.69	32.00	50.92	49.58	−109.41	−107.86	492.95	487.16
T36	0.1612	−16.01	230.17	−364.83	32.69	32.00	50.38	49.04	−111.19	−109.63	497.90	492.09
T3*	0.1603	−15.99	236.15	−383.83	32.39	31.68	57.25	55.84	−133.65	−132.24	319.26	313.63
T4	0.1591	−15.97	235.65	−383.28	36.16	35.46	95.55	94.15	−25.85	−24.45	103.41	97.80
T41	0.1619	−16.07	230.17	−368.68	32.71	32.00	52.01	50.59	−107.44	−106.02	479.45	473.77
T42	0.1618	−16.07	230.17	−368.36	32.71	32.00	52.10	50.69	−106.95	−105.52	479.07	473.38
T43	0.1616	−16.06	230.17	−367.71	32.70	32.00	51.96	50.56	−107.12	−105.66	481.04	475.33
T44	0.1613	−16.03	230.17	−366.23	32.70	32.00	51.41	50.04	−108.28	−106.76	487.48	481.72
T45	0.1615	−16.03	230.17	−366.42	32.70	32.00	51.02	49.65	−109.75	−108.24	490.58	484.83
T46	0.1608	−16.01	230.17	−365.07	32.69	32.00	51.26	49.92	−108.15	−106.59	490.16	484.36
T5	0.1641	−16.01	201.83	−437.18	37.73	37.01	99.98	98.55	−26.39	−24.96	105.57	99.85
T51	0.1617	−16.07	230.16	−368.28	32.70	32.00	52.08	50.68	−106.96	−105.52	479.34	473.65
T52	0.1616	−16.07	230.17	−368.39	32.70	32.00	52.08	50.67	−107.00	−105.56	479.34	473.65
T53	0.1613	−16.04	230.17	−366.53	32.70	32.00	51.39	50.02	−108.50	−106.99	487.35	481.61
T54	0.1614	−16.05	230.16	−367.05	32.70	32.00	51.64	50.26	−107.85	−106.37	484.55	478.82
T55	0.1615	−16.04	230.17	−366.98	32.70	32.00	51.61	50.23	−107.98	−106.49	484.86	479.12
T56	0.1611	−16.02	230.17	−365.58	32.69	32.00	51.47	50.12	−107.73	−106.19	487.71	481.93
T6	0.1609	−15.98	236.10	−383.49	30.67	29.96	32.24	30.82	−213.02	−211.61	478.15	472.50
T61	0.1619	−16.08	230.17	−369.08	32.71	32.00	52.20	50.78	−106.97	−105.56	477.43	471.77
T62	0.1620	−16.08	230.16	−369.25	32.71	32.00	51.74	50.32	−108.66	−107.26	481.23	475.57
T63	0.1619	−16.07	230.17	−368.62	32.71	32.00	52.47	51.06	−105.79	−104.37	475.50	469.82
T64	0.1616	−16.05	230.17	−367.06	32.70	32.00	51.86	50.48	−107.14	−105.66	482.56	476.83
T65	0.1617	−16.06	230.17	−367.70	32.70	32.00	51.89	50.49	−107.37	−105.91	481.65	475.94
T66	0.1614	−16.03	230.17	−366.36	32.70	32.00	51.66	50.29	−107.47	−105.96	485.11	479.36
T7	0.1607	−15.95	235.79	−372.55	30.71	29.51	34.98	31.09	−206.40	−209.93	440.17	439.47
T8	0.1607	−15.96	235.85	−372.69	30.77	29.92	35.82	33.70	−187.58	−187.59	480.61	476.38
T9	0.1604	−15.90	235.06	−371.30	30.60	29.75	35.83	33.71	−185.67	−185.68	476.33	472.11
UNEDF0	0.1606	−16.07	230.16	−404.03	31.79	30.54	49.19	45.06	−185.74	−189.77	288.17	287.97
UNEDF1	0.1588	−15.82	220.16	−404.55	30.13	28.98	43.60	39.98	−176.51	−179.55	325.14	323.98
v070	0.1576	−15.82	231.44	−385.84	29.48	27.99	1.78	−3.58	−355.26	−361.80	590.30	592.66
v075	0.1576	−15.82	231.44	−385.84	29.32	27.99	4.16	−0.37	−337.15	−342.04	587.17	587.88
v080	0.1575	−15.81	231.32	−385.59	29.17	27.99	5.99	2.18	−322.32	−325.76	586.48	585.74
v090	0.1575	−15.81	231.32	−385.59	28.93	27.99	7.59	4.99	−303.36	−304.39	596.81	593.66
v100	0.1575	−15.81	231.31	−385.59	28.74	27.99	10.32	8.68	−282.41	−281.51	593.52	588.45
v105	0.1575	−15.81	231.32	−385.59	28.66	27.99	8.26	7.03	−286.35	−284.63	617.96	612.06
v110	0.1575	−15.81	231.32	−385.59	28.58	27.99	8.32	7.47	−282.21	−279.74	624.72	618.07
Z	0.1590	−15.99	330.49	−65.17	27.96	26.81	−46.15	−49.78	−655.06	−658.13	496.51	495.38
ZR1a	0.1726	−17.00	398.96	185.92	10.57	9.83	−56.19	−57.67	−472.74	−471.26	109.21	103.29
ZR1b	0.1726	−17.00	398.96	185.92	19.23	18.49	−30.20	−31.68	−472.74	−471.26	109.21	103.29
ZR1c	0.1726	−17.00	398.96	185.92	32.23	31.49	8.79	7.31	−472.74	−471.26	109.21	103.29
ZR2a	0.1733	−17.01	324.97	−185.19	2.35	1.61	−80.96	−82.44	−398.93	−397.45	481.04	475.10
ZR2b	0.1733	−17.01	324.97	−185.19	12.67	11.93	−49.97	−51.46	−398.93	−397.45	481.04	475.10
ZR2c	0.1733	−17.01	324.97	−185.19	28.17	27.42	−3.50	−4.98	−398.93	−397.45	481.04	475.10
ZR3a	0.1754	−17.01	198.93	−476.04	−138.30	−139.05	−503.21	−504.70	−273.50	−272.00	774.32	768.33
ZR3b	0.1754	−17.01	198.93	−476.04	−99.78	−100.53	−387.65	−389.15	−273.50	−272.00	774.32	768.33
ZR3c	0.1754	−17.01	198.93	−476.04	−42.00	−42.75	−214.32	−215.81	−273.50	−272.00	774.32	768.33
Zs	0.1630	−15.89	233.48	−369.28	28.00	26.68	−25.01	−29.46	−396.98	−401.60	883.03	883.38
Zs*	0.1625	−15.97	235.02	−369.49	30.14	28.79	−0.00	−4.59	−327.87	−332.78	724.71	725.35

TABLE III. Nuclear structural properties of Skyrme models. The surface parameters σ_o, σ_δ, and S_S are calculated using a semi-infinite interface from Eqs. (120), (122), and (123), respectively. The neutron skin thicknesses r_{np} and dipole polarizabilities α_D are calculated using the droplet model and the hydrodynamical model from Eqs. (125) and (127), respectively. Also, the surface correction for the neutron skin thicknesses from Eq. (126) has been included.

Model	σ_o MeV/fm^2	σ_δ MeV/fm^2	S_S MeV	$r_{np}(^{208}$Pb) fm	$r_{np}(^{48}$Ca) fm	$\alpha_D(^{208}$Pb) fm^3	$\alpha_D(^{48}$Ca) fm^3
BSk1	0.909	1.539	25.53	0.089	0.096	21.936	2.151
BSk2	0.908	1.624	26.92	0.093	0.099	21.984	2.165
BSk2′	0.906	1.618	26.82	0.093	0.099	21.964	2.162
BSk3	0.883	1.558	25.83	0.090	0.097	21.853	2.144
BSk4	0.951	1.786	29.60	0.100	0.104	22.449	2.231
BSk5	0.961	2.155	35.72	0.117	0.115	22.790	2.302
BSk6	1.011	1.932	32.03	0.107	0.109	22.870	2.290
BSk7	1.017	1.978	32.79	0.109	0.111	23.002	2.309
BSk8	1.053	1.918	31.61	0.106	0.108	22.661	2.266
BSk9	1.075	3.095	51.00	0.151	0.137	23.724	2.480
BSk10	0.997	2.935	48.30	0.145	0.133	23.283	2.419
BSk11	0.969	2.906	47.96	0.145	0.133	23.303	2.419
BSk12	0.966	2.885	47.62	0.144	0.132	23.251	2.412
BSk13	0.964	2.912	48.06	0.145	0.133	23.317	2.421
BSk14	1.031	3.238	53.44	0.157	0.141	24.129	2.536
BSk15	1.032	2.767	45.60	0.139	0.129	22.912	2.365
BSk16	1.046	2.846	46.97	0.142	0.131	23.154	2.398
BSk17	1.054	2.930	48.36	0.145	0.133	23.363	2.427
BSk18	0.975	2.700	44.55	0.137	0.127	22.790	2.346
BSk19	1.007	2.634	43.38	0.134	0.125	22.550	2.315
BSk20	1.002	2.656	43.73	0.134	0.126	22.606	2.322
BSk21	0.976	2.633	43.61	0.135	0.126	22.732	2.335
BSk22	0.986	3.778	62.67	0.173	0.149	23.514	2.499
BSk23	0.979	3.178	52.72	0.154	0.138	23.153	2.421
BSk24	0.971	2.615	43.38	0.134	0.126	22.731	2.333
BSk25	0.948	2.080	34.37	0.112	0.112	22.199	2.231
BSk26	0.996	2.647	43.72	0.135	0.126	22.673	2.329
E	1.061	0.877	14.44	0.054	0.070	19.953	1.872
Es	1.076	0.424	6.88	0.026	0.050	19.241	1.742
f−	1.156	3.362	54.79	0.155	0.138	22.046	2.306
f+	1.161	3.293	53.60	0.153	0.136	21.869	2.282
f0	1.157	3.319	54.07	0.154	0.137	21.947	2.292
FPLyon	1.056	3.275	53.31	0.154	0.138	22.829	2.390
Gs	0.943	6.175	102.32	0.242	0.191	29.586	3.343
Gs1	1.098	3.486	57.38	0.167	0.148	25.989	2.767
Gs2	1.196	2.676	44.09	0.141	0.134	27.404	2.864
Gs3	1.956	0.262	3.94	−0.009	0.039	27.666	2.495
Gs4	0.885	0.085	1.40	−0.045	0.024	38.774	3.430
Gs5	0.975	0.639	10.57	0.030	0.066	29.996	2.830
Gs6	1.137	0.012	0.20	−0.042	0.019	33.722	2.935
GSkI	1.046	4.437	73.11	0.192	0.161	24.680	2.671
GSkII	1.048	3.703	61.09	0.172	0.150	24.714	2.633
KDE	1.089	3.234	52.11	0.149	0.134	21.478	2.234
KDE0v	1.083	3.438	56.21	0.157	0.138	21.423	2.240
KDE0v1	1.107	4.074	65.59	0.171	0.146	20.856	2.208
LNS	0.950	4.315	66.79	0.172	0.147	21.132	2.251
MSk1	0.920	2.576	42.70	0.133	0.125	22.612	2.317
MSk2	0.907	2.537	42.05	0.131	0.124	22.514	2.303
MSk3	0.909	1.534	25.43	0.088	0.096	21.723	2.128
MSk4	0.896	1.527	25.31	0.088	0.096	21.703	2.125
MSk5	0.896	1.539	25.51	0.089	0.096	21.737	2.130
MSk5*	0.989	1.658	27.65	0.095	0.101	22.244	2.196
MSk6	0.903	1.614	26.75	0.092	0.099	21.953	2.161

TABLE III. (*Continued.*)

Model	σ_o MeV/fm^2	σ_δ MeV/fm^2	S_S MeV	$r_{np}(^{208}\mathrm{Pb})$ fm	$r_{np}(^{48}\mathrm{Ca})$ fm	$\alpha_D(^{208}\mathrm{Pb})$ fm^3	$\alpha_D(^{48}\mathrm{Ca})$ fm^3
MSk7	0.905	1.607	26.64	0.092	0.099	21.980	2.163
MSk8	0.887	1.550	25.70	0.089	0.097	21.837	2.142
MSk9	0.917	1.650	27.35	0.094	0.100	22.057	2.175
MSkA	1.052	3.627	61.18	0.175	0.152	25.449	2.714
MSL0	1.060	4.351	71.37	0.192	0.163	26.666	2.900
NRAPR	1.040	4.337	70.99	0.186	0.157	23.468	2.524
PRC45	0.000	0.000	0.00	0.023	0.034	10.247	0.890
RATP	1.180	3.069	50.38	0.151	0.137	24.336	2.548
Rs	0.944	5.515	91.34	0.227	0.183	29.109	3.255
SAMi	1.126	3.288	54.23	0.161	0.145	26.381	2.798
SAMi-T	1.245	3.707	59.87	0.169	0.148	24.931	2.659
Sefm068	1.103	20.828	341.42	0.319	0.218	11.266	1.299
Sefm074	1.041	6.272	102.72	0.236	0.186	26.714	2.997
Sefm081	0.978	5.265	86.05	0.216	0.176	27.731	3.076
Sefm09	0.906	4.212	68.83	0.191	0.164	29.165	3.188
Sefm1	0.827	3.241	52.94	0.163	0.149	30.774	3.303
SGI	1.116	4.319	72.54	0.201	0.169	29.802	3.270
SGII	0.925	2.717	44.88	0.142	0.134	26.454	2.760
SGOI	1.497	8.281	131.62	0.243	0.184	18.689	2.083
SGOII	1.345	22.667	359.78	0.315	0.215	10.244	1.180
SI	0.924	1.533	25.66	0.089	0.095	20.849	2.036
SI′	0.924	2.303	38.54	0.124	0.119	22.808	2.317
SII	1.208	4.144	71.50	0.190	0.158	23.448	2.511
SIII	1.020	1.885	32.99	0.113	0.113	24.139	2.423
SIII*	1.070	2.766	47.88	0.145	0.132	22.484	2.317
SIV	1.361	5.172	88.21	0.224	0.181	28.651	3.182
SK255	1.061	6.586	109.30	0.238	0.185	23.621	2.634
SK272	1.063	6.082	101.77	0.228	0.179	23.077	2.551
SKa	1.205	5.680	95.03	0.229	0.182	26.915	2.997
Ska25s20	0.937	4.185	68.47	0.179	0.152	22.217	2.370
Ska35s15	0.893	2.382	39.40	0.124	0.118	21.551	2.185
Ska35s20	0.916	3.999	66.15	0.177	0.150	22.379	2.380
Ska35s25	0.934	6.111	101.25	0.227	0.179	23.164	2.563
Ska45s20	0.895	3.839	64.09	0.174	0.149	22.497	2.385
SKb	1.205	3.558	59.53	0.181	0.162	34.818	3.808
SkI1	1.099	15.631	256.03	0.374	0.255	37.213	4.570
SkI2	1.057	7.084	117.43	0.258	0.198	28.864	3.292
SkI3	1.193	6.797	112.57	0.248	0.192	26.513	2.993
SkI4	1.129	3.998	65.56	0.182	0.157	26.389	2.847
SkI5	1.150	9.290	155.16	0.296	0.217	29.168	3.400
SkI6	1.093	15.522	254.71	0.374	0.255	37.393	4.591
SkM	1.020	3.782	61.96	0.173	0.150	24.394	2.601
SkM1	1.057	0.240	3.93	0.013	0.041	19.861	1.770
SkM*	1.057	3.701	60.63	0.171	0.150	24.990	2.665
SkMP	1.107	5.207	86.48	0.221	0.180	29.453	3.280
SkO	0.946	5.130	84.00	0.210	0.172	26.018	2.864
SkO′	0.938	4.440	72.78	0.191	0.160	24.595	2.661
SkP	0.992	2.449	39.76	0.124	0.119	21.708	2.207
SKRA	1.024	4.009	65.92	0.180	0.154	24.415	2.617
SkS1	1.037	2.834	46.25	0.141	0.132	24.098	2.503
SkS2	1.041	3.369	55.08	0.161	0.144	25.004	2.645
SkS3	1.035	4.095	66.94	0.186	0.160	27.369	2.968
SkS4	1.038	2.474	40.14	0.127	0.122	23.385	2.395
SkSC1	0.962	1.405	22.98	0.081	0.090	20.930	2.031
SkSC2	0.977	1.574	25.76	0.090	0.101	24.990	2.480
SkSC3	0.975	1.381	22.59	0.080	0.091	21.871	2.127

TABLE III. (*Continued.*)

Model	σ_o MeV/fm^2	σ_δ MeV/fm^2	S_S MeV	$r_{np}(^{208}\text{Pb})$ fm	$r_{np}(^{48}\text{Ca})$ fm	$\alpha_D(^{208}\text{Pb})$ fm^3	$\alpha_D(^{48}\text{Ca})$ fm^3
SkSC4	0.964	1.379	22.56	0.079	0.088	20.258	1.959
SkSC4o	0.964	1.060	17.34	0.063	0.078	20.903	1.990
SkSC5	0.961	1.357	22.21	0.077	0.085	18.541	1.780
SkSC6	0.981	1.569	25.65	0.090	0.101	25.162	2.497
SkSC10	0.993	1.770	28.95	0.100	0.111	28.411	2.876
SkSC11	0.964	1.379	22.56	0.079	0.088	20.258	1.959
SkSC14	0.980	2.689	43.98	0.135	0.126	22.498	2.313
SkSC15	0.969	1.611	26.34	0.090	0.097	21.588	2.122
SkSP.1	1.469	2.543	41.41	0.130	0.125	24.063	2.476
SkT	0.929	2.062	35.69	0.123	0.124	28.523	2.925
SkT1a	0.995	3.866	63.16	0.172	0.149	23.177	2.465
SkT2a	0.998	3.881	63.40	0.173	0.149	23.228	2.472
SkT3a	0.996	3.804	62.10	0.171	0.148	23.540	2.503
SkT4a	0.984	6.208	102.27	0.232	0.182	24.584	2.737
SkT5a	1.020	7.439	120.03	0.249	0.191	24.356	2.750
SkT6a	0.987	2.609	42.64	0.131	0.124	22.319	2.287
SkT7a	1.044	2.774	45.40	0.139	0.129	23.206	2.398
SkT8a	1.045	2.816	46.07	0.140	0.129	22.896	2.367
SkT9a	1.056	2.847	46.64	0.141	0.131	23.182	2.401
SkTK	1.345	4.179	66.33	0.170	0.145	19.878	2.100
SKX	0.895	2.490	41.65	0.129	0.122	21.631	2.202
SkX414	0.883	15.049	268.95	0.350	0.239	20.844	2.456
SkX450	0.846	9.140	169.43	0.303	0.218	23.847	2.733
SkX500	0.878	23.654	413.91	0.378	0.249	15.428	1.838
SKXce	0.889	2.460	41.17	0.129	0.122	22.448	2.290
Skxcsb	0.876	2.681	44.92	0.137	0.126	21.800	2.234
SKXm	0.927	2.652	43.72	0.133	0.124	21.524	2.202
Skxs15	0.927	2.838	46.24	0.137	0.126	21.028	2.159
Skxs20	0.947	4.709	76.69	0.190	0.158	21.548	2.317
Skxs25	0.964	7.170	116.95	0.241	0.185	22.023	2.459
Skxta	0.921	2.559	42.72	0.132	0.123	21.684	2.213
Skxtb	0.902	2.553	42.73	0.132	0.123	21.756	2.220
Skz0	1.079	3.358	55.08	0.157	0.139	22.229	2.327
Skz1	1.079	2.833	46.48	0.138	0.127	21.090	2.166
Skz2	1.079	2.262	37.10	0.116	0.112	19.859	1.991
Skz3	1.079	1.972	32.35	0.104	0.104	19.229	1.902
Skz4	1.079	1.611	26.42	0.089	0.093	18.451	1.792
Skzm1	1.079	4.535	74.39	0.194	0.162	24.767	2.686
SLy0	1.145	3.610	59.14	0.165	0.144	22.754	2.402
SLy1	1.150	3.620	59.31	0.165	0.144	22.764	2.403
SLy2	1.144	3.620	59.25	0.165	0.144	22.725	2.399
SLy230a	1.148	3.295	54.06	0.154	0.137	22.111	2.310
SLy230b	1.138	3.520	57.86	0.162	0.143	22.632	2.382
SLy3	1.140	3.495	57.24	0.161	0.142	22.486	2.364
SLy4	1.138	3.519	57.83	0.162	0.143	22.635	2.383
SLy5	1.143	3.661	59.96	0.166	0.145	22.814	2.412
SLy6	1.093	3.452	56.88	0.161	0.142	22.605	2.375
SLy7	1.076	3.388	56.02	0.159	0.141	22.543	2.364
SLy8	1.139	3.574	58.56	0.164	0.143	22.705	2.394
SLy9	1.057	3.689	62.85	0.176	0.151	24.172	2.570
SLy10	1.008	2.797	46.75	0.140	0.128	21.549	2.215
SQMC1	1.231	2.091	37.99	0.128	0.122	24.321	2.464
SQMC2	0.963	1.942	34.79	0.119	0.117	24.459	2.464
SQMC3	1.203	6.418	104.97	0.213	0.167	17.172	1.859
SQMC600	1.373	5.239	81.39	0.195	0.161	21.997	2.391
SQMC650	1.217	4.938	77.20	0.190	0.159	22.331	2.418

TABLE III. (*Continued.*)

Model	σ_o MeV/fm^2	σ_δ MeV/fm^2	S_S MeV	$r_{np}(^{208}$Pb) fm	$r_{np}(^{48}$Ca) fm	$\alpha_D(^{208}$Pb) fm^3	$\alpha_D(^{48}$Ca) fm^3
SQMC700	1.086	4.685	73.69	0.186	0.156	22.293	2.403
SQMC750	0.997	4.542	71.28	0.180	0.152	21.656	2.322
SSK	1.098	3.859	62.93	0.169	0.146	21.733	2.298
SV	1.543	8.400	140.69	0.290	0.216	32.880	3.838
SV-bas	0.971	2.735	44.94	0.137	0.128	22.747	2.344
SV-min	0.957	3.205	52.34	0.152	0.137	23.038	2.409
SVI	0.888	1.205	21.26	0.079	0.090	23.443	2.269
SVII	0.864	1.119	19.75	0.074	0.086	23.076	2.219
SV-K218	0.977	2.921	47.63	0.143	0.131	22.973	2.383
SV-K226	0.974	2.851	46.68	0.141	0.130	22.921	2.372
SV-K241	0.968	2.641	43.55	0.134	0.126	22.619	2.323
SV-Kap00	0.971	2.849	46.78	0.141	0.131	23.006	2.381
SV-Kap02	0.971	2.777	45.61	0.139	0.129	22.840	2.357
SV-Kap06	0.971	2.701	44.40	0.136	0.127	22.675	2.333
SV-mas07	1.080	3.698	60.69	0.172	0.150	25.078	2.675
SV-mas08	1.020	3.106	51.01	0.151	0.137	23.644	2.471
SV-mas10	0.931	2.519	41.41	0.129	0.122	22.234	2.271
SV-sym28	0.958	1.670	27.46	0.094	0.100	21.886	2.159
SV-sym32	0.980	4.015	66.00	0.179	0.153	23.720	2.536
SV-sym34	0.986	5.535	91.09	0.218	0.175	24.796	2.736
SV-tls	0.977	2.789	45.85	0.139	0.129	22.893	2.364
T	1.002	2.415	39.41	0.125	0.121	23.396	2.391
T1	0.995	3.866	63.16	0.172	0.149	23.177	2.465
T11	1.152	3.754	61.26	0.169	0.146	22.924	2.429
T12	1.150	3.740	61.07	0.168	0.146	22.911	2.427
T13	1.149	3.744	61.15	0.168	0.146	22.927	2.429
T14	1.148	3.738	61.05	0.168	0.146	22.911	2.427
T15	1.149	3.752	61.23	0.169	0.146	22.922	2.429
T16	1.152	3.751	61.25	0.169	0.146	22.935	2.431
T1*	0.984	3.823	62.66	0.172	0.148	23.192	2.464
T2	0.998	3.881	63.40	0.173	0.149	23.228	2.472
T21	1.161	3.801	61.98	0.170	0.147	22.997	2.440
T22	1.159	3.783	61.70	0.169	0.147	22.970	2.436
T23	1.158	3.778	61.65	0.169	0.147	22.970	2.436
T24	1.157	3.788	61.82	0.170	0.147	23.001	2.440
T25	1.153	3.736	61.06	0.168	0.146	22.933	2.429
T26	1.150	3.705	60.57	0.167	0.146	22.874	2.421
T3	0.995	3.805	62.17	0.171	0.149	23.566	2.507
T31	1.167	3.817	62.28	0.171	0.148	23.051	2.448
T32	1.167	3.846	62.72	0.171	0.148	23.098	2.455
T33	1.165	3.806	62.11	0.170	0.148	23.036	2.445
T34	1.166	3.834	62.53	0.171	0.148	23.072	2.451
T35	1.161	3.788	61.90	0.170	0.147	23.038	2.445
T36	1.161	3.757	61.34	0.169	0.147	22.945	2.432
T3*	0.984	3.795	62.20	0.171	0.149	23.463	2.494
T4	0.984	6.208	102.27	0.232	0.182	24.584	2.737
T41	1.182	3.919	63.79	0.173	0.149	23.195	2.470
T42	1.180	3.915	63.77	0.173	0.149	23.207	2.471
T43	1.177	3.899	63.55	0.173	0.149	23.194	2.469
T44	1.172	3.848	62.81	0.172	0.148	23.128	2.458
T45	1.171	3.827	62.41	0.171	0.148	23.061	2.449
T46	1.166	3.822	62.50	0.171	0.148	23.132	2.457
T5	1.020	7.439	120.03	0.249	0.191	24.356	2.750
T51	1.187	3.937	64.14	0.174	0.150	23.265	2.479
T52	1.183	3.926	64.01	0.174	0.150	23.261	2.478
T53	1.179	3.873	63.20	0.172	0.149	23.176	2.465

TABLE III. (*Continued.*)

Model	σ_o MeV/fm^2	σ_δ MeV/fm^2	S_S MeV	$r_{np}(^{208}\mathrm{Pb})$ fm	$r_{np}(^{48}\mathrm{Ca})$ fm	$\alpha_D(^{208}\mathrm{Pb})$ fm^3	$\alpha_D(^{48}\mathrm{Ca})$ fm^3
T54	1.178	3.884	63.36	0.173	0.149	23.190	2.467
T55	1.180	3.888	63.40	0.173	0.149	23.180	2.467
T56	1.173	3.857	63.00	0.172	0.149	23.172	2.464
T6	0.987	2.609	42.64	0.131	0.124	22.319	2.287
T61	1.191	3.959	64.46	0.175	0.150	23.284	2.482
T62	1.190	3.931	63.97	0.174	0.150	23.217	2.473
T63	1.189	3.969	64.62	0.175	0.150	23.308	2.486
T64	1.185	3.918	63.88	0.174	0.150	23.241	2.475
T65	1.182	3.910	63.71	0.173	0.149	23.208	2.471
T66	1.182	3.895	63.55	0.173	0.149	23.216	2.471
T7	1.044	2.774	45.40	0.139	0.129	23.206	2.398
T8	1.045	2.816	46.07	0.140	0.129	22.896	2.367
T9	1.056	2.847	46.64	0.141	0.131	23.182	2.401
UNEDF0	0.978	3.436	56.25	0.161	0.143	23.769	2.508
UNEDF1	0.854	2.748	45.32	0.140	0.130	23.936	2.478
v070	0.886	1.321	21.90	0.078	0.088	21.110	2.041
v075	0.893	1.399	23.19	0.082	0.091	21.335	2.073
v080	0.891	1.449	24.03	0.084	0.093	21.480	2.094
v090	0.895	1.503	24.91	0.087	0.095	21.634	2.115
v100	0.895	1.585	26.27	0.091	0.098	21.870	2.149
v105	0.894	1.520	25.21	0.088	0.095	21.685	2.123
v110	0.894	1.522	25.22	0.088	0.095	21.688	2.123
Z	0.994	0.446	7.36	0.028	0.051	19.341	1.755
ZR1a	0.000	0.000	0.00	−0.086	0.007	46.375	4.026
ZR1b	0.000	0.000	0.00	−0.022	0.022	24.644	2.140
ZR1c	0.000	0.000	0.00	0.007	0.030	14.472	1.256
ZR2a	0.000	0.000	0.00	−0.784	−0.162	283.176	24.586
ZR2b	0.000	0.000	0.00	−0.062	0.013	38.095	3.307
ZR2c	0.000	0.000	0.00	0.001	0.028	16.576	1.439
ZR3a	0.000	0.000	0.00	0.060	0.042	−3.243	−0.282
ZR3b	0.000	0.000	0.00	0.063	0.043	−4.485	−0.389
ZR3c	0.000	0.000	0.00	0.081	0.048	−10.547	−0.916
Zs	1.035	0.527	8.53	0.032	0.055	19.339	1.766
Zs*	1.060	1.397	22.69	0.079	0.088	20.128	1.947

TABLE IV. Neutron star properties of Skyrme models. Subscripts n indicate values for stars of mass $nM_\odot$. −1 indicates where $M > M_{\max}$. Radii and masses have units of km and $M_\odot$, respectively. Other quantities are dimensionless.

Model	$R_{1.2}$	$\Lambda_{1.2}$	$\bar{I}_{1.2}$	BE/$M_{1.2}$	$R_{1.4}$	$\Lambda_{1.4}$	$\bar{I}_{1.4}$	BE/$M_{1.4}$	$R_{1.6}$	$\Lambda_{1.6}$	$\bar{I}_{1.6}$	BE/$M_{1.6}$	$M_{\max}$
BSk1	−1	−1	−1	−1	−1	−1	−1	−1	−1	−1	−1	−1	0.09
BSk2	−1	−1	−1	−1	−1	−1	−1	−1	−1	−1	−1	−1	0.09
BSk2′	−1	−1	−1	−1	−1	−1	−1	−1	−1	−1	−1	−1	0.09
BSk3	−1	−1	−1	−1	−1	−1	−1	−1	−1	−1	−1	−1	0.09
BSk4	−1	−1	−1	−1	−1	−1	−1	−1	−1	−1	−1	−1	0.95
BSk5	6.62	11.5	5.83	0.159	−1	−1	−1	−1	−1	−1	−1	−1	1.20
BSk6	8.89	160.7	9.89	0.095	8.74	46.9	7.54	0.122	8.27	9.4	5.68	0.162	1.64
BSk7	9.07	185.1	10.23	0.093	8.94	55.9	7.81	0.118	8.56	13.0	5.97	0.153	1.67
BSk8	8.72	143.0	9.62	0.098	8.58	41.3	7.35	0.124	8.09	7.8	5.52	0.167	1.63
BSk9	10.85	576.5	13.74	0.073	10.78	207.0	10.50	0.091	10.60	71.0	8.21	0.113	1.91
BSk10	9.78	257.3	11.06	0.087	9.30	59.2	7.88	0.118	−1	−1	−1	−1	1.53
BSk11	9.97	296.8	11.47	0.085	9.55	73.9	8.26	0.113	−1	−1	−1	−1	1.57
BSk12	9.92	284.7	11.35	0.086	9.48	69.5	8.15	0.114	−1	−1	−1	−1	1.56

TABLE IV. (*Continued.*)

Model	$R_{1.2}$	$\Lambda_{1.2}$	$\bar{I}_{1.2}$	$BE/M_{1.2}$	$R_{1.4}$	$\Lambda_{1.4}$	$\bar{I}_{1.4}$	$BE/M_{1.4}$	$R_{1.6}$	$\Lambda_{1.6}$	$\bar{I}_{1.6}$	$BE/M_{1.6}$	M_{max}
BSk13	10.04	311.6	11.61	0.084	9.64	79.2	8.39	0.111	−1	−1	−1	−1	1.58
BSk14	11.01	622.8	14.02	0.071	10.90	216.6	10.61	0.090	10.65	70.7	8.20	0.113	1.86
BSk15	10.05	332.9	11.82	0.082	9.84	100.0	8.85	0.106	9.37	24.6	6.65	0.138	1.70
BSk16	10.24	377.2	12.24	0.080	10.06	119.3	9.21	0.102	9.68	32.5	7.00	0.131	1.74
BSk17	10.38	414.1	12.55	0.078	10.21	133.3	9.45	0.100	9.86	37.9	7.21	0.127	1.76
BSk18	10.40	420.5	12.60	0.078	10.24	136.5	9.50	0.099	9.90	39.5	7.27	0.126	1.77
BSk19	10.51	455.7	12.86	0.077	10.41	156.5	9.82	0.096	10.19	51.2	7.67	0.120	1.86
BSk20	11.41	846.6	15.21	0.067	11.46	328.4	11.83	0.082	11.45	134.4	9.48	0.099	2.18
BSk21	12.22	1423.2	17.59	0.059	12.39	603.7	13.85	0.072	12.51	262.3	11.23	0.085	2.50
BSk22	12.90	1985.5	19.39	0.055	13.07	845.8	15.18	0.067	13.19	379.2	12.26	0.080	2.58
BSk23	12.58	1695.1	18.51	0.057	12.75	720.2	14.53	0.069	12.86	317.9	11.75	0.082	2.54
BSk24	12.22	1426.2	17.61	0.059	12.40	605.2	13.86	0.072	12.51	262.9	11.24	0.085	2.50
BSk25	11.94	1272.6	17.05	0.061	12.14	544.7	13.49	0.073	12.28	239.5	10.99	0.087	2.52
BSk26	11.43	859.4	15.26	0.066	11.49	332.4	11.88	0.082	11.48	136.8	9.52	0.099	2.18
E	−1	−1	−1	−1	−1	−1	−1	−1	−1	−1	−1	−1	0.15
Es	−1	−1	−1	−1	−1	−1	−1	−1	−1	−1	−1	−1	0.15
f−	11.48	859.6	15.26	0.066	11.52	331.3	11.86	0.082	11.49	134.3	9.48	0.099	2.15
f+	11.51	854.2	15.24	0.067	11.54	328.3	11.82	0.082	11.49	131.2	9.43	0.099	2.13
f0	11.50	856.5	15.25	0.067	11.53	329.4	11.83	0.082	11.49	132.2	9.45	0.099	2.14
FPLyon	10.78	541.1	13.46	0.074	10.67	185.3	10.22	0.093	10.43	60.3	7.93	0.116	1.86
Gs	−1	−1	−1	−1	−1	−1	−1	−1	−1	−1	−1	−1	0.00
Gs1	11.70	1054.3	16.14	0.064	11.76	397.7	12.46	0.079	11.74	160.8	9.91	0.095	2.14
Gs2	10.74	602.6	13.94	0.072	10.77	226.5	10.77	0.089	10.69	84.2	8.53	0.109	1.98
Gs3	8.87	162.7	9.87	0.096	8.75	42.0	7.58	0.121	8.35	9.6	5.79	0.158	1.66
Gs4	−1	−1	−1	−1	−1	−1	−1	−1	−1	−1	−1	−1	0.00
Gs5	−1	−1	−1	−1	−1	−1	−1	−1	−1	−1	−1	−1	0.00
Gs6	−1	−1	−1	−1	−1	−1	−1	−1	−1	−1	−1	−1	0.00
GSkI	12.00	1143.9	16.50	0.063	11.94	404.2	12.47	0.079	11.76	147.6	9.68	0.098	1.98
GSkII	10.93	566.5	13.58	0.074	10.61	162.1	9.88	0.096	9.86	33.0	7.00	0.132	1.65
KDE	10.84	552.5	13.58	0.073	10.77	198.2	10.39	0.092	10.58	68.4	8.15	0.113	1.92
KDE0v	11.19	656.2	14.24	0.071	11.11	236.9	10.88	0.088	10.92	84.4	8.53	0.109	1.95
KDE0v1	11.54	797.2	14.97	0.068	11.44	284.6	11.39	0.085	11.25	102.1	8.89	0.105	1.97
LNS	11.14	614.7	13.91	0.072	10.83	183.4	10.18	0.094	10.24	44.5	7.43	0.124	1.70
MSk1	9.36	190.0	10.26	0.093	8.84	40.3	7.29	0.126	−1	−1	−1	−1	1.50
MSk2	8.98	136.1	9.48	0.100	8.07	17.5	6.24	0.148	−1	−1	−1	−1	1.42
MSk3	−1	−1	−1	−1	−1	−1	−1	−1	−1	−1	−1	−1	0.09
MSk4	−1	−1	−1	−1	−1	−1	−1	−1	−1	−1	−1	−1	0.09
MSk5	−1	−1	−1	−1	−1	−1	−1	−1	−1	−1	−1	−1	0.09
MSk5*	−1	−1	−1	−1	−1	−1	−1	−1	−1	−1	−1	−1	1.02
MSk6	−1	−1	−1	−1	−1	−1	−1	−1	−1	−1	−1	−1	0.09
MSk7	−1	−1	−1	−1	−1	−1	−1	−1	−1	−1	−1	−1	0.09
MSk8	−1	−1	−1	−1	−1	−1	−1	−1	−1	−1	−1	−1	0.09
MSk9	−1	−1	−1	−1	−1	−1	−1	−1	−1	−1	−1	−1	0.78
MSkA	12.43	1542.0	17.99	0.058	12.53	620.1	13.94	0.072	12.56	255.9	11.12	0.086	2.30
MSL0	11.85	1089.5	16.28	0.063	11.79	381.9	12.28	0.080	11.59	135.5	9.49	0.099	1.94
NRAPR	11.87	990.0	15.84	0.065	11.73	341.8	11.90	0.082	11.47	116.2	9.15	0.103	1.92
PRC45	16.25	6170.0	27.21	0.041	16.30	2509.8	20.86	0.052	16.31	1168.2	16.61	0.062	2.91
RATP	10.19	364.1	12.12	0.081	9.99	112.7	9.09	0.103	9.57	29.3	6.87	0.133	1.72
Rs	13.06	2268.4	20.18	0.053	13.18	910.3	15.50	0.066	13.20	375.2	12.24	0.080	2.27
SAMi	11.6	862.3	15.25	0.067	11.6	323.5	11.74	0.083	11.5	122.4	9.28	0.101	2.04
SAMi-T	11.6	856.7	15.22	0.067	11.6	322.5	11.73	0.083	11.5	122.8	9.28	0.101	2.06
Sefm068	21.11	16644.1	40.36	0.028	20.77	8147.9	30.36	0.038	20.41	3583.7	23.16	0.048	2.68
Sefm074	13.15	2232.0	20.05	0.053	13.21	874.3	15.31	0.067	13.18	352.7	12.02	0.081	2.22
Sefm081	12.71	1864.7	19.01	0.056	12.78	719.6	14.52	0.070	12.74	283.8	11.39	0.085	2.16
Sefm09	12.32	1594.7	18.19	0.058	12.40	615.7	13.93	0.072	12.38	243.3	10.96	0.088	2.13
Sefm1	−1	−1	−1	−1	−1	−1	−1	−1	−1	−1	−1	−1	0.00

TABLE IV. (*Continued.*)

Model	$R_{1.2}$	$\Lambda_{1.2}$	$\bar{I}_{1.2}$	BE/$M_{1.2}$	$R_{1.4}$	$\Lambda_{1.4}$	$\bar{I}_{1.4}$	BE/$M_{1.4}$	$R_{1.6}$	$\Lambda_{1.6}$	$\bar{I}_{1.6}$	BE/$M_{1.6}$	M_{max}
SGI	12.53	1765.9	18.72	0.056	12.67	714.3	14.49	0.069	12.72	298.2	11.55	0.084	2.31
SGII	10.30	406.3	12.47	0.079	10.04	117.7	9.17	0.103	9.41	24.5	6.63	0.139	1.66
SGOI	13.96	2428.2	20.56	0.052	13.92	962.2	15.72	0.065	13.84	401.5	12.43	0.079	2.41
SGOII	21.76	18412.2	41.25	0.028	21.15	8286.5	30.19	0.038	20.54	3276.7	22.51	0.049	2.52
SI	−1	−1	−1	−1	−1	−1	−1	−1	−1	−1	−1	−1	0.12
SI′	11.43	891.6	15.41	0.066	11.52	346.1	12.04	0.081	11.55	146.4	9.70	0.097	2.24
SII	12.05	1014.6	15.95	0.064	11.94	360.9	12.10	0.081	11.74	132.7	9.44	0.100	2.02
SIII	−1	−1	−1	−1	−1	−1	−1	−1	−1	−1	−1	−1	1.18
SIII*	9.35	184.0	10.19	0.093	9.00	47.1	7.53	0.122	−1	−1	−1	−1	1.58
SIV	12.93	1931.4	19.21	0.055	13.02	782.8	14.85	0.068	13.05	328.5	11.83	0.082	2.36
SK255	13.62	2565.7	20.88	0.052	13.64	999.2	15.89	0.065	13.58	404.7	12.44	0.079	2.24
SK272	13.64	2547.1	20.85	0.052	13.68	1008.3	15.93	0.064	13.64	417.9	12.55	0.078	2.30
SKa	13.00	1976.2	19.34	0.055	13.05	777.7	14.82	0.068	13.02	314.4	11.69	0.083	2.25
Ska25s20	11.78	925.0	15.55	0.066	11.59	304.1	11.56	0.084	11.23	95.4	8.74	0.107	1.84
Ska35s15	8.54	93.2	8.69	0.108	−1	−1	−1	−1	−1	−1	−1	−1	1.38
Ska35s20	12.07	1122.7	16.41	0.063	11.96	388.6	12.33	0.080	11.72	136.4	9.50	0.099	1.94
Ska35s25	13.58	2607.5	20.99	0.051	13.63	1028.2	16.02	0.064	13.60	423.3	12.59	0.078	2.27
Ska45s20	12.35	1339.4	17.26	0.060	12.31	487.8	13.10	0.076	12.16	184.6	10.22	0.093	2.06
SKb	11.83	1277.1	17.20	0.060	11.97	485.0	13.31	0.074	12.01	206.7	10.60	0.090	2.20
SkI1	−1	−1	−1	−1	−1	−1	−1	−1	−1	−1	−1	−1	0.00
SkI2	13.57	3002.4	21.96	0.049	13.77	1265.5	17.03	0.061	13.89	563.0	13.60	0.073	2.52
SkI3	13.58	2845.4	21.61	0.050	13.77	1222.7	16.84	0.061	13.90	552.3	13.52	0.073	2.59
SkI4	12.19	1441.0	17.65	0.059	12.31	581.0	13.71	0.073	12.36	241.7	10.96	0.087	2.29
SkI5	14.21	3974.1	24.09	0.046	14.47	1772.7	18.80	0.056	14.66	827.3	15.12	0.067	2.75
SkI6	−1	−1	−1	−1	−1	−1	−1	−1	−1	−1	−1	−1	0.00
SkM	10.86	534.0	13.36	0.075	10.53	152.5	9.74	0.098	9.84	32.5	6.99	0.132	1.67
SkM1	−1	−1	−1	−1	−1	−1	−1	−1	−1	−1	−1	−1	0.14
SkM*	10.55	433.0	12.66	0.078	10.16	115.8	9.13	0.103	9.10	16.0	6.14	0.151	1.61
SkMP	12.59	1718.6	18.56	0.057	12.65	666.3	14.21	0.071	12.62	264.6	11.19	0.086	2.19
SkO	12.65	1735.3	18.60	0.057	12.67	656.0	14.14	0.071	12.58	252.4	11.04	0.087	2.10
SkO′	12.22	1302.6	17.12	0.061	12.17	464.8	12.93	0.077	12.00	170.2	10.02	0.095	2.00
SkP	−1	−1	−1	−1	−1	−1	−1	−1	−1	−1	−1	−1	0.13
SKRA	11.28	682.9	14.34	0.070	11.03	215.2	10.58	0.091	10.56	59.1	7.88	0.118	1.76
SkS1	−1	−1	−1	−1	−1	−1	−1	−1	−1	−1	−1	−1	0.77
SkS2	−1	−1	−1	−1	−1	−1	−1	−1	−1	−1	−1	−1	0.59
SkS3	10.64	454.5	12.78	0.078	−1	−1	−1	−1	−1	−1	−1	−1	1.35
SkS4	−1	−1	−1	−1	−1	−1	−1	−1	−1	−1	−1	−1	0.38
SkSC1	−1	−1	−1	−1	−1	−1	−1	−1	−1	−1	−1	−1	0.10
SkSC2	6.74	17.7	6.27	0.146	−1	−1	−1	−1	−1	−1	−1	−1	1.24
SkSC3	−1	−1	−1	−1	−1	−1	−1	−1	−1	−1	−1	−1	0.09
SkSC4	−1	−1	−1	−1	−1	−1	−1	−1	−1	−1	−1	−1	0.12
SkSC4o	−1	−1	−1	−1	−1	−1	−1	−1	−1	−1	−1	−1	0.11
SkSC5	−1	−1	−1	−1	−1	−1	−1	−1	−1	−1	−1	−1	0.15
SkSC6	6.88	21.5	6.49	0.141	−1	−1	−1	−1	−1	−1	−1	−1	1.26
SkSC10	9.07	197.0	10.38	0.092	8.84	51.9	7.69	0.120	−1	−1	−1	−1	1.58
SkSC11	−1	−1	−1	−1	−1	−1	−1	−1	−1	−1	−1	−1	0.12
SkSC14	9.18	166.0	9.94	0.096	8.62	32.7	7.00	0.131	−1	−1	−1	−1	1.48
SkSC15	−1	−1	−1	−1	−1	−1	−1	−1	−1	−1	−1	−1	0.09
SkSP.1	6.98	24.2	6.64	0.138	−1	−1	−1	−1	−1	−1	−1	−1	1.30
SkT	11.04	730.1	14.65	0.069	11.08	277.9	11.33	0.085	11.04	107.0	9.00	0.104	2.04
SkT1a	11.42	772.5	14.83	0.068	11.26	257.6	11.09	0.087	10.93	81.2	8.44	0.110	1.83
SkT2a	11.42	770.8	14.82	0.068	11.25	256.9	11.08	0.087	10.93	80.9	8.43	0.110	1.83
SkT3a	11.81	769.0	14.79	0.069	11.55	257.0	11.07	0.087	11.15	81.6	8.44	0.110	1.84
SkT4a	13.32	2345.3	20.35	0.053	13.37	919.5	15.52	0.066	13.33	371.8	12.18	0.080	2.23
SkT5a	13.23	2173.6	19.88	0.054	13.20	806.7	14.96	0.068	13.05	303.1	11.56	0.084	2.08
SkT6a	8.80	120.8	9.22	0.102	8.02	17.6	6.25	0.147	−1	−1	−1	−1	1.43

TABLE IV. (*Continued.*)

Model	$R_{1.2}$	$\Lambda_{1.2}$	$\bar{I}_{1.2}$	BE/$M_{1.2}$	$R_{1.4}$	$\Lambda_{1.4}$	$\bar{I}_{1.4}$	BE/$M_{1.4}$	$R_{1.6}$	$\Lambda_{1.6}$	$\bar{I}_{1.6}$	BE/$M_{1.6}$	M_{max}
SkT7a	9.05	147.0	9.65	0.098	8.33	24.0	6.60	0.140	−1	−1	−1	−1	1.44
SkT8a	9.97	315.3	11.66	0.083	9.75	94.1	8.73	0.107	9.27	22.5	6.54	0.140	1.69
SkT9a	9.99	322.1	11.72	0.083	9.78	96.5	8.78	0.106	9.31	23.4	6.59	0.139	1.70
SkTK	10.48	380.9	12.26	0.080	10.21	116.6	9.16	0.103	9.73	30.4	6.91	0.133	1.73
SKX	9.12	143.2	9.59	0.099	−1	−1	−1	−1	−1	−1	−1	−1	1.39
Skχ414	11.9	952.0	15.69	0.065	11.9	368.4	12.19	0.080	11.8	151.7	9.77	0.096	2.21
Skχ450	11.6	799.4	14.93	0.068	11.5	301.6	11.54	0.084	11.4	117.0	9.18	0.102	2.10
Skχ500	11.6	885.4	15.40	0.066	11.6	353.7	12.09	0.080	11.7	151.1	9.77	0.096	2.28
SKXce	9.51	203.2	10.43	0.092	8.85	38.3	7.21	0.128	−1	−1	−1	−1	1.47
Skxcsb	10.7	417.1	12.54	0.079	10.4	127.7	9.35	0.101	9.8	32.7	7.00	0.131	1.72
SKXm	−1	−1	−1	−1	−1	−1	−1	−1	−1	−1	−1	−1	0.59
Skxs15	7.40	25.7	6.67	0.139	−1	−1	−1	−1	−1	−1	−1	−1	1.22
Skxs20	11.72	819.0	15.04	0.068	11.38	246.4	10.94	0.088	10.76	62.3	7.96	0.117	1.72
Skxs25	13.52	2287.4	20.17	0.053	13.42	831.1	15.07	0.068	13.20	304.2	11.56	0.084	2.05
Skxta	8.9	109.2	8.99	0.105	−1	−1	−1	−1	−1	−1	−1	−1	1.33
Skxtb	9.6	188.4	10.23	0.094	8.8	32.2	6.97	0.132	−1	−1	−1	−1	1.45
Skz−1	10.71	425.2	12.55	0.079	−1	−1	−1	−1	−1	−1	−1	−1	1.37
Skz0	−1	−1	−1	−1	−1	−1	−1	−1	−1	−1	−1	−1	0.73
Skz1	8.15	62.9	7.98	0.116	−1	−1	−1	−1	−1	−1	−1	−1	1.35
Skz2	8.08	72.7	8.26	0.112	7.73	15.7	6.16	0.148	−1	−1	−1	−1	1.49
Skz3	8.95	169.4	10.02	0.094	8.90	55.3	7.81	0.117	8.68	15.7	6.17	0.147	1.74
Skz4	−1	−1	−1	−1	−1	−1	−1	−1	−1	−1	−1	−1	0.16
SLy0	11.49	837.9	15.16	0.067	11.47	315.3	11.67	0.083	11.38	120.0	9.24	0.101	2.06
SLy1	11.48	836.1	15.15	0.067	11.47	314.6	11.67	0.083	11.37	119.8	9.23	0.101	2.06
SLy2	11.50	845.0	15.20	0.067	11.49	318.3	11.70	0.083	11.39	121.2	9.26	0.101	2.06
SLy230a	11.51	886.3	15.39	0.066	11.56	340.2	11.95	0.081	11.54	139.3	9.56	0.098	2.16
SLy230b	11.46	821.6	15.09	0.067	11.45	309.5	11.62	0.083	11.35	118.1	9.20	0.102	2.06
SLy3	11.39	786.2	14.92	0.068	11.38	295.0	11.49	0.084	11.27	112.3	9.10	0.103	2.05
SLy4	11.46	821.2	15.09	0.067	11.45	309.3	11.62	0.083	11.35	118.0	9.20	0.102	2.06
SLy5	11.55	873.3	15.33	0.066	11.54	328.8	11.80	0.082	11.45	125.8	9.34	0.100	2.07
SLy6	11.58	887.9	15.39	0.066	11.57	334.2	11.86	0.082	11.49	129.7	9.40	0.100	2.09
SLy7	11.60	898.5	15.44	0.066	11.60	337.7	11.90	0.082	11.52	131.8	9.44	0.100	2.09
SLy8	11.49	838.7	15.17	0.067	11.48	316.1	11.68	0.083	11.38	120.5	9.25	0.101	2.06
SLy9	12.27	1322.5	17.21	0.060	12.32	513.9	13.29	0.075	12.29	212.4	10.58	0.090	2.23
SLy10	11.22	693.7	14.46	0.070	11.20	262.2	11.18	0.086	11.11	100.8	8.88	0.105	2.04
SQMC1	−1	−1	−1	−1	−1	−1	−1	−1	−1	−1	−1	−1	0.18
SQMC2	−1	−1	−1	−1	−1	−1	−1	−1	−1	−1	−1	−1	0.13
SQMC3	14.00	2251.4	20.10	0.053	13.89	874.2	15.31	0.067	13.75	356.7	12.07	0.081	2.39
SQMC600	−1	−1	−1	−1	−1	−1	−1	−1	−1	−1	−1	−1	0.93
SQMC650	10.35	341.6	11.87	0.083	9.69	72.1	8.21	0.114	−1	−1	−1	−1	1.51
SQMC700	11.25	648.7	14.13	0.071	10.96	199.8	10.39	0.092	10.44	52.6	7.69	0.120	1.74
SQMC750	11.69	880.2	15.35	0.067	11.51	293.5	11.46	0.085	11.19	94.3	8.73	0.107	1.86
SSK	11.64	879.0	15.35	0.066	11.59	323.2	11.74	0.083	11.44	119.8	9.23	0.102	2.03
SV	13.79	3243.3	22.44	0.048	14.01	1390.2	17.49	0.060	14.16	636.5	14.05	0.071	2.65
SV-bas	−1	−1	−1	−1	−1	−1	−1	−1	−1	−1	−1	−1	1.04
SV-min	10.44	411.3	12.50	0.079	10.12	116.7	9.15	0.103	9.41	23.0	6.56	0.140	1.65
SVI	−1	−1	−1	−1	−1	−1	−1	−1	−1	−1	−1	−1	0.11
SVII	−1	−1	−1	−1	−1	−1	−1	−1	−1	−1	−1	−1	0.11
SV-K218	−1	−1	−1	−1	−1	−1	−1	−1	−1	−1	−1	−1	0.87
SV-K226	−1	−1	−1	−1	−1	−1	−1	−1	−1	−1	−1	−1	0.99
SV-K241	−1	−1	−1	−1	−1	−1	−1	−1	−1	−1	−1	−1	1.10
SV-Kap00	10.51	457.2	12.87	0.077	10.36	149.6	9.71	0.097	10.04	44.3	7.44	0.124	1.79
SV-Kap02	9.67	240.2	10.87	0.089	9.24	57.5	7.84	0.118	−1	−1	−1	−1	1.55
SV-Kap06	−1	−1	−1	−1	−1	−1	−1	−1	−1	−1	−1	−1	0.32
SV-mas07	11.70	1012.0	15.95	0.064	11.71	371.5	12.22	0.080	11.62	144.5	9.64	0.098	2.07
SV-mas08	10.45	419.5	12.58	0.078	10.19	126.5	9.33	0.101	9.68	30.7	6.92	0.133	1.70

TABLE IV. (*Continued.*)

Model	$R_{1.2}$	$\Lambda_{1.2}$	$\bar{I}_{1.2}$	$BE/M_{1.2}$	$R_{1.4}$	$\Lambda_{1.4}$	$\bar{I}_{1.4}$	$BE/M_{1.4}$	$R_{1.6}$	$\Lambda_{1.6}$	$\bar{I}_{1.6}$	$BE/M_{1.6}$	M_{max}
SV-mas10	−1	−1	−1	−1	−1	−1	−1	−1	−1	−1	−1	−1	0.26
SV-sym28	−1	−1	−1	−1	−1	−1	−1	−1	−1	−1	−1	−1	0.09
SV-sym32	11.42	739.4	14.64	0.069	11.12	224.9	10.69	0.090	10.53	55.5	7.77	0.120	1.70
SV-sym34	12.84	1777.2	18.73	0.056	12.79	650.3	14.10	0.071	12.61	240.5	10.88	0.089	2.02
SV-tls	−1	−1	−1	−1	−1	−1	−1	−1	−1	−1	−1	−1	1.09
T	8.69	117.6	9.17	0.103	8.02	18.6	6.32	0.146	−1	−1	−1	−1	1.44
T1	11.42	772.5	14.83	0.068	11.26	257.6	11.09	0.087	10.93	81.2	8.44	0.110	1.83
T11	11.57	889.2	15.40	0.066	11.56	333.3	11.85	0.082	11.47	127.8	9.37	0.100	2.07
T12	11.57	891.0	15.41	0.066	11.57	333.9	11.85	0.082	11.48	128.3	9.38	0.100	2.07
T13	11.59	897.8	15.44	0.066	11.58	336.0	11.88	0.082	11.49	129.5	9.40	0.100	2.07
T14	11.58	896.5	15.43	0.066	11.58	335.7	11.87	0.082	11.49	129.4	9.40	0.100	2.08
T15	11.58	896.5	15.43	0.066	11.58	335.5	11.87	0.082	11.49	129.1	9.39	0.100	2.07
T16	11.58	891.5	15.41	0.066	11.57	334.0	11.85	0.082	11.48	128.2	9.38	0.100	2.07
T1*	11.44	781.5	14.87	0.068	11.28	260.9	11.12	0.087	10.95	82.4	8.47	0.110	1.84
T2	11.42	770.8	14.82	0.068	11.25	256.9	11.08	0.087	10.93	80.9	8.43	0.110	1.83
T21	11.58	892.5	15.41	0.066	11.57	334.0	11.85	0.082	11.47	128.0	9.37	0.100	2.07
T22	11.57	889.6	15.40	0.066	11.56	333.2	11.84	0.082	11.47	127.7	9.37	0.100	2.07
T23	11.58	892.7	15.41	0.066	11.57	334.2	11.86	0.082	11.48	128.3	9.38	0.100	2.07
T24	11.59	903.1	15.46	0.066	11.59	337.5	11.89	0.082	11.50	130.2	9.41	0.100	2.07
T25	11.57	890.4	15.40	0.066	11.57	333.9	11.85	0.082	11.48	128.5	9.38	0.100	2.07
T26	11.56	882.5	15.37	0.066	11.55	331.6	11.83	0.082	11.47	127.4	9.36	0.100	2.07
T3	11.39	768.6	14.81	0.068	11.24	258.0	11.10	0.087	10.92	82.0	8.46	0.110	1.84
T31	11.58	895.2	15.43	0.066	11.57	334.9	11.86	0.082	11.48	128.7	9.38	0.100	2.07
T32	11.60	909.1	15.49	0.066	11.60	339.2	11.91	0.082	11.50	130.8	9.42	0.100	2.07
T33	11.58	894.5	15.42	0.066	11.57	334.7	11.86	0.082	11.48	128.5	9.38	0.100	2.07
T34	11.59	903.7	15.46	0.066	11.59	337.5	11.89	0.082	11.49	129.9	9.40	0.100	2.07
T35	11.59	901.9	15.46	0.066	11.59	337.3	11.89	0.082	11.50	130.2	9.41	0.100	2.08
T36	11.56	882.5	15.37	0.066	11.55	331.4	11.83	0.082	11.46	127.1	9.36	0.100	2.07
T3*	11.45	792.5	14.93	0.068	11.30	266.2	11.18	0.086	10.99	85.2	8.53	0.109	1.84
T4	13.32	2345.3	20.35	0.053	13.37	919.5	15.52	0.066	13.33	371.8	12.18	0.080	2.23
T41	11.59	904.4	15.47	0.066	11.58	337.3	11.89	0.082	11.49	129.5	9.40	0.100	2.07
T42	11.61	911.8	15.50	0.066	11.60	339.6	11.91	0.082	11.50	130.7	9.42	0.100	2.07
T43	11.61	912.3	15.50	0.066	11.60	340.0	11.92	0.082	11.51	131.1	9.42	0.100	2.07
T44	11.60	907.3	15.48	0.066	11.59	338.7	11.90	0.082	11.50	130.7	9.42	0.100	2.07
T45	11.57	891.4	15.41	0.066	11.57	333.8	11.85	0.082	11.47	128.0	9.37	0.100	2.07
T46	11.62	916.0	15.52	0.066	11.61	341.8	11.94	0.082	11.53	132.6	9.45	0.099	2.08
T5	13.23	2173.6	19.88	0.054	13.20	806.7	14.96	0.068	13.05	303.1	11.56	0.084	2.08
T51	11.61	912.7	15.50	0.066	11.60	340.1	11.92	0.082	11.51	131.0	9.42	0.100	2.07
T52	11.61	915.1	15.51	0.066	11.61	340.8	11.93	0.082	11.51	131.4	9.43	0.100	2.07
T53	11.60	905.0	15.47	0.066	11.59	337.9	11.90	0.082	11.50	130.2	9.41	0.100	2.07
T54	11.60	909.5	15.49	0.066	11.60	339.3	11.91	0.082	11.51	130.8	9.42	0.100	2.07
T55	11.60	905.8	15.47	0.066	11.59	338.1	11.90	0.082	11.50	130.2	9.41	0.100	2.07
T56	11.61	915.1	15.51	0.066	11.61	341.4	11.93	0.082	11.52	132.2	9.44	0.100	2.08
T6	8.80	120.8	9.22	0.102	8.02	17.6	6.25	0.147	−1	−1	−1	−1	1.43
T61	11.60	909.2	15.49	0.066	11.59	338.7	11.90	0.082	11.50	130.1	9.41	0.100	2.07
T62	11.57	894.1	15.42	0.066	11.57	333.9	11.85	0.082	11.47	127.5	9.36	0.100	2.06
T63	11.62	919.9	15.54	0.066	11.61	342.2	11.94	0.082	11.52	132.0	9.44	0.100	2.07
T64	11.61	912.9	15.50	0.066	11.60	340.2	11.92	0.082	11.51	131.3	9.43	0.100	2.07
T65	11.60	909.1	15.49	0.066	11.60	338.9	11.91	0.082	11.50	130.5	9.41	0.100	2.07
T66	11.61	912.4	15.50	0.066	11.60	340.4	11.92	0.082	11.51	131.5	9.43	0.100	2.08
T7	9.05	147.0	9.65	0.098	8.33	24.0	6.60	0.140	−1	−1	−1	−1	1.44
T8	9.97	315.3	11.66	0.083	9.75	94.1	8.73	0.107	9.27	22.5	6.54	0.140	1.69
T9	9.99	322.1	11.72	0.083	9.78	96.5	8.78	0.106	9.31	23.4	6.59	0.139	1.70
UNEDF0	−1	−1	−1	−1	−1	−1	−1	−1	−1	−1	−1	−1	1.01
UNEDF1	−1	−1	−1	−1	−1	−1	−1	−1	−1	−1	−1	−1	1.13
v070	−1	−1	−1	−1	−1	−1	−1	−1	−1	−1	−1	−1	0.11
v075	−1	−1	−1	−1	−1	−1	−1	−1	−1	−1	−1	−1	0.10

TABLE IV. (*Continued.*)

Model	$R_{1.2}$	$\Lambda_{1.2}$	$\bar{I}_{1.2}$	BE/$M_{1.2}$	$R_{1.4}$	$\Lambda_{1.4}$	$\bar{I}_{1.4}$	BE/$M_{1.4}$	$R_{1.6}$	$\Lambda_{1.6}$	$\bar{I}_{1.6}$	BE/$M_{1.6}$	M_{max}
v080	−1	−1	−1	−1	−1	−1	−1	−1	−1	−1	−1	−1	0.10
v090	−1	−1	−1	−1	−1	−1	−1	−1	−1	−1	−1	−1	0.09
v100	−1	−1	−1	−1	−1	−1	−1	−1	−1	−1	−1	−1	0.09
v105	−1	−1	−1	−1	−1	−1	−1	−1	−1	−1	−1	−1	0.09
v110	−1	−1	−1	−1	−1	−1	−1	−1	−1	−1	−1	−1	0.09
Z	−1	−1	−1	−1	−1	−1	−1	−1	−1	−1	−1	−1	0.17
ZR1a	−1	−1	−1	−1	−1	−1	−1	−1	−1	−1	−1	−1	0.00
ZR1b	−1	−1	−1	−1	−1	−1	−1	−1	−1	−1	−1	−1	0.00
ZR1c	−1	−1	−1	−1	−1	−1	−1	−1	−1	−1	−1	−1	0.11
ZR2a	−1	−1	−1	−1	−1	−1	−1	−1	−1	−1	−1	−1	0.00
ZR2b	−1	−1	−1	−1	−1	−1	−1	−1	−1	−1	−1	−1	0.00
ZR2c	−1	−1	−1	−1	−1	−1	−1	−1	−1	−1	−1	−1	0.09
ZR3a	−1	−1	−1	−1	−1	−1	−1	−1	−1	−1	−1	−1	0.00
ZR3b	−1	−1	−1	−1	−1	−1	−1	−1	−1	−1	−1	−1	0.00
ZR3c	−1	−1	−1	−1	−1	−1	−1	−1	−1	−1	−1	−1	0.00
Zs	−1	−1	−1	−1	−1	−1	−1	−1	−1	−1	−1	−1	0.15
Zs*	−1	−1	−1	−1	−1	−1	−1	−1	−1	−1	−1	−1	0.12

APPENDIX B: PARAMETERS AND PROPERTIES FOR RELATIVISTIC MEAN-FIELD AND RELATIVISTIC MEAN-FIELD POINT-COUPLING MODELS

This Appendix contains Tables V–X.

TABLE V. Parameters of RMF models. Masses, A, α_1, and α_2 are in MeV. Other quantities are dimensionless.

	M_n	m_σ	m_ω	m_ρ	m_δ	g_σ	g_ω	g_ρ	
Model	A	B	C	α_1	α'_1	α_2	α'_2	α'_3	g_δ
Linear finite-range models (type 1)									
H1 [96]	939	550	783	770		11.079	13.806	5.258	
L1 [97]	938	550	783			10.3	12.6		
L2 [97]	938	546.94	780			11.397	14.248		
L3 [97]	938	492.26	780			10.692	14.87		
LBF [45]	938	615	1008	763		12.334	17.619	10.378	
LHS [97]	938.9	520	783	770		10.481	13.814	8.0849	
LW [97]	938.9	550	783			9.574	11.672		
LZ [97]	938	551.31	780	763		11.193	13.826	10.8883	
RMF201 [98]	938.9	550	783	763		10.974	13.636	7.1007	
RMF202 [96]	938.9	550	783	763		10.963	13.62	7.1089	
RMF203 [96]	938.9	550	783	763		10.951	13.604	7.117	
RMF204 [96]	938.9	550	783	763		10.94	13.588	7.125	
RMF205 [96]	938.9	550	783	763		10.929	13.572	7.1331	
RMF206 [96]	938.9	550	783	763		10.917	13.556	7.141	
$\sigma^3 + \sigma^4$ models (type 2)									
CS [99]	938	492.45	780	763		10.144	12.969	9.5757	
	2598.9062	−39.371							
E [99]	938	502.71	780	763		10.317	13.031	9.0408	
	2418.6655	−36.8858							
ER [99]	938	500.55	780	763		10.279	13.025	9.3045	
	2415.7714	−36.4817							

TABLE V. (*Continued.*)

	M_n	m_σ	m_ω	m_ρ	m_δ	g_σ	g_ω	g_ρ	
Model	A	B	C	α_1	α_1'	α_2	α_2'	α_3'	g_δ
FAMA1 [100]	939	500	783	763		10.13	12.782	9.1007	
	2639.2391	−39.0652							
FAMA2 [100]	939	500	783	763		10.076	12.782	9.1007	
	2381.9744	−34.3879							
FAMA3 [100]	939	500	783	763		10.022	12.782	9.1007	
	2128.2523	−29.8203							
FAMA4 [100]	939	500	783	763		9.967	12.782	9.1007	
	1878.0575	−25.3612							
FAMA5 [100]	939	500	783	763		9.913	12.782	9.1007	
	1631.375	−21.0095							
FAMB1 [100]	939	500	783	763		9.125	10.81	9.3601	
	3746.48	−44.9319							
FAMB2 [100]	939	500	783	763		9.043	10.81	9.3601	
	3218.7987	−34.1835							
FAMB3 [100]	939	500	783	763		8.962	10.81	9.3601	
	2705.5114	−23.9087							
FAMB4 [100]	939	500	783	763		8.881	10.81	9.3601	
	2206.3502	−14.0938							
FAMB5 [100]	939	500	783	763		8.8	10.81	9.3601	
	1721.0554	−4.7255							
FAMC1 [100]	939	500	783	763		9.125	10.81	7.1316	
	3746.4804	−44.9319							
FAMC2 [100]	939	500	783	763		9.043	10.81	7.1316	
	3218.7987	−34.1835							
FAMC3 [100]	939	500	783	763		8.962	10.81	7.1316	
	2705.5114	−23.9087							
FAMC4 [100]	939	500	783	763		8.881	10.81	7.1316	
	2206.3502	−14.0938							
FAMC5 [100]	939	500	783	763		8.8	10.81	7.1316	
	1721.0554	−4.7255							
GL1 [101]	938	550	782	770		9.927	10.595	8.1944	
	5147.0545	−67.8296							
GL2 [101]	938	550	782	770		9.369	9.458	8.4198	
	6775.8518	−77.8025							
GL3 [101]	938	550	782	770		8.781	8.153	8.6165	
	9274.389	−73.8021							
GL4 [101]	938	550	782	770		9.747	10.595	8.1944	
	3745.6742	−37.0367							
GL5 [101]	938	550	782	770		9.129	9.458	8.4198	
	4477.5734	−23.6735							
GL6 [101]	938	550	782	770		8.424	8.153	8.6165	
	4936.0904	33.8202							
GL7 [101]	938	550	782	770		9.568	10.595	8.1944	
	2422.3306	−8.9769							
GL8 [101]	938	550	782	770		8.892	9.458	8.4198	
	2374.4572	23.2645							
GL82 [102]	938	550	782	770		8.795	9.17	9.7163	
	2641.9492	42.8425							
GL9 [101]	938	550	782	770		8.08	8.153	8.6165	
	1226.9159	119.305							
GM1 [103]	939	550	782	770		9.57	10.596	8.1953	
	2425.744	−8.9767							
GM2 [103]	939	550	782	770		8.43	8.7	8.5412	
	1956.649	67.0741							
GM3 [103]	939	550	782	770		8.782	8.7	8.5412	
	5506.668	−14.3991							

TABLE V. (*Continued.*)

	M_n	m_σ	m_ω	m_ρ	m_δ	g_σ	g_ω	g_ρ	
Model	A	B	C	α_1	α_1'	α_2	α_2'	α_3'	g_δ
GPS [104]	938	550	783	770		8.122	8.282	8.7472	
	1047.4868	120.9956							
Hybrid [105]	939	508.194	782.501	763		10.308	12.868	8.9246	
	2490.3102	−36.7323							
MS2 [106]	939	500	782.65	763		10.004	12.783	8.4018	
	2070.843	−29.0764							
MTVTC [107]	938	400	783	769		6.394	8.721	8.5392	
	2122.69	−4.0453							
NL-VT1 [108]	938.9	484.307	780	763		9.813	12.65	9.2686	
	2620.6604	−38.0773							
NLρ [109]	939	500	782.65	763		8.144	9.234	7.5374	
	3517.1282	−21.113							
NL06 [45]	938.9	492.363	780	763		9.996	12.729	9.4606	
	2604.1246	−37.9776							
NL065 [45]	938.9	491.871	780	763		9.322	11.732	9.504	
	2229.8882	−25.0851							
NL07 [45]	938.9	478.975	780	763		8.51	10.702	9.6204	
	2061.9209	−13.1752							
NL075 [45]	938.9	454.871	780	763		7.512	9.515	9.851	
	1889.569	1.9706							
NL1 [97]	938	492.25	795.359	763		10.138	13.285	9.9514	
	2401.9432	−36.2646							
NL1J4 [110]	938	492.25	795.359	763		10.156	13.322	9.2021	
	2388.061	−36.227							
NL1J5 [110]	938	492.25	795.359	763		10.156	13.322	11.1605	
	2388.061	−36.227							
NL2 [97]	938	504.89	780	763		9.111	11.493	10.7732	
	454.6493	13.7844							
NL3 [111]	939	508.194	782.501	763		10.217	12.868	8.948	
	2058.3179	−28.885							
NL3-II [111]	939	507.68	781.869	763		10.202	12.854	8.96	
	2050.4249	−28.939							
NL3*[112]	939	502.5742	782.6	763		10.094	12.806	9.1496	
	2132.9667	−30.1486							
NL4 [113]	938	508.194	782.474	763.9		10.216	12.867	8.72	
	2058.5153	−28.882							
NLB [114]	939	510	783	770		9.696	12.589	8.544	
	400	1.6667							
NLB1 [97]	938.9	470	783	770		8.758	11.805	7.5039	
	1482.8058	−16.8112							
NLB2 [97]	938.9	485	783	770		9.727	12.894	7.0587	
	1868.8446	−28.1254							
NLC [114]	939	500.8	783	770		9.752	12.204	8.6597	
	2500	−33.3333							
NLD [115]	939	476.7	783	770		8.266	10.866	8.9861	
	749.7915	8.3333							
NLM [110]	939	500	783	763		8.811	10.355	7.2071	
	3701.1489	−43.528							
NLM2 [110]	939	500	783	763		8.912	10.331	7.2071	
	4137.9892	−49.5989							
NLM3 [110]	939	500	783	763		9.225	10.956	7.8332	
	3761.5286	−45.3841							
NLM4 [110]	939	500	783	763		8.496	10.355	7.2071	
	1725.0455	−5.6021							
NLM5 [110]	939	500	783	763		10.252	13.087	6.1864	
	2441.1254	−38.7177							

TABLE V. (*Continued.*)

Model	M_n A	m_σ B	m_ω C	m_ρ α_1	m_δ α_1'	g_σ α_2	g_ω α_2'	g_ρ α_3'	g_δ
NLM6 [110]	939 3701.1489	500 −43.528	783	763		8.811	10.355	9.4776	
NLRA [116]	939 1591.6041	515 −16.3173	782.6	764		9.627	11.904	9.0484	
NLRA1 [117]	939 1985.0992	515.7 −27.5565	783	763		10.362	12.921	8.8118	
NLS [118]	938.9 2096.8362	499.2361 −28.2795	780	763		9.924	12.58	9.9169	
NLSH [111]	939 1363.5098	526.059 −15.8337	783	763		10.444	12.945	8.766	
NLZ [108]	938.9 2665.3353	488.67 −40.2243	780	763		9.813	12.65	9.2686	
NLZ2 [108]	938.9 2714.4499	493.15 −41.4013	780	763		10.137	12.908	9.1125	
P-067 [119]	938.9 2652.0749	488.67 −29.74	780	763		8.91	11.02	9.69	
P-070 [119]	938.9 2646.1551	488.67 −24.48	780	763		8.45	10.26	9.69	
P-075 [119]	938.9 2577.0906	488.67 −3.69	780	763		7.58	8.73	9.69	
P-080 [119]	938.9 2661.9412	488.67 30.07	780	763		7.22	7.94	9.69	
Q1 [120]	939 2300.6709	505.8769 −33.1203	782	770		10.182	12.833	8.5572	
RMF301 [98]	938.9 4591.8652	550	783	763		8.774	8.85	8.4469	
RMF302 [98]	938.9 4885.1743	550	783	763		8.727	8.719	8.4662	
RMF303 [98]	938.9 4946.8176	550	783	763		8.717	8.692	8.47	
RMF304 [98]	938.9 5009.5667	550	783	763		8.708	8.666	8.4738	
RMF305 [98]	938.9 5138.2713	550	783	763		8.69	8.612	8.4815	
RMF306 [98]	938.9 5271.503	550	783	763		8.617	8.559	8.489	
RMF307 [98]	938.9 5339.9459	550	783	763		8.662	8.531	8.4928	
RMF308 [98]	938.9 5409.5813	550	783	763		8.653	8.504	8.4966	
RMF309 [98]	938.9 5552.6372	550	783	763		8.635	8.45	8.5041	
RMF310 [98]	938.9 5777.2432	550	783	763		8.609	8.367	8.5153	
RMF311 [98]	938.9 5854.9512	550	783	763		8.6	8.34	8.519	
RMF312 [98]	938.9 5934.127	550	783	763		8.591	8.312	8.5227	
RMF313 [98]	938.9 6097.0451	550	783	763		8.574	8.256	8.5301	
RMF314 [98]	938.9 6181.2894	550	783	763		8.565	8.228	8.5337	
RMF315 [98]	938.9 6223.4113	550	783	763		8.561	8.214	8.5356	
RMF316 [98]	938.9 6266.2617	550	783	763		8.557	8.2	8.5374	

TABLE V. (*Continued.*)

	M_n	m_σ	m_ω	m_ρ	m_δ	g_σ	g_ω	g_ρ	
Model	A	B	C	α_1	α_1'	α_2	α_2'	α_3'	g_δ
RMF317 [98]	938.9	550	783	763		8.548	8.172	8.5411	
	6353.872								
RMF401 [98]	938.9	550	783	763		9.706	10.4	8.1706	
	4473.4385	−48.7165							
RMF402 [98]	938.9	550	783	763		9.699	10.4	8.1706	
	4412.7561	−42.7972							
RMF403 [98]	938.9	550	783	763		9.589	10.178	8.2163	
	4673.5702	−48.3159							
RMF404 [98]	938.9	550	783	763		9.581	10.178	8.2163	
	4606.954	−44.1382							
RMF405 [98]	938.9	550	783	763		9.573	10.178	8.2163	
	4540.4661	−45.3292							
RMF406 [98]	938.9	550	783	763		8.82	8.719	8.4662	
	5877.751	−23.7336							
RMF407 [98]	938.9	550	783	763		9.47	9.951	8.2609	
	4889.1222	−47.5762							
RMF408 [98]	938.9	550	783	763		9.462	9.951	8.2609	
	4815.6069	−45.9034							
RMF409 [98]	938.9	550	783	763		9.453	9.951	8.2609	
	4742.3558	−44.2383							
RMF410 [98]	938.9	550	783	763		9.445	9.951	8.2609	
	4669.2777	−42.5812							
RMF411 [98]	938.9	550	783	763		9.35	9.717	8.3042	
	5119.4647	−46.3323							
RMF412 [98]	938.9	550	783	763		9.341	9.717	8.3042	
	5038.0403	−44.4534							
RMF413 [98]	938.9	550	783	763		9.332	9.717	8.3042	
	4956.8799	−42.5842							
RMF414 [98]	938.9	550	783	763		9.323	9.717	8.3042	
	4875.976	−40.7247							
RMF415 [98]	938.9	550	783	763		9.227	9.478	8.3463	
	5363.2919	−49.4879							
RMF416 [98]	938.9	550	783	763		9.218	9.478	8.3463	
	5272.6359	−42.2327							
RMF417 [98]	938.9	550	783	763		9.208	9.478	8.3463	
	5182.262	−40.1238							
RMF418 [98]	938.9	550	783	763		9.198	9.478	8.3463	
	5092.2129	−46.8404							
RMF419 [98]	938.9	550	783	763		9.102	9.232	8.3873	
	5617.868	−51.1364							
RMF420 [98]	938.9	550	783	763		9.092	9.232	8.3873	
	5598.896	−38.9086							
RMF421 [98]	938.9	550	783	763		9.082	9.232	8.3873	
	5415.1675	−49.1802							
RMF422 [98]	938.9	550	783	763		8.975	8.98	8.4273	
	5878.2873	−36.7536							
RMF423 [98]	938.9	550	783	763		8.964	8.98	8.4273	
	5763.9074	−34.0083							
RMF424 [98]	938.9	550	783	763		8.605	8.45	8.5041	
	5218.6965	8.0393							
RMF425 [98]	938.9	550	783	763		8.592	8.45	8.5041	
	5077.2813	11.4216							
RMF426 [98]	938.9	550	783	763		8.579	8.45	8.5041	
	4936.6039	14.7742							
RMF427 [98]	938.9	550	783	763		8.525	8.172	8.5411	
	6077.7223	6.7892							

TABLE V. (*Continued.*)

Model	M_n A	m_σ B	m_ω C	m_ρ α_1	m_δ α_1'	g_σ α_2	g_ω α_2'	g_ρ α_3'	g_δ
RMF428 [98]	938.9	550	783	763		8.511	8.172	8.5411	
	5911.2069	10.8626							
RMF429 [98]	938.9	550	783	763		8.497	8.172	8.5411	
	5745.7781	14.8959							
RMF430 [98]	938.9	550	783	763		8.483	8.172	8.5411	
	5581.3565	18.8893							
RMF431 [98]	938.9	550	783	763		8.468	8.172	8.5411	
	5417.9559	22.8431							
RMF432 [98]	938.9	550	783	763		8.454	8.172	8.5411	
	5255.5807	26.7577							
RMF433 [98]	938.9	550	783	763		8.44	8.172	8.5411	
	5094.2173	30.6335							
RMF434 [98]	938.9	550	783	763		8.426	8.172	8.5411	
	4933.8423	34.4706							
RSk1*[110]	939	440	783	769		6.848	8.267	7.6884	
	3464.3031	−15.7274							
S271 [121]	939	505	783	763		9.006	10.806	9.2431	
	2439.5057	−17.2993							
SMFT1 [122]	939	571	784			10.736	11.822		
	3784.6339	−61.5398							
SMFT2 [122]	939	550	782.6			9.853	11.179		
	2973.4849	−40.6319							
SRK3M5 [123]	939	500	783	763		10.391	13.566	4.1944	
	1704.4689	−26.7765							
SRK3M7 [123]	939	500	783	763		8.132	9.598	7.5199	
	1662.4187	17.3974							
VT [99]	938.9	483.42	780	763		9.791	12.657	9.2264	
	2597.8434	−38.1282							
			$\sigma^3+\sigma^4+\omega_0^4$ models (type 3)						
BM-A [124]	939	550	782.6			12.418	15.063		
	2422.3439	189.005	0.02387						
BM-B [124]	939	550	782.6			12.412	15.333		
	1208.2956	232.2355	0.023605						
BM-C [124]	939	550	782.6			12.361	15.45		
	356.4405	255.5887	0.022954						
DJM [124]	939	571	784			11.586	13.382		
	2145.1224	6.0898	0.005835						
DJM-C [124]	939	571	784			11.725	13.878		
	1188.2784	25.1398	0.006352						
EMFT1 [122]	939	571	784			11.96	13.651		
	3270.4105		0.006771						
EMFT2 [122]	939	550	782.6			12.412	15.333		
	1208.3309	232.2445	0.023606						
HD [125]	939	550	783	770		9.359	10.374	7.832	
	2751.5039	−30.4992	−0.000775						
LB [125]	939	550	783	770		10.105	12.113	6.2192	
	809.5827	12.9403	0.005188						
MB [125]	939	550	783	770		10.596	14.295	6.1622	
	−3330.9553	168.2078	0.020449						
MS1 [126]	939	485	783	770		9.999	13.46	8.4788	
	1446.4825	1.351	0.00394						
MS3 [127]	939	485	782.5	763		10.538	14.728	8.402	
	297.331	56.9669	0.01						
NLSV1 [128]	939	510.0349	783	763		10.125	12.727	8.9839	
	1823.4159	−15.388	0.001563						

TABLE V. (*Continued.*)

Model	M_n	m_σ	m_ω	m_ρ	m_δ	g_σ	g_ω	g_ρ	
	A	B	C	α_1	α_1'	α_2	α_2'	α_3'	g_δ
NLSV2 [128]	939	519.812	783	763		10.32	12.882	9.0029	
	1353.7836	−0.3675	0.002628						
PK1 [129]	939.573	514.0891	784.254	763		10.322	13.013	9.0594	
	1611.9248	−9.9976	0.00194						
TM1 [130]	938	511.198	783	770		10.029	12.614	9.2644	
	1427.1675	0.6183	0.002817						
TM2 [130]	938	526.443	783	770		11.469	14.638	9.3566	
	876.9212	4.6076	0.001841						
Z271 [121]	939	465	783	763		7.031	8.406	9.5011	
	1072.4396	63.6907	0.01						
			$\sigma^3+\sigma^4+\omega^4+$ cross terms models (type 4)						
BigApple [131]	939	492.73	782.5	763		9.670	12.316	14.162	
	2352.4181	−31.68	0.0001					0.0949	
BKA20 [132]	939	509.877	782	770		10.106	12.695	12.3301	
	1612.0359	9.9833	0.005	0.00101	1.41×10^{-4}	7.5098			
BKA22 [132]	939	497.8578	782	770		10.634	13.935	12.9459	
	2175.3524	11.3082	0.005	0.26076	1.24×10^{-4}	7.402			
BKA24 [132]	939	492.7872	782	770		10.798	14.405	11.7885	
	2474.0994	16.6266	0.005	0.42371	1.94×10^{-4}	5.6568			
BSR1 [133]	939	502.2322	782.5	763		10.514	13.488	14.985	
	3010.537	−14.9667		0.44738	7.32×10^{-4}	6.0367	0.01556	0.015	
BSR2 [133]	939	495.7634	782.5	763		10.656	13.958	14.3269	
	3607.3398	−9.7648		0.76296	7.79×10^{-4}	5.7579	0.0135	0.0148	
BSR3 [133]	939	497.8349	782.5	763		10.444	13.522	13.1171	
	2732.0169	−0.8486		0.35758	1.598×10^{-3}	5.8541	0.01253	0.001	
BSR4 [133]	939	491.4826	782.5	763		10.503	13.801	12.1297	
	3883.7798	−23.4863		0.86865	9.9×10^{-5}	5.0665	0.00514	0.0105	
BSR5 [133]	939	492.7682	782.5	763		10.341	13.462	11.1828	
	3542.8015	−26.0815		0.69664	7.3×10^{-5}	4.4886	0.00155	0.0053	
BSR6 [133]	939	490.2424	782.5	763		10.486	13.812	10.3945	
	3476.5727	−17.4849		0.68755	5.22×10^{-4}	1.3435	0.00414	0.0115	
BSR7 [133]	939	491.8668	782.5	763		10.32	13.451	10.0961	
	3066.7089	−21.5312		0.4609	4.73×10^{-4}	1.1985	0.00331	0.003	
BSR8 [133]	939	506.5058	782.5	763		10.629	13.66	14.9908	
	1636.3149	12.4514	0.005	0.00722	2.72×10^{-4}	5.7105	0.01597	0.0152	
BSR9 [133]	939	500.5111	782.5	763		10.761	14.111	14.6741	
	1919.0082	21.8004	0.005	0.20346	5.07×10^{-4}	6.0544	0.01163	0.0136	
BSR10 [133]	939	499.5263	782.5	763		10.73	14.043	13.6901	
	1978.4409	14.2496	0.005	0.16341	2.98×10^{-4}	6.2794	0.00475	0.0098	
BSR11 [133]	939	497.2074	782.5	763		10.719	14.125	12.1916	
	1966.539	23.3484	0.005	0.21015	6.53×10^{-4}	5.4807	0.00221	0.0046	
BSR12 [133]	939	499.1246	782.5	763		10.618	13.887	10.9646	
	2092.7579	10.2259	0.005	0.24836	5×10^{-6}	2.3432	0.01276	0.0029	
BSR13 [133]	939	495.1821	782.5	763		10.667	14.12	10.1481	
	2028.2493	18.7645	0.005	0.23677	4.41×10^{-4}	1.3451	0.00548	0.0036	
BSR14 [133]	939	494.9388	782.5	763		10.601	14.031	10.0044	
	2101.6473	15.7193	0.005	0.31746	1.67×10^{-4}	0.9303	0.00528	0.0032	
BSR15 [133]	939	503.4384	782.5	763		11.052	14.656	14.9872	
	886.6689	61.2708	0.01	0.01186	2×10^{-5}	5.6482	0.01552	0.0155	
BSR16 [133]	939	501.3704	782.5	763		11.024	14.666	14.5219	
	918.6591	60.2792	0.01	0.00886	5.3×10^{-5}	5.098	0.01569	0.0158	
BSR17 [133]	939	499.3813	782.5	763		10.958	14.596	13.4111	
	997.6173	57.9698	0.01	0.00807	1.08×10^{-4}	5.255	0.01309	0.0085	
BSR18 [133]	939	497.272	782.5	763		11.019	14.775	11.9484	
	1029.6705	60.7499	0.01	0.02899	1.56×10^{-4}	3.9918	0.00902	0.0096	

TABLE V. (*Continued.*)

Model	M_n	m_σ	m_ω	m_ρ	m_δ	g_σ	g_ω	g_ρ	
	A	B	C	α_1	α_1'	α_2	α_2'	α_3'	g_δ
BSR19 [133]	939	495.8239	782.5	763		10.919	14.647	10.7105	
	1158.9515	55.2713	0.01	0.06904	2.3×10^{-5}	2.4606	0.00779	0.0075	
BSR20 [133]	939	490.8349	782.5	763		11.108	15.198	10.0884	
	1532.8118	63.7487	0.01	0.27928	8×10^{-6}	2.3391	0.00274	0.0041	
BSR21 [133]	939	490.6891	782.5	763		11.032	15.016	10.0067	
	1070.1795	59.5637	0.01	0.04091	1.11×10^{-4}	1.0917	0.00163	0.0073	
C1 [120]	939	505.8768	782	770		9.771	12.376	8.1748	
	2223.3213			0.62879					
FSU-I [134]	939	491.5	782.5	763		10.592	14.302	9.0374	
	843.9895	49.9354	0.01						
FSU-II [134]	939	491.5	782.5	763		10.592	14.302	9.7269	
	843.9895	49.9354	0.01					0.02	
FSU-III [134]	939	491.5	782.5	763		10.592	14.302	10.6027	
	843.9895	49.9354	0.01					0.04	
FSU-IV [134]	939	491.5	782.5	763		10.592	14.302	13.4266	
	843.9895	49.9354	0.01					0.08	
FSU-V [134]	939	491.5	782.5	763		10.592	14.302	14.8389	
	843.9895	49.9354	0.01				0.02	0.06	
FSU2H [135]	939	497.479	782.5	763		10.135	13.02	14.0453	
	2082.8811	−23.3854	0.001333					0.09	
FSU2R [135]	939	497.479	782.5	763		10.372	13.505	14.3675	
	1724.4503	−3.2403	0.004					0.09	
FSUGarnet [136]	939	496.939	782.5	763		10.505	13.70	13.89	
	1889.5804	−7.207	0.0039					0.0868	
FSUGold [137]	939	491.5	782.5	763		10.592	14.302	11.7673	
	843.9895	49.9354	0.01					0.06	
FSUGold4 [138]	939	491	782.5	763		10.592	14.302	13.5138	
	843.9895	49.9354	0.01					0.08	
FSUGold5 [138]	939	490.25	782.5	763		10.592	14.302	16.3739	
	843.9895	49.9354	0.01					0.1	
FSUGZ00 [139]	939	495.763	782.5	770		10.656	13.958	14.3269	
	3607.2922	−9.7654		0.76306	7.79×10^{-4}	5.7578	0.0135	0.0148	
FSUGZ03 [139]	939	500.511	782.5	770		10.761	14.111	14.6741	
	1918.936	21.8007	0.005	0.20344	5.07×10^{-4}	6.0544	0.01162	0.0136	
FSUGZ06 [139]	939	501.37	782.5	770		11.024	14.666	14.5219	
	918.5666	60.2782	0.01	0.00888	5.3×10^{-5}	5.0981	0.01569	0.0158	
G1 [120]	939	506.7126	782	770		9.869	12.128	8.7769	
	2977.3341	−47.692	0.003994	0.15629	2.267×10^{-3}	−1.1156			
G2 [120]	939	520.2999	782	770		10.496	12.762	8.1671	
	4912.0724	3.5599	0.002703	1.29931	2.34×10^{-4}	1.3694			
G2*[140]	939	520.2999	782	770		10.496	12.762	11.7873	
	4912.0724	3.5599	0.002703	1.29931	2.34×10^{-4}	10.2025			
HC [125]	939	550	783	770		9.545	10.453	9.1223	
	3624.768	−43.2285	−0.000039					0.087	
IOPB-I [136]	939	500.487	782.5	762.5		10.393	13.341	11.119	
	2072.328	−14.802	0.00291					0.0479	
IUFSU [127]	939	491.5	782.5	763		9.971	13.032	13.59	
	1675.8785	0.4877	0.005					0.092	
LA [125]	939	550	783	770		10.194	12.159	8.3503	
	966.619	13.7061	0.00542					0.047	
MA [125]	939	550	783	770		10.337	13.439	8.5895	
	−2678.1449	131.6257	0.015849					0.0646	
NL3v1 [141]	939	508.194	782.5	763		10.217	12.868	9.2141	
	2058.3362	−28.8943						0.01	

TABLE V. (*Continued.*)

Model	M_n A	m_σ B	m_ω C	m_ρ α_1	m_δ α_1'	g_σ α_2	g_ω α_2'	g_ρ α_3'	g_δ
NL3v2 [141]	939	508.194	782.5	763		10.217	12.868	9.5341	
	2058.3362	−28.8943						0.02	
NL3v3 [141]	939	508.194	782.5	763		10.217	12.868	9.7057	
	2058.3362	−28.8943						0.025	
NL3v4 [141]	939	508.194	782.5	763		10.217	12.868	9.8944	
	2058.3362	−28.8943						0.03	
NL3v5 [141]	939	508.194	782.5	763		10.217	12.868	10.2956	
	2058.3362	−28.8943						0.04	
NL3v6 [141]	939	508.194	782.5	763		10.217	12.868	10.7517	
	2058.3362	−28.8943						0.05	
PCSB0 [142]	939	550	783	770		10.429	11.774	10.273	
	3284.7926	−43.5566						0.0557	
PCSB1 [142]	939	550	783	770		10.488	11.928	10.357	
	2918.3759	−27.5871	0.001667					0.057	
PCSB2 [142]	939	550	783	770		10.548	12.088	10.443	
	2543.3831	−10.9677	0.003333					0.0583	
PCSB3 [142]	939	550	783	770		10.611	12.254	10.531	
	2161.8037	6.326	0.005					0.0597	
PCSB4 [142]	939	550	783	770		10.675	12.427	10.62	
	1770.5205	24.3485	0.006667					0.061	
PCSB5 [142]	939	550	783	770		10.742	12.608	10.714	
	1371.0912	43.1672	0.008333					0.0624	
QMC-RMF1 [143]	939	491.5	782.5	763		7.54	8.43	10.88	
	2938.3431	11.3124						0.2221	
QMC-RMF2 [143]	939	491.5	782.5	763		7.82	8.99	11.24	
	2828.9574	−3.3657						0.1985	
QMC-RMF3 [143]	939	491.5	782.5	763		8.32	9.76	11.02	
	3407.0313	−28.7504						0.1232	
QMC-RMF4 [143]	939	491.5	782.5	763		8.21	9.94	12.18	
	2130.4872	−9.541						0.2111	
S271v1 [141]	939	505	783	763		9.006	10.806	9.4004	
	2440.9325	−17.323						0.01	
S271v2 [141]	939	505	783	763		9.006	10.806	9.5659	
	2440.9325	−17.323						0.02	
S271v3 [141]	939	505	783	763		9.006	10.806	9.7405	
	2440.9325	−17.323						0.03	
S271v4 [141]	939	505	783	763		9.006	10.806	9.925	
	2440.9325	−17.323						0.04	
S271v5 [141]	939	505	783	763		9.006	10.806	10.1204	
	2440.9325	−17.323						0.05	
S271v6 [141]	939	505	783	763		9.006	10.806	10.3278	
	2440.9325	−17.323						0.06	
SIG-OM [144]	939	505.9263	783	763		10.043	12.767	8.9504	
	1563.2837	12.4601			2.171×10^{-3}				
SVI−1 [145]	939	524.527	783	763		9.676	11.603	8.928	
				−1.29922	2.686×10^{-3}				
SVI−2 [145]	939	524.024	783	763		9.641	11.565	8.984	
				−1.29784	2.64×10^{-3}				
TM1*[146]	938	511.21	783	770		11.197	14.979	10.0028	
	3919.6376	55.6685	0.002674	1.60218	1.55×10^{-4}	2.8428			
TM1e [147]	938	511.198	783	770		10.029	12.614	13.9714	
	1427.1675	0.6143	0.002817					0.0858	
XS [127]	939	491.5	782.5	763		11.446	16.066	14.6274	
	5.9229	124.1138	0.015					0.08	
Z271*[140]	939	464.805	783	763		7.037	8.419	11.5108	
	1072.6543	63.7483	0.009971					0.06	

TABLE V. (*Continued.*)

Model	M_n	m_σ	m_ω	m_ρ	m_δ	g_σ	g_ω	g_ρ	
	A	B	C	α_1	α_1'	α_2	α_2'	α_3'	g_δ
Z271s1 [141]	939	465	783	763		7.031	8.406	9.8182	
	1072.3734	63.6909	0.01				0.02		
Z271s2 [141]	939	465	783	763		7.031	8.406	10.1732	
	1072.3734	63.6909	0.01				0.04		
Z271s3 [141]	939	465	783	763		7.031	8.406	10.5698	
	1072.3734	63.6909	0.01				0.06		
Z271s4 [141]	939	465	783	763		7.031	8.406	11.0167	
	1072.3734	63.6909	0.01				0.08		
Z271s5 [141]	939	465	783	763		7.031	8.406	11.5254	
	1072.3734	63.6909	0.01				0.1		
Z271s6 [141]	939	465	783	763		7.031	8.406	12.1119	
	1072.3734	63.6909	0.01				0.12		
Z271v1 [141]	939	465	783	763		7.031	8.406	9.6198	
	1072.3734	63.6909	0.01					0.02	
Z271v2 [141]	939	465	783	763		7.031	8.406	9.7466	
	1072.3734	63.6909	0.01					0.04	
Z271v3 [141]	939	465	783	763		7.031	8.406	9.8118	
	1072.3734	63.6909	0.01					0.05	
Z271v4 [141]	939	465	783	763		7.031	8.406	9.8784	
	1072.3734	63.6909	0.01					0.06	
Z271v5 [141]	939	465	783	763		7.031	8.406	9.9464	
	1072.3734	63.6909	0.01					0.07	
Z271v6 [141]	939	465	783	763		7.031	8.406	10.0158	
	1072.3734	63.6909	0.01					0.08	
			δ meson models (type 7)						
HA [125]	939	550	783	770	980	9.515	10.438	12.113	5.361
	3546.975	−42.6563	-1.42×10^{-4}					0.02662	
HB [125]	939	550	783	770	980	9.297	10.339	10.732	5.017
	2548.732	−28.21	-1.05×10^{-3}						
NLδ [148]	939	550	783	769	980	8.144	9.234	7.5374	5.617
	3517.128	−21.11							

TABLE VI. Parameters of density-dependent RMF (type 5) models. Masses are in MeV and n_0 has units of fm^{-3}. Other entries are dimensionless.

Model	M_n	m_σ	m_ω	m_ρ	$\Gamma_\sigma(n_0)$	a_σ	b_σ	c_σ	
	$\Gamma_\omega(n_0)$	a_ω	b_ω	c_ω	d_ω	$\Gamma_\rho(n_0)$	a_ρ	n_0	d_σ
DD [149]	939.0	547.2	783.0	763.0	10.685	1.3715	0.6441	1.0346	0.5676
	13.312	1.3856	0.5217	0.8700	0.6190	7.278	0.4987	0.1487	
DDF [150]	939.0	555.0	783.0	763.0	11.024	1.4867	0.1956	0.4282	0.8823
	13.575	1.5449	0.1838	0.4397	0.8707	7.290	0.4479	0.1469	
DD-ME1 [151]	939.0	549.5	783.0	763.0	10.443	1.3854	0.9781	1.5342	0.4661
	12.894	1.3879	0.8525	1.3566	0.4957	7.611	0.5008	0.1520	
DD-ME2 [152]	939.0	550.1	783.0	763.0	10.540	1.3881	1.0943	1.7057	0.4421
	13.019	1.3892	0.9240	1.4620	0.4775	7.367	0.5647	0.1520	
DDME-X [107]	938.5	547.333	783.0	763.0	10.707	1.3970	1.3350	2.0671	0.4016
	13.339	1.3936	1.0191	1.6060	0.4556	7.238	0.6202	0.1520	
DD2 [153]	938.9	546.2	783.0	763.0	10.687	1.3576	0.6344	1.0054	0.5758
	13.342	1.3697	0.4965	0.8178	0.6385	7.254	0.5189	0.1490	
MPE [154]	938.919	559.114	783.0	763.0	11.1052	1.2078	0.4421	0.6023	0.7439
	13.5784	1.1936	0.1958	0.2778	1.0954	7.525	0.4877	0.1419	
PKDD [129]	938.9	555.5	783.0	763.0	10.739	1.3274	0.4351	0.6917	0.6942
	13.148	1.3422	0.3712	0.6114	0.7384	8.600	0.1833	0.1496	
TW-99 [155]	939.0	550.0	783.0	763.0	10.729	1.3655	0.2261	0.4097	0.9020
	13.290	1.4025	0.1726	0.3443	0.9840	7.322	0.5150	0.1530	

TABLE VII. Parameters of RMF-PC (type 6) models.

Model	M_n (MeV) $\alpha_{\rm TV}$ (MeV^{-2})	$\alpha_{\rm S}$ (MeV^{-2}) $\gamma_{\rm TV}$ (MeV^{-8})	$\beta_{\rm S}$ (MeV^{-5}) $\alpha_{\rm TS}$ (MeV^{-2})	$\gamma_{\rm S}$ (MeV^{-8}) η_1 (MeV^{-5})	$\alpha_{\rm V}$ (MeV^{-2}) η_2 (MeV^{-8})	$\gamma_{\rm V}$ (MeV^{-8}) η_3 (MeV^{-5})
FZ0 [156]	939 3.842×10^{-5}	-4.371×10^{-4}			3.373×10^{-4}	
PC-F1 [157]	939 3.468×10^{-5}	-3.836×10^{-4}	7.686×10^{-11}	-2.904×10^{-17}	2.593×10^{-4}	-3.879×10^{-18}
PC-F2 [157]	939 3.241×10^{-5}	-3.836×10^{-4}	7.684×10^{-11} 2.34×10^{-6}	-2.911×10^{-17}	2.594×10^{-4}	-3.823×10^{-18}
PC-F3 [157]	939 3.549×10^{-5}	-3.836×10^{-4}	7.685×10^{-11}	-2.906×10^{-17}	2.593×10^{-4}	-3.873×10^{-18}
PC-F4 [157]	939 3.937×10^{-5}	-3.836×10^{-4}	7.681×10^{-11} -5.92×10^{-6}	-2.911×10^{-17}	2.594×10^{-4}	-3.844×10^{-18}
PC-PK1 [158]	939 2.950×10^{-5}	-3.963×10^{-4}	8.665×10^{-11}	-3.807×10^{-17}	2.690×10^{-4}	-3.642×10^{-18}

TABLE VIII. The same as Table II, except for RMF and RMF-PC models.

Model	n_0	E_0	K_0	Q_0	J_1	J_2	L_1	L_2	$K_{\rm sym,1}$	$K_{\rm sym,2}$	$Q_{\rm sym,1}$	$Q_{\rm sym,2}$
Linear finite-range models (type 1)												
H1	0.1485	−15.75	547.98	2156.48	27.03	25.95	91.90	88.46	95.36	93.56	−500.97	−541.41
L1	0.1767	−18.52	626.43	2231.43	22.91	21.69	79.56	75.69	85.46	81.83	−709.62	−788.55
L2	0.1418	−16.78	579.31	2325.86	20.14	19.08	72.21	68.85	99.22	97.43	−559.89	−607.50
L3	0.1345	−18.24	625.85	2573.09	19.91	18.87	72.94	69.59	104.01	102.15	−653.15	−713.38
LBF	0.1525	−17.01	584.53	2262.38	48.04	46.93	155.39	151.94	94.82	92.58	−587.49	−641.77
LHS	0.1484	−15.79	549.20	2161.57	36.09	35.01	119.12	115.68	95.43	93.62	−503.55	−544.35
LW	0.1937	−15.75	545.87	1878.52	23.37	22.11	78.36	74.46	78.14	74.95	−549.19	−605.20
LZ	0.1491	−17.01	584.40	2287.76	49.86	48.77	161.01	157.63	96.26	94.15	−582.35	−635.07
RMF201	0.1524	−16.30	564.00	2189.73	33.45	32.35	111.28	107.79	94.42	92.37	−541.18	−588.32
RMF202	0.1526	−16.30	562.93	2184.29	33.50	32.40	111.30	107.91	94.30	92.25	−539.16	−586.05
RMF203	0.1529	−16.30	563.07	2182.68	33.58	32.48	111.53	108.12	94.18	92.12	−539.88	−586.94
RMF204	0.1532	−16.30	563.19	2181.02	33.65	32.55	111.76	108.33	94.06	91.99	−540.57	−587.80
RMF205	0.1535	−16.30	563.30	2179.32	33.73	32.62	111.99	108.54	93.94	91.86	−541.24	−588.63
RMF206	0.1538	−16.30	563.40	2177.57	33.80	32.70	112.21	108.75	93.82	91.73	−541.87	−589.42
$\sigma^3+\sigma^4$ models (type 2)												
CS	0.1496	−16.16	187.08	−292.34	41.91	40.88	134.25	131.32	133.22	136.58	433.68	513.65
E	0.1498	−16.12	221.50	23.24	39.61	38.57	127.57	124.57	129.41	132.22	317.84	380.92
ER	0.1486	−16.15	220.61	−22.24	40.44	39.41	129.62	126.62	125.26	127.77	316.52	376.77
FAMA1	0.1485	−16.00	200.08	−302.99	39.03	38.02	123.46	120.54	111.50	113.25	348.55	403.22
FAMA2	0.1485	−16.00	225.13	−117.29	39.03	38.02	123.24	120.30	105.81	107.07	270.86	314.31
FAMA3	0.1485	−16.00	250.18	53.25	39.03	38.02	123.03	120.06	100.23	101.04	199.44	233.15
FAMA4	0.1485	−16.00	275.22	208.85	39.03	38.02	122.82	119.82	94.78	95.17	134.03	159.35
FAMA5	0.1485	−16.00	300.27	349.70	39.03	38.02	122.60	119.58	89.44	89.45	74.38	92.54
FAMB1	0.1485	−16.00	200.07	−594.04	37.94	37.02	110.98	108.41	33.70	33.12	153.00	157.38
FAMB2	0.1485	−16.00	225.11	−465.56	37.94	37.02	110.81	108.22	29.84	29.17	113.53	115.85
FAMB3	0.1485	−16.00	250.15	−355.75	37.94	37.02	110.63	108.04	26.11	25.37	79.24	80.02
FAMB4	0.1485	−16.00	275.18	−264.24	37.94	37.02	110.46	107.86	22.50	21.72	49.79	49.46

TABLE VIII. (*Continued.*)

Model	n_0	E_0	K_0	Q_0	J_1	J_2	L_1	L_2	$K_{\mathrm{sym},1}$	$K_{\mathrm{sym},2}$	$Q_{\mathrm{sym},1}$	$Q_{\mathrm{sym},2}$
FAMB5	0.1485	−16.00	300.22	−190.68	37.94	37.02	110.28	107.67	19.01	18.21	24.83	23.77
FAMC1	0.1485	−16.00	200.07	−594.04	28.93	28.01	83.97	81.40	33.70	33.12	153.00	157.38
FAMC2	0.1485	−16.00	225.11	−465.56	28.94	28.01	83.79	81.21	29.84	29.17	113.53	115.85
FAMC3	0.1485	−16.00	250.15	−355.75	28.94	28.01	83.62	81.03	26.11	25.37	79.24	80.02
FAMC4	0.1485	−16.00	275.18	−264.24	28.94	28.01	83.45	80.84	22.50	21.72	49.79	49.46
FAMC5	0.1485	−16.00	300.22	−190.68	28.94	28.01	83.27	80.66	19.01	18.21	24.83	23.77
GL1	0.1530	−16.30	200.01	−619.06	33.44	32.50	97.30	94.68	33.64	33.08	156.87	161.46
GL2	0.1531	−16.30	200.12	−608.67	33.42	32.52	93.97	91.58	9.07	8.77	102.07	100.16
GL3	0.1531	−16.31	200.13	−580.54	33.37	32.52	91.23	89.08	−8.66	−8.42	77.17	73.42
GL4	0.1531	−16.31	250.23	−380.65	33.46	32.52	97.04	94.38	26.00	25.28	81.79	82.57
GL5	0.1531	−16.31	250.21	−455.05	33.42	32.52	93.64	91.25	2.92	2.64	56.77	54.11
GL6	0.1536	−16.36	250.71	−548.56	33.47	32.62	91.22	89.08	−13.21	−12.87	57.61	54.17
GL7	0.1530	−16.30	299.96	−215.24	33.44	32.50	96.57	93.94	18.74	17.94	26.42	25.23
GL8	0.1531	−16.31	300.28	−384.97	33.42	32.52	93.33	90.91	−2.69	−2.90	28.53	25.90
GL82	0.1451	−16.00	285.90	−451.10	37.09	36.24	103.56	101.34	−8.13	−8.06	38.05	35.30
GL9	0.1531	−16.31	300.25	−611.67	33.37	32.52	90.65	88.49	−17.32	−16.85	51.42	48.33
GM1	0.1533	−16.36	300.95	−217.37	33.49	32.54	96.77	94.08	18.81	18.00	26.32	25.13
GM2	0.1532	−16.34	300.51	−508.19	33.39	32.52	91.65	89.40	−12.20	−12.00	40.12	37.24
GM3	0.1531	−16.32	240.11	−513.40	33.37	32.50	91.94	89.71	−6.53	−6.47	59.04	55.74
GPS	0.1499	−15.96	299.76	−591.71	33.34	32.50	90.74	88.61	−16.88	−16.41	49.82	46.81
Hybrid	0.1483	−16.24	230.30	−69.33	38.34	37.32	121.72	118.73	109.70	111.16	268.62	314.15
MS2	0.1485	−15.75	250.33	80.62	36.04	35.02	114.11	111.11	100.25	101.04	194.72	227.96
MTVTC	0.1526	−16.30	239.83	−512.75	33.33	32.47	91.83	89.61	−6.53	−6.46	58.98	55.68
NL-VT1	0.1498	−16.10	179.04	−487.88	40.05	39.03	126.55	123.65	115.59	117.76	418.40	483.30
NLρ	0.1602	−16.05	240.81	−464.69	31.29	30.37	87.07	84.62	3.65	3.36	64.04	61.34
NL06	0.1474	−16.05	195.18	−366.38	40.34	39.34	127.11	124.20	109.31	110.96	358.41	412.58
NL065	0.1498	−16.37	256.97	−219.78	39.97	38.99	120.64	117.81	56.54	55.90	122.50	132.72
NL07	0.1499	−16.49	276.59	−296.19	39.47	38.54	114.96	112.34	22.37	21.60	51.93	51.60
NL075	0.1510	−16.64	281.34	−419.41	39.86	38.98	112.90	110.50	−0.29	−0.53	38.60	35.94
NL1	0.1518	−16.42	211.20	−31.24	44.53	43.48	143.12	140.13	139.14	142.82	368.46	444.64
NL1J4	0.1521	−16.42	211.96	7.06	41.08	40.03	133.19	130.17	142.58	146.53	369.76	448.50
NL1J5	0.1521	−16.42	211.96	7.06	51.09	50.03	163.21	160.19	142.58	146.53	369.76	448.50
NL2	0.1457	−17.03	399.63	68.18	44.82	43.88	132.47	129.70	21.25	20.11	−50.49	−52.02
NL3	0.1483	−16.24	271.94	205.46	38.44	37.42	121.67	118.63	100.37	101.06	151.43	180.78
NL3-II	0.1492	−16.26	271.99	224.48	38.74	37.72	122.81	119.77	102.74	103.55	152.87	183.38
NL3*	0.1500	−16.31	258.55	124.08	39.73	38.70	125.75	122.72	104.71	105.72	188.71	223.62
NL4	0.1477	−16.16	270.71	196.06	37.28	36.26	118.03	115.01	99.25	99.88	151.49	180.37
NLB	0.1485	−15.77	421.34	728.43	36.04	35.02	111.38	108.30	56.44	54.96	−130.14	−132.75
NLB1	0.1625	−15.79	280.52	108.96	34.10	33.05	105.62	102.53	76.48	76.18	93.09	107.72
NLB2	0.1628	−15.79	245.92	546.83	34.23	33.12	114.53	111.38	154.50	159.16	224.19	287.92
NLC	0.1485	−15.77	224.48	−278.08	36.01	35.02	110.83	107.98	76.93	76.92	212.08	235.60
NLD	0.1485	−15.77	343.37	−75.65	35.95	35.02	104.17	101.54	14.39	13.53	−10.66	−12.29
NLM	0.1601	−16.00	200.12	−600.83	30.99	30.02	89.79	87.08	33.81	33.27	156.75	161.43
NLM2	0.1601	−17.00	200.10	−675.96	30.99	30.02	89.72	87.01	33.86	33.34	166.05	171.14
NLM3	0.1451	−16.00	200.13	−592.19	30.93	30.02	90.08	87.52	33.68	33.08	151.91	156.21
NLM4	0.1601	−16.00	300.31	−196.19	30.99	30.02	89.07	86.31	18.54	17.71	23.84	22.42
NLM5	0.1601	−16.00	200.27	221.52	31.12	30.02	106.31	103.28	172.85	179.75	416.66	523.85
NLM6	0.1601	−16.00	200.12	−600.83	40.99	40.02	119.81	117.09	33.81	33.27	156.75	161.43
NLRA	0.1571	−16.25	320.88	217.36	39.90	38.87	122.09	119.00	63.04	62.19	20.00	26.17
NLRA1	0.1468	−16.15	285.76	282.01	37.50	36.49	118.55	115.51	95.53	95.89	114.69	138.69
NLS	0.1502	−16.49	263.83	62.35	43.16	42.14	134.84	131.85	94.19	94.67	166.63	194.61
NLSH	0.1461	−16.36	356.11	604.68	37.16	36.15	116.83	113.76	80.52	79.91	−31.88	−24.54
NLZ	0.1415	−13.72	143.02	−647.37	37.63	36.68	117.24	114.48	97.79	98.90	418.71	469.21
NLZ2	0.1510	−16.06	172.29	−411.39	40.06	39.02	128.81	125.88	137.01	140.78	488.01	577.76
P-067	0.1572	−16.31	231.67	−413.32	42.06	41.07	125.16	122.35	46.97	46.35	143.15	151.27
P-070	0.1633	−16.25	245.18	−396.48	42.85	41.86	125.17	122.40	28.49	27.78	92.04	93.47

TABLE VIII. (*Continued.*)

Model	n_0	E_0	K_0	Q_0	J_1	J_2	L_1	L_2	$K_{\mathrm{sym},1}$	$K_{\mathrm{sym},2}$	$Q_{\mathrm{sym},1}$	$Q_{\mathrm{sym},2}$
P-075	0.1734	−16.51	271.46	−440.18	43.94	42.97	124.13	121.53	−1.75	−1.98	46.71	43.52
P-080	0.1616	−15.84	260.09	−529.83	40.53	39.65	112.07	109.83	−14.52	−14.17	55.97	52.52
Q1	0.1437	−15.21	226.89	−87.42	35.16	34.18	110.62	107.74	94.85	95.45	234.92	268.83
RMF301	0.1530	−16.30	253.86	−489.08	33.37	32.50	92.12	89.88	−6.28	−6.25	52.45	49.30
RMF302	0.1530	−16.30	249.71	−502.35	33.37	32.50	91.88	89.66	−7.44	−7.35	54.57	51.33
RMF303	0.1530	−16.30	248.88	−504.90	33.37	32.50	91.83	89.62	−7.67	−7.57	54.98	51.73
RMF304	0.1530	−16.30	248.04	−507.42	33.37	32.50	91.78	89.57	−7.89	−7.78	55.40	52.13
RMF305	0.1530	−16.30	246.37	−512.37	33.37	32.50	91.69	89.49	−8.34	−8.21	56.23	52.92
RMF306	0.1530	−16.30	244.69	−517.17	33.36	32.50	91.60	89.41	−8.78	−8.63	57.05	53.72
RMF307	0.1530	−16.30	243.84	−519.53	33.36	32.50	91.55	89.37	−9.00	−8.84	57.46	54.11
RMF308	0.1530	−16.30	243.00	−521.86	33.36	32.50	91.51	89.32	−9.21	−9.04	57.87	54.50
RMF309	0.1530	−16.30	241.30	−526.40	33.36	32.50	91.41	89.24	−9.64	−9.45	58.68	55.28
RMF310	0.1530	−16.30	238.75	−532.97	33.36	32.50	91.28	89.12	−10.27	−10.04	59.89	56.45
RMF311	0.1530	−16.30	237.89	−535.10	33.36	32.50	91.23	89.08	−10.48	−10.24	60.29	56.83
RMF312	0.1530	−16.30	237.03	−537.19	33.36	32.50	91.19	89.04	−10.68	−10.44	60.69	57.22
RMF313	0.1530	−16.30	235.31	−541.28	33.35	32.50	91.10	88.97	−11.09	−10.82	61.49	57.98
RMF314	0.1530	−16.30	234.44	−543.30	33.35	32.50	91.06	88.93	−11.29	−11.01	61.88	58.36
RMF315	0.1530	−16.30	234.01	−544.26	33.35	32.50	91.03	88.91	−11.39	−11.10	62.08	58.55
RMF316	0.1530	−16.30	233.57	−545.23	33.35	32.50	91.01	88.89	−11.49	−11.20	62.28	58.74
RMF317	0.1530	−16.30	232.70	−547.19	33.35	32.50	90.97	88.85	−11.69	−11.39	62.67	59.12
RMF401	0.1530	−16.30	230.00	−477.84	33.43	32.50	96.36	93.79	23.66	23.04	99.83	100.50
RMF402	0.1455	−15.74	231.20	−443.97	31.82	30.93	90.93	88.46	16.78	16.22	81.77	80.95
RMF403	0.1530	−16.30	230.00	−486.56	33.42	32.50	95.65	93.13	18.63	18.06	91.30	90.87
RMF404	0.1488	−15.99	231.38	−464.20	32.53	31.63	92.64	90.19	15.01	14.49	81.31	80.19
RMF405	0.1530	−16.30	234.00	−470.81	33.42	32.50	95.62	93.10	18.07	17.50	86.53	85.93
RMF406	0.1530	−16.30	233.99	−520.06	33.37	32.50	91.98	89.76	−5.86	−5.80	62.04	58.72
RMF407	0.1530	−16.30	230.00	−493.82	33.41	32.50	94.97	92.50	13.91	13.42	83.96	82.66
RMF408	0.1530	−16.30	232.00	−486.57	33.41	32.50	94.96	92.49	13.64	13.15	81.79	80.44
RMF409	0.1530	−16.30	234.00	−479.45	33.41	32.50	94.94	92.47	13.37	12.88	79.66	78.25
RMF410	0.1530	−16.30	236.00	−472.45	33.41	32.50	94.93	92.46	13.11	12.62	77.55	76.09
RMF411	0.1530	−16.30	230.00	−500.11	33.40	32.50	94.32	91.90	9.49	9.09	77.79	75.82
RMF412	0.1530	−16.30	232.00	−493.59	33.40	32.50	94.31	91.89	9.24	8.84	75.85	73.85
RMF413	0.1530	−16.30	234.00	−487.20	33.40	32.50	94.30	91.88	8.98	8.58	73.94	71.90
RMF414	0.1530	−16.30	236.00	−480.94	33.40	32.50	94.28	91.86	8.73	8.33	72.07	69.99
RMF415	0.1596	−16.78	231.39	−528.37	34.78	33.85	98.19	95.69	9.15	8.76	80.79	78.75
RMF416	0.1530	−16.30	232.00	−500.18	33.40	32.50	93.69	91.32	5.12	4.82	71.04	68.54
RMF417	0.1530	−16.30	234.00	−494.57	33.40	32.50	93.68	91.31	4.87	4.58	69.35	66.83
RMF418	0.1648	−17.18	239.38	−523.72	35.87	34.92	101.71	99.12	11.50	11.04	80.75	78.99
RMF419	0.1648	−17.17	232.95	−549.87	35.85	34.90	101.00	98.45	7.52	7.17	81.02	78.73
RMF420	0.1502	−15.95	227.45	−500.29	32.80	31.93	91.29	89.00	0.39	0.24	67.16	64.24
RMF421	0.1687	−17.47	238.73	−548.29	36.66	35.70	103.62	100.99	9.13	8.73	80.99	78.88
RMF422	0.1530	−16.30	229.99	−518.27	33.38	32.50	92.54	90.27	−2.10	−2.17	65.99	62.86
RMF423	0.1530	−16.30	231.99	−514.26	33.38	32.50	92.53	90.26	−2.32	−2.38	64.70	61.56
RMF424	0.1530	−16.30	245.99	−524.01	33.36	32.50	91.39	89.22	−10.08	−9.88	56.95	53.58
RMF425	0.1530	−16.30	247.99	−523.22	33.36	32.50	91.37	89.20	−10.27	−10.06	56.25	52.90
RMF426	0.1530	−16.30	249.99	−522.59	33.36	32.50	91.36	89.19	−10.46	−10.24	55.57	52.23
RMF427	0.1530	−16.30	235.99	−546.22	33.35	32.50	90.95	88.83	−11.98	−11.67	61.58	58.05
RMF428	0.1530	−16.30	237.99	−545.84	33.35	32.50	90.94	88.82	−12.16	−11.85	60.95	57.43
RMF429	0.1530	−16.30	239.99	−545.62	33.35	32.50	90.93	88.81	−12.34	−12.02	60.34	56.84
RMF430	0.1530	−16.30	241.99	−545.55	33.35	32.50	90.92	88.79	−12.52	−12.19	59.75	56.27
RMF431	0.1530	−16.30	243.99	−545.64	33.35	32.50	90.91	88.78	−12.69	−12.36	59.18	55.71
RMF432	0.1530	−16.30	245.99	−545.88	33.35	32.50	90.89	88.77	−12.87	−12.53	58.64	55.19
RMF433	0.1530	−16.30	247.99	−546.28	33.35	32.50	90.88	88.76	−13.04	−12.70	58.12	54.68
RMF434	0.1530	−16.30	249.99	−546.83	33.35	32.50	90.87	88.75	−13.21	−12.87	57.62	54.19
RSk1*	0.1601	−15.77	216.75	−530.11	30.93	30.05	84.07	81.79	−7.55	−7.41	70.39	66.77
S271	0.1485	−16.24	271.32	−295.39	37.41	36.48	108.90	106.28	23.09	22.33	55.90	55.77

TABLE VIII. (*Continued.*)

Model	n_0	E_0	K_0	Q_0	J_1	J_2	L_1	L_2	$K_{\mathrm{sym},1}$	$K_{\mathrm{sym},2}$	$Q_{\mathrm{sym},1}$	$Q_{\mathrm{sym},2}$
SMFT1	0.1577	−13.80	173.19	−456.40	18.60	17.58	58.90	55.96	86.75	87.36	315.09	351.34
SMFT2	0.1629	−13.85	212.28	−268.68	18.45	17.43	55.88	52.94	61.24	60.84	174.00	188.41
SRK3M5	0.1500	−16.00	299.95	967.25	24.56	23.50	85.52	82.46	143.66	146.79	60.92	96.54
SRK3M7	0.1500	−16.00	299.95	−363.94	29.61	28.73	82.03	79.69	−2.34	−2.56	27.14	24.62
VT	0.1530	−16.09	172.81	−482.63	40.77	39.74	129.83	126.88	127.09	130.15	464.14	543.21
$\sigma^3+\sigma^4+\omega_0^4$ models (type 3)												
BM-A	0.1789	−15.17	188.47	−436.81	20.83	19.63	55.37	51.91	−17.17	−18.08	−31.08	−36.10
BM-B	0.1562	−13.47	170.81	−504.71	18.48	17.42	48.43	45.47	−15.21	−15.61	−1.95	−5.33
BM-C	0.1418	−12.36	163.19	−547.67	16.99	16.02	44.21	41.51	−14.03	−14.21	9.79	7.02
DJM	0.1719	−14.81	244.96	148.09	21.40	20.22	66.65	62.98	35.25	32.64	−284.08	−303.13
DJM-C	0.1814	−15.67	329.61	229.25	23.18	21.90	72.57	68.48	21.33	17.14	−434.53	−469.15
EMFT1	0.1587	−13.56	166.32	4.41	19.70	18.61	59.94	56.62	32.29	30.48	−158.09	−166.13
EMFT2	0.1562	−13.47	170.82	−504.71	18.48	17.42	48.42	45.47	−15.21	−15.61	−1.95	−5.33
HD	0.1772	−16.22	284.47	−101.28	36.78	35.71	109.09	106.00	45.42	44.64	88.54	93.48
LB	0.1839	−15.26	316.79	−51.68	33.12	31.92	100.39	96.74	29.69	27.18	−253.55	−268.85
MB	0.1903	−15.07	341.75	−1376.15	33.77	32.49	93.72	89.98	−27.07	−28.10	−27.62	−32.75
MS1	0.1345	−13.89	209.98	−305.33	32.52	31.58	97.64	94.85	33.09	31.84	−54.56	−55.15
MS3	0.1484	−15.75	250.00	−563.95	36.06	35.00	105.53	102.38	1.17	−0.20	−106.68	−111.17
NLSV1	0.1491	−16.26	270.20	−74.48	38.32	37.31	117.71	114.70	60.01	58.98	−30.95	−27.90
NLSV2	0.1491	−16.48	296.67	−144.91	38.42	37.39	116.84	113.78	42.99	41.49	−112.90	−116.14
PK1	0.1485	−16.30	283.26	−26.55	38.73	37.70	119.18	116.10	56.76	55.48	−88.18	−88.97
TM1	0.1453	−16.26	281.41	−285.30	37.89	36.91	113.80	110.86	34.96	33.65	−65.52	−66.93
TM2	0.1324	−16.16	344.38	266.36	37.00	36.01	116.26	113.12	57.83	56.10	−230.98	−239.19
Z271	0.1485	−16.24	271.18	−734.69	36.77	35.94	101.04	98.91	−16.89	−16.41	52.10	49.01
$\sigma^3+\sigma^4+\omega^4+$ cross terms models (type 4)												
BigApple	0.1547	−16.34	227.17	−208.12	33.12	31.32	40.72	39.83	74.61	87.73	1495.37	1127.02
BKA20	0.1460	−15.93	237.99	−464.72	33.31	32.24	79.05	75.39	−10.82	−15.04	192.33	198.33
BKA22	0.1473	−15.91	225.42	−283.08	34.32	33.19	82.85	78.83	−4.14	−8.79	128.35	133.73
BKA24	0.1471	−15.95	227.21	−273.52	35.34	34.20	88.78	84.83	−10.34	−14.94	110.53	112.17
BSR1	0.1481	−16.02	240.09	−34.86	32.21	31.05	63.88	59.43	17.36	13.04	471.96	467.76
BSR2	0.1487	−16.03	239.94	−48.04	32.67	31.50	66.30	62.02	1.19	−3.13	423.07	403.20
BSR3	0.1497	−16.09	230.82	−113.87	33.91	32.76	74.97	70.50	0.04	−7.69	449.95	397.27
BSR4	0.1504	−16.08	238.81	4.87	34.35	33.18	77.50	73.27	−15.05	−20.66	440.56	419.91
BSR5	0.1508	−16.12	235.92	−10.01	35.62	34.47	87.54	83.41	−7.83	−14.12	359.81	346.76
BSR6	0.1493	−16.13	235.78	−7.57	36.78	35.62	89.77	85.68	−43.81	−49.55	392.95	352.01
BSR7	0.1494	−16.18	232.04	−18.60	38.41	37.28	103.22	99.19	−9.85	−16.95	272.07	198.40
BSR8	0.1470	−16.04	231.19	−290.61	32.25	31.09	64.57	60.29	2.42	−0.69	254.00	237.52
BSR9	0.1474	−16.07	232.72	−296.99	32.79	31.63	68.11	63.93	−8.06	−11.30	225.43	202.34
BSR10	0.1475	−16.06	227.56	−254.91	33.89	32.73	75.00	70.86	−12.62	−16.50	217.41	204.72
BSR11	0.1468	−16.08	226.83	−312.46	34.83	33.69	82.74	78.79	−20.42	−24.72	183.51	172.43
BSR12	0.1474	−16.10	232.39	−290.24	35.14	34.00	81.96	77.91	−38.14	−44.23	412.92	324.13
BSR13	0.1473	−16.13	228.78	−294.32	36.96	35.83	94.98	91.10	−36.70	−41.70	206.04	138.90
BSR14	0.1474	−16.18	235.53	−316.97	37.44	36.32	97.66	93.86	−37.05	−41.96	184.81	112.50
BSR15	0.1456	−16.03	226.95	−512.65	32.13	30.98	65.75	61.81	−19.20	−21.36	158.20	128.00
BSR16	0.1457	−16.05	225.03	−503.19	32.39	31.25	66.26	62.34	−21.89	−24.17	184.02	152.20
BSR17	0.1465	−16.05	221.85	−489.78	33.13	31.99	71.41	67.47	−28.47	−31.59	214.21	176.35
BSR18	0.1459	−16.05	221.15	−485.80	33.88	32.74	76.46	72.65	−39.11	−42.24	236.55	199.37
BSR19	0.1468	−16.08	220.94	−484.34	34.93	33.79	83.27	79.50	−46.75	−50.15	242.52	194.63
BSR20	0.1462	−16.09	223.43	−508.30	35.67	34.55	91.69	88.07	−37.01	−39.93	106.40	82.63
BSR21	0.1452	−16.12	220.39	−468.34	37.07	35.97	96.50	92.96	−43.19	−46.03	85.82	67.41
C1	0.1459	−16.19	304.03	−132.71	33.00	32.03	97.48	94.63	28.27	26.61	−7.91	−11.76
FSU-I	0.1482	−16.28	229.56	−524.03	38.46	37.42	112.71	109.63	3.94	2.64	−97.69	−101.74
FSU-II	0.1482	−16.28	229.56	−524.03	36.60	35.49	91.04	87.40	−65.50	−68.37	151.84	156.81
FSU-III	0.1482	−16.28	229.56	−524.03	35.15	33.90	75.80	71.73	−74.78	−74.40	390.67	398.21
FSU-IV	0.1482	−16.28	229.56	−524.03	32.94	31.43	55.23	52.16	−20.85	−16.78	339.65	249.89
FSU-V	0.1482	−16.28	229.56	−524.03	32.31	30.96	52.88	49.47	5.49	5.38	106.64	79.67

TABLE VIII. (*Continued.*)

Model	n_0	E_0	K_0	Q_0	J_1	J_2	L_1	L_2	$K_{\mathrm{sym},1}$	$K_{\mathrm{sym},2}$	$Q_{\mathrm{sym},1}$	$Q_{\mathrm{sym},2}$
FSU2H	0.1505	−16.26	237.98	−24.62	32.19	30.55	46.00	44.51	81.07	86.92	899.99	652.38
FSU2R	0.1505	−16.27	237.97	−135.44	32.30	30.69	48.80	46.90	55.36	55.87	355.61	190.26
FSUGarnet	0.1532	−16.23	229.71	13.52	32.48	30.92	53.20	50.97	58.91	59.48	282.06	137.39
FSUGold	0.1482	−16.28	229.56	−524.03	33.95	32.56	64.29	60.44	−55.96	−51.40	465.74	425.65
FSUGold4	0.1486	−16.53	231.98	−535.15	33.07	31.54	55.21	52.17	−19.90	−15.92	333.15	242.01
FSUGold5	0.1492	−16.92	235.62	−551.96	32.32	30.68	47.88	46.09	28.72	23.40	−63.74	−102.81
FSUGZ00	0.1488	−16.03	240.25	−47.08	32.61	31.44	66.51	62.19	0.97	−3.39	422.40	402.09
FSUGZ03	0.1474	−16.07	232.72	−297.03	32.72	31.56	68.20	64.02	−8.38	−11.63	226.06	202.86
FSUGZ06	0.1458	−16.05	225.23	−503.49	32.34	31.19	66.41	62.46	−22.19	−24.49	184.81	152.95
G1	0.1532	−16.14	214.96	−361.52	39.43	38.50	125.35	123.25	89.89	96.96	33.71	95.38
G2	0.1536	−16.07	214.87	−438.76	32.77	31.75	91.89	88.80	2.71	0.48	27.11	22.06
G2*	0.1536	−16.07	214.87	−438.76	31.46	30.40	73.19	69.70	−18.50	−21.92	197.34	197.45
HC	0.1686	−15.75	231.95	−390.72	32.30	31.01	62.96	58.54	−102.78	−99.02	836.28	933.82
IOPB-I	0.1490	−16.10	222.65	−116.46	34.74	33.36	67.91	63.70	−48.42	−40.12	880.94	873.03
IUFSU	0.1547	−16.40	231.55	−289.77	32.94	31.31	49.54	47.24	23.26	28.64	561.38	369.13
LA	0.1794	−15.46	301.71	−145.52	34.78	33.49	82.95	78.68	−59.88	−61.78	251.91	264.53
MA	0.1791	−15.93	347.54	−1280.97	33.72	32.40	75.61	71.50	−74.14	−74.56	265.07	265.76
NL3v1	0.1483	−16.24	271.80	205.37	37.13	36.08	104.68	101.29	3.02	0.71	105.62	128.87
NL3v2	0.1483	−16.24	271.80	205.37	36.11	34.99	91.76	87.79	−42.92	−46.14	379.90	442.43
NL3v3	0.1483	−16.24	271.80	205.37	35.64	34.49	86.29	82.10	−54.15	−56.09	545.84	633.24
NL3v4	0.1483	−16.24	271.80	205.37	35.23	34.03	81.33	76.98	−60.06	−59.81	713.22	819.96
NL3v5	0.1483	−16.24	271.80	205.37	34.45	33.17	72.69	68.26	−58.99	−52.86	1017.30	1128.98
NL3v6	0.1483	−16.24	271.80	205.37	33.75	32.39	65.40	61.16	−45.75	−33.55	1257.86	1323.57
PCSB0	0.1501	−16.00	240.24	−278.13	33.29	32.02	64.57	60.02	−100.40	−95.26	974.75	1087.73
PCSB1	0.1501	−16.00	240.27	−343.64	33.30	32.02	64.47	60.02	−95.87	−90.54	899.35	977.73
PCSB2	0.1500	−15.99	239.98	−411.26	33.29	32.00	64.33	60.00	−92.07	−86.76	828.78	880.95
PCSB3	0.1500	−16.00	240.08	−479.42	33.29	32.00	64.22	60.00	−88.79	−83.58	764.92	797.32
PCSB4	0.1501	−16.00	240.25	−546.62	33.31	32.01	64.22	60.03	−85.95	−80.91	707.13	724.70
PCSB5	0.1501	−16.01	240.26	−612.23	33.32	32.02	64.14	60.03	−83.59	−78.76	655.43	662.25
QMC-RMF1	0.1599	−16.10	259.78	−495.40	32.89	31.05	44.48	38.09	−190.31	−161.95	1100.59	1306.37
QMC-RMF2	0.1609	−16.33	263.73	−450.55	32.75	30.86	40.60	35.33	−169.06	−132.25	1351.97	1384.80
QMC-RMF3	0.1569	−16.06	229.80	−482.13	33.62	31.98	49.16	43.67	−164.33	−142.93	1208.05	1344.09
QMC-RMF4	0.1619	−16.13	278.82	−310.52	30.43	28.60	31.31	29.70	−54.85	−27.61	1487.24	1049.59
S271v1	0.1485	−16.24	271.27	−295.65	36.70	35.75	98.83	95.98	−41.20	−44.12	−41.99	−53.77
S271v2	0.1485	−16.24	271.27	−295.65	36.06	35.07	90.23	86.90	−84.43	−90.44	23.75	15.13
S271v3	0.1485	−16.24	271.27	−295.65	35.48	34.44	82.72	78.88	−113.52	−121.11	161.48	181.56
S271v4	0.1485	−16.24	271.27	−295.65	34.95	33.84	76.09	71.77	−132.58	−139.61	329.14	391.87
S271v5	0.1485	−16.24	271.27	−295.65	34.46	33.28	70.14	65.45	−144.20	−148.69	506.10	611.13
S271v6	0.1485	−16.24	271.27	−295.65	34.00	32.75	64.76	59.82	−150.08	−150.47	681.68	817.26
SIG-OM	0.1495	−16.30	265.60	−233.41	38.06	37.03	115.24	112.04	44.15	41.19	−37.09	−49.30
SVI−1	0.1495	−16.30	264.09	−490.34	38.06	37.07	119.53	116.62	95.88	95.98	196.31	207.97
SVI−2	0.1487	−16.31	271.61	−455.14	38.03	37.05	118.96	116.10	91.37	91.45	186.68	198.91
TM1*	0.1433	−15.64	273.43	−516.29	35.05	34.01	93.47	90.18	−17.71	−20.57	72.19	68.66
TM1e	0.1453	−16.26	281.41	−285.30	33.12	31.39	42.21	40.03	−13.26	3.71	1156.44	843.52
XS	0.1484	−16.30	229.98	−702.80	33.35	31.83	58.15	54.97	−30.22	−28.80	169.13	128.26
Z271*	0.1481	−16.24	271.10	−734.60	41.36	40.17	89.11	83.36	−178.74	−198.18	257.15	306.97
Z271s1	0.1485	−16.24	271.18	−734.69	35.82	34.97	89.12	86.90	−65.45	−64.91	246.25	144.84
Z271s2	0.1485	−16.24	271.18	−734.69	34.90	34.09	78.51	76.65	−93.75	−92.33	472.11	301.73
Z271s3	0.1485	−16.24	271.18	−734.69	34.02	33.28	69.32	67.83	−104.75	−104.61	659.64	457.85
Z271s4	0.1485	−16.24	271.18	−734.69	33.19	32.54	61.50	60.20	−103.31	−106.05	769.08	580.68
Z271s5	0.1485	−16.24	271.18	−734.69	32.41	31.85	54.92	53.58	−93.99	−99.80	795.13	655.18
Z271s6	0.1485	−16.24	271.18	−734.69	31.69	31.21	49.40	47.82	−80.24	−88.19	751.38	676.63
Z271v1	0.1485	−16.24	271.18	−734.69	36.21	35.36	93.26	90.90	−64.73	−66.45	−2.74	−17.49
Z271v2	0.1485	−16.24	271.18	−734.69	35.71	34.82	86.53	83.64	−99.33	−104.97	35.36	15.62
Z271v3	0.1485	−16.24	271.18	−734.69	35.48	34.55	83.46	80.26	−113.06	−120.52	72.28	58.17
Z271v4	0.1485	−16.24	271.18	−734.69	35.26	34.30	80.56	77.02	−124.92	−133.90	116.15	113.22

TABLE VIII. (*Continued.*)

Model	n_0	E_0	K_0	Q_0	J_1	J_2	L_1	L_2	$K_{sym,1}$	$K_{sym,2}$	$Q_{sym,1}$	$Q_{sym,2}$
Z271v5	0.1485	−16.24	271.18	−734.69	35.05	34.05	77.81	73.92	−135.18	−145.29	164.64	177.78
Z271v6	0.1485	−16.24	271.18	−734.69	34.85	33.81	75.19	70.96	−144.07	−154.88	216.10	249.30
Density-dependent models (type 5)												
DD	0.1488	−16.02	240.34	133.31	32.70	31.64	58.89	55.98	−95.65	−95.36	595.16	576.63
DDF	0.1470	−16.04	223.35	−760.26	32.68	31.63	58.70	55.98	−141.49	−139.90	484.83	467.46
DD-ME1	0.1523	−16.23	246.36	314.22	34.15	33.10	58.43	55.47	−101.53	−101.34	722.02	705.07
DD-ME2	0.1520	−16.14	251.31	477.60	33.37	32.31	54.23	51.27	−87.15	−87.22	794.29	776.77
DDME-X	0.1516	−16.06	265.85	878.41	33.33	32.26	52.71	49.69	−70.92	−71.42	820.29	796.88
DD2	0.1492	−16.02	243.58	165.60	32.74	31.68	57.99	55.03	−93.80	−93.39	618.50	597.47
MPE	0.1381	−15.84	246.94	−1.18	31.73	30.74	60.08	57.21	−74.68	−74.39	515.20	504.82
PKDD	0.1496	−16.27	262.51	−120.13	37.85	36.80	93.14	90.23	−81.11	−80.62	40.14	24.05
TW-99	0.1532	−16.27	241.27	−543.91	33.88	32.79	58.31	55.34	−126.05	−125.00	560.11	537.77
Relativistic point-coupling models (type 6)												
FZ0	0.1399	−16.24	563.09	2280.37	40.51	39.47	133.11	129.81	98.91	98.04	−519.77	−560.89
PC-F1	0.1509	−16.17	254.60	−289.85	38.78	37.76	120.06	117.05	74.40	74.56	67.31	78.64
PC-F2	0.1509	−16.17	255.08	−282.86	38.61	37.01	118.73	114.33	66.92	70.25	46.51	62.04
PC-F3	0.1510	−16.19	254.88	−287.36	39.28	38.26	121.59	118.57	75.12	74.74	66.75	78.07
PC-F4	0.1510	−16.18	254.90	−282.52	38.63	39.08	121.91	122.37	94.10	86.69	120.92	122.63
PC-PK1	0.1530	−16.12	238.25	−65.58	36.66	35.61	115.99	112.92	94.75	95.53	62.42	76.18
δ meson models (type 7)												
HA	0.1697	−15.63	232.98	−370.53	32.01	30.64	61.04	55.04	−148.73	−135.72	894.56	1163.06
HB	0.1797	−16.24	297.91	−4.98	37.68	36.79	122.85	121.55	117.30	148.05	347.64	426.75
NLδ	0.1602	−16.05	240.82	−464.71	31.51	30.75	104.30	102.85	102.53	127.69	346.03	304.88

TABLE IX. The same as Table III except for RMF models.

Model	σ_o MeV/fm^2	σ_δ MeV/fm^2	S_S MeV	$r_{np}(^{208}Pb)$ fm	$r_{np}(^{48}Ca)$ fm	$\alpha_D(^{208}Pb)$ fm^3	$\alpha_D(^{48}Ca)$ fm^3
Linear finite-range models (type 1)							
H1	1.485	5.462	94.20	0.247	0.199	39.243	4.492
L1	1.930	4.927	75.67	0.206	0.180	40.976	4.668
L2	1.480	3.746	66.62	0.211	0.189	53.985	6.151
L3	1.749	4.185	77.10	0.239	0.205	61.277	7.113
LBF	1.546	10.133	171.68	0.290	0.210	21.397	2.452
LHS	1.632	8.318	143.52	0.293	0.216	30.991	3.599
LW	1.937	5.509	79.58	0.204	0.178	38.410	4.392
LZ	1.546	10.618	182.62	0.298	0.214	21.154	2.430
RMF201	1.553	7.043	119.37	0.267	0.204	31.196	3.578
RMF202	1.556	7.046	119.32	0.266	0.204	31.087	3.565
RMF203	1.559	7.077	119.69	0.267	0.204	30.987	3.554
RMF204	1.562	7.108	120.05	0.267	0.204	30.887	3.542
RMF205	1.565	7.138	120.41	0.267	0.204	30.787	3.531
RMF206	1.568	7.168	120.76	0.267	0.204	30.686	3.520
$\sigma^3 + \sigma^4$ models (type 2)							
CS	1.147	11.361	194.97	0.328	0.232	28.711	3.393
E	1.167	10.213	175.11	0.316	0.227	29.566	3.474
ER	1.160	10.389	179.09	0.318	0.228	29.108	3.421
FAMA1	1.111	9.754	168.20	0.311	0.225	29.744	3.485

TABLE IX. (*Continued.*)

Model	σ_o MeV/fm^2	σ_δ MeV/fm^2	S_S MeV	$r_{np}(^{208}\text{Pb})$ fm	$r_{np}(^{48}\text{Ca})$ fm	$\alpha_D(^{208}\text{Pb})$ fm^3	$\alpha_D(^{48}\text{Ca})$ fm^3
FAMA2	1.150	9.613	165.77	0.309	0.223	29.505	3.451
FAMA3	1.190	9.486	163.59	0.307	0.222	29.292	3.421
FAMA4	1.230	9.372	161.62	0.305	0.221	29.099	3.394
FAMA5	1.271	9.268	159.82	0.303	0.220	28.922	3.369
FAMB1	0.935	7.457	128.60	0.269	0.203	26.911	3.064
FAMB2	0.978	7.382	127.31	0.268	0.202	26.778	3.045
FAMB3	1.022	7.316	126.17	0.266	0.201	26.660	3.029
FAMB4	1.066	7.257	125.15	0.265	0.201	26.554	3.014
FAMB5	1.112	7.203	124.22	0.264	0.200	26.458	3.000
FAMC1	0.935	5.324	91.82	0.239	0.192	34.567	3.909
FAMC2	0.978	5.269	90.87	0.237	0.191	34.397	3.885
FAMC3	1.022	5.221	90.04	0.236	0.190	34.246	3.863
FAMC4	1.066	5.178	89.29	0.235	0.189	34.111	3.844
FAMC5	1.112	5.139	88.62	0.233	0.189	33.990	3.827
GL1	0.804	5.431	91.81	0.226	0.181	27.273	3.029
GL2	0.705	4.696	79.36	0.205	0.168	25.601	2.793
GL3	0.595	3.925	66.32	0.181	0.154	23.890	2.551
GL4	0.885	5.374	90.81	0.224	0.180	27.105	3.006
GL5	0.794	4.691	79.27	0.205	0.168	25.589	2.791
GL6	0.707	4.052	68.33	0.184	0.156	24.000	2.571
GL7	0.968	5.306	89.70	0.222	0.179	26.996	2.990
GL8	0.889	4.693	79.30	0.205	0.168	25.592	2.792
GL82	0.782	4.871	85.31	0.211	0.170	23.462	2.549
GL9	0.819	4.103	69.34	0.187	0.157	24.286	2.607
GM1	0.972	5.328	89.95	0.222	0.179	26.938	2.984
GM2	0.845	4.334	73.20	0.194	0.162	24.778	2.677
GM3	0.718	4.275	72.24	0.192	0.161	24.685	2.663
GPS	0.805	4.082	69.96	0.189	0.159	24.733	2.658
Hybrid	1.131	9.287	160.30	0.305	0.222	29.834	3.484
MS2	1.188	8.726	150.48	0.300	0.220	31.770	3.710
MTVTC	1.192	7.047	119.33	0.266	0.204	30.994	3.553
NL-VT1	1.143	10.731	183.99	0.323	0.230	29.851	3.523
NLrho	0.972	5.357	87.83	0.220	0.179	28.600	3.185
NL06	1.116	10.256	177.75	0.318	0.228	29.228	3.433
NL065	1.164	8.907	152.71	0.292	0.214	27.000	3.119
NL07	1.153	8.086	138.58	0.277	0.206	26.134	2.988
NL075	1.149	7.837	133.65	0.269	0.202	25.113	2.855
NL1	1.233	12.479	212.07	0.334	0.234	27.088	3.209
NL1J4	1.239	11.515	195.44	0.329	0.232	29.401	3.484
NL1J5	1.239	14.710	249.66	0.347	0.238	23.820	2.829
NL2	1.299	8.621	150.57	0.280	0.206	22.853	2.598
NL3	1.196	9.037	155.98	0.300	0.219	29.271	3.406
NL3-II	1.209	9.198	158.12	0.301	0.219	29.016	3.378
NL3*	1.214	9.711	166.35	0.307	0.222	28.561	3.335
NL4	1.187	8.673	150.12	0.297	0.218	30.181	3.509
NLB	1.418	7.690	132.61	0.279	0.209	29.705	3.417
NLB1	1.462	9.108	147.92	0.293	0.217	32.431	3.805
NLB2	1.420	10.391	168.55	0.314	0.227	34.791	4.142
NLC	1.099	8.176	141.00	0.290	0.215	30.675	3.555
NLD	1.290	7.245	124.93	0.270	0.204	28.821	3.292
NLM	1.008	6.178	101.33	0.242	0.192	31.122	3.532
NLM2	1.005	5.990	98.25	0.238	0.189	30.661	3.466
NLM3	0.913	5.700	99.83	0.249	0.196	32.988	3.737
NLM4	1.199	5.960	97.75	0.237	0.189	30.586	3.456

TABLE IX. (*Continued.*)

Model	σ_o MeV/fm^2	σ_δ MeV/fm^2	S_S MeV	$r_{np}(^{208}\mathrm{Pb})$ fm	$r_{np}(^{48}\mathrm{Ca})$ fm	$\alpha_D(^{208}\mathrm{Pb})$ fm^3	$\alpha_D(^{48}\mathrm{Ca})$ fm^3
NLM5	1.258	9.094	149.15	0.303	0.224	38.269	4.543
NLM6	1.008	8.744	143.41	0.272	0.202	24.040	2.748
NLRA	1.279	8.878	147.47	0.281	0.208	25.809	2.970
NLRA1	1.174	8.438	146.63	0.293	0.216	29.640	3.434
NLS	1.223	10.477	179.31	0.310	0.222	26.069	3.041
NLSH	1.237	7.754	135.18	0.281	0.210	28.913	3.322
NLZ	0.958	9.780	174.18	0.326	0.233	33.137	3.914
NLZ2	1.131	11.009	187.75	0.326	0.231	30.047	3.554
P-067	1.149	9.631	159.91	0.289	0.211	24.741	2.856
P-070	1.161	9.535	154.34	0.278	0.204	23.010	2.639
P-075	1.155	8.885	138.18	0.252	0.190	20.141	2.272
P-080	0.951	6.810	111.00	0.233	0.181	21.471	2.382
Q1	1.076	8.097	142.73	0.297	0.220	32.761	3.813
RMF301	0.756	4.361	73.73	0.195	0.163	24.893	2.692
RMF302	0.738	4.292	72.55	0.193	0.161	24.738	2.670
RMF303	0.735	4.277	72.31	0.192	0.161	24.707	2.666
RMF304	0.731	4.263	72.07	0.192	0.161	24.675	2.661
RMF305	0.724	4.235	71.59	0.191	0.160	24.612	2.652
RMF306	0.717	4.206	71.11	0.190	0.160	24.548	2.643
RMF307	0.713	4.192	70.86	0.190	0.159	24.516	2.639
RMF308	0.710	4.177	70.62	0.189	0.159	24.484	2.634
RMF309	0.702	4.148	70.13	0.188	0.158	24.419	2.625
RMF310	0.691	4.104	69.37	0.187	0.158	24.320	2.611
RMF311	0.688	4.089	69.12	0.186	0.157	24.287	2.606
RMF312	0.684	4.073	68.86	0.186	0.157	24.253	2.601
RMF313	0.676	4.043	68.35	0.185	0.156	24.185	2.592
RMF314	0.673	4.028	68.09	0.184	0.156	24.152	2.587
RMF315	0.671	4.020	67.96	0.184	0.156	24.134	2.585
RMF316	0.669	4.012	67.83	0.184	0.156	24.117	2.582
RMF317	0.665	3.997	67.57	0.183	0.155	24.082	2.577
RMF401	0.835	5.255	88.83	0.221	0.178	26.879	2.973
RMF402	0.773	4.665	81.55	0.216	0.177	28.751	3.166
RMF403	0.817	5.114	86.45	0.217	0.176	26.566	2.929
RMF404	0.784	4.781	82.34	0.214	0.175	27.557	3.030
RMF405	0.823	5.110	86.39	0.217	0.176	26.558	2.928
RMF406	0.707	4.277	72.30	0.192	0.161	24.705	2.665
RMF407	0.797	4.973	84.08	0.213	0.173	26.254	2.885
RMF408	0.801	4.972	84.05	0.213	0.173	26.251	2.884
RMF409	0.804	4.971	84.04	0.213	0.173	26.249	2.884
RMF410	0.808	4.970	84.02	0.213	0.173	26.246	2.883
RMF411	0.778	4.833	81.71	0.209	0.171	25.942	2.840
RMF412	0.782	4.833	81.70	0.209	0.171	25.941	2.840
RMF413	0.785	4.832	81.68	0.209	0.171	25.939	2.840
RMF414	0.789	4.831	81.67	0.209	0.171	25.938	2.840
RMF415	0.811	5.184	85.20	0.209	0.170	24.230	2.653
RMF416	0.762	4.693	79.34	0.205	0.169	25.631	2.796
RMF417	0.766	4.693	79.34	0.205	0.169	25.631	2.796
RMF418	0.867	5.587	89.88	0.212	0.171	23.209	2.549
RMF419	0.831	5.416	87.13	0.207	0.168	22.926	2.508
RMF420	0.715	4.386	75.06	0.200	0.166	26.013	2.825
RMF421	0.872	5.721	90.63	0.209	0.169	22.222	2.436
RMF422	0.719	4.413	74.60	0.196	0.163	25.008	2.708
RMF423	0.723	4.414	74.62	0.196	0.163	25.011	2.709
RMF424	0.712	4.154	70.23	0.188	0.159	24.433	2.627
RMF425	0.716	4.157	70.28	0.188	0.159	24.439	2.628
RMF426	0.721	4.160	70.32	0.189	0.159	24.445	2.628

TABLE IX. (*Continued.*)

Model	σ_o MeV/fm^2	σ_δ MeV/fm^2	S_S MeV	$r_{np}(^{208}\text{Pb})$ fm	$r_{np}(^{48}\text{Ca})$ fm	$\alpha_D(^{208}\text{Pb})$ fm^3	$\alpha_D(^{48}\text{Ca})$ fm^3
RMF427	0.672	4.003	67.67	0.184	0.156	24.096	2.579
RMF428	0.677	4.007	67.73	0.184	0.156	24.104	2.580
RMF429	0.681	4.010	67.79	0.184	0.156	24.112	2.581
RMF430	0.685	4.014	67.85	0.184	0.156	24.120	2.583
RMF431	0.690	4.017	67.92	0.184	0.156	24.129	2.584
RMF432	0.694	4.021	67.98	0.184	0.156	24.136	2.585
RMF433	0.699	4.024	68.03	0.184	0.156	24.144	2.586
RMF434	0.703	4.028	68.09	0.184	0.156	24.152	2.587
RSk1*	1.013	5.790	94.97	0.232	0.186	30.128	3.392
S271	1.041	6.989	120.52	0.260	0.198	26.640	3.015
SMFT1	0.838	3.256	53.94	0.173	0.169	51.295	5.754
SMFT2	0.962	3.235	52.46	0.166	0.165	50.202	5.618
SRK3M5	1.336	6.152	105.38	0.269	0.213	48.168	5.653
SRK3M7	1.031	4.696	80.44	0.217	0.178	31.145	3.455
VT	1.174	11.477	194.02	0.328	0.232	29.498	3.495
$\sigma^3+\sigma^4+\omega_0^4$ models (type 3)							
BM-A	0.976	3.856	58.73	0.173	0.164	41.735	4.667
BM-B	0.832	2.991	49.86	0.163	0.163	50.473	5.614
BM-C	0.748	2.505	44.55	0.156	0.163	57.787	6.405
DJM	1.097	4.410	68.99	0.197	0.177	44.292	5.033
DJM-C	1.368	5.071	76.53	0.205	0.179	39.922	4.549
EMFT1	0.830	3.829	63.18	0.193	0.179	50.640	5.750
EMFT2	0.832	2.990	49.85	0.163	0.163	50.468	5.613
HD	1.151	7.373	113.02	0.237	0.184	23.706	2.669
LB	1.435	7.840	117.24	0.247	0.192	27.824	3.190
MB	1.792	7.513	109.81	0.233	0.184	25.636	2.910
MS1	1.024	7.314	134.74	0.302	0.224	37.493	4.374
MS3	1.287	8.605	148.46	0.298	0.219	31.584	3.683
NLSV1	1.183	8.574	147.47	0.291	0.214	28.446	3.289
NLSV2	1.206	8.170	140.51	0.282	0.210	27.638	3.177
PK1	1.202	8.629	148.80	0.292	0.214	28.196	3.260
TM1	1.152	7.832	137.04	0.282	0.210	28.311	3.249
TM2	1.157	7.422	138.18	0.296	0.219	31.408	3.619
Z271	1.001	6.022	103.85	0.239	0.186	25.413	2.830
$\sigma^3+\sigma^4+\omega^4+$ cross terms models (type 4)							
BigApple	1.218	3.166	53.12	0.155	0.139	23.120	2.416
BKA20	1.083	4.921	85.82	0.220	0.178	27.637	3.047
BKA22	1.122	5.569	96.56	0.235	0.186	27.757	3.094
BKA24	1.132	6.356	110.31	0.253	0.195	28.273	3.191
BSR1	1.122	3.870	66.85	0.187	0.159	26.104	2.805
BSR2	1.127	4.213	72.60	0.197	0.165	26.340	2.854
BSR3	1.141	5.088	87.27	0.220	0.177	26.760	2.951
BSR4	1.142	5.553	94.96	0.231	0.183	27.176	3.023
BSR5	1.147	6.496	110.89	0.251	0.194	27.557	3.109
BSR6	1.151	7.165	123.12	0.265	0.201	27.791	3.163
BSR7	1.157	8.259	141.86	0.284	0.211	27.869	3.208
BSR8	1.125	3.871	67.20	0.188	0.160	26.235	2.821
BSR9	1.140	4.237	73.43	0.199	0.166	26.465	2.870
BSR10	1.136	4.953	85.80	0.218	0.177	26.865	2.957
BSR11	1.131	5.775	100.36	0.240	0.188	27.695	3.096
BSR12	1.139	6.063	105.07	0.246	0.191	27.835	3.125
BSR13	1.146	7.403	128.36	0.273	0.205	28.384	3.244
BSR14	1.156	7.596	131.65	0.276	0.207	28.153	3.222
BSR15	1.121	3.912	68.35	0.191	0.162	26.701	2.878

TABLE IX. (*Continued.*)

Model	σ_o MeV/fm^2	σ_δ MeV/fm^2	S_S MeV	$r_{np}(^{208}\text{Pb})$ fm	$r_{np}(^{48}\text{Ca})$ fm	$\alpha_D(^{208}\text{Pb})$ fm^3	$\alpha_D(^{48}\text{Ca})$ fm^3
BSR16	1.124	4.061	70.93	0.196	0.164	26.757	2.894
BSR17	1.126	4.671	81.29	0.213	0.174	27.247	2.987
BSR18	1.126	5.361	93.55	0.232	0.184	28.085	3.123
BSR19	1.134	6.227	108.21	0.251	0.195	28.555	3.220
BSR20	1.136	6.984	121.70	0.268	0.204	29.328	3.345
BSR21	1.140	7.618	133.36	0.280	0.209	29.049	3.334
C1	1.142	6.325	110.37	0.259	0.200	31.341	3.565
FSU-I	1.194	8.995	155.33	0.300	0.219	29.224	3.399
FSU-II	1.194	7.343	126.80	0.271	0.205	28.503	3.257
FSU-III	1.194	5.994	103.50	0.243	0.190	27.667	3.102
FSU-IV	1.194	3.805	65.71	0.184	0.157	25.490	2.730
FSU-V	1.194	3.278	56.61	0.166	0.146	24.674	2.601
FSU2R	1.210	3.249	55.53	0.163	0.144	24.547	2.584
FSU2H	1.207	3.214	54.94	0.162	0.144	24.612	2.589
FSUGarnet	1.223	3.634	61.39	0.174	0.151	24.872	2.647
FSUGold	1.194	4.841	83.59	0.215	0.174	26.680	2.929
FSUGold4	1.207	3.786	65.25	0.183	0.156	25.255	2.701
FSUGold5	1.227	2.768	47.59	0.146	0.133	23.513	2.432
FSUGZ00	1.127	4.248	73.16	0.198	0.165	26.475	2.872
FSUGZ03	1.139	4.260	73.83	0.200	0.166	26.603	2.888
FSUGZ06	1.125	4.093	71.46	0.197	0.165	26.888	2.911
G1	1.088	9.503	160.50	0.299	0.218	27.847	3.240
G2	0.959	6.069	102.33	0.243	0.191	29.586	3.339
G2*	0.959	4.346	73.28	0.198	0.166	27.195	2.963
HC	0.986	4.407	69.83	0.184	0.157	24.383	2.634
IUFSU	1.241	3.603	60.45	0.171	0.148	24.167	2.564
LA	1.360	6.561	99.75	0.222	0.177	24.373	2.724
MA	1.656	5.621	85.55	0.204	0.167	23.915	2.634
NL3v1	1.197	7.960	137.40	0.283	0.211	28.946	3.332
NL3v2	1.197	7.081	122.22	0.266	0.202	28.573	3.256
NL3v3	1.197	6.686	115.40	0.259	0.198	28.384	3.218
NL3v4	1.197	6.316	109.02	0.251	0.194	28.171	3.177
NL3v5	1.197	5.640	97.35	0.236	0.186	27.756	3.097
NL3v6	1.197	5.034	86.89	0.220	0.178	27.311	3.014
PCSB0	0.934	4.274	73.18	0.196	0.164	25.669	2.778
PCSB1	0.945	4.257	72.89	0.196	0.163	25.630	2.773
PCSB2	0.954	4.216	72.23	0.195	0.163	25.566	2.763
PCSB3	0.966	4.182	71.64	0.193	0.162	25.484	2.751
PCSB4	0.977	4.165	71.32	0.193	0.162	25.415	2.742
PCSB5	0.988	4.131	70.73	0.192	0.161	25.333	2.731
QMC-RMF1	0.964	3.242	53.21	0.154	0.138	22.888	2.395
QMC-RMF2	1.031	3.179	51.97	0.151	0.136	22.806	2.381
QMC-RMF3	0.999	3.866	64.27	0.176	0.151	23.766	2.533
QMC-RMF4	1.168	2.587	42.11	0.131	0.125	23.514	2.418
S271v1	1.041	6.507	112.21	0.251	0.193	26.531	2.984
S271v2	1.041	6.063	104.56	0.242	0.189	26.410	2.952
S271v3	1.041	5.656	97.53	0.233	0.184	26.285	2.920
S271v4	1.041	5.279	91.04	0.224	0.179	26.153	2.887
S271v5	1.041	4.930	85.02	0.215	0.174	26.015	2.854
S271v6	1.041	4.605	79.42	0.207	0.170	25.871	2.820
SIG-OM	1.190	8.460	145.24	0.289	0.213	28.486	3.291
SVI−1	1.196	8.331	143.02	0.286	0.212	28.216	3.253
SVI−2	1.194	8.180	140.94	0.284	0.211	28.122	3.237
TM1*	1.072	5.999	105.93	0.249	0.194	28.464	3.199

TABLE IX. (*Continued.*)

Model	σ_o MeV/fm^2	σ_δ MeV/fm^2	S_S MeV	$r_{np}(^{208}\mathrm{Pb})$ fm	$r_{np}(^{48}\mathrm{Ca})$ fm	$\alpha_D(^{208}\mathrm{Pb})$ fm^3	$\alpha_D(^{48}\mathrm{Ca})$ fm^3
TM1e	1.152	2.951	51.63	0.156	0.139	23.821	2.481
XS	1.195	3.661	63.16	0.178	0.153	24.671	2.626
Z271*	0.998	5.866	101.35	0.225	0.177	21.480	2.353
Z271s1	1.001	5.425	93.55	0.225	0.179	25.250	2.786
Z271s2	1.001	4.889	84.31	0.212	0.172	25.059	2.738
Z271s3	1.001	4.401	75.90	0.199	0.165	24.845	2.688
Z271s4	1.001	3.953	68.17	0.186	0.157	24.607	2.636
Z271s5	1.001	3.537	61.00	0.174	0.150	24.341	2.580
Z271s6	1.001	3.149	54.30	0.160	0.142	24.045	2.520
Z271v1	1.001	5.688	98.10	0.231	0.182	25.371	2.811
Z271v2	1.001	5.380	92.78	0.224	0.179	25.319	2.792
Z271v3	1.001	5.233	90.25	0.221	0.177	25.291	2.782
Z271v4	1.001	5.091	87.80	0.218	0.175	25.263	2.772
Z271v5	1.001	4.953	85.42	0.214	0.173	25.233	2.762
Z271v6	1.001	4.819	83.11	0.211	0.171	25.203	2.752
Density-dependent models (type 5)							
DD	1.202	4.871	83.88	0.217	0.176	27.756	3.059
DDF	1.216	4.917	85.37	0.220	0.178	28.212	3.116
DD-ME1	1.199	4.961	84.12	0.212	0.172	25.670	2.814
DD-ME2	1.192	4.560	77.42	0.202	0.167	25.702	2.798
DDME-X	1.197	4.475	76.11	0.200	0.166	25.629	2.785
DD2	1.213	4.807	82.63	0.214	0.175	27.487	3.023
MPE	1.085	4.126	74.68	0.208	0.172	28.964	3.158
PKDD	1.227	7.342	126.00	0.266	0.201	26.745	3.040
TW-99	1.296	4.918	83.07	0.211	0.172	25.771	2.824
δ meson models (type 7)							
HA	0.997	7.725	121.87	0.263	0.202	31.872	3.688
HB	1.196	11.619	176.45	0.301	0.218	28.330	3.350
NLδ	0.818	11.376	186.50	0.338	0.241	42.141	5.113

TABLE X. The same as Table IV except for RMF and RMF-PC models.

Model	$R_{1.2}$	$\Lambda_{1.2}$	$\bar{I}_{1.2}$	BE/$M_{1.2}$	$R_{1.4}$	$\Lambda_{1.4}$	$\bar{I}_{1.4}$	BE/$M_{1.4}$	$R_{1.6}$	$\Lambda_{1.6}$	$\bar{I}_{1.6}$	BE/$M_{1.6}$	$M_{\max}$
Linear finite-range models (type 1)													
H1	14.38	3377.0	23.07	0.047	14.69	1675.2	18.49	0.057	14.95	855.1	15.24	0.066	3.05
L1	13.30	2280.0	20.23	0.053	13.59	1070.3	16.22	0.063	13.82	531.1	13.39	0.074	2.79
L2	14.45	3465.5	23.27	0.047	14.78	1750.4	18.72	0.056	15.06	903.7	15.48	0.065	3.13
L3	14.71	4179.8	24.31	0.045	15.07	1984.1	19.56	0.054	15.38	1056.4	16.20	0.063	3.25
LBF	14.44	4217.2	24.35	0.045	14.82	2003.0	19.53	0.054	15.14	1039.3	16.11	0.063	3.11
LHS	14.49	3855.5	23.86	0.046	14.82	1889.5	19.12	0.055	15.11	960.4	15.74	0.065	3.08
LW	12.71	1737.9	18.63	0.056	12.96	788.2	14.90	0.068	13.15	379.1	12.26	0.079	2.60
LZ	14.42	4416.8	24.60	0.045	14.83	2053.7	19.78	0.053	15.18	1091.2	16.35	0.062	3.16
RMF201	14.42	3523.2	23.32	0.047	14.73	1733.9	18.67	0.056	14.99	880.5	15.37	0.066	3.04
RMF202	14.41	3512.1	23.30	0.047	14.72	1728.0	18.65	0.056	14.98	877.4	15.35	0.066	3.04
RMF203	14.41	3501.4	23.28	0.047	14.71	1722.0	18.64	0.056	14.97	874.1	15.34	0.066	3.03
RMF204	14.40	3490.4	23.26	0.047	14.71	1716.0	18.62	0.056	14.97	870.8	15.32	0.066	3.03
RMF205	14.40	3479.7	23.24	0.047	14.70	1710.2	18.60	0.056	14.96	867.6	15.31	0.066	3.03
RMF206	14.39	3469.0	23.22	0.047	14.70	1704.4	18.58	0.056	14.95	864.4	15.29	0.066	3.02

TABLE X. (*Continued.*)

Model	$R_{1.2}$	$\Lambda_{1.2}$	$\bar{I}_{1.2}$	$BE/M_{1.2}$	$R_{1.4}$	$\Lambda_{1.4}$	$\bar{I}_{1.4}$	$BE/M_{1.4}$	$R_{1.6}$	$\Lambda_{1.6}$	$\bar{I}_{1.6}$	$BE/M_{1.6}$	M_{max}
$\sigma^3 + \sigma^4$ models (type 2)													
CS	14.24	3665.3	23.47	0.046	14.54	1718.7	18.61	0.056	14.77	839.7	15.16	0.067	2.93
E	14.26	3599.1	23.36	0.047	14.55	1695.0	18.54	0.056	14.78	832.1	15.12	0.067	2.94
ER	14.27	3664.9	23.48	0.046	14.57	1728.1	18.64	0.056	14.80	849.0	15.21	0.066	2.94
FAMA1	14.21	3498.9	23.14	0.047	14.48	1626.0	18.30	0.057	14.68	785.2	14.88	0.068	2.88
FAMA2	14.23	3522.6	23.20	0.047	14.51	1645.5	18.37	0.057	14.72	799.4	14.95	0.067	2.88
FAMA3	14.25	3545.4	23.25	0.047	14.53	1663.8	18.43	0.057	14.75	812.6	15.02	0.067	2.89
FAMA4	14.27	3566.7	23.30	0.047	14.56	1680.9	18.49	0.057	14.78	824.5	15.08	0.067	2.89
FAMA5	14.29	3588.1	23.35	0.047	14.58	1697.1	18.54	0.056	14.80	835.0	15.13	0.067	2.90
FAMB1	14.00	3075.7	22.08	0.049	14.15	1310.1	17.16	0.060	14.21	582.8	13.70	0.073	2.52
FAMB2	14.04	3144.9	22.22	0.049	14.21	1354.1	17.33	0.060	14.30	612.3	13.89	0.072	2.54
FAMB3	14.07	3206.0	22.34	0.049	14.26	1391.9	17.47	0.059	14.37	637.1	14.04	0.071	2.55
FAMB4	14.10	3241.3	22.44	0.048	14.30	1425.1	17.59	0.059	14.43	658.5	14.17	0.071	2.57
FAMB5	14.13	3267.0	22.53	0.048	14.34	1455.0	17.70	0.059	14.48	677.6	14.28	0.070	2.58
FAMC1	13.66	2410.2	20.50	0.052	13.75	1002.2	15.90	0.064	13.76	439.1	12.71	0.077	2.47
FAMC2	13.73	2500.6	20.73	0.052	13.84	1057.4	16.14	0.063	13.88	471.2	12.95	0.076	2.48
FAMC3	13.78	2570.6	20.92	0.051	13.91	1103.2	16.34	0.063	13.98	498.0	13.14	0.075	2.50
FAMC4	13.83	2632.6	21.09	0.051	13.97	1143.1	16.51	0.062	14.05	520.9	13.30	0.074	2.51
FAMC5	13.87	2689.1	21.23	0.051	14.03	1178.4	16.65	0.062	14.12	541.2	13.44	0.074	2.52
GL1	13.77	2577.1	20.92	0.051	13.85	1069.6	16.19	0.063	13.86	464.8	12.90	0.076	2.46
GL2	13.62	2361.1	20.37	0.053	13.64	943.3	15.63	0.065	13.58	387.0	12.30	0.080	2.26
GL3	13.50	2189.9	19.92	0.054	13.47	849.9	15.18	0.067	13.34	331.7	11.83	0.082	2.10
GL4	13.86	2708.4	21.26	0.051	13.99	1159.9	16.58	0.062	14.05	520.2	13.29	0.075	2.49
GL5	13.74	2529.9	20.80	0.052	13.83	1050.3	16.11	0.064	13.83	453.9	12.82	0.077	2.32
GL6	13.62	2356.8	20.36	0.053	13.66	950.7	15.66	0.065	13.60	392.9	12.35	0.079	2.17
GL7	13.93	2813.0	21.51	0.050	14.09	1227.5	16.84	0.061	14.18	560.5	13.56	0.073	2.51
GL8	13.83	2641.2	21.10	0.051	13.94	1124.2	16.43	0.063	13.99	498.5	13.14	0.075	2.36
GL82	14.06	3147.2	22.22	0.049	14.23	1354.7	17.33	0.060	14.30	608.8	13.87	0.072	2.38
GL9	13.73	2493.4	20.71	0.052	13.80	1029.4	16.02	0.064	13.78	438.9	12.70	0.077	2.21
GM1	13.92	2796.7	21.48	0.050	14.08	1219.9	16.81	0.061	14.17	556.8	13.54	0.073	2.51
GM2	13.76	2539.0	20.83	0.051	13.85	1061.1	16.16	0.063	13.85	459.9	12.86	0.077	2.26
GM3	13.64	2388.1	20.44	0.052	13.69	968.2	15.74	0.065	13.64	404.4	12.44	0.079	2.22
GPS	13.81	2611.9	21.02	0.051	13.90	1090.7	16.28	0.063	13.90	470.1	12.94	0.076	2.23
Hybrid	14.24	3524.0	23.21	0.047	14.52	1650.9	18.39	0.057	14.74	805.1	14.98	0.067	2.90
MS2	14.23	3407.5	22.96	0.047	14.49	1592.4	18.18	0.057	14.69	773.0	14.81	0.068	2.88
MTVTC	13.57	2339.1	20.33	0.053	13.64	957.8	15.70	0.065	13.61	402.7	12.43	0.079	2.22
NL-VT1	14.19	3482.6	23.09	0.047	14.45	1607.1	18.23	0.057	14.64	769.5	14.79	0.068	2.86
NLrho	13.41	2074.5	19.61	0.054	13.44	838.9	15.12	0.067	13.39	348.5	11.99	0.081	2.24
NL06	14.22	3580.6	23.30	0.047	14.50	1667.6	18.44	0.057	14.71	807.7	14.99	0.067	2.89
NL065	14.17	3395.1	22.88	0.047	14.41	1552.6	18.03	0.058	14.58	731.4	14.59	0.069	2.72
NL07	14.11	3272.1	22.53	0.048	14.32	1445.9	17.67	0.059	14.44	667.7	14.22	0.070	2.56
NL075	14.04	3139.0	22.21	0.049	14.21	1350.8	17.32	0.060	14.29	607.8	13.86	0.072	2.41
NL1	14.25	3767.1	23.65	0.046	14.57	1778.8	18.80	0.056	14.82	874.3	15.34	0.066	2.96
NL1J4	14.26	3618.2	23.40	0.047	14.55	1703.0	18.56	0.056	14.78	835.8	15.14	0.067	2.95
NL1J5	14.21	4007.3	24.02	0.045	14.58	1914.7	19.19	0.055	14.87	950.2	15.70	0.065	2.99
NL2	14.33	3871.0	23.83	0.046	14.65	1837.0	18.97	0.055	14.90	903.7	15.48	0.065	2.77
NL3	14.28	3565.5	23.30	0.047	14.56	1682.4	18.50	0.057	14.79	826.3	15.09	0.067	2.91
NL3-II	14.27	3554.5	23.28	0.047	14.56	1676.3	18.48	0.057	14.78	823.2	15.07	0.067	2.91
NL3*	14.26	3557.3	23.28	0.047	14.54	1672.1	18.46	0.057	14.76	818.4	15.05	0.067	2.90
NL4	14.28	3537.5	23.25	0.047	14.56	1668.5	18.45	0.057	14.78	819.4	15.05	0.067	2.90
NLB	14.33	3496.7	23.20	0.047	14.61	1670.8	18.46	0.057	14.84	828.2	15.10	0.067	2.87
NLB1	13.91	2765.6	21.41	0.050	14.08	1227.3	16.85	0.061	14.21	574.7	13.66	0.073	2.68
NLB2	14.07	3076.3	22.07	0.049	14.29	1386.3	17.46	0.059	14.47	670.7	14.24	0.070	2.87
NLC	14.14	3280.4	22.58	0.048	14.36	1478.4	17.78	0.059	14.52	698.4	14.40	0.070	2.77
NLD	14.14	3230.0	22.44	0.048	14.35	1444.0	17.66	0.059	14.50	678.5	14.28	0.070	2.59
NLM	13.46	2130.7	19.76	0.054	13.50	867.8	15.27	0.067	13.48	367.4	12.15	0.080	2.39

TABLE X. (*Continued.*)

Model	$R_{1.2}$	$\Lambda_{1.2}$	$\bar{I}_{1.2}$	$BE/M_{1.2}$	$R_{1.4}$	$\Lambda_{1.4}$	$\bar{I}_{1.4}$	$BE/M_{1.4}$	$R_{1.6}$	$\Lambda_{1.6}$	$\bar{I}_{1.6}$	$BE/M_{1.6}$	M_{max}
NLM2	13.45	2122.7	19.74	0.054	13.49	860.1	15.23	0.067	13.45	361.6	12.10	0.081	2.38
NLM3	13.84	2688.5	21.21	0.051	13.95	1135.8	16.48	0.062	13.99	503.1	13.17	0.075	2.51
NLM4	13.64	2383.5	20.43	0.052	13.76	1016.5	15.96	0.064	13.82	456.6	12.84	0.077	2.44
NLM5	14.04	3000.4	21.92	0.049	14.26	1356.3	17.35	0.060	14.44	658.8	14.17	0.070	2.89
NLM6	13.89	2846.4	21.58	0.050	14.00	1189.1	16.69	0.062	14.02	515.6	13.26	0.075	2.44
NLRA	14.16	3285.3	22.63	0.048	14.40	1501.5	17.86	0.058	14.57	714.2	14.49	0.069	2.74
NLRA1	14.29	3583.0	23.34	0.047	14.59	1696.6	18.54	0.056	14.81	835.8	15.14	0.067	2.91
NLS	14.26	3677.9	23.50	0.046	14.56	1730.2	18.65	0.056	14.79	846.1	15.19	0.067	2.88
NLSH	14.35	3658.7	23.50	0.046	14.65	1749.3	18.71	0.056	14.89	868.6	15.31	0.066	2.93
NLZ	14.15	3464.4	23.04	0.047	14.41	1587.6	18.16	0.058	14.59	753.6	14.71	0.068	2.85
NLZ2	14.21	3510.8	23.16	0.047	14.48	1631.4	18.32	0.057	14.68	789.2	14.90	0.068	2.91
P-067	14.05	3204.7	22.34	0.049	14.24	1386.6	17.45	0.059	14.34	632.4	14.01	0.071	2.59
P-070	13.94	2947.2	21.80	0.050	14.09	1256.8	16.96	0.061	14.15	558.2	13.54	0.073	2.47
P-075	13.73	2554.5	20.87	0.051	13.80	1048.2	16.10	0.064	13.78	445.0	12.75	0.077	2.26
P-080	13.76	2599.5	20.98	0.051	13.83	1061.5	16.16	0.064	13.79	444.9	12.75	0.077	2.19
Q1	14.24	3464.2	23.09	0.047	14.51	1620.5	18.28	0.057	14.71	788.1	14.89	0.068	2.88
RMF301	13.69	2452.0	20.60	0.052	13.75	1004.8	15.91	0.064	13.73	426.5	12.61	0.078	2.25
RMF302	13.67	2422.7	20.53	0.052	13.72	988.0	15.83	0.065	13.69	416.3	12.53	0.078	2.23
RMF303	13.66	2416.8	20.51	0.052	13.72	984.6	15.82	0.065	13.68	414.2	12.51	0.078	2.22
RMF304	13.66	2411.0	20.50	0.052	13.71	981.3	15.80	0.065	13.67	412.1	12.50	0.079	2.22
RMF305	13.65	2399.4	20.47	0.052	13.70	974.6	15.77	0.065	13.66	408.0	12.47	0.079	2.21
RMF306	13.64	2387.3	20.44	0.052	13.69	967.8	15.74	0.065	13.64	403.9	12.43	0.079	2.20
RMF307	13.64	2381.5	20.42	0.052	13.68	964.4	15.73	0.065	13.63	401.8	12.42	0.079	2.20
RMF308	13.63	2375.6	20.41	0.052	13.68	961.1	15.71	0.065	13.63	399.7	12.40	0.079	2.20
RMF309	13.63	2363.8	20.38	0.052	13.66	954.2	15.68	0.065	13.61	395.5	12.37	0.079	2.19
RMF310	13.61	2345.6	20.33	0.053	13.65	944.0	15.63	0.065	13.58	389.1	12.32	0.080	2.18
RMF311	13.61	2339.6	20.32	0.053	13.64	940.5	15.61	0.065	13.58	387.0	12.30	0.080	2.17
RMF312	13.60	2333.6	20.30	0.053	13.63	937.1	15.60	0.065	13.57	384.8	12.28	0.080	2.17
RMF313	13.60	2321.7	20.27	0.053	13.62	930.1	15.57	0.066	13.55	380.6	12.25	0.080	2.16
RMF314	13.59	2315.8	20.26	0.053	13.62	926.7	15.55	0.066	13.54	378.5	12.23	0.080	2.16
RMF315	13.59	2312.5	20.25	0.053	13.61	924.9	15.54	0.066	13.54	377.4	12.22	0.080	2.16
RMF316	13.59	2309.6	20.24	0.053	13.61	923.1	15.53	0.066	13.53	376.4	12.21	0.080	2.15
RMF317	13.58	2303.5	20.22	0.053	13.60	919.7	15.52	0.066	13.52	374.2	12.20	0.080	2.15
RMF401	13.79	2611.6	21.02	0.051	13.90	1098.6	16.32	0.063	13.93	483.6	13.03	0.076	2.44
RMF402	13.87	2740.8	21.34	0.050	13.99	1165.3	16.60	0.062	14.04	517.1	13.27	0.075	2.45
RMF403	13.77	2573.4	20.92	0.051	13.86	1074.9	16.22	0.063	13.88	469.1	12.93	0.076	2.40
RMF404	13.81	2644.9	21.10	0.051	13.92	1112.6	16.38	0.063	13.95	488.4	13.07	0.076	2.41
RMF405	13.77	2583.6	20.95	0.051	13.87	1082.1	16.25	0.063	13.89	473.6	12.96	0.076	2.41
RMF406	13.63	2373.0	20.40	0.052	13.67	958.9	15.70	0.065	13.62	398.5	12.39	0.079	2.21
RMF407	13.74	2536.4	20.82	0.052	13.83	1052.3	16.12	0.064	13.83	455.3	12.83	0.077	2.37
RMF408	13.74	2542.2	20.84	0.052	13.83	1056.0	16.14	0.064	13.84	457.7	12.84	0.077	2.37
RMF409	13.75	2547.3	20.85	0.051	13.84	1059.8	16.15	0.064	13.85	459.9	12.86	0.077	2.37
RMF410	13.75	2553.0	20.86	0.051	13.84	1063.4	16.17	0.063	13.86	462.2	12.88	0.077	2.37
RMF411	13.72	2501.6	20.73	0.052	13.79	1030.6	16.02	0.064	13.78	442.3	12.73	0.077	2.33
RMF412	13.72	2507.4	20.74	0.052	13.80	1034.7	16.04	0.064	13.79	444.7	12.75	0.077	2.34
RMF413	13.73	2512.8	20.76	0.052	13.80	1038.4	16.06	0.064	13.80	447.0	12.76	0.077	2.34
RMF414	13.73	2518.4	20.77	0.052	13.81	1042.1	16.07	0.064	13.81	449.3	12.78	0.077	2.34
RMF415	13.62	2358.6	20.37	0.053	13.67	959.3	15.70	0.065	13.64	404.3	12.44	0.079	2.29
RMF416	13.70	2472.5	20.65	0.052	13.76	1013.5	15.95	0.064	13.75	432.1	12.65	0.078	2.30
RMF417	13.70	2479.1	20.67	0.052	13.77	1017.5	15.96	0.064	13.75	434.4	12.67	0.078	2.30
RMF418	13.58	2299.8	20.22	0.053	13.63	935.0	15.59	0.065	13.59	393.6	12.36	0.079	2.29
RMF419	13.54	2245.2	20.07	0.053	13.57	903.5	15.44	0.066	13.52	374.0	12.20	0.080	2.25
RMF420	13.69	2472.4	20.65	0.052	13.75	1008.8	15.93	0.064	13.73	426.8	12.61	0.078	2.27
RMF421	13.51	2203.8	19.96	0.053	13.54	886.5	15.36	0.066	13.48	366.5	12.14	0.080	2.25
RMF422	13.64	2393.9	20.45	0.052	13.69	969.6	15.75	0.065	13.65	405.2	12.44	0.079	2.24
RMF423	13.65	2400.4	20.47	0.052	13.70	973.7	15.77	0.065	13.66	407.7	12.46	0.079	2.24
RMF424	13.64	2378.1	20.42	0.052	13.68	962.7	15.72	0.065	13.63	400.6	12.41	0.079	2.19

TABLE X. (*Continued.*)

Model	$R_{1.2}$	$\Lambda_{1.2}$	$\bar{I}_{1.2}$	BE/$M_{1.2}$	$R_{1.4}$	$\Lambda_{1.4}$	$\bar{I}_{1.4}$	BE/$M_{1.4}$	$R_{1.6}$	$\Lambda_{1.6}$	$\bar{I}_{1.6}$	BE/$M_{1.6}$	M_{max}
RMF425	13.64	2384.3	20.43	0.052	13.69	966.3	15.73	0.065	13.64	402.8	12.43	0.079	2.20
RMF426	13.65	2390.4	20.45	0.052	13.69	969.8	15.75	0.065	13.65	404.9	12.44	0.079	2.20
RMF427	13.59	2314.4	20.25	0.053	13.61	926.0	15.55	0.066	13.54	378.0	12.23	0.080	2.15
RMF428	13.60	2320.6	20.27	0.053	13.62	929.7	15.56	0.066	13.55	380.2	12.25	0.080	2.16
RMF429	13.60	2327.1	20.28	0.053	13.63	933.3	15.58	0.065	13.56	382.5	12.26	0.080	2.16
RMF430	13.60	2333.3	20.30	0.053	13.64	937.0	15.60	0.065	13.57	384.6	12.28	0.080	2.16
RMF431	13.61	2339.3	20.32	0.053	13.64	940.5	15.62	0.065	13.58	386.7	12.30	0.080	2.16
RMF432	13.61	2345.4	20.33	0.053	13.65	944.1	15.63	0.065	13.58	388.9	12.31	0.080	2.16
RMF433	13.62	2351.4	20.35	0.053	13.65	947.6	15.65	0.065	13.59	391.0	12.33	0.079	2.17
RMF434	13.62	2357.5	20.36	0.053	13.66	951.0	15.66	0.065	13.60	393.0	12.35	0.079	2.17
RSk1*	13.21	1844.6	18.93	0.056	13.17	712.1	14.45	0.070	13.03	277.2	11.31	0.086	2.09
S271	14.09	3216.4	22.36	0.048	14.28	1403.8	17.52	0.059	14.40	646.9	14.10	0.071	2.56
SMFT1	13.07	1804.4	18.82	0.056	13.22	788.2	14.88	0.068	13.33	365.2	12.14	0.080	2.59
SMFT2	12.82	1606.4	18.20	0.057	12.95	693.3	14.36	0.070	13.04	310.3	11.68	0.083	2.47
SRK3M5	14.15	3123.1	22.26	0.049	14.42	1470.3	17.75	0.059	14.64	728.5	14.57	0.069	2.97
SRK3M7	13.73	2494.6	20.72	0.052	13.84	1058.0	16.15	0.063	13.88	469.0	12.93	0.076	2.35
VT	14.18	3447.6	23.01	0.047	14.43	1586.6	18.16	0.058	14.62	757.3	14.73	0.068	2.86
$\sigma^3+\sigma^4+\omega_0^4$ models (type 3)													
BM-A	11.28	604.7	13.83	0.073	10.75	155.1	9.76	0.098	−1	−1	−1	−1	1.49
BM-B	11.55	696.0	14.37	0.070	11.01	180.4	10.12	0.095	−1	−1	−1	−1	1.50
BM-C	11.79	790.0	14.88	0.068	11.25	208.9	10.49	0.092	−1	−1	−1	−1	1.51
DJM	12.73	1486.7	17.78	0.059	12.76	598.3	13.80	0.072	12.70	243.7	10.95	0.088	1.98
DJM-C	12.69	1489.1	17.79	0.059	12.74	604.3	13.83	0.072	12.69	247.1	10.99	0.087	1.97
EMFT1	12.71	1431.6	17.59	0.059	12.69	557.3	13.54	0.073	12.57	220.0	10.66	0.090	1.92
EMFT2	11.55	696.0	14.37	0.070	11.01	180.4	10.12	0.095	−1	−1	−1	−1	1.50
HD	13.56	2273.1	20.15	0.053	13.66	964.2	15.73	0.065	13.72	432.5	12.66	0.078	2.76
LB	13.21	1887.7	19.06	0.055	13.27	773.1	14.79	0.068	13.24	323.8	11.77	0.082	2.10
MB	12.64	1369.7	17.36	0.060	12.50	486.4	13.06	0.076	12.13	159.5	9.84	0.097	1.76
MS1	14.13	3321.8	22.66	0.048	14.33	1465.8	17.73	0.059	14.44	668.8	14.23	0.070	2.35
MS3	13.95	2936.9	21.78	0.050	14.06	1223.8	16.83	0.061	14.05	519.9	13.28	0.075	2.11
NLSV1	14.19	3396.8	22.89	0.047	14.43	1556.5	18.04	0.058	14.60	733.5	14.60	0.069	2.57
NLSV2	14.19	3386.9	22.86	0.048	14.43	1542.0	17.99	0.058	14.58	720.8	14.53	0.069	2.47
PK1	14.21	3444.6	23.01	0.047	14.46	1585.5	18.15	0.058	14.63	750.8	14.69	0.068	2.55
TM1	14.20	3425.7	22.94	0.047	14.43	1557.6	18.04	0.058	14.58	724.5	14.55	0.069	2.45
TM2	14.39	4194.3	24.32	0.045	14.76	1998.4	19.44	0.054	15.05	1003.2	15.93	0.064	2.72
Z271	13.89	2795.0	21.45	0.050	13.97	1151.0	16.54	0.062	13.93	480.7	13.01	0.076	2.08
$\sigma^3+\sigma^4+\omega^4+$ cross terms models (type 4)													
BigApple	12.87	1761.5	18.70	0.056	13.09	795.8	14.93	0.067	13.26	382.6	12.27	0.079	2.62
BKA20	13.57	2286.9	20.18	0.053	13.62	934.6	15.59	0.065	13.59	392.7	12.35	0.079	2.11
BKA22	13.61	2350.9	20.35	0.053	13.68	966.1	15.74	0.065	13.65	410.1	12.48	0.079	2.13
BKA24	13.70	2499.2	20.72	0.052	13.78	1028.9	16.02	0.064	13.76	438.0	12.70	0.078	2.14
BSR1	13.44	2163.2	19.87	0.053	13.59	947.1	15.66	0.065	13.70	438.4	12.71	0.077	2.51
BSR2	13.41	2109.8	19.72	0.054	13.53	909.8	15.48	0.066	13.61	414.0	12.52	0.078	2.43
BSR3	13.52	2235.2	20.05	0.053	13.64	957.7	15.70	0.065	13.70	433.1	12.67	0.077	2.43
BSR4	13.55	2287.6	20.19	0.053	13.68	985.8	15.83	0.064	13.76	449.7	12.79	0.077	2.49
BSR5	13.71	2511.3	20.78	0.052	13.86	1087.7	16.28	0.063	13.95	499.2	13.15	0.075	2.54
BSR6	13.70	2505.3	20.75	0.052	13.82	1070.7	16.21	0.063	13.90	484.3	13.04	0.076	2.47
BSR7	13.92	2900.8	21.71	0.050	14.09	1264.7	16.99	0.061	14.20	581.9	13.70	0.073	2.58
BSR8	13.27	1940.3	19.22	0.055	13.31	792.1	14.89	0.068	13.27	329.7	11.82	0.082	2.05
BSR9	13.29	1961.6	19.28	0.055	13.33	792.9	14.89	0.068	13.27	325.5	11.78	0.082	2.04
BSR10	13.43	2115.5	19.72	0.054	13.48	862.3	15.24	0.067	13.43	359.0	12.07	0.081	2.07
BSR11	13.57	2296.3	20.21	0.053	13.62	932.8	15.58	0.065	13.57	388.2	12.31	0.080	2.08
BSR12	13.53	2249.1	20.08	0.053	13.58	917.3	15.51	0.066	13.54	384.4	12.28	0.080	2.09
BSR13	13.73	2568.1	20.90	0.051	13.80	1051.4	16.11	0.064	13.77	442.9	12.73	0.077	2.11
BSR14	13.78	2648.4	21.10	0.051	13.86	1091.0	16.29	0.063	13.84	462.2	12.88	0.077	2.13

TABLE X. (*Continued.*)

Model	$R_{1.2}$	$\Lambda_{1.2}$	$\bar{I}_{1.2}$	$BE/M_{1.2}$	$R_{1.4}$	$\Lambda_{1.4}$	$\bar{I}_{1.4}$	$BE/M_{1.4}$	$R_{1.6}$	$\Lambda_{1.6}$	$\bar{I}_{1.6}$	$BE/M_{1.6}$	M_{max}
BSR15	13.11	1744.4	18.62	0.057	13.04	660.5	14.16	0.071	12.82	244.4	10.92	0.088	1.86
BSR16	13.10	1740.9	18.61	0.057	13.03	658.2	14.14	0.071	12.81	243.1	10.91	0.088	1.85
BSR17	13.19	1828.7	18.88	0.056	13.13	693.5	14.35	0.070	12.91	257.9	11.08	0.087	1.87
BSR18	13.30	1950.2	19.24	0.055	13.24	740.8	14.61	0.069	13.04	276.2	11.28	0.086	1.88
BSR19	13.41	2089.4	19.64	0.054	13.37	798.5	14.91	0.068	13.18	300.5	11.53	0.084	1.90
BSR20	13.63	2401.1	20.47	0.052	13.63	938.6	15.60	0.065	13.49	365.2	12.12	0.081	1.96
BSR21	13.71	2549.5	20.84	0.052	13.73	1003.4	15.90	0.064	13.61	394.5	12.35	0.079	1.96
C1	14.11	3187.3	22.30	0.049	14.32	1406.3	17.53	0.059	14.45	658.5	14.17	0.071	2.59
FSU-I	14.00	3092.5	22.11	0.049	14.13	1296.2	17.11	0.061	14.14	555.0	13.52	0.074	2.14
FSU-II	13.49	2200.3	19.95	0.053	13.43	833.4	15.09	0.067	13.22	307.8	11.59	0.084	1.88
FSU-III	13.11	1744.3	18.62	0.057	13.00	641.6	14.05	0.071	12.72	227.2	10.73	0.090	1.82
FSU-IV	12.70	1414.3	17.52	0.060	12.61	520.0	13.30	0.075	12.34	184.0	10.20	0.094	1.80
FSU-V	12.70	1422.2	17.55	0.059	12.62	527.5	13.35	0.074	12.37	188.8	10.26	0.093	1.80
FSU2H	13.17	1931.5	19.22	0.055	13.35	860.9	15.26	0.066	13.48	406.1	12.46	0.078	2.42
FSU2R	13.00	1726.1	18.58	0.057	13.09	727.3	14.55	0.069	13.11	314.3	11.69	0.083	2.11
FSUGarnet	13.00	1749.6	18.65	0.056	13.10	740.3	14.62	0.069	13.14	321.3	11.76	0.082	2.12
FSUGold	12.87	1527.0	17.91	0.058	12.76	559.5	13.55	0.074	12.48	197.1	10.37	0.092	1.80
FSUGold4	12.70	1413.9	17.52	0.060	12.61	520.4	13.30	0.075	12.34	184.4	10.20	0.093	1.80
FSUGold5	12.57	1350.7	17.29	0.060	12.50	500.3	13.17	0.075	12.25	178.5	10.13	0.094	1.80
FSUGZ00	13.41	2112.1	19.73	0.054	13.53	910.8	15.48	0.066	13.61	414.4	12.52	0.078	2.43
FSUGZ03	13.30	1963.4	19.28	0.055	13.33	793.7	14.90	0.068	13.27	325.9	11.78	0.082	2.04
FSUGZ06	13.10	1742.2	18.62	0.057	13.03	658.6	14.15	0.071	12.81	243.2	10.91	0.088	1.85
G1	14.15	3368.1	22.79	0.048	14.37	1511.2	17.89	0.058	14.51	700.0	14.41	0.070	2.46
G2	13.60	2327.5	20.29	0.053	13.63	937.2	15.60	0.065	13.57	387.2	12.30	0.080	2.14
G2*	13.12	1763.5	18.68	0.056	13.10	691.7	14.34	0.070	12.99	274.5	11.29	0.086	2.05
HC	12.42	1241.8	16.89	0.061	12.47	502.4	13.21	0.075	12.48	219.0	10.68	0.089	2.30
IUFSU	12.69	1480.3	17.76	0.059	12.74	602.4	13.82	0.072	12.70	247.9	11.00	0.087	2.00
LA	12.77	1476.5	17.74	0.059	12.75	575.5	13.66	0.073	12.63	228.4	10.75	0.089	1.95
MA	12.34	1155.2	16.53	0.062	12.12	386.4	12.28	0.080	11.50	102.1	8.86	0.106	1.66
NL3v1	14.07	3172.1	22.27	0.049	14.29	1411.3	17.55	0.059	14.45	672.6	14.25	0.070	2.77
NL3v2	13.88	2784.1	21.46	0.050	14.08	1245.5	16.92	0.061	14.23	591.8	13.77	0.072	2.76
NL3v3	13.81	2654.7	21.16	0.051	14.00	1193.9	16.71	0.062	14.16	567.8	13.61	0.073	2.76
NL3v4	13.75	2556.1	20.92	0.051	13.94	1151.5	16.55	0.062	14.10	550.2	13.50	0.073	2.76
NL3v5	13.65	2423.3	20.57	0.052	13.85	1094.6	16.31	0.063	14.01	526.9	13.35	0.074	2.77
NL3v6	13.57	2341.7	20.34	0.052	13.77	1059.8	16.17	0.063	13.95	513.3	13.25	0.074	2.77
PCSB0	13.23	1861.5	18.98	0.056	13.34	803.9	14.96	0.068	13.43	368.0	12.16	0.080	2.55
PCSB1	13.13	1749.4	18.65	0.056	13.20	731.2	14.57	0.069	13.21	316.2	11.72	0.083	2.24
PCSB2	13.05	1656.5	18.35	0.057	13.06	669.7	14.22	0.071	13.01	276.5	11.32	0.085	2.07
PCSB3	12.97	1578.5	18.09	0.058	12.94	617.8	13.91	0.072	12.81	244.7	10.94	0.088	1.96
PCSB4	12.90	1504.9	17.84	0.059	12.82	570.8	13.62	0.073	12.62	214.6	10.59	0.090	1.88
PCSB5	12.83	1442.4	17.62	0.059	12.71	528.0	13.35	0.074	12.43	188.0	10.25	0.093	1.82
QMC-RMF1	11.73	839.6	15.16	0.067	11.69	322.1	11.73	0.083	11.56	123.4	9.29	0.101	1.96
QMC-RMF2	11.84	934.2	15.59	0.065	11.86	361.8	12.15	0.080	11.81	149.2	9.73	0.097	2.05
QMC-RMF3	12.14	1038.9	16.06	0.064	12.15	404.0	12.53	0.078	12.11	171.8	10.07	0.094	2.16
QMC-RMF4	12.04	1151.6	16.55	0.062	12.17	478.0	13.05	0.075	12.23	211.6	10.58	0.090	2.23
S271v1	13.85	2741.2	21.34	0.050	13.96	1152.9	16.55	0.062	13.99	504.7	13.18	0.075	2.38
S271v2	13.61	2376.5	20.41	0.052	13.68	971.1	15.76	0.065	13.66	415.3	12.52	0.078	2.36
S271v3	13.41	2099.1	19.68	0.054	13.45	854.5	15.20	0.067	13.44	362.7	12.11	0.081	2.36
S271v4	13.24	1913.7	19.14	0.055	13.29	781.3	14.83	0.068	13.28	332.4	11.86	0.082	2.36
S271v5	13.11	1782.4	18.75	0.056	13.17	734.9	14.59	0.069	13.18	314.3	11.71	0.083	2.36
S271v6	13.01	1692.8	18.47	0.057	13.08	704.6	14.42	0.070	13.10	303.1	11.61	0.083	2.37
SIG-OM	14.14	3311.9	22.65	0.048	14.36	1479.9	17.78	0.059	14.49	687.1	14.33	0.070	2.55
SVI−1	14.23	3453.5	23.04	0.047	14.49	1595.8	18.19	0.057	14.67	761.4	14.75	0.068	2.73
SVI−2	14.24	3474.1	23.08	0.047	14.50	1608.8	18.24	0.057	14.68	769.8	14.79	0.068	2.74
TM1*	13.93	2864.3	21.62	0.050	14.05	1210.4	16.77	0.062	14.08	527.2	13.34	0.074	2.22
TM1e	13.07	1785.8	18.76	0.056	13.18	763.3	14.74	0.068	13.23	335.4	11.89	0.082	2.18

TABLE X. (*Continued.*)

Model	$R_{1.2}$	$\Lambda_{1.2}$	$\bar{I}_{1.2}$	$\mathrm{BE}/M_{1.2}$	$R_{1.4}$	$\Lambda_{1.4}$	$\bar{I}_{1.4}$	$\mathrm{BE}/M_{1.4}$	$R_{1.6}$	$\Lambda_{1.6}$	$\bar{I}_{1.6}$	$\mathrm{BE}/M_{1.6}$	M_{max}
XS	12.57	1286.1	17.04	0.061	12.36	433.9	12.67	0.078	11.80	123.5	9.26	0.102	1.68
Z271*	12.88	1513.7	17.85	0.059	12.46	443.3	12.71	0.078	11.45	88.6	8.56	0.110	1.63
Z271s1	13.54	2247.4	20.07	0.053	13.49	856.8	15.21	0.067	13.28	316.8	11.68	0.083	1.88
Z271s2	13.18	1811.6	18.83	0.056	13.05	653.3	14.11	0.071	12.70	220.4	10.65	0.090	1.79
Z271s3	12.89	1527.5	17.91	0.059	12.71	534.1	13.38	0.074	12.29	171.2	10.00	0.095	1.75
Z271s4	12.66	1351.5	17.29	0.060	12.48	466.4	12.92	0.077	12.03	145.0	9.62	0.099	1.72
Z271s5	12.49	1239.1	16.86	0.061	12.31	426.4	12.61	0.078	11.84	129.8	9.37	0.101	1.71
Z271s6	12.36	1164.7	16.57	0.062	12.18	400.9	12.41	0.079	11.71	120.3	9.21	0.102	1.70
Z271v1	13.59	2328.9	20.29	0.053	13.53	872.6	15.28	0.067	13.24	307.2	11.57	0.084	1.81
Z271v2	13.27	1905.9	19.11	0.056	13.05	647.4	14.07	0.072	12.48	184.8	10.18	0.094	1.70
Z271v3	13.11	1725.1	18.55	0.057	12.83	561.3	13.54	0.074	12.14	146.4	9.62	0.099	1.68
Z271v4	12.95	1567.3	18.04	0.058	12.63	494.2	13.09	0.076	11.86	120.5	9.19	0.103	1.66
Z271v5	12.81	1434.5	17.58	0.060	12.46	443.5	12.72	0.078	11.63	103.2	8.87	0.107	1.65
Z271v6	12.67	1323.9	17.17	0.061	12.31	405.7	12.42	0.080	11.46	91.8	8.64	0.109	1.64
Density-dependent models (type 5)													
DD	13.05	1755.7	18.67	0.056	13.16	750.3	14.68	0.069	13.23	334.8	11.89	0.082	2.43
DDF	12.12	987.6	15.81	0.065	11.99	353.4	12.02	0.081	11.77	130.2	9.40	0.100	1.98
DD-ME1	12.99	1716.7	18.55	0.057	13.12	740.7	14.63	0.069	13.20	334.0	11.88	0.082	2.46
DD-ME2	13.01	1752.4	18.66	0.056	13.16	766.5	14.77	0.068	13.26	352.5	12.03	0.081	2.50
DDME-X	13.17	1883.9	19.08	0.055	13.34	839.8	15.15	0.067	13.47	396.9	12.39	0.079	2.58
DD2	13.04	1757.3	18.68	0.056	13.16	753.7	14.69	0.069	13.23	337.9	11.91	0.081	2.44
MPE	13.56	2191.9	19.93	0.053	13.68	951.8	15.67	0.065	13.76	436.2	12.70	0.077	2.51
PKDD	13.65	2439.9	20.57	0.052	13.73	1006.2	15.92	0.064	13.73	435.2	12.68	0.078	2.35
TW-99	12.38	1183.2	16.65	0.062	12.34	446.3	12.82	0.077	12.24	180.0	10.17	0.093	2.10
Relativistic point-coupling models (type 6)													
FZ0	17.19	6423.2	26.60	0.042	17.20	2727.3	20.96	0.051	17.23	1413.6	17.15	0.060	3.22
PC-F1	−1	−1	−1	−1	−1	−1	−1	−1	−1	−1	−1	−1	0.62
PC-F2	−1	−1	−1	−1	−1	−1	−1	−1	−1	−1	−1	−1	0.00
PC-F3	−1	−1	−1	−1	−1	−1	−1	−1	−1	−1	−1	−1	0.62
PC-F4	−1	−1	−1	−1	−1	−1	−1	−1	−1	−1	−1	−1	0.00
PC-PK1	−1	−1	−1	−1	−1	−1	−1	−1	−1	−1	−1	−1	0.61
δ meson models (type 7)													
HA	12.31	1172.9	16.62	0.062	12.37	476.8	13.05	0.075	12.40	212.5	10.59	0.090	2.33
HB	13.79	2587.5	20.98	0.051	13.95	1138.2	16.49	0.062	14.06	528.7	13.35	0.074	2.74
NLδ	13.95	2820.4	21.53	0.050	14.11	1238.7	16.89	0.061	14.21	570.9	13.63	0.073	2.55

APPENDIX C: PARAMETERS AND PROPERTIES OF GOGNY MODELS

This Appendix contains Tables XI–XIII.

TABLE XI. Parameters of Gogny models. For each interaction, the first row corresponds quantities with subscript $i = 1$ and the second row to $i = 2$. W_i, B_i, H_i, and M_i are in MeV, μ_i in fm, t_{3i} in MeV $\text{fm}^{3+3\alpha_i}$, while x_{3i} and α_i are dimensionless. We do not discuss more complex Gogny models having parameters with $i = 3$.

Model	W_i	B_i	$\mathbf{H}_i$	M_i	μ_i	t_{3i}	x_{3i}	α_i
D1 [159]	−402.400	−100.0000	−496.200	−23.5600	0.7	1350.000	1	1/3
	−21.3000	−11.770	37.270	−68.8100	1.2			
D1M [160]	−12797.57	14048.85	−15144.43	11963.81	0.5	1562.220	1	1/3
	490.9500	−752.270	675.120	−693.570	1.0			
D1M*[161]	−17242.014	19604.4056	−20699.986	16408.3344	0.5	1561.220	1	1/3
	675.386	−982.815	905.665	−878.006	1.0			
D1MK [20]	−17242.014	19604.4056	−20699.986	16408.6002	0.5	1561.7167	1	1/3
	642.600	−941.150	865.572	−845.3008	1.0	0	−1	1
D1N [162]	−2047.610	1700.0000	−2414.930	1519.3500	0.8	1609.460	1	1/3
	293.020	−300.780	414.590	−316.8400	1.2			
D1P [163]	−372.890	62.6900	−464.510	−31.4900	0.9	1025.900	1.16	1/3
	34.6200	−14.080	70.950	−20.9600	1.44	256.020	−2.007	0.92
D1PK [20]	−465.028	155.1345	−506.775	117.7499	0.9	981.0654	1	1/3
	34.6200	−14.080	70.950	−41.3518	1.44	534.1557	−1	1
D1S [159]	−1720.300	1300.00	−1813.530	1397.600	0.7	1390.600	1	1/3
	103.640	−163.480	162.810	−223.930	1.2			
D250 [159]	−1045.960	900.00	−1127.639	1009.162	0.7	1350.000	1	2/3
	45.731	−121.465	102.549	−184.271	1.2			
D260 [159]	1396.200	−2000.00	1232.414	−1972.945	0.7	1300.500	1	1/3
	−171.827	174.285	−105.179	121.308	1.2			
D280 [159]	1689.093	−2000.00	1097.591	−2400.662	0.7	1301.000	1	1/3
	−194.420	190.813	−89.561	176.047	1.2			
D300 [159]	673.794	−1000.00	446.057	−1036.897	0.7	1450.000	1	2/3
	−115.173	103.365	−43.235	55.678	1.2			
GT2 [164]	2311.000	−3480.00	2962.00	−2800.00	0.7	1400.000	1	1/3
	−339.000	388.000	−370.000	260.000	1.2			

TABLE XII. The same as Table II except for Gogny models.

Model	n_0	E_0	K_0	Q_0	J_1	J_2	L_1	L_2	K_{sym1}	K_{sym2}	Q_{sym1}	Q_{sym2}
D1	0.1665	−16.32	229.35	−473.47	31.90	30.69	21.11	18.33	−277.61	−274.62	615.98	616.79
D1M	0.1647	−16.04	224.75	−456.81	29.72	28.54	24.61	24.82	−157.87	−133.21	806.61	735.63
D1M*	0.1650	−16.07	225.20	−458.33	31.24	30.24	41.19	43.16	−80.22	−47.09	811.72	706.21
D1MK	0.1650	−16.08	225.24	−458.44	33.85	32.99	52.41	54.86	−69.71	−36.83	766.16	664.14
D1N	0.1613	−15.98	225.76	−449.23	30.13	29.59	31.92	33.55	−183.85	−168.56	518.82	440.17
D1P	0.1698	−15.27	254.10	−329.36	33.98	32.75	53.08	50.26	−164.08	−159.35	406.62	408.31
D1PK	0.1633	−16.02	260.01	−316.42	33.85	32.99	56.53	54.91	−152.69	−149.82	402.40	397.27
D1S	0.1633	−16.02	202.82	−544.42	31.94	31.12	22.23	22.41	−252.95	−241.50	682.29	644.22
D250	0.1580	−15.86	249.71	−387.56	32.35	31.56	24.81	24.81	−299.17	−289.33	513.59	484.31
D260	0.1601	−16.27	259.10	−362.01	31.84	30.10	24.28	17.58	−290.81	−298.60	487.57	539.16
D280	0.1525	−16.35	284.80	−268.80	34.87	33.13	53.19	46.52	−205.92	−211.83	288.67	326.06
D300	0.1562	−16.23	298.98	−232.31	32.43	31.22	29.75	25.83	−312.50	−315.05	336.25	359.50
GT2	0.1612	−16.03	227.88	−453.45	35.42	33.93	12.75	5.013	−423.72	−445.80	617.85	740.97

TABLE XIII. The same as Table IV except for Gogny models.

Model	$R_{1.2}$	$\Lambda_{1.2}$	$\bar{I}_{1.2}$	BE/$M_{1.2}$	$R_{1.4}$	$\Lambda_{1.4}$	$\bar{I}_{1.4}$	BE/$M_{1.4}$	$R_{1.6}$	$\Lambda_{1.6}$	$\bar{I}_{1.6}$	BE/$M_{1.6}$	M_{max}
D1	−1	−1	−1	−1	−1	−1	−1	−1	−1	−1	−1	−1	0.0081
D1M	9.97	347.4	12.00	0.081	9.88	116.4	9.17	0.102	9.61	33.9	7.07	0.129	1.74
D1M*	11.32	816.7	15.07	0.067	11.36	316.9	11.69	0.083	11.32	123.4	9.30	0.101	2.04
D1MK	11.79	1007.2	15.93	0.064	11.81	379.2	12.30	0.079	11.75	152.1	9.77	0.097	2.08
D1N	8.14	59.3	7.86	0.119	−1	−1	−1	−1	−1	−1	−1	−1	1.23
D1P	11.09	606.1	13.92	0.072	10.95	210.2	10.53	0.091	10.69	69.1	8.16	0.113	1.89
D1PK	11.63	888.3	15.39	0.066	11.59	328.3	11.78	0.083	11.46	123.0	9.28	0.101	2.07
D1S	−1	−1	−1	−1	−1	−1	−1	−1	−1	−1	−1	−1	0.016
D250	−1	−1	−1	−1	−1	−1	−1	−1	−1	−1	−1	−1	0.0001
D260	−1	−1	−1	−1	−1	−1	−1	−1	−1	−1	−1	−1	0.014
D280	11.33	655.1	14.16	0.071	10.98	194.2	10.32	0.093	10.22	41.4	7.32	0.127	1.65
D300	−1	−1	−1	−1	−1	−1	−1	−1	−1	−1	−1	−1	0.72
GT2	−1	−1	−1	−1	−1	−1	−1	−1	−1	−1	−1	−1	0.0007

[1] M. Dutra, O. Lourenço, J. S. Sá Martins, A. Delfino, J. R. Stone, and P. D. Stevenson, Phys. Rev. C **85**, 035201 (2012).
[2] M. Dutra, O. Lourenço, S. S. Avancini, B. V. Carlson, A. Delfino, D. P. Menezes, C. Providência, S. Typel, and J. R. Stone, Phys. Rev. C **90**, 055203 (2014).
[3] B. V. Carlson, M. Dutra, O. Lourenço, and J. Margueron, Phys. Rev. C **107**, 035805 (2023).
[4] S. Typel, Particles **1**, 2 (2018).
[5] D. Vautherin and D. M. Brink, Phys. Rev. C **5**, 626 (1972).
[6] B. K. Agrawal, S. K. Dhiman, and R. Kumar, Phys. Rev. C **73**, 034319 (2006).
[7] N. Chamel, S. Goriely, and J. M. Pearson, Nucl. Phys. A **812**, 72 (2008).
[8] N. Chamel, S. Goriely, and J. M. Pearson, Phys. Rev. C **80**, 065804 (2009).
[9] A. W. Steiner, M. Prakash, J. M. Lattimer, and P. J. Ellis, Phys. Rep. **411**, 325 (2005).
[10] B. A. Nikolaus, T. Hoch, and D. G. Madland, Phys. Rev. C **46**, 1757 (1992).
[11] C. Gonzalez-Boquera, M. Centelles, X. Viñas, and A. Rios, Phys. Rev. C **96**, 065806 (2017).
[12] J. M. Lattimer, Particles **6**, 30 (2023).
[13] W. D. Myers and W. J. Swiatecki, Nucl. Phys. A **336**, 267 (1980).
[14] W. D. Myers and W. J. Swiatecki, Ann. Phys. (NY) **84**, 186 (1974).
[15] J. M. Lattimer and M. Prakash, Phys. Rep. **621**, 127 (2016).
[16] M. Warda, X. Viñas, X. Roca-Maza, and M. Centelles, Phys. Rev. C **80**, 024316 (2009).
[17] D. Adhikari, H. Albataineh, D. Androic, K. Aniol, D. S. Armstrong, T. Averett, C. A. Gayoso, S. Barcus, V. Bellini, R. S. Beminiwattha *et al.*, Phys. Rev. Lett. **126**, 172502 (2021).
[18] D. Adhikari, H. Albataineh, D. Androic, K. A. Aniol, D. S. Armstrong, T. Averett, C. A. Gayoso, S. K. Barcus, V. Bellini, R. S. Beminiwattha *et al.*, Phys. Rev. Lett. **129**, 042501 (2022).
[19] G. Giacalone, G. Nijs, and W. van der Scheee, Phys. Rev. Lett. **131**, 202302 (2023).
[20] S. Tagami, T. Wakasa, M. Takechi, J. Matsui, and M. Yahiro, Results Phys. **33**, 105155 (2022).
[21] J. Birkhan, M. Miorelli, S. Bacca, S. Bassauer, C. Bertulani, G. Hagen, H. Matsubara, P. von Neumann-Cosel, T. Papenbrock, N. Pietralla, V. Y. Ponomarev, A. Richter, A. Schwenk, and A. Tamii, Phys. Rev. Lett. **118**, 252501 (2017).
[22] A. Tamii, Phys. Rev. Lett. **107**, 062502 (2011).
[23] J. M. Lattimer and F. D. Swesty, Nucl. Phys. A **535**, 331 (1991).
[24] T. Zhao and J. M. Lattimer, Phys. Rev. D **106**, 123002 (2022).
[25] J. M. Lattimer and M. Prakash, Astrophys. J. **550**, 426 (2001).
[26] D. G. Ravenhall and C. J. Pethick, Astrophys. J. **424**, 846 (1994).
[27] S. Postnikov, M. Prakash, and J. M. Lattimer, Phys. Rev. D **82**, 024016 (2010).
[28] T. Zhao and J. M. Lattimer, Phys. Rev. D **98**, 063020 (2018).
[29] K. Yagi and N. Yunes, Phys. Rep. **681**, 1 (2017).
[30] M. Bagchi, Mon. Not. R. Astron. Soc.: Lett. **413**, L47 (2011).
[31] M. Samyn, S. Goriely, P.-H. Heenen, J. M. Pearson, and F. Tondeur, Nucl. Phys. A **700**, 142 (2002).
[32] S. Goriely, M. Samyn, P.-H. Heenen, J. M. Pearson, and F. Tondeur, Phys. Rev. C **66**, 024326 (2002).
[33] M. Samyn, S. Goriely, and J. M. Pearson, Nucl. Phys. A **725**, 69 (2003).
[34] S. Goriely, M. Samyn, M. Bender, and J. M. Pearson, Phys. Rev. C **68**, 054325 (2003).
[35] M. Samyn, S. Goriely, M. Bender, and J. M. Pearson, Phys. Rev. C **70**, 044309 (2004).
[36] S. Goriely, M. Samyn, J. M. Pearson, and M. Onsi, Nucl. Phys. A **750**, 425 (2005).
[37] S. Goriely, M. Samyn, and J. M. Pearson, Nucl. Phys. A **773**, 279 (2006).
[38] S. Goriely, M. Samyn, and J. M. Pearson, Phys. Rev. C **75**, 064312 (2007).
[39] S. Goriely and J. M. Pearson, Phys. Rev. C **77**, 031301(R) (2008).

[40] S. Goriely, N. Chamel, and J. M. Pearson, Phys. Rev. Lett. **102**, 152503 (2009).
[41] S. Goriely, N. Chamel, and J. M. Pearson, Phys. Rev. C **82**, 035804 (2010).
[42] S. Goriely, N. Chamel, and J. M. Pearson, Phys. Rev. C **88**, 024308 (2013).
[43] J. Friedrich and P.-G. Reinhard, Phys. Rev. C **33**, 335 (1986).
[44] T. Lesinski, K. Bennaceur, T. Duguet, and J. Meyer, Phys. Rev. C **74**, 044315 (2006).
[45] M. Dutra (private communication).
[46] L. Guo-Qiang, J. Phys. G **17**, 1 (1991).
[47] B. K. Agrawal, S. Shlomo, and V. K. Au, Phys. Rev. C **72**, 014310 (2005).
[48] L. G. Cao, U. Lombardo, C. W. Shen, and N. V. Giai, Phys. Rev. C **73**, 014313 (2006).
[49] F. Tondeur, S. Goriely, J. M. Pearson, and M. Onsi, Phys. Rev. C **62**, 024308 (2000).
[50] M. Farine, J. M. Pearson, and F. Tondeur, Nucl. Phys. A **696**, 396 (2001).
[51] S. Goriely, F. Tondeur, and J. M. Pearson, At. Data Nucl. Data Tables **77**, 311 (2001).
[52] M. M. Sharma, G. A. Lalazissis, J. König, and P. Ring, Phys. Rev. Lett. **74**, 3744 (1995).
[53] L.-W. Chen, C. M. Ko, B.-A. Li, and J. Xu, Phys. Rev. C **82**, 024321 (2010).
[54] S. J. Lee and A. Z. Mekjian, Phys. Rev. C **63**, 044605 (2001).
[55] M. Rayet, M. Arnould, G. Paulus, and F. Tondeur, Astron. Astrophys. **116**, 183 (1982).
[56] S. Shen, G. Colò, and X. Roca-Maza, Phys. Rev. C **99**, 034322 (2019).
[57] N. Van Giai and H. Sagawa, Phys. Lett. B **106**, 379 (1981).
[58] Q.-b. Shen, Y.-l. Han, H.-r. Guo *et al.*, Phys. Rev. C **80**, 024604 (2009).
[59] J. M. Lattimer and D. G. Ravenhall, Astrophys. J. **223**, 314 (1978).
[60] M. Beiner, H. Flocard, N. Van Giai, and P. Quentin, Nucl. Phys. A **238**, 29 (1975).
[61] M. J. Giannoni and P. Quentin, Phys. Rev. C **21**, 2076 (1980).
[62] B. K. Agrawal, S. Shlomo, and V. Kim Au, Phys. Rev. C **68**, 031304(R) (2003).
[63] H. S. Köhler, Nucl. Phys. A **258**, 301 (1976).
[64] P.-G. Reinhard and H. Flocard, Nucl. Phys. A **584**, 467 (1995).
[65] W. Nazarewicz, J. Dobaczewski, T. R. Werner, J. A. Maruhn, P.-G. Reinhard, K. Rutz, C. R. Chinn, A. S. Umar, and M. R. Strayer, Phys. Rev. C **53**, 740 (1996).
[66] H. Krivine, J. Treiner, and O. Bohigas, Nucl. Phys. A **336**, 155 (1980).
[67] X. Li and P.-H. Heenen, Phys. Rev. C **54**, 1617 (1996).
[68] J. Bartel, P. Quentin, M. Brack, C. Guet, and H.-B. Håkansson, Nucl. Phys. A **386**, 79 (1982).
[69] L. Bennour, P.-H. Heenen, P. Bonche, J. Dobaczewski, and H. Flocard, Phys. Rev. C **40**, 2834 (1989).
[70] P.-G. Reinhard, D. J. Dean, W. Nazarewicz, J. Dobaczewski, J. A. Maruhn, and M. R. Strayer, Phys. Rev. C **60**, 014316 (1999).
[71] J. Dobaczewski, H. Flocard, and J. Treiner, Nucl. Phys. A **422**, 103 (1984).
[72] M. Rashdan, Mod. Phys. Lett. A **15**, 1287 (2000).
[73] J. Gómez, C. Prieto, and J. Navarro, Nucl. Phys. A **549**, 125 (1992).
[74] J. M. Pearson, Y. Aboussir, A. Dutta, R. Nayak, M. Farine, and F. Tondeur, Nucl. Phys. A **528**, 1 (1991).
[75] Y. Aboussir, J. M. Pearson, A. Dutta, and F. Tondeur, Nucl. Phys. A **549**, 155 (1992).
[76] J. M. Pearson and R. C. Nayak, Nucl. Phys. A **668**, 163 (2000).
[77] M. Onsi, H. Przysiezniak, and J. M. Pearson, Phys. Rev. C **50**, 460 (1994).
[78] C. J. Pethick, D. G. Ravenhall, and C. P. Lorenz, Nucl. Phys. A **584**, 675 (1995).
[79] C. M. Ko, H. C. Pauli, M. Brack, and G. E. Brown, Nucl. Phys. A **236**, 269 (1974).
[80] J. Treiner and H. Krivine, J. Phys. G: Nucl. Phys. **2**, 285 (1976).
[81] B. A. Brown, Phys. Rev. C **58**, 220 (1998).
[82] Y. Lim and J. W. Holt, Phys. Rev. C **95**, 065805 (2017).
[83] R. Obaid and A. Alzubadi, East Eur. J. Phys. **2**, 76 (2023).
[84] B. A. Brown, G. Shen, G. C. Hillhouse, J. Meng, and A. Trzcińska, Phys. Rev. C **76**, 034305 (2007).
[85] J. Margueron, J. Navarro, and N. V. Giai, Phys. Rev. C **66**, 014303 (2002).
[86] E. Chabanat, Technical Report (Lyon-1 University, 1995).
[87] E. Chabanat, P. Bonche, P. Haensel, J. Meyer, and R. Schaeffer, Nucl. Phys. A **627**, 710 (1997).
[88] E. Chabanat, P. Bonche, P. Haensel, J. Meyer, and R. Schaeffer, Nucl. Phys. A **635**, 231 (1998).
[89] P. A. M. Guichon and A. W. Thomas, Phys. Rev. Lett. **93**, 132502 (2004).
[90] P. A. M. Guichon, H. H. Matevosyan, N. Sandulescu, and A. W. Thomas, Nucl. Phys. A **772**, 1 (2006).
[91] P. Klüpfel, P.-G. Reinhard, T. J. Bürvenich, and J. A. Maruhn, Phys. Rev. C **79**, 034310 (2009).
[92] F. Tondeur, M. Brack, M. Farine, and J. M. Pearson, Nucl. Phys. A **420**, 297 (1984).
[93] T. Lesinski, M. Bender, K. Bennaceur, T. Duguet, and J. Meyer, Phys. Rev. C **76**, 014312 (2007).
[94] M. Kortelainen, J. McDonnell, W. Nazarewicz, P.-G. Reinhard, J. Sarich, N. Schunck, M. V. Stoitsov, and S. M. Wild, Phys. Rev. C **85**, 024304 (2012).
[95] J. M. Pearson and S. Goriely, Phys. Rev. C **64**, 027301 (2001).
[96] S. Haddad, Europhys. Lett. **48**, 505 (1999).
[97] P.-G. Reinhard, Rep. Prog. Phys. **52**, 439 (1989).
[98] A. ben Ali Dadi, Phys. Rev. C **82**, 025203 (2010).
[99] M. Rufa, P.-G. Reinhard, J. A. Maruhn, W. Greiner, and M. R. Strayer, Phys. Rev. C **38**, 390 (1988).
[100] J. Piekarewicz, Phys. Rev. C **66**, 034305 (2002).
[101] N. K. Glendenning, *Compact Stars: Nuclear Physics, Particle Physics and General Relativity* (Springer, New York, 2012).
[102] N. K. Glendenning, Phys. Lett. B **114**, 392 (1982).
[103] N. K. Glendenning and S. A. Moszkowski, Phys. Rev. Lett. **67**, 2414 (1991).
[104] S. K. Ghosh, S. C. Phatak, and P. K. Sahu, Z. Phys. A: Hadrons Nucl. **352**, 457 (1995).
[105] J. Piekarewicz and M. Centelles, Phys. Rev. C **79**, 054311 (2009).
[106] H. Mueller and B. D. Serot, Nucl. Phys. A **606**, 508 (1996).
[107] C.-J. Xia, T. Maruyama, A. Li, B. Y. Sun, W.-H. Long, and Y.-X. Zhang, Commun. Theor. Phys. **74**, 095303 (2022).

[108] M. Bender, K. Rutz, P.-G. Reinhard, J. A. Maruhn, and W. Greiner, Phys. Rev. C **60**, 034304 (1999).
[109] B. Liu, V. Greco, V. Baran, M. Colonna, and M. Di Toro, Phys. Rev. C **65**, 045201 (2002).
[110] M. Centelles, M. Del Estal, and X. Vinas, Nucl. Phys. A **635**, 193 (1998).
[111] G. A. Lalazissis, J. König, and P. Ring, Phys. Rev. C **55**, 540 (1997).
[112] G. A. Lalazissis, S. Karatzikos, R. Fossion, D. P. Arteaga, A. V. Afanasjev, and P. Ring, Phys. Lett. B **671**, 36 (2009).
[113] B. Nerlo-Pomorska and J. Sykut, Int. J. Mod. Phys. E **13**, 75 (2004).
[114] B. D. Serot and J. D. Walecka, Int. J. Mod. Phys. E **06**, 515 (1997).
[115] B. D. Serot, Rep. Prog. Phys. **55**, 1855 (1992).
[116] K. Chung, C. S. Wang, A. J. Santiago, and J. W. Zhang, Eur. Phys. J. A **9**, 453 (2000).
[117] M. Rashdan, Phys. Rev. C **63**, 044303 (2001).
[118] P. G. Reinhard, Z. Phys. A: At. Nucl. **329**, 257 (1988).
[119] A. Sulaksono, T. Mart, and C. Bahri, Phys. Rev. C **71**, 034312 (2005).
[120] R. J. Furnstahl, B. D. Serot, and H.-B. Tang, Nucl. Phys. A **615**, 441 (1997).
[121] C. J. Horowitz and J. Piekarewicz, Phys. Rev. Lett. **86**, 5647 (2001).
[122] S. Gmuca, Z. Phys. A: Hadrons Nucl. **342**, 387 (1992).
[123] M. Centelles, X. Vinas, M. Barranco, S. Marcos, and R. J. Lombard, Nucl. Phys. A **537**, 486 (1992).
[124] S. Gmuca, Nucl. Phys. A **547**, 447 (1992).
[125] J. K. Bunta and Š. Gmuca, Phys. Rev. C **68**, 054318 (2003).
[126] H. Müller and B. D. Serot, Phys. Rev. C **52**, 2072 (1995).
[127] F. J. Fattoyev and J. Piekarewicz, Phys. Rev. C **82**, 025805 (2010).
[128] M. M. Sharma, A. R. Farhan, and S. Mythili, Phys. Rev. C **61**, 054306 (2000).
[129] W. Long, J. Meng, N. V. Giai, and S.-G. Zhou, Phys. Rev. C **69**, 034319 (2004).
[130] Y. Sugahara and H. Toki, Nucl. Phys. A **579**, 557 (1994).
[131] F. J. Fattoyev, C. J. Horowitz, J. Piekarewicz, and B. Reed, Phys. Rev. C **102**, 065805 (2020).
[132] B. K. Agrawal, Phys. Rev. C **81**, 034323 (2010).
[133] S. K. Dhiman, R. Kumar, and B. K. Agrawal, Phys. Rev. C **76**, 045801 (2007).
[134] B.-J. Cai and L.-W. Chen, Phys. Rev. C **85**, 024302 (2012).
[135] L. Tolos, M. Centelles, and A. Ramos, Astrophys. J. **834**, 3 (2016).
[136] T. Miyatsu, M.-K. Cheoun, K. Kim, and K. Saito, Phys. Lett. B **8**43, 138013 (2023).
[137] B. G. Todd-Rutel and J. Piekarewicz, Phys. Rev. Lett. **95**, 122501 (2005).
[138] J. Piekarewicz and S. P. Weppner, Nucl. Phys. A **778**, 10 (2006).
[139] R. Kumar, B. K. Agrawal, and S. K. Dhiman, Phys. Rev. C **74**, 034323 (2006).
[140] A. Sulaksono and T. Mart, Phys. Rev. C **74**, 045806 (2006).
[141] C. J. Horowitz and J. Piekarewicz, Phys. Rev. C **66**, 055803 (2002).
[142] B. K. Pradhan, D. Chatterjee, R. Gandhi, and J. Schaffner-Bielich, Nucl. Phys. A **1030**, 122578 (2023).
[143] M. G. Alford, L. Brodie, A. Haber, and I. Tews, Phys. Rev. C **106**, 055804 (2022).
[144] M. M. Haidari and M. M. Sharma, Nucl. Phys. A **803**, 159 (2008).
[145] M. M. Sharma, Phys. Lett. B **666**, 140 (2008).
[146] M. Del Estal, M. Centelles, X. Vinas, and S. K. Patra, Phys. Rev. C **63**, 024314 (2001).
[147] H. Shen, F. Ji, J. Hu, and K. Sumiyoshi, Astrophys. J. **891**, 148 (2020).
[148] D. P. Menezes and C. Providência, Phys. Rev. C **70**, 058801 (2004).
[149] S. Typel, Phys. Rev. C **71**, 064301 (2005).
[150] T. Klähn, D. Blaschke, S. Typel, E. N. E. van Dalen, A. Faessler, C. Fuchs, T. Gaitanos, H. Grigorian, A. Ho, E. E. Kolomeitsev *et al.*, Phys. Rev. C **74**, 035802 (2006).
[151] T. Nikšić, D. Vretenar, P. Finelli, and P. Ring, Phys. Rev. C **66**, 024306 (2002).
[152] G. A. Lalazissis, T. Nikšić, D. Vretenar, and P. Ring, Phys. Rev. C **71**, 024312 (2005).
[153] S. Typel, G. Röpke, T. Klähn, D. Blaschke, and H. H. Wolter, Phys. Rev. C **81**, 015803 (2010).
[154] J.-J. Li and A. Sedrakian, Astrophys. J. **957**, 41 (2023).
[155] S. Typel and H. H. Wolter, Nucl. Phys. A **656**, 331 (1999).
[156] J. J. Rusnak and R. J. Furnstahl, Nucl. Phys. A **627**, 495 (1997).
[157] T. J. Bürvenich, D. G. Madland, J. A. Maruhn, and P.-G. Reinhard, Phys. Rev. C **65**, 044308 (2002).
[158] P.-W. Zhao, Z.-P. Li, J.-M. Yao, J. Meng *et al.*, Phys. Rev. C **82**, 054319 (2010).
[159] J. P. Blaizot, J. Berger, J. Dechargé, and M. Girod, Nucl. Phys. A **591**, 435 (1995).
[160] S. Goriely, S. Hilaire, M. Girod, and S. Péru, Phys. Rev. Lett. **102**, 242501 (2009).
[161] C. Gonzalez-Boquera, M. Centelles, X. Viñas, and L. M. Robledo, Phys. Lett. B **779**, 195 (2018).
[162] F. Chappert, M. Girod, and S. Hilaire, Phys. Lett. B **668**, 420 (2008).
[163] M. Farine, D. Von-Eiff, P. Schuck, J. Berger, J. Dechargé, and M. Girod, J. Phys. G **25**, 863 (1999).
[164] T. Otsuka, T. Matsuo, and D. Abe, Phys. Rev. Lett. **97**, 162501 (2006).